ABSTRACT

Title of Document: MECHANISTIC-BASED DESIGN-INTEGRATED RELIABILITY VALIDATION FRAMEWORK FOR MECHANICAL SYSTEMS.

Omer Yousif, PhD in Reliability Engineering, 2015

Directed By: Professor, Mohammad Modarres, Mechanical Engineering Department

New product design challenges, related to customer needs, product usage and environments, face companies when they expand their product offerings to new markets; Some of the main challenges are: the lack of quantifiable information, product experience and field data. Designing reliable products under such challenges requires flexible reliability assessment processes that can capture the variables and parameters affecting the product overall reliability and allow different design scenarios to be assessed. These challenges also suggest a mechanistic (Physics of Failure-PoF) reliability approach would be a suitable framework to be used for reliability assessment. Mechanistic Reliability recognizes the primary factors affecting design reliability.

This research views the designed entity as a "system of components required to deliver specific operations"; it addresses the above mentioned challenges by; Firstly: developing a design synthesis that allows a descriptive operations/ system components relationships to be realized; Secondly: developing component's mathematical damage models that evaluate components Time to Failure (TTF) distributions given: 1) the

descriptive design model, 2) customer usage knowledge and 3) design material properties; Lastly: developing a procedure that integrates components' damage models to assess the mechanical system's reliability over time.

Analytical and numerical simulation models were developed to capture the relationships between operations and components, the mathematical damage models and the assessment of system's reliability. The process was able to affect the design form during the conceptual design phase by providing stress goals to meet component's reliability target. The process was able to numerically assess the reliability of a system based on component's mechanistic TTF distributions, besides affecting the design of the component during the design embodiment phase. The process was used to assess the reliability of an internal combustion engine manifold during design phase; results were compared to reliability field data and found to produce conservative reliability results.

The research focused on mechanical systems, affected by independent mechanical failure mechanisms that are influenced by the design process. Assembly and manufacturing stresses and defects' influences are not a focus of this research.

MECHANISTIC-BASED DESIGN-INTEGRATED RELIABILITY VALIDATION FRAMEWORK FOR MECHANICAL SYSTEMS

By

Omer Yousif

Dissertation submitted to the Faculty of the Graduate School of the
University of Maryland, College Park, in partial fulfillment
of the requirements for the degree of
Doctor of Philosophy
2015

Advisory Committee:

Professor Mohammad Modarres (Chair)
Professor Ali Mosleh
Associate Professor Linda Schmidt
Professor Mohamad Al-Sheikhly (Dean Representative)
Assistant Professor Monifa Vaughn-Cooke

PREFACE

Considering the process of developing new mechanical system products, the amount of time spent on designing, validating and testing the system is by far the most costly and time consuming activity among the rest of the product delivery processes. If the first design iteration successfully passed through virtual validation check processes (FEA, CFD…etc.), made it to physical testing but failed to pass its requirements, a modification or complete redesign for the system would need to be implemented before progressing to the next product development process. Many reasons lead to this mismatch between virtual verification checks outcome and physical verifications, one of them is the uncontrolled physical environment randomness that affects physical testing; which is not captured during deterministic virtual verification assessments; besides, the lack of an organized reliability assessment process that can be implemented during the virtual verification phases.

Most of mechanical systems fail due to physical material failures. Those failures are produced by degradation mechanisms, such as fatigue, wear, corrosion…etc., that create internal and/or external damages produced by environment stresses. Those stresses, besides the rate of system usage and material capacity to resist those damaging mechanisms, lead over time to component failures that hinder the successful operation of the system. Mechanical systems are also required to deliver specific system tasks (will be called operations in this research); those operations, indirectly, are the main cause of system failures. The demand on the system to deliver these operations is the primary driver that leads to failure. Being able to identify the operations affecting specific component and how that effect is being carried out is a difficult task to visually recognize for complicated systems. A tool that helps the system analyst to recognize the relationships between system operations and components and recognize interactions and influences between system components is very important in assessing the system reliability.

Another issue related to the reliability of mechanical systems is the mismatch between reliability predictions produced by processes like RBD and FTA and product reliability data collected during customer usage. Generally RBD and FTA processes, originally developed for electronic components, underestimates mechanical systems reliability in comparison with observed data during customer usage phase. A process developed specifically for mechanical systems and mechanical failures is needed.

In this research, a framework is developed to allow coupling of the design synthesis of mechanical systems to mechanistic-based damage models. The final goal of this coupling is to assess components time-to-failure (TTF) distributions and use that to assess the mechanical system (TTF) distribution and reliability.

DEDICATION

I would like to dedicate this thesis to my parents Hassan and Asma for their unconditional love and support

ACKNOWLEDGEMENTS

I would like to express my special appreciation and thanks to professor Mohammad Modarres my advisor for his encouragement, inspiration and advice to write this dissertation.

I would also like to thank my committee: professor Ali Mosleh, doctor Linda Schmidt, professor Mohamad Al-Sheikhly and doctor Monifa Vaughn-Cooke for taking the time to review this work and for their valuable inputs and advice.

I would like also to thank my mentor and friend Jose Nazario for his encouragement; a special thanks also to my friend Mark Zimmerman for his moral support. I would also like to thank my Circle Club friends for their inspiration and continuous encouragement.

Special thanks to my family, Naima, Noon, Jewiriya and Osama, for their unconditional support and encouragement during this research.

Finally I thank Allah for giving me the energy, will and guidance to complete this work.

TABLE OF CONTENTS

LIST OF TABLES

LIST OF FIGURES

NOMENCLATURE

3D	Three Dimensional
AGREE	Advisory Group on the Reliability of Electronic Equipment
ALT	Accelerated Life Test
CAD	Computer-Aided Design
CFD	Computational Fluid Dynamics
CDF	Cumulative Density Function
COV	Coefficient of Variation
CPU	Central Processing Unit
DOF	Degree of Freedom
DOFS	Degrees of Freedom
ETA	Event Tree Analysis
FEA	Finite Element Analysis
FEM	Finite Element Model
FTA	Fault Tree Analysis
FMEA	Failure Mode and Effect Analysis
FMECA	Failure Mode and Effect Criticality Analysis
GUI	Graphical User Interface
IC	Internal Combustion
LS	Least Squares
MDRV	Mechanistic-Based Design Integrated Reliability Validation Process
MLE	Maximum Likelihood Estimator
PDF	Probability Density Function

PDP	Product Development Process
PoF	Physics of Failure
PRA	Probabilistic Risk Assessment
RBD	Reliability Block Diagram
TTF	Time to Failure
TTM	Time to Market

Chapter 1. Introduction

1.1 Research Motivation

As companies expand into new markets by developing new products or marketing existing ones, they normally face the challenge of delivering value products that keep them competitive to survive in those markets. The environment, customer usage and product perception in these new markets might be different than what those products were designed for. A process that recognizes and models those differences and their impact on products durability and reliability would help to accurately predict these products future performance.

Due to the complexity of modern engineering systems and the short time to market (TTM) allocated to complete PDP, the time required to assess the reliability of these systems is becoming a critical component of the success of the product delivery process. A systematic, structured reliability assessment process that recognizes the parameters affecting design reliability and can easily be used by engineers during the product development phases is needed to help make the right design decisions to influence the reliability of these products during early design phases.

Reliability is defined as the probability that an item will perform a required function without failure under stated conditions for a specified period of time [1]. Based on this definition, understanding the functionality, customer usage, operational environments and life goals of a system is very essential to assess its reliability. In this research, an attempt is made to integrate those reliability elements into a mechanistic-based, design integrated reliability evaluation process. The physics of failure methodology of reliability assessment will be integrated to the design entity and the design development process. The main focus of this research will be on mechanical systems and degradation type mechanical failures as presented in Table 3-1.

Chapter-1 of this dissertation outlines the contribution and scope of this research work. The literature review of reliability and product engineering, the history of reliability integration during design processes and summary of the currently used processes are presented in Chapter 2. Chapter 3 introduces the new mechanistic reliability process; The process of design synthesis needed to capture the design elements essential to reliability validation is demonstrated; Damage and degradation models are developed for fatigue type failures to assess component reliability; System reliability and availability processes are developed and demonstrated through short examples and an overview of the integration between the design process and reliability validation process is summarized at the end. Chapter 4 shows through generic example how the mechanistic reliability methodology can be integrated to the system of components design process. Chapter 5 demonstrates the component mechanistic reliability process integration to design through practical example of an internal combustion engine manifold design problem. Lastly, Chapter 6 presents a discussion about the proposed process, conclusions of this research work, and recommendations for future work.

1.2 Contributions

The key characteristic descriptions for this thesis work are: automation, streamlining and integration related to reliability engineering processes of mechanical systems. This research identifies the need for a design integrated, physics-based reliability framework to bridge gaps that hinders the *automation* and *streamlining* of reliability assessment during the design process of mechanical systems. The mechanistic aspect of this process refers to the mechanization related to the *integration* process of design synthesis and the integration of physics of failure (PoF) approach. Considering mechanical systems and mechanical failure modes, this dissertation contributes the following to address this need:

1. *Reliability-centered design synthesis process*: An automated algorithm was developed to integrate design synthesis models, PoF damage models, expert knowledge and relevant information needed to evaluate system reliability (Figure 3-38).
2. *Component's reliability assessment process*: leveraging interrelationships revealed by the design synthesis step, a process was developed to generate components' time to failure (TTF) distributions using: product usage information and PoF damage models. Damage path mathematical model was introduced with statistical data management process.
3. *System reliability assessment process*: leveraging component's TTF distributions and interrelationships revealed by the design synthesis process, a reliability assessment method for mechanical systems was developed. Three damage operators (**SYNC1**, **SYNC2** & **ASYNC**) that govern the interrelationship between components' and system level damage was introduced and demonstrated through examples.
4. *Damage model implementation to system availability assessment*: Mathematical models and algorithms for (**SYNC1**, **SYNC2** & **ASYNC**) damage behavior for system availability was introduced and demonstrated.

1.3 Scope of Work

This research will address the mechanical system reliability problem by leveraging design synthesis methods, focusing on failure events caused by failure mechanisms with known physics-based damage models. The following assumptions about the mechanical system, under investigation, are assumed true:

1. components are assumed to be independent of each other
2. system operations are assumed to be independent of each other
3. failure mechanisms are not influencing each other in terms of accelerating or decelerating the damage process progression.
4. the mechanical failure modes follow Palmgren–Miner linear damage hypothesis [2] [3].
5. the mechanical system: operations' descriptive models, coupling relationships and component interaction are assumed linear. Possible cases of nonlinearity could exist but not in the scope of this research.

The research will attempt to deliver the above-mentioned goals by:

1) develop a design synthesis that provides sufficient knowledge about the system to allow PoF reliability assessment to be implemented
2) develop generic PoF reliability assessment process using the system synthesis developed and
3) demonstrate the process through examples

The research will focus on reliability assessment of the design given the knowledge about: system usage, stress agents affecting the system and the damage behavior of the design materials.

Chapter 2 Literature review

This research focuses on the framework of design-integrated physics-based reliability processes. The assumption that design synthesis is an important aspect to describe design goals, entities, functions, environment, usage…etc leads us to focus on understanding the key characteristics of this topic; besides design processes that integrates reliability engineering within their framework.

At the end of World War II, with statistics and mass production well established, Reliability Engineering emerged as a new science; the catalyst came in the form of an electronic component, the vacuum tube [4]. Vacuum tubes were used in several electronic products such as radars, radios, sound reproductions, large phone network, television, etc. Due to its numerous failure modes and its extensive use in electronic components, during World War II, vacuum tubes were by far the most unreliable component used in electronic systems [5]. It is this experience with the vacuum tubes that prompted the US Department of Defense (DoD) to initiate a series of studies for looking into these failures after the war; these efforts eventually consolidated and gave birth to a new discipline, Reliability Engineering [4].

Design research is the field of engineering concerned with the physical embodiment of man-made things; how these things perform their jobs, and how they work; besides how designers work, how they think, and how they carry out design activity. Design research is also concerned with what is achieved at the end of a purposeful design activity, how an artificial thing appears, what it means besides concerned with the embodiment of configurations. Design research is a systematic search and acquisition of knowledge related to design and design activity [6]. The influence of systems analysis and systems theory on design established the grounds for the foundation of “systematic design methods”. The Conference on Design Methods, organized by J. C. Jones and D. G. Thornley in 1963 was the first scientific approach to design methods in England [6].

This chapter will review the design engineering processes in general with more focus on design methodologies and design representation elements and techniques; besides a review of reliability engineering with more focus on design-integrated reliability methods and techniques. A literature summary to this chapter is presented on the last section.

2.1 Design Engineering

Although design continues to remain a mysterious activity for many, it has been recognized as an important activity for more than 4,000 years. Around 2,000 BC, Hammurabi, King of Babylon, enacted a law which both recognized design and made it dangerous [7]; Hammurabi’s code mentions: "If a designer/builder has designed/built a house for a man and his work is not good, and if the house he has designed/built falls in and kills the householder, that designer/builder shall be slain." [7]. Design research has a number of goals including: gaining a better understanding of design, developing tools to aid human designers, and the potential automation of some design tasks [7]. Engineering design is the process of satisfying requirements by developing and synthesizing building blocks into meaningful designs that meet the requirements to fulfill needs and desires [8].

Design synthesis is the area of research that focuses on developing guidelines, methods and tools for supporting creation of such solutions [8].

Dieter and Schmidt [9] recognized that good design requires both analysis and synthesis. Typically we approach complex problems like design by decomposing the problem into manageable parts. Because we need to understand how the part will perform in service, we must be able to calculate as much about the part's expected behavior as possible before it exists in a physical form by using the appropriate discipline of science and engineering science and the necessary computational tools. This process is called analysis; it usually involves the simplification of the world through models. Synthesis involves the identification of the design elements that will comprise the product, its decomposition into parts, and the combination of the part solutions into a total workable system [9].

Gero [7] described the design activity as: "a goal-oriented, constrained, decision-making, exploration and learning activity which operates within a context which depends on the designer's perception of the context".

Zheng et al [10] considered the design of a product system as the synthesis of various candidate systems in fulfilling design requirement. The design requirement includes (1) the need for the system as suggested by customers or users and (2) the effort limited to produce the system. The need further has two aspects: (i) the time-insensitive need, and (ii) the time-sensitive need. The second- (ii) - commonly refers to the delivery time of a system. The effort limited is basically about the cost (for producing the system) which can always be converted into a monetary measure

Modern design engineering processes distinguish between design sciences and design methodology; Design science uses scientific methods to analyze the structures of technical systems and their relationships with the environment [11]. Design methodology, however is a concrete course of action for the design of technical systems that derives its knowledge from design science and cognitive psychology, and from practical experience in different domains. It includes plans of action that link working steps and design phases according to content and organization [11].

Decisions made during conceptual design have significant influence on cost, performance, reliability, safety and environmental impact of the product [12]. It has been estimated that design decisions account for more than 75% of final product costs [12], [13], [14], [15].

2.1.1 Design Methodologies Overview

Design methodologies aim at developing processes that allows idea to be transferred to products; some of these processes address the design as a process and some as an entity that need to be synthesized; some processes try to integrate the two aspects: the process and the entity form. Some of the commonly known methodologies are:

1. Systematic Design
2. Axiomatic Design
3. Theory of Inventive Problem Solving (TIPS or TRIZ)
4. Design by Analogy

The first two are design processes that follow a systematic breakdown of the system main functions into sub-functions; Systematic Design method starts by producing a system functional structure that is based on flow and conversion of materials, energy and signals through sub functions that are connected together to produce the system's overall function; Axiomatic Design on the other hand will focus on identifying the most feasible design solution to the generic functional structure.

Theory of Inventive Problem Solving (TIPS or TRIZ in the original Russian name) presumes that the most effective solutions are achieved when an inventor solves a technical problem that contains contradiction; TRIZ applies strategies and tools to find a design solution that overcomes the need for trade-off between design parameters.

Design by Analogy is a design method that depends on acquiring knowledge from one design and apply that knowledge to design a similar product; due to its focus on how to develop a design solution, design-by-analogy is more of a design synthesis procedure than a complete design method process.

The following sections will focus on reviewing Systematic Design and Axiomatic Design due to their comprehensive description of the design as an object and a process

Systematic Design:

Modern systematic design methodology ideas were developed in Germany and pioneered by Erkens in the 1920s. He insisted on a step-by-step approach based on constant testing and evaluation, and also on balancing of conflicting demands, a process that must be continued until a network of ideas-the design-emerges [11].

Pahl and Beitz outlined and defined Systematic Design as a design method in their seminal textbook, Engineering Design: A Systematic Approach. They broke down the design process into four main steps [11]:

1. Planning and task clarification: The purpose of this step is to collect information about the requirements that have to be fulfilled by the product, and any existing constraints and their importance. This activity results in the specification of information in a form of a requirements list [11].
2. Conceptual Design: This phase determines the principle solution which is achieved by abstracting the essential problems, establishing function structures, searching for suitable working principles and then combining those principles into a working structure. This phase results in the specification of a principle solution [11].
3. Embodiment Design: during this phase, designers starting from a concept (working structure, principle solution) determine the construction structure (overall layout) of a technical system in line with technical and economic criteria. Embodiment design results in the specification of a layout or many valid layouts [11].
4. Detail Design: this is the phase of the design process in which arrangement, forms, dimensions and surface properties of all of the individual parts are finally laid down. Materials would be specified, production possibilities assessed, cost estimated and all the drawings and other production documents produced during this phase. The detail design phase results in the specification of information in the form of production documentation [11].

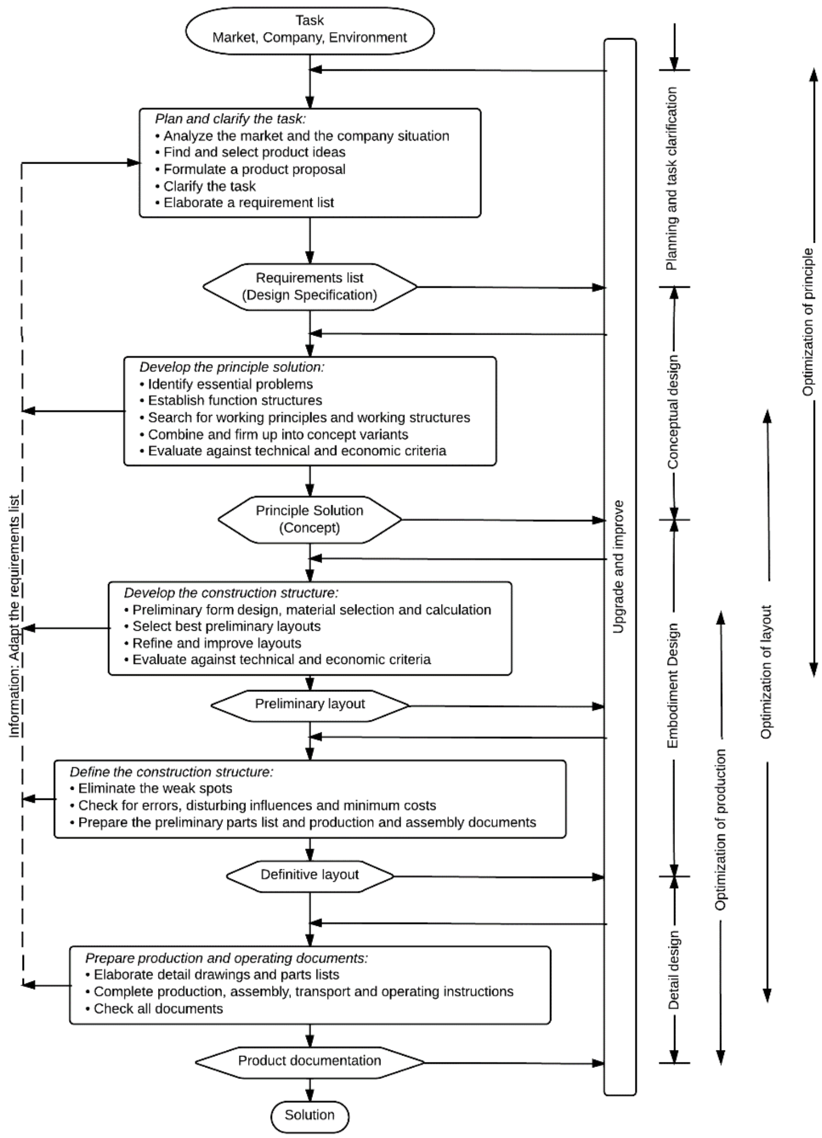

Figure 2-1: Steps in the planning and design process of the Systematic Design method [11]

Figure 2-1 shows the process steps as outlined by Pahl & Beitz [11]. The most popular step in systematic design is the establishment of a functional structure. The functional structure is a solution-neutral network of functional representations that leads to the delivery of the main system function outputs; systematic design adopts the idea that artifacts are systems connected to the environment by means of inputs and outputs [16]; a system can be divided into subsystems; what belong to a particular system is determined by the system boundary. Inputs and outputs cross the system boundary to be converted, channeled, mixed, transported, displayed…etc. Pahl and Beitz identified three forms of inputs and outputs; energy, material and signal.

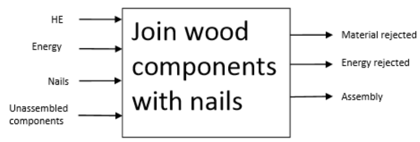

Figure 2-2: Top Level Functional Structure of a Nail Gun

The top-level functional structure can be decomposed until the design concept features were realized enough to start the physical system components design. Figure 2-3 shows the decomposed main functional structure of a pneumatic nail gun; both of these two functional structures are solution independent, i.e. they do not specify what kind of components would satisfy those functional requirements.

The graphical functional structure representation to the design domain allows functional flows to be recognized. Considering a system that is required to deliver specific operations, a set of functions working together to deliver a specific operation can be considered as a definition to what that operation is; i.e. an operation can be defined as a set of functions working together to deliver an objective system purpose; the capabilities of functional structures will be utilized, as will be demonstrated in Chapter 3, to recognize a descriptive model for the mechanical system.

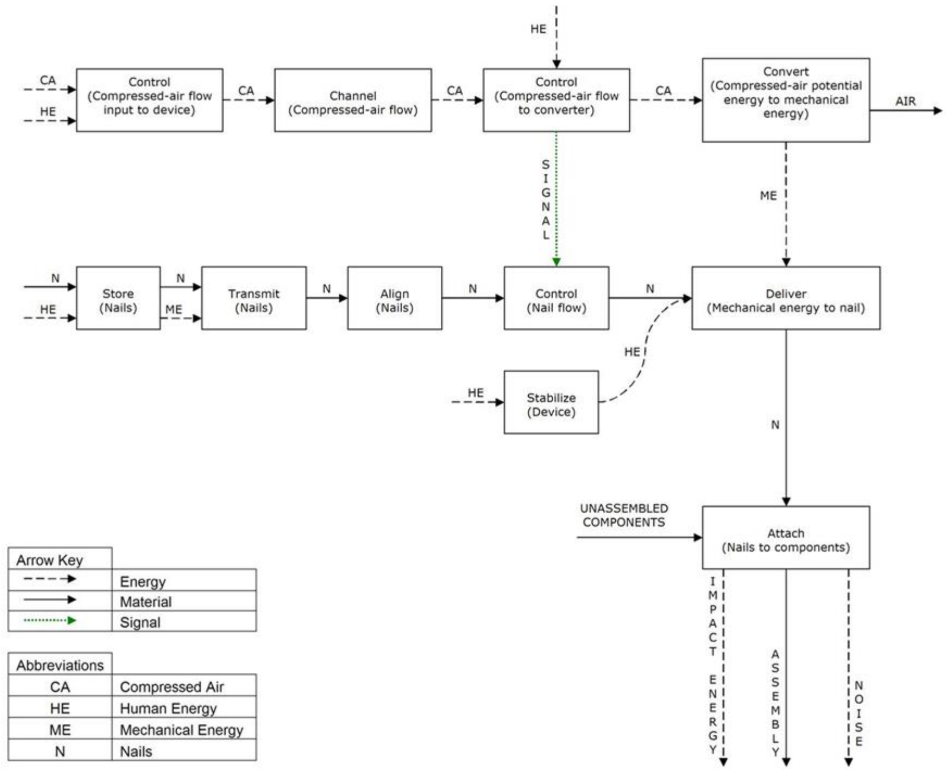

Figure 2-3: Expanded Level Functional Structure of a Nail Gun

Axiomatic Design

Axiomatic Design was advanced by Nam P. Suh in the mid-1970s with the goal to develop a scientific, generalized, codified, and systematic procedure for design [17]. According to Suh, design may be defined as the creation of synthesized solutions in the form of products, processes or systems that satisfy perceived needs through the mapping between the functional requirements (FRs) in the functional domain and the design parameters (DPs) in the physical domain, through the proper selection of DPs that satisfy FRs [18].

In Axiomatic design framework; the world of design is made up of four domains: the customer domain, the functional domain, the physical domain, and the process domain. The customer domain is characterized by the attributes (CAs) that the customer is looking for in a product or process or system or materials. In the functional domain, the customer needs are specified in terms of functional requirements (FRs) and constraints (Cs). In order to satisfy the specified FRs, we conceive design parameters (DPs) in the physical domain. Finally, to produce the product specified in terms of DPs, we develop a process that is characterized by process variables (PVs) in the process domain [19].

Axiomatic design methodology is based on two Axioms [19], these two axioms are identified by examining the common elements that are present in a good design:

- The Independence Axiom: maintains the independence of the functional requirements (FRs).
- The Information Axiom: Minimize the information content of the design; this axiom states that among those designs that satisfy the Independence Axiom the design with the smallest information content is the best design.

In summary the Axiomatic Design methodology assumes a relationship between a vector that represents $\{FRs\}$ and another vector that represents $\{DPs\}$ as the following system representation:

$$\{FRs\}=[A]\{DPs\} \qquad \textbf{Equation 2-1}$$

$[A]$ is called the Design Matrix, it is a characterization to the design space. For a 3 FRs and 3 DPs system;

$$\begin{Bmatrix} FR_1 \\ FR_2 \\ FR_3 \end{Bmatrix} = \begin{bmatrix} A_{11} & A_{12} & A_{13} \\ A_{21} & A_{22} & A_{23} \\ A_{31} & A_{32} & A_{33} \end{bmatrix} \begin{Bmatrix} DP_1 \\ DP_2 \\ DP_3 \end{Bmatrix} \qquad \textbf{Equation 2-2}$$

Considering the first axiom, Axiomatic Design calls a system like Equation 2-3's uncoupled design

$$\begin{Bmatrix} FR_1 \\ FR_2 \\ FR_3 \end{Bmatrix} = \begin{bmatrix} A_{11} & 0 & 0 \\ 0 & A_{22} & 0 \\ 0 & 0 & A_{33} \end{bmatrix} \begin{Bmatrix} DP_1 \\ DP_2 \\ DP_3 \end{Bmatrix} \qquad \textbf{Equation 2-3}$$

and a system like Equation 2-4's a decoupled design;

$$\begin{Bmatrix} FR_1 \\ FR_2 \\ FR_3 \end{Bmatrix} = \begin{bmatrix} A_{11} & 0 & 0 \\ A_{21} & A_{22} & 0 \\ A_{31} & A_{32} & A_{33} \end{bmatrix} \begin{Bmatrix} DP_1 \\ DP_2 \\ DP_3 \end{Bmatrix} \qquad \text{Equation 2-4}$$

where, DPs are being determined from the top (DP_1) to the bottom (DP_3), in a sequence.

Axiomatic design assumes that for a system to satisfy the first axiom it has to be uncoupled or decoupled; any other forms of the design matrix are called a coupled design. Axiomatic design considers coupled designs as not robust and cannot survive random variations of DPs and the environment surrounding the design [19].

The matrix representation to the design domain allows coupling relationships between functions and physical components to be developed and system performance to be studied further, as will be shown in Chapter 3.

2.1.2 Design Representation Overview

The purpose of design representation is to provide the semantics and syntax for specifying and manipulating design information [20]. An ordinal mechanical design produces blueprints of a mechanical system which represents shape, size of parts and their configuration. However, the blue prints do not represent the functions of a mechanical system; In other words, it is difficult for a user to identify the functions or designers' intention of each part correctly. Therefore it is very useful to represent all kinds of information of a design systematically [21]. On the other hand, the ability to analyze design behavior under variety of conditions drives the need to model a design analytically to gain feedback on likely or potential behavior before design decisions are made [22].

The design representation discussion brings attention to concepts like function, behavior, structure, state, purpose in the context of product engineering. These concepts has been discussed and define differently by design researchers, [23] [24] [25] [24] [10], Table 2-1 shows a summary of these concepts definitions in the context of design engineering. The majority of the design community accepts the idea that the function domain is a subset of the behavior domain and that the behavior domain can be divided into two main subsets of intended and unintended behavior. Zhang et al [10] summarized the differences in definitions for four design schools, (Table 2-2).

Table 2-1: Summary of concepts definitions related to design engineering framework

	Technical definitions in context of design engineering
Function	The design intent, what the device is designed for, what is performed by an artifact and what an artifact does [23]. The purposes of the design being designed, i.e., its teleology, a description of behavior abstracted by human through recognition of the behavior in order to utilize it [24].
Purpose	The reason why an artifact exists or what it is intended for [25], it defines intentional functions and why an artifact is and does what it does, what the artifact is for [23].
Behavior	Is the manner in which an artifact acts under specified condition; how the artifact does what it does [23]. The set of attributes derivable from structure or expected of structure, sequential in nature, and recognized by changes of state [24]. The response of the system when it receives stimuli [10].
Structure	Is what constitutes an artifact or defines its constitution [23]. Design description represents the artifact’s elements and their relationships [26].
State	Refers to a structure’s state, an instantaneous time representation to the structure [24].

A naïve understanding of conceptual design may lead one to believe that a function perspective of an artifact is adequate; however, any realistic conceptual design review process demands that the designer be able to answer performance questions that arise from secondary characteristics of a design, better known as behavior [22]. Understanding and predicting behavior is the key to creating designs that react with its environment. Behavior, other than intended behavior, is not modeled directly during the conceptual design phase because the focus is on assuring and improving functionality, which is a subset of possible behaviors [22]. As the design progresses to the embodiment phase the behavior and structure of the design start to emerge and if it was well recognized it could play significant role in the performance of the designed system. Combining form, function, and behavior can satisfy all necessary criteria for a representation system [22].

Table 2-2: Different schools of the design modeling; Definitions survey [10]

	American	Japanese	European	Australian
Function	what the device is for	description of behavior abstracted by human through recognition of the behavior	the usefulness of the behavior, perceived by the human user	the thing an artifact performs
Behavior	what the device does	what the device does	a description of the system in terms of its allowable states, the system's variables, and how those variables are related	the manner in which an artifact acts under specified conditions
Structure	what the device is	what the device is	how the behavior is realized.	what constitutes an artifact (or defines its constitution).

The focus of the coming subsections will be on exploring design representation methods. The methods are grouped with commonalities in relation to: functional, behavioral, environmental, physical and user interaction representational models. Some of these methods has reliability modeling integrated to the process which will be explored on the Reliability Engineering overview, section 2.2.

Functional Basis

Functionality is a representation mapping the intrinsic properties of an object in the perceptual and interactive space of an agent. It is characterized as an extension of purposive and active vision, active perception and task-oriented approaches [27].

In the functional basis approach, the designer firstly determines the entire function by analyzing the specifications of the product to be designed and built. He or she then divides the function recursively into sub-functions, a process that produces a functional structure. Secondly, for each divided sub-function, the designer uses a catalog to look up the most appropriate functional element a component or a set of components that perform a function. Finally, he/she composes a design solution from those selected elements [28]. This methodology defines function as the transformation between input and output of energy, material, and information. Although widely accepted, this definition has trouble representing a function that does not transform something [28].

Pahl and Beitz [11] listed five generally valid functions and three types of flow at a very high level of abstraction. Hundal [29] presented a list of six basic function "data base" with more specific subfunctions under every category. After analyzing the functions described in Collins' work [30] and considering consumer products, Fadel et al [31] derived four basic types of functions: Motion, Power/Matter, Control, and Enclosure. Table 2-3 shows a summary of the functions recognized by Pahl & Beitz, Hundal and Fadel et al. (numbers between brackets next to Hundal's functions are the number of subfunctions recognized by him).

Table 2-3: Basic Functions Sets recognized by: Pahl & Beitz, Hundal and Fadel et al.

Pahl & Beitz [11]	Hundal [29]	Fadel et al [31]
Change	Channel (4)	Motion
Vary	Store/Supply (2)	Control
Connect	Connect (13)	Power/Matter
Channel	Branch (5)	Enclose
Store	Change Magnitude (5)	
	Convert (10)	

The functional basis research grew out of various researchers' needs to describe and compare product functionality and to create a formal function representation that would advance design methods and lead to repeatable models [32]. In 2002, Stone, Hirtz, Szykman, Wood & McAdams [32], through funding from the NIST, collaborated to review and reconcile the previous functional basis effort developed by NIST teams. The new reconciled functional basis, resulting from the comparison and combination of the NIST taxonomy and functional basis was called Reconciled Functional Basis, shown in Table 2-4 to Table 2-6.

The reconciled flow set in Table 2-4 contains three class primary flows: material, signal and energy. The material level has five further specified secondary categories with an expanded list of tertiary categories. The signal class has two further specified secondary categories with an expanded list of tertiary categories. The energy class has 13 further specified secondary categories with an expanded list of tertiary categories; Table 2-5 is a more specific breakdown of the Energy class. To achieve more detail when specifying product information, the power conjugate complements of effort and flow can be used [32]. The reconciled functional basis taxonomy will be adopted for modeling systems' functional structures in this MDRV research work.

Table 2-4: Functional basis reconciled flow set [32]

Class (Primary)	Secondary	Tertiary	Correspondents
Material	Human		Hand, foot, head
	Gas		Homogeneous
	Liquid		Incompressible, compressible, homogeneous
	Solid	Object	Rigid-body, elastic-body, widget
		Particulate	
		Composite	
	Plasma		
	Mixture	Gas-gas	
		Liquid-liquid	
		Solid-solid	Aggregate
		Solid-Liquid	
		Liquid-Gas	
		Solid-Gas	
		Solid-Liquid-Gas	
		Colloidal	Aerosol
Signal	Status	Auditory	Tone, word
		Olfactory	
		Tactile	Temperature, pressure, roughness
		Taste	
		Visual	Position, displacement
	Control	Analog	Oscillatory
		Discrete	Binary
Energy	Human		
	Acoustic		
	Biological		
	Chemical		
	Electrical		
	Electromagnetic	Optical	
		Solar	
	Hydraulic		
	Magnetic		
	Mechanical	Rotational	
		Translational	
	Pneumatic		
	Radioactive/Nuclear		
	Thermal		

→ overall increasing degree of specification

Table 2-5: Power conjugate complements for the energy class of flows [32]

Class (Primary)	Secondary	Tertiary	Power conjugate complements	
			Effort analogy	Flow analogy
Energy			Effort	Flow
	Human		Force	Velocity
	Acoustic		Pressure	Particle velocity
	Biological		Pressure	Volumetric flow
	Chemical		Affinity	Reaction rate
	Electrical		Electromotive force	Current
	Electromagnetic		Effort	Flow
		Optical	Intensity	Velocity
		Solar	Intensity	Velocity
	Hydraulic		Pressure	Volumetric flow
	Magnetic		Magnetomotive force	Magnetic flux rate
	Mechanical		Effort	Flow
		Rotational	Torque	Angular velocity
		Translational	Force	Linear velocity
	Pneumatic		Pressure	Mass flow
	Radioactive/Nuclear		Intensity	Decay rate
	Thermal		Temperature	Heat flow

Table 2-6: Functional basis reconciled function set [32]

Class (Primary)	Secondary	Tertiary	Correspondents
Branch	Separate		Isolate, sever, disjoin
		Divide	Detach, isolate, release, sort, split, disconnect, subtract
		Extract	Refine, filter, purify, percolate, strain, clear
		Remove	Cut, drill, lathe, polish, sand
	Distribute		Diffuse, dispel, disperse, dissipate, diverge, scatter
Channel	Import		Form entrance, allow, input, capture
	Export		Dispose, eject, emit, empty, remove, destroy, eliminate
	Transfer		Carry, deliver
		Transport	Advance, lift, move
		Transmit	Conduct, convey
	Guide		Direct, shift, steer, straighten, switch
		Translate	Move, relocate
		Rotate	Spin, turn
		Allow DOF	Constrain, unfasten, unlock
Connect	Couple		Associate, connect
		Join	Assemble, fasten
		Link	Attach
	Mix		Add, blend, coalesce, combine, pack
Control Magnitude	Actuate		Enable, initiate, start, turn-on
	Regulate		Control, equalize, limit, maintain
		Increase	Allow, open
		Decrease	Close, delay, interrupt
	Change		Adjust, modulate, clear, demodulate, invert, normalize, rectify, reset, scale, vary, modify
		Increment	Amplify, enhance, magnify, multiply
		Decrement	Attenuate, dampen, reduce
		Shape	Compact, compress, crush, pierce, deform, form
		Condition	Prepare, adapt, treat
	Stop		End, halt, pause, interrupt, restrain
		Prevent	Disable, turn-off
		Inhibit	Shield, insulate, protect, resist
Convert	Convert		Condense, create, decode, differentiate, digitize, encode, evaporate, generate, integrate, liquefy, process, solidify, transform
Provision	Store		Accumulate
		Contain	Capture, enclose
		Collect	Absorb, consume, fill, reserve
	Supply		Provide, replenish, retrieve
Signal	Sense		Feel, determine
		Detect	Discern, perceive, recognize
		Measure	Identify, locate
	Indicate		Announce, show, denote, record, register
		Track	Mark, time
		Display	Emit, expose, select
	Process		Compare, calculate, check
Support	Stabilize		Steady
	Secure		Constrain, hold, place, fix
	Position		Align, locate, orient
	→	overall increasing degree of specification	

Function & Behavior Modeling

Karnopp and Rosenberg [33] developed the foundation of behavior-based representation with bond graphs [22]. Morten Lind [34] developed the Multilevel Flow Modeling for the representation of goals and functions of complex process plants. In Lind's MFM, functions represent roles a plant subsystem plays in achieving system goal. Multilevel Flow Modeling represents a system as an artifact i.e. as a man-made purposeful system. Plant functions are represented by a set of mass energy, activity and information flow structures on several levels of abstraction. MFM represents a system along two dimensions, functions goals and physical components. Functions in MFM describe organizational aspects and not behavioral aspects of the system [34].

The Goal Tree Success Tree Master Plant Logic Diagram (GTST-MLD) process, developed by Modarres [35] is a hybrid of a hieratical Goal Tree Success Tree and a Master Logic Diagram. While Goal Tress Success Tree represents the functionality of system starting with functional objective at the top, Master Logic Diagram represents the interrelationship between the components of the system, see Figure 2-4

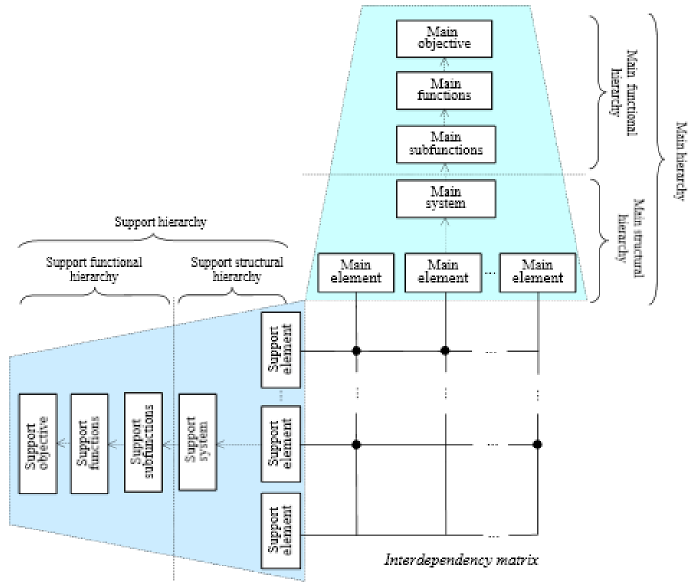

Figure 2-4: A combined GTST-MLD framework, Modarres & Cheon [36]

Modarres [35], [36] framework is a functional decomposition used to describe and model complex physical systems in terms of objects, relationships, and qualities through GTST diagram. The process views the functional hierarchy as the central backbone of the system model describing the system's state-time behavior [36], all other hierarchies can be defined with respect to their relation to the functional hierarchy, see Figure 2-5.

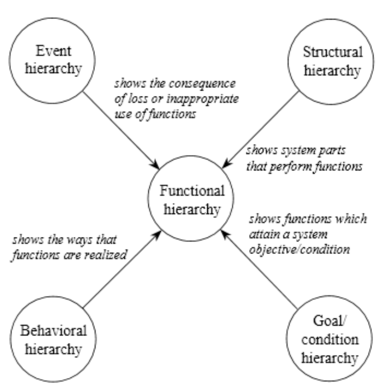

Figure 2-5: Function-centered system description, Modarres & Cheon [36]

Modarres and Cheon [36] demonstrated GTST capabilities to capture system dynamic behavior through conservation laws, where potential behaviors (intended and unintended) for a system in terms of the behavior of its subordinates, consistent with conservation laws, can be developed and used in functional modeling.

Smith and Clarkson [37] developed a method that combines entity-relationship diagrams to describe design concepts through functional decomposition. This method, hierarchically, describes the requirements those concepts satisfy; the description is then analyzed for potential failures through: 1) aspects of the concept that would generate detrimental effects, 2) aspects that would transfer that effect, and 3) aspects that would be affected. Smith and Clarkson [37] adopted Rosenman & Gero's definition for Function, Behavior and Purpose, they used what they referred to as Group Diagram or Entity-Relationship Diagram to represent groups graphically; Figure 2-6 shows a group diagram for two entities; the authors, graphically, presented the interrelationships between group entities, see Figure 2-7. Figure 2-8 shows a brake system control case study developed by Smith and Clarkson [37].

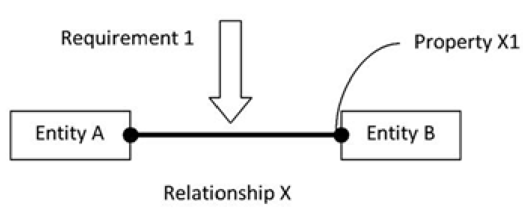

Figure 2-6: Group Diagram [37]

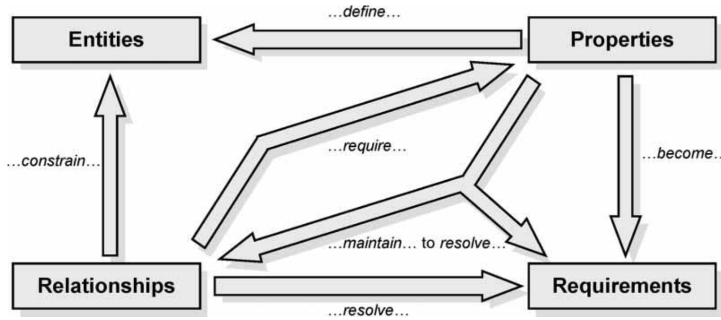

Figure 2-7: Group Entities and the links between them per Smith & Clarkson [37]

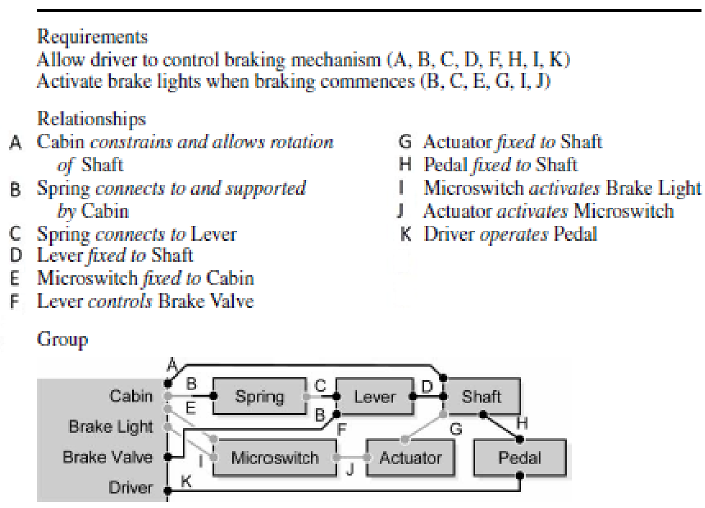

Figure 2-8: Brake System Control, developed by Smith & Clarkson [37]

Function & Behavior Modeling: Environment Perspective

Deng et al [38] expanded the function-behavior-Structure model to include environment representation based on the concept of causal process description from functional representation theory [39] and Umeda et al's physical phenomenon technique of behavior representation [40]; they [38] identified two kinds of relationships between the design and its environmental elements: geometric relation and physical interaction.

Geometric relation refers to the assembly or connection style between the design and its environmental elements. Physical interaction refers to the situation where the source environmental elements provide input actions to the design and the design generates output actions to target environmental elements. Deng et al [38] focused on modeling only intended behavior by using input-output flow of actions to represent both the overall intended behavior of the design, as well as any of its sub-behaviors. Behavior was represented by a set of driving inputs (required physical interactions from its source environment to the design), and a set of functional outputs (desired physical interactions from the design to its target environment).

Function & Behavior Modeling, User Perspective

Operator interaction with an engineering system affects the durability and reliability of the system significantly. Trained and experienced users tend to efficiently operate that system, prolong its life and have reasonable expectations about its performance. Operator interaction with an engineering system represents one of the environmental inputs to that system; hence identifying these inputs is critical to the performance, operability and reliability of that system. Mitchell [41] proposed an Operator Function Model (OFM) that is “dynamic and analytic”. A dynamic representation requires that operators activities be modeled within the context of changing system state and analytic representation is one that can be easily coded into software and readily used to characterize the semantics a user interface, operator aid or tutor requires [42]. The OFM is a hierarchic network of nodes connected together, where nodes in the top specify the major operator functions and nodes at the bottom define operator actions; Figure 2-9 shows a generic OFM network [42]. Top functions are decomposed into subfunctions and subfunctions are decomposed into tasks and tasks are decomposed into actions. The number of subfunctions level in the OFM varies based on the application. The arcs in the model connecting nodes at the same level represent system triggering events or the successful completion of operator activity. Arcs can be thought of as both pre-conditions and initiating events. Hierarchically, arcs often define the expected temporal flow of control activity in a dynamic system [42].

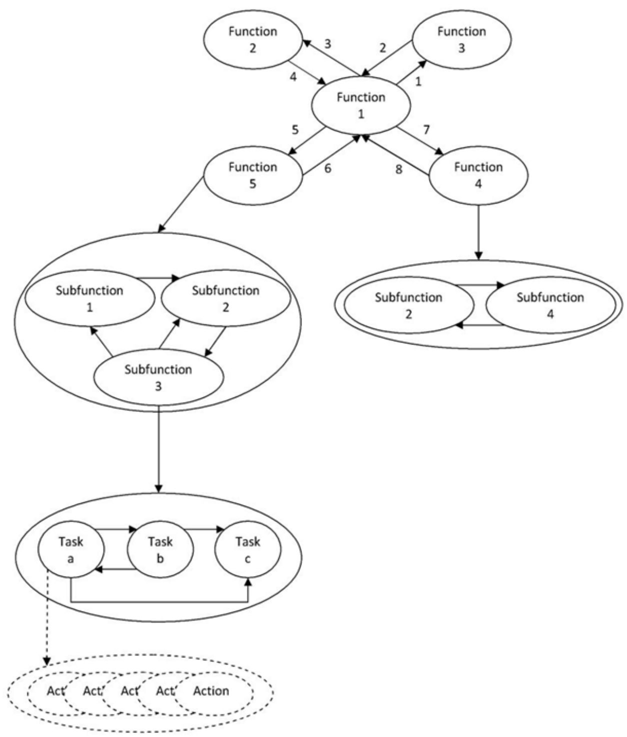

Figure 2-9: Generic OFM Network [42]

Assembly Interaction Modeling

Suh's Axiomatic Design methodology has an implicit assembly representation through design matrix. His method, as discussed in 0, provides a matrix presentation that links the system components (design parameters vector) to design functions (functional requirements vector); this representation provides the functional interrelationships between the components but not the physical one.

$$\begin{Bmatrix} FR_1 \\ FR_2 \\ FR_3 \end{Bmatrix} = \begin{bmatrix} A_{11} & A_{12} & A_{13} \\ A_{21} & A_{22} & A_{23} \\ A_{31} & A_{32} & A_{33} \end{bmatrix} \begin{Bmatrix} DP_1 \\ DP_2 \\ DP_3 \end{Bmatrix}$$

Equation 2-5

McAdams et al. [14] presented a process to characterize the structural and flow interactions between artifacts in a product; the representation generated was called: “assembly model”. They identified four types of structural interactions: Couple, Secure, Position and Guide. Their proposed modeling process allows flow interactions to be represented. Their methodology recognizes two types of functionalities delivered by artifacts within a system: conceptual functionality and supporting functionality. Artifacts that are capable of directly solving the functions described by the product’s functional model have conceptual functionality; artifacts that do not directly solve the main functionality of the product but support the delivery of the conceptual functionality have supporting functionality; example to supporting functionality are threaded fasteners. Supporting functionalities are important enough that without them the overall product functionality might not be achieved. The assembly model graphically depicts all connections that exist between product artifacts and classifies each connection using functional terms defined in the Functional Basis [32]”. Figure 2-10 and Figure 2-11 show McAdams et al structural connection representations and an assembly model as an example on how they get implemented to model flow and structural connections between artifacts components of a vegetable peeler.

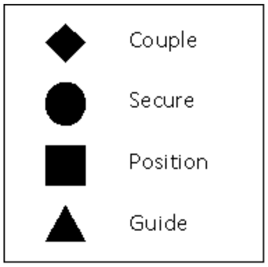

Figure 2-10: McAdams et al. [14] Assembly Model representation for structural connections, see next figure for an example

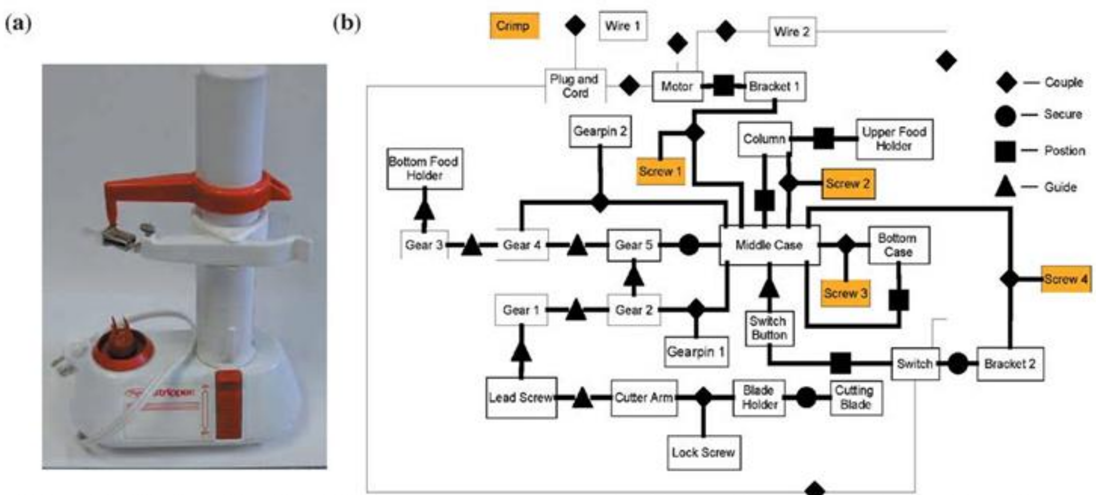

Figure 2: ***(a)*** *The Dazey Vegetable Peeler was reverse engineered to produce the assembly model shown.* ***(b)*** *Assembly model constructed for the Dazey vegetable peeler. Boxes represent individual product artifacts. Energy flow interactions are represented by regular line connections, material flow interactions by bold lines, and signal flow interactions by dashed lines. The four symbols overlaid on the flow connections represent the structural interactions (supporting functionality) between the connected artifacts.*

Figure 2-11: Vegetable Peeler Assembly Model; as represented by McAdams et al [14];

Interactions between artifacts are denoted by lines: single weighted lines for energy domain connections, bold lines for material domain connections, and dashed lines for signal domain connections. The four structural type connections: couple, secure, position and guide, have special symbols presented on the upper right side of the picture.

2.2 Reliability Engineering

Reliability engineering is the science of designing products and processes to be reliable [43] To ensure their products have sufficient level of reliability, modern engineering organizations assess the reliability of their new products during the design phase (Reliability Prediction) and test it during the prototype validation and verification phase (Reliability Testing); Service and maintenance plans are also developed for on-service products to prolong their life and reduce the customer dissatisfaction due to failure incidents (Reliability Monitoring).

Most of the methodologies available for reliability assessment were originally developed for electrical and electronic systems; for such systems, it is relatively easier to perform repetitive tests to produce many failure samples in a fairly short period of time [44]. In contrast to electronic systems there are usually no abrupt failures in mechanical systems, for which degradation processes leading to failure happen on a slower time scale [44]. Due to the above mentioned definition and practices of reliability; the science of reliability engineering has been strongly tied to the statistics and probability theory.

In this section the available reliability-during- design processes and frameworks were reviewed and summarized.

2.2.1 Reliability Evaluation in Product Design Phase

Reliability of a product is directly related to the probability of product failure events as presented by Equation 2-6;

$$R(t) = 1 - F(t) \qquad \textbf{Equation 2-6}$$

where; $R(t) \equiv$ the reliability of a product at a specific time (t)

$F(t) \equiv$ the probability of failure at that time.

When failure analysis and prevention are coupled with product's design from its conception, potentially shorter design times and fewer redesigns are necessary to arrive at a final product design [45]. Techniques used to improve reliability can be categorized as data-oriented and designer-oriented methods. Data-oriented methods are statistical and make reliability a mathematical function; designer-oriented methods are not concerned with calculating reliability, but with improving it by finding faults in the design [37]. While methods like Fault Tree, Failure Modes and Effects Analysis (FMEA) can be used during conceptual design, they are usually applied later when more detail of the embodiment design is known [37].

Currently Failure Modes and Effect Analysis (FMEA), Fault Tree Analysis and Fault Tree (FTA) and Failure Modes and Effects Criticality Analysis (FMECA) are the most popular methods to identify the potential failure modes during the design phase of engineered products. These methods identify the failure modes during the design phase but do not provide a solution to how the failure risk can be managed. FMEA and FMECA also do not provide failure analysis on the system level. Traditional FMEA needs a systematic approach capable of capturing a wider range of failure modes, applicable early in the design stage [46]. FTA (fault tree analysis) performs the reverse. It starts with an undesirable top event and isolates possible causes at each successive lower level of the hierarchy in order to establish the prime cause(s). FTA is more powerful in the sense that it forces the designers to consider all the causes of unacceptable top events [47]. However, the analysis is not pursued far enough, and the prime causes are not revealed [48]. Although a well-accepted technique, large system-level fault trees are often difficult to understand, and to build due to the complex logic involved [49]. The weakness of both FMEA and FTA is that the basic sources of unacceptable behavior cannot be identified [48].

Assessing and analyzing the reliability of a system during the design conception phase prolongs the design duration but it produce initial reliability estimates and highlights design parameters critical to reliability which can be improved and/or optimized to save more time and cost later on, during the product validation and verification phase of the product development process [12], [13], [14], [15].

When the above mentioned reliability assessment tools and processes are used in concurrency with design tools, the process would be called design for reliability (DFR). According to MIL-HDBK-338B [50]: Design for reliability is the process of selecting a part or material and applying it in such a manner that results in high reliability under the worst case actual use conditions. Such an effort requires a structured approach during the part selection and design process. This process should include:

1) Definition of operating environments
2) Establishment of lifetime requirements
3) Use of reliability models to estimate lifetime under use conditions
4) Estimates of reliability during the useful life
5) Stress derating
6) Analysis and design modifications to ensure robustness

Dieter and Schmidt [9] summarized the steps for integrating reliability in design as shown in Table 2-7; the design for reliability process starts at the conceptual design and continues to production and data feedback during service.

Table 2-7: Reliability activities throughout design, production and service [9]

Design Stage	Design Activity
Conceptual design	Problem definition: Estimate reliability requirement Determine likely service environment
Embodiment design	Configuration design: Investigate redundancy Provide accessibility for maintenance Parametric Design: Select highly reliable components Build and test physical and computer prototypes Full environment tests Establish failure modes/ FMEA Estimate MTBF User trials/modifications
Detail design	Produce & test preproduction prototypes Final estimate of reliability
Production	Production models: Further environment tests Establish quality assurance program
Service	Deliver to customer: Feedback field failures and MTBFs to designers Repair and replace Retirement from service

Functional Design and Reliability Assessment

A reliability method that is specifically tailored to conceptual design and is commensurate with the type of information available during conceptual design would be valuable as an effective means of augmenting the set of tools available to the designer [51] [37]. Conceptual reliability is concerned with the reduction of conceptual failures, failures committed to during conceptual design; i.e. less design effort will be necessary to ensure reliability during the detailed stages of design if the design's concept is conceptually reliable. [37].

Reliability of a system has always been related to probability of failure and the failure rate of its subsystems and components. Tumer and Stone [52] developed theoretical foundations of a matrix-based approach to derive similarities that exist between different failure modes, by mapping system failures to functionality of each system component. The function-failure method is proposed to design new products with solutions for functions that eliminate or reduce the potential of a failure mode. Their method builds on the knowledge developed about a product through functionality modeling and links failure modes to system sub-functions. The method helps when designing or redesigning components or sub-functions for a system by offering failure modes to guard against during the design phase. According to Tumer and Stone [47] components have a "commonality" they share at some basic level in terms of their functionality and failure modes, this basic level of commonality is explored by decomposing the knowledge about functionality and failures via matrix manipulations.

Smith and Clarkson [37] developed a method that combines entity-relationship diagrams, see section 0, to describe design concepts with functional decomposition to describe the requirements those concepts satisfy. The description is then analyzed for potential failures through

1. aspects of the concept that would generate detrimental effects
2. aspects that would transfer that effect
3. aspects that would be affected

The conceptual reliability method by Smith and Clarkson [37] consists of a representation and analysis method. The representation provides the designer with a language to describe the commitments made by the concept under analysis. The analysis method allows the description to be analyzed so as to reveal potential reliability problems. Smith and Clarkson [37] categorized two types of conceptual failures: functional errors and behavioral errors; (see Figure 2-12). Functional errors occur when the functions chosen do not fulfill the product's purpose; behavioral errors occur when the behavior realized does not fulfill the associated product function. According to Smith and Clarkson [37] functional error occurs when the functional specification or requirements developed for the product do not address the whole problem; behavioral error occurs when the detailed design fails to accomplish one of its functions due to inadequate product performance [37]. This categorization of error looks at consequence, and not concerned with its cause. After the design has been described as a group, it can be analyzed to determine how its conceptual reliability can be improved; potential failures are also revealed and if they are serious, then an attempt is made to eliminate them [37].

Figure 2-12: Functional and behavioral failure per Smith and Clarkson [37]

This method is similar to the functional design method [11] that analyzes the flow of energy, material and information to determine the extent to which this transfer could generate detrimental effects. The distinction between the two approaches is related to the method by which the design is represented. Smith and Clarkson [37] method uses relationships that doesn't need transfers, whereas Pahl and Beitz's [11] functional modeling relationships are based on energy, materials and information transfer. Additionally, Smith and Clarkson [37] method emphasizes the interrelationships between requirements and design concepts, as well as the development of requirements, while these are only implicit in the transfer-oriented functional methods [37]. Smith and Clarkson [37] concluded that they developed a method to describe the design through a language used to represent a concept and a simple analysis technique applied to the representation in order to reveal potential reliability issues. They concluded that the method is limited by its bias towards conceptual design and the language used to describe the concepts. Although the method has a degree of formality, it still relies on users' understanding of the design concept and therefore not considered suitable for automation.

Ormon et al. [53] developed a generic simulation model for predicting system reliability without knowing the exact failure rate for the components in the system; the simulation model estimates mission reliability, average time to failure for the system, and average mission cost. Triangular distribution parameters for components with unknown failure rates, mission length, and component and mission costs were used. The process is similar to conventional reliability assessment tools; it uses minimum, maximum and most likely value for failure rate probability. A triangular probability distribution is used where probability of failure is zero at minimum and maximum possible values and 50% at the most likely failure rate. Ormon et al [54] elaborated on their simulation based model and included an analytical solution. They provided three general procedure; using both simulation and analytic solution techniques for predicting system reliability and average mission cost; the three solution options are:

- Simulation-based:
    1. Component level simulation analysis: this method assesses the failure rate and time to failure for components that do not have known failure rates using inverse transformation method [55];
    2. Subsystem level simulation analysis: If the failure rate for a subsystem is known or has been generated from the triangular probability density function, then subsystem reliability can be computed directly.
- Analytical-based:
    1. Analytic prediction model: The analytic solution is achieved by modeling the system at the subsystem level, and using conditional probability when the subsystem failure rate is unknown; a PDF of the failure rate for components in subsystem could be established using the triangular distribution of the minimum, mode and maximum estimates on the failure rate from expert assessment.

Ormon et al [54] concludes, “the analytic approach is superior to the simulation-based prediction models”

Tumer et al. [56] introduced a system-level reliability analysis method for assessing the dependability of alternative conceptual design architectures. The method enables the analysis of criticality and sensitivity of components to system-level requirements. Based on component connections and their failure probability; they developed a directed representation called Configuration Graph (CG); they made following assumptions for their method:

1. component fails independently of each other
2. inputs of any components are from different sources
3. the function provided by a component fails if any of its inputs fails or the component fails
4. the function of a serial connector fails if any of its inputs fails
5. the function of a parallel connector fails if all its inputs fail

A component fails to function correctly either because it has failed or because it has an input that has failed; their system modeling [56] approach is similar to several existing reliability modeling techniques, like FTA and RBD, but differ in the technique used, while FTA and RBD are hierarchical in their structure, CG is an acyclic graph that defines the component connectivity from sources to sinks. There was no clear definition to what is a source or a sink in their framework. Their methodology did not specify the source of connectivity between components; they have used electrical power system schematic to develop the interrelationship between components without mentioning whether the schematic is a functional, behavioral or physical. Physics of failure representation or modeling does not exist in this method.

Avontuur & Werff [15] developed an automated reliability analysis method during the conceptual design phase of drive trains used in infrastructure works such as movable bridges, lock gates and storm surge barriers; what they considered a conceptual phase would include high level of embodiment design in a CAD environment. This automated technique relies on finite element equations for the analysis of structures. Their process decomposes the drive train into two main functions; carrying loads and executing motion. Finite elements theory was adapted to describe these two functions. The function "carrying load" is expressed through the following equations systems [15]:

$$\mathrm{D}^{\mathrm{T}} \cdot \underline{\sigma} = \underline{f} \qquad \textbf{Equation 2-7}$$

where $\underline{f}$ represents the external loads and $\underline{\sigma}$ the internal element stresses. The function "executing motion" is expressed with the following equations system [15]:

$$\underline{\epsilon} = \mathrm{D} \cdot \underline{u} \qquad \textbf{Equation 2-8}$$

where $\underline{u}$ represents the nodal displacement and $\underline{\epsilon}$ the element deformation.

A zero element stress represents a failure mode for an element that might fail to fulfill the function carrying load because it is broken. A zero element deformation represents a failure mode of an element that might fail to fulfill the function executing motion if it is blocked; The vector $\underline{\sigma}_0 = 0$ represents the prescribed elemental stresses of the failed elements.

$$\mathrm{D}_{\mathrm{cc}}^{\mathrm{T}} \cdot \underline{\sigma}_{\mathrm{c}} = \underline{f_c} - \mathrm{D}_{0\mathrm{c}}^{\mathrm{T}} \cdot \underline{\sigma}_0 \qquad \textbf{Equation 2-9}$$

$$\begin{pmatrix} \mathrm{D}_{cc} \\ \mathrm{D}_{0\mathrm{c,prescribed}} \end{pmatrix} \left(\underline{u}_c\right) = \begin{pmatrix} 0 - \mathrm{D}_{c0} \cdot \underline{u}_0 \\ 0 - \mathrm{D}_{00,\mathrm{prescribed}} \cdot \underline{u}_0 \end{pmatrix} \qquad \textbf{Equation 2-10}$$

The matrices $\mathbf{D}_{0\mathrm{c,prescribed}}$ and $\mathbf{D}_{00,\mathrm{prescribed}}$ are sub-matrices of $\mathbf{D}_0$ corresponding with failing deformations, that are prescribed to be zero [15]. The formulation presented above was used by Avontuur & Werff [15] to express the failure state of the drive train system components; i.e. when it is not possible to find a permissible stress distribution $\underline{\sigma}_c$, or kinematical permissible displacement field $\underline{u}_c$; the combination of failing components is a failure mode. All failure modes are found by trying all combinations; the structure fails, when the above system of equations cannot be solved for the prescribed loads and displacements, an unsolvable set of equations is the mathematical representation of a failing drive train [15]. The theory presented above was implemented by Avontuur & Werff to in an algorithm that finds the minimal cut sets of a fault tree by trying all combinations of failing elemental deformations and stresses; they [15] also outlined the following design steps for their process algorithm:

1. The designer creates design concepts and defines functions of the structure
2. He decomposes these functions into the basic functions carrying load and executing motion
3. The software helps the designer to build a component model of the design concepts; for each function a separate model is necessary.
4. The software translated the component model into a finite element model; generates the minimal cut sets of the fault tress and quantifies the fault tree.

Avontuur & Werff [15] process could work at a design phase where component failure modes and rates were identified; the process allows the automation of creating fault tree cut sets.

The Master Logic Diagram section of the GTST-MLD framework presented by Modarres [35], (in section 0), shows the interrelationships among the independent functions (or systems) and the independent support functions, the MLD, in success space, can show the manner in which various functions, subfunctions and hardware interact to achieve the overall system objective, on the other hand, an MLD (in failure space) can show the logical representation of the causes for failure of functions (or systems). The MLD (in success or failure space) can easily map the propagation of the effect of failure, i.e. establish the trajectories of event failure propagation. The analysis of the MLD is straightforward; using a combinatorial approach or Boolean reduction method one can provide an assessment to system reliability [57], similar to the typical Fault Tree Analysis method. The reliability process of GTST-MLD is limited to static reliability, reliability is not presented as a function in time; the process also doesn't support quantitative physics of failure model or prime causal representation.

Axiomatic Design and Reliability Assessment

Trewn and Yang [58] developed a procedure to assess system functional reliability; they defined functional reliability as the likelihood of successfully providing necessary functions that a system or a component is intended to deliver. Their intent was to lay the foundations for reliability improvement in the conceptual design phase. Trewn and Yang procedure is based on leveraging the Axiomatic Design approach to map functional requirements {FRs} to {DPs} through the equation:

$$\{FRs\}=[A]\{DPs\} \qquad \textbf{Equation 2-11}$$

where: $[A]\equiv$ Design matrix that maps functional requirements to design parameters

Trewn and Yang expanded Equation 2-11to:

$$\{FRs\}=[A]\{DPs\}=[A]^{\circ}[B]\{SS\} = [D]\{SS\} \qquad \textbf{Equation 2-12}$$

where: $[A]\equiv$ Design matrix that maps functional requirements to design parameters

[B]≡ Design matrix that maps components to design parameters;

$b_{jk}\equiv$ element of the matrix [B] that maps the kth component to the jth design parameter. The element b_{jk} is binary, 0 = no relationship and 1 = related

$\{SS\}\equiv$ component space vector

$[D] = [A]°[B]\equiv$ Design matrix that maps FRs to components space vector

Trewn and Yang [58] defined system functional reliability by the following equation:

$$R_s = \prod_{i=1}^{m} P(FR_i) \qquad \textbf{Equation 2-13}$$

where: $P(FR_i)$ is the probability that FR_i is successfully delivered and

$$P(FR_i) = \prod_{k=1}^{n} (1 - P_k)^{d_{ik}} \qquad \textbf{Equation 2-14}$$

where: d_{ik} ≡ entry of D matrix in ith row and kth column

P_k ≡ failure probability of component k

Trewn and Yang [58] concluded that the system functional reliability would be represented through the following model:

$$R_s = \prod_{i=1}^{m} \prod_{k=1}^{n} (1 - P_k)^{d_{ik}} \qquad \textbf{Equation 2-15}$$

where:$R_s\equiv$ the reliability of the subfunction under assessment

Trewn and Yang [58] procedure provides a good organizational framework, especially for multifunctional systems; to represent the system components and their contribution in delivering the required system functions. The process is limited to series system and does not have a behavioral or PoF representation.

Citti et al. [59], by leveraging the knowledge developed about a system through the Axiomatic Design method, developed what they called an Axiomatic Design for Reliability process. The process follows a functional and physical system breakdown to identify all subsystems and element components. By doing a reliability estimation to elementary components they can build what they called a Reliability Matrix. Citti et al [59] defined Reliability Matrix as a matrix that couples FRs and DPs through the reliability of components to achieve the FRs. To find out if each of the Reliability Matrix elements would be an "R" or a "0", a question would need to be answered: "Does the probability of satisfying the function i- (FR_i) depend on the reliability of the component j- (DP_j)?"; (R_{ij}) shows the reliability value of the component (j) in relation to the function (i).

$$\{FRs\} = [R]\{DPs\} \qquad \textbf{Equation 2-16}$$

where [R] is the reliability matrix.

The contribution of each component to the reliability function can be assessed for each row (neglecting the "0"s) through the equations:

$$R_{Series} = \prod_{i=1}^{n} R_i \qquad \textbf{Equation 2-17}$$

$$R_{Parallel} = 1 - \prod_{i=1}^{n} (1 - R_i) \qquad \textbf{Equation 2-18}$$

Citti et al. mentioned that the Reliability Matrix [R] should capture all the correlations that existed in the Design Matrix [A] beside other correlations that reflects the reliability interrelationships between FRs and DPs; that is, because the failure of a component, even when it is not directly involved in performing a function may prevent that function from being achieved [59]. Citti et al [59] representation provides a qualitative and quantitative representation to the reliability of the design space; the procedure separates the design domain from the reliability performance; it leverages expert's knowledge to develop the reliability matrix but does not provide a systematic methodology to map the design matrix to the reliability matrix.

2.3 Mechanical Systems Failure Models and Damage Theory

In context of engineered system usage, failures are the result of the existence of source challenges and conditions occurring in a particular scenario, the system has an inherent capacity to withstand such challenges, which capacity may be reduced by specific internal or external conditions; when challenges surpass the capacity of the system, a failure may occur [57]. Many failure models that address this perspective exist, Pecht and Dashgupta [60] summarized them in the list below:

- *Stress-Strength Model*: for this model, an item would fail if and only if the challenge (i.e stress) exceeds the capacity (i.e. strength); an example to this model is the yielding of a steel bar when its exposed to tensile loading and a transistor with voltage applied across the emitter-collector.
- *Damage-Endurance Model*: for this model the challenge (i.e. stress) causes damage that accumulates irreversibly. The aggregate of challenges and external conditions leads to the metric represented as cumulative damage. The item fails when and only when the cumulative damage exceeds the item damage endurance. This is the most suitable framework to model mechanical failure modes (Table 3-1) such as mechanical fatigue, corrosion, wear, and metal embrittlement.
- *Challenge-Response Model*: for this model a system element would fail the system when it's challenged (needed) and doesn't perform the response (requirement) expected; an example to this model is the emergency brake of a car, telephone switching and most computer software failures.

- *Tolerance-Requirements Model*: for this model system performance characteristic is satisfactory if and only if it fails within acceptable tolerance limits. Example of this is a copier machine and instrument where gradual degradation eventually results in a user deciding that performance quality is unacceptable.

The Damage-Endurance Model explicitly highlights the process of system degradation due to usage over time. With some modifications, the Stress-Strength and Challenge-Response models, as related to mechanical systems, can be absorbed in this model. The Tolerance-Requirement Model is a system level failure model and unique as related to PoF approach; the Tolerance-Endurance Model is not in the focus of this research.

The word degradation and damage have, sometimes, been synonymously used in the literature of failure modeling; with degradation seen an unobservable abstract that triggers failure upon hitting a threshold and with the observables such as crack growth seen as manifestations of damage, Singpurwalla [61] proposed a generalized framework that treats the former as the cumulative hazard and the latter as a covariate or a marker that influences the former; considering that the covariates and markers are influential variables that are precursors to failure; Markers are often a function of time and as such are best described by stochastic process models, namely by marker processes.

Degradation is regarded as the irreversible accumulation of damage throughout life that ultimately leads to failure [62]. Whereas the term “damage” itself is not defined, it is claimed that damage manifests as corrosion, cracks, physical wear (i.e. the depletion of material), etc [61]. Degradation and damage are abstract constructs, used to predict the life of engineered systems.

Considering the process of fatigue damage accumulation, several cumulative fatigue damage models exist. Palmegran-Miner damage theory is a linear damage rule (LDR) and the most popular due to its simplified linearity where the accumulated damage is modeled as: $D = \sum n_i / N_{f_i}$ where D denotes the damage and n_i and N_{f_i} are the applied cycles and the total cycles to failure; the main deficiency with LDR are its load level independence, load sequence independence and lack of load interaction accountability [63]. To remedy the deficiencies associated with LDR, Richart and Newmark [64] introduced the concept of damage curve (D-r diagram), $(r = n/N_f)$, and speculated that the D-r curves ought to be different at different stress levels; Marco and Starkey [65] used the D-r curve to propose the first nonlinear load-dependent damage theory represented by a power relationship, $D = \sum r_i^{x_i}$ where x_i is a variable quantity related to the ith loading level; Miner's rule is a special case of this model with $x_i = 1$. On the other hand, the concept of change in endurance limit due to prestress exerted an important influence on subsequent cumulative fatigue damage research [63]. Kommers [66] and Bennett [67] further investigated the effect of fatigue prestressing on endurance properties using a two-level step loading method; their experimental results suggested that the reduction in endurance strength should be used as a damage measure but they did not correlate this damage parameter to the life fraction [63], this kind of correlation was first deduced by Henry [68] and later by Gatts [69] [70] and Bluhm [71]. All of the damage models based on endurance limit reduction are nonlinear and able to account for the load sequence effect. None of these models however take into account load interaction effects [63]. Fatemi and Yang [63] summarized more than 50 fatigue damage models proposed since Palmgren damage accumulation concept and Miner's LDR were introduced; they highlighted six major categories in cumulative fatigue damage modeling exist:

1. Linear damage evolution and linear summation
2. Nonlinear damage curve and two-stage linearization approaches
3. Life curve modifications to account for load interactions
4. Approaches based on crack growth concept
5. Models based on Continuum Damage Mechanics (CDM)
6. Energy-based methods

The applicability of each model varies from case to case. Consequently, the Palmegren-Miner LDR is still dominantly used in design, inspite of its shortcomings [63].

2.4 Summary of Reliability Integration within Design Processes

In this section, design methodologies were reviewed with more emphasis on Systematic Design and Axiomatic Design. Systematic design methodology presents a streamlined design process; it explicitly identifies the phases of design going from: conceptual, embodiment to detailed design; its use for functional structures give the design a graphical representation and a structure to study the flow of energy, material and signal to visualize how the design main function is delivered. On the other hand Axiomatic design is concerned with the design as an entity and how that entity can optimally be designed; it has the capability to develop a naïve mathematical representation to realize the interrelationships between functional requirements and design parameters.

Developing a design integrated reliability process has been the focus for many who are working in the design and reliability engineering fields. Reliability is one of the design process goals; other goals like: safety, manufacturability, maintenance, quality…etc. also require focus to meet the customer expectations. The taxonomy of the design research although precise to describe the design contextual entities yet generic to capture those mentioned goals. The literature review of design-integrated mechanistic-based reliability engineering methods reveals the following:

1) The physics-based (or mechanistic-based) reliability models have proven to be the most comprehensive representation, capable of bringing many influential factors into the life and reliability models of the components [44].
2) History search into the design representation and its usage in reliability modeling revealed that functional representation is the dominating design representation methodology; behavioral modeling and a mechanistic integrated design process does not exist, see Table 2-8.
3) Direct assembly representation and reliability integrated process that captures the physical interactions or interrelationships between components does not exist either, see Table 2-8.

Table 2-8 shows a summary list of available design integrated reliability assessment processes. The framework developed through this research intends to bridge the gaps recognized by (2) and (3) above.

Table 2-8: Summary of available design integrated reliability methods; Ormon et al [54] ; Avontuur & Werff [15] , Smith and Clarkson [37] ; Tumer et al [47] ; Modarres [35] [36] ; Trewn and Yang [58] ; Citi et al [59] ;

	Process	Functional Representation	Behavior Representation	Operation Representation	Assembly Representation	Physical Description (PoF)	Relationship between components	Applications to PDP	Comments
Simulation-Based Special Applications	Ormon et al	No	No	Single Mission, Finite Duration Nonrepairable Exponential Distribution	No	No	Logical; Independent Series &Parallel	Conceptual Design	Simulation-based and analytical quantitative reliability assessment System level assessment System is a number of subsystems connected in-series Subsystems are components that are connected in-series or parallel (active or stand-by redundancy)
Simulation-Based Special Applications	Avontuur & Werff	No	No	limited system functional operations	No	No	Logical; Independent Series & Parallel	Conceptual Design	Quantitative reliability assessment their software algorithm was not completely presented Domain specific (drive train systems)
Functional Basis Methods	Smith and Clarkson	Entity-Relationship Diagrams	No	No	No	No	structural	Limited Application to Conceptual Design, it needs relationships between entities to be defined on the physical level	Qualitative reliability assessment System level assessment Design functional representation and analysis framework Relationships are defined based on the users' understanding of the design concept Does not provide a quantitative measure of reliability
Functional Basis Methods	Tumer et al.	Configuration Graph	No	system schematic representation is used to develop CG	No	No	did not specify	Conceptual Design	Quantitative reliability assessment System level assessment component connectivity from sources to sinks lacks details Domain specific (electrical power systems)
Functional Basis Methods	Modarres	GTST-MLD	No	single system objective hierarchical representation functional path dependent	No	No	Logical representation	Conceptual Design Embodiment Design	Qualitative and quantitative reliability assessment Physically Independent support functions (subsystems)
Axiomatic Methods	Trewn and Yang	through functional decomposition	No	system design and reliability matrix could be created to represent how the system perform different operations	indirect representation through design matrix, no interaction representation	No	indirect connections if the same function is performed by more than one component; Independent logical relationship	Conceptual Design Embodiment Design	Multi-Functional Representation Functions in Series Static Reliability
Axiomatic Methods	Citi et al	through functional decomposition	No	subjective mapping of design matrix to reliability matrix	indirect representation through design matrix, no interaction representation	No	indirect connections if the same function is performed by more than one component; Independent logical relationship	Conceptual Design Embodiment Design	Multi-Functional Representation Functions in Series Static Reliability Expert's Knowledge Leveraged to map design matrix to reliability matrix

Chapter 3 The Mechanistic-Based, Design-Integrated Reliability Validation Process

The main goal of this research is to develop a cohesive design-integrated reliability assessment framework that captures the causes and mechanisms affecting the failure behavior of mechanical systems. This framework consists of many models that captures: *what* the system is; *how* it delivers design-intended operations; *what* physics-based mechanisms cause its failure; and *how* components failure propagates through the system to cause system failure. The framework consists of a set of causal models connected together to allow the reliability of mechanical systems to be assessed and to understand system elements and design parameters that has significant impact on the design operational reliability.

According to Pearl [72] a causal model is a pair $= \langle D, \theta_D \rangle$, consisting of a causal structure D and a set of parameters θ_D compatible with D. The parameters θ_D assign a function $x_i = f_i(pa_i, u_i)$ to each $X_i \in V$ and a probability measure $P(u_i)$ to each u_i, where PA_i are the parents of X_i in D and where each U_i is a random disturbance distributed according to $P(u_i)$ independently of all other u. In this thesis framework, the failure causal structure for the mechanical system components (section 3.2) is a set of damage models {D} that capture the set of mechanical stresses, product usage, material properties …etc. $\{\theta_D\}$ causing components to fail. On the system level (section 3.3), the causal structure is a set of relations $\{\mathbf{SYNC1}, \mathbf{SYNC2}, \mathbf{ASYNC}\}$ that organize system damage behavior through a prior knowledge about the system operations, functions and components, developed from a descriptive model (section 3.1). The basic knowledge needed about the system is related to: *what* components participate in delivering system operations; *how* components collaborate to deliver those operations; *what* failure mechanisms affect components and *how* components failure propagate through the system to cause its failure. This knowledge is accumulated to assess system operational reliability. This thesis is attempting to maximize the value of available relevant information about the system to assess its reliability--an attempt to reflect the mechanistic methodology on system availability modeling (section 3.4) is also presented and demonstrated.

Figure 3-1 shows a simplified flowchart of the mechanistic design reliability process; the process elaborates and links each of the modules necessary to assess systems reliability. The following sections will present the mathematical models and the process besides demonstrating how MDRV can be implemented using a simplified example.

The main focus of this research will be on modeling degradation-type mechanical failures. Mechanical failures are defined by Collins [73] as any change in size, shape, or material properties of a structure, machine, or machine component that renders it incapable of satisfactorily performing its intended function. Tumer and Stone [52] presented a list of mechanical failure modes adopted from Collins [73] (outlined in Table 3-1). The categories highlighted in red color bold fonts are degradation type failure modes.

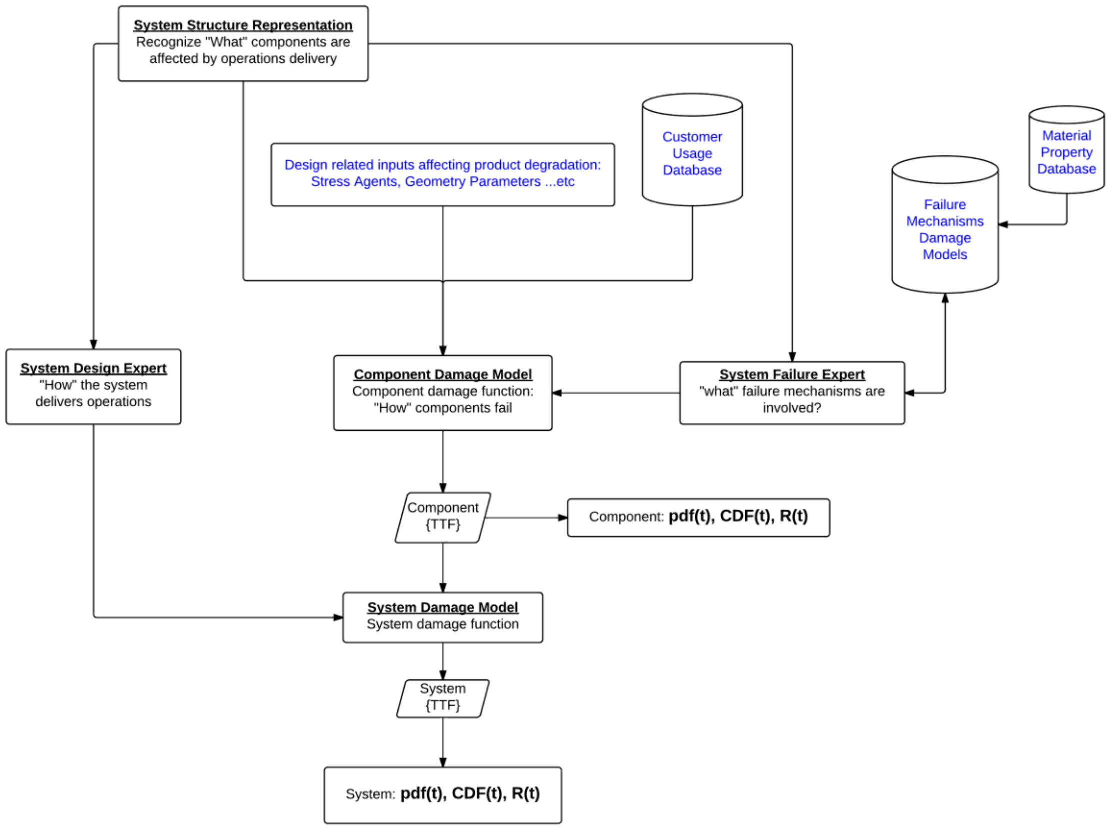

Figure 3-1: Mechanistic reliability: process outline

Table 3-1: Mechanical Failure Modes, Tumer & Stone's [52] adopted from Collins [73]; red color categories are degradation type failures

Main Category	Sub
Elastic Deformation	force induced
	temperature induced
Yielding	
Brinnelling	
Ductile rupture	
Brittle fracture	
Fatigue	high-cycle
	low-cycle
	thermal
	surface
	impact
	corrosion
	fretting
Corrosion	direct chemical attack
	galvanic
	pitting
	intergranular
	selective leaching
	erosion
	cavitation
	hydrogen damage
	biological
	stress
Wear	adhesive
	abrasive
	corrosive
	surface fatigue
	deformation
	impact
	fretting

Main Category	Sub
Impact	fracture
	deformation
	wear
	fretting
Fretting	fatigue
	wear
	corrosion
Creep	
Thermal relaxation	
Stress rupture	
Thermal shock	
Galling and seizure	
Spalling	
Radiation damage	
Buckling	
Creep buckling	
Stress corrosion	
Corrosion wear	
Corrosion fatigue	
Creep and fatigue	

The context of MDRV is the design reliability of a system of components, primarily affected by physics-based failures where physics-based degradation can mathematically be modeled; given sufficient knowledge about system usage and system components' materials and design forms. MDRV adopts a system level perspective to the design entity; the definitions summarized by Table 3-2 are adopted for this research.

Table 3-2: MDRV important definitions

Term	Technical definitions in context of MDRV
Reliability	The probability that a system design delivers its intended operations over a period of time without physics-based failures under some specified conditions of use.
Operation	Discretization to customer usage for the system; also represents the primary need and requirement expected from the system; Structurally: an operation is a set of system functions organized by-design intent to deliver customer needs. Operations are the primary system purpose and what the system is expected to deliver in MDRV.
Function	The primary building block of an operation; the lowest level of a system functional structure.
Component	Physical entity that is characterized by specific physical properties and capable of delivering at least one required function.
Behavior	The response of a system component when it receives stimuli [10]. In reliability context we are concerned with *Failure Behavior*; the degradation response of the system when it receives stress stimuli
Structure	Design description represents the artifact's elements and their relationships [26].
Failure	Emergent, time dependent system property caused by system usage and consumption of material capacity, it leads to system being incapable of delivering intended operations.
Damage	A marker, measures the depleting of material capacity to resist stimuli effects; when it reaches 100% the material reaches failure state.
Degradation	Damage increase rate.
Mechanistic	Mechanically determined; in context of MDRV: a design aspect that emerges from design synthesis.

3.1 System Synthesis

3.1.1 System Structure Representation: Recognizing Operations, Functions and Components Coupling Relationships

A functional structure, such as the one shown in Figure 3-2, is normally the first developed system representation. The main goal of the system is to deliver specific set of operations, which are the main goal for the components' functions to achieve.

Operations/ Functions Organization

An operation, in this mechanistic framework, is a set of required functions that achieves system goals. An operation path highlights the set of required functions that achieve operations in a system functional structure; Figure 3-3 shows two operations paths on a system functional structure.

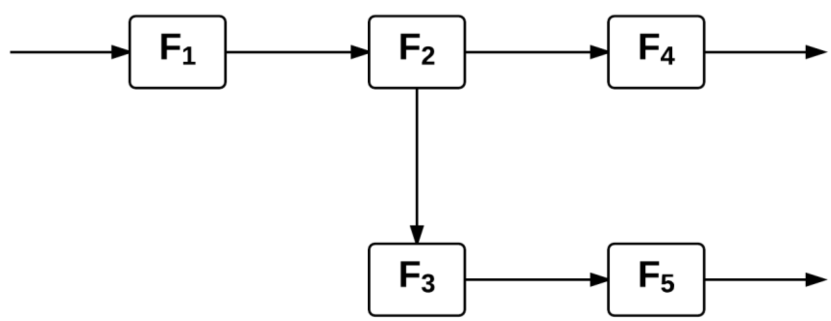

Figure 3-2: Example of a system functional structure

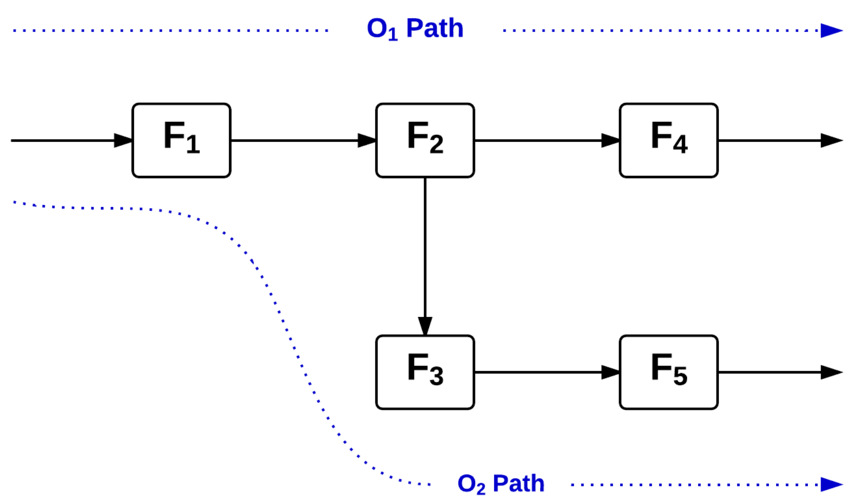

Figure 3-3: Operations paths demonstrated on a system functional structure

Operations path recognition on functional structures is important to assessing the system expected life; it provides the basic initial knowledge to recognize system components degraded by the operations identified. Operations and functions can symbolically be organized by vector sets: $\{O\}$ and $\{F\}$ respectively, assuming a linear descriptive model. Equation 3-1 below organizes the relationship between these two vector spaces; $\boldsymbol{OF}$ is the Functions Order Matrix

$$\{O\} = \boldsymbol{OF} \times \{F\} \qquad \textbf{Equation 3-1}$$

where: $\{O\} \equiv$ vector representation of system operations

$\{F\} \equiv$ vector representation of all system functions

$\boldsymbol{OF} \equiv m \times n$ matrix; Functions Order Matrix. (m) is number of system operations and (n) is number of system functions

$$\begin{Bmatrix} O_1 \\ O_2 \\ \vdots \\ O_m \end{Bmatrix} = \begin{bmatrix} A_1^1 & A_1^2 & \cdots & A_1^n \\ A_2^1 & A_2^2 & \cdots & A_2^n \\ \vdots & \vdots & \ddots & \vdots \\ A_m^1 & A_m^2 & \cdots & A_m^n \end{bmatrix} \times \begin{Bmatrix} F_1 \\ F_2 \\ \vdots \\ F_n \end{Bmatrix}$$ **Equation 3-2**

$$\boldsymbol{OF} = \begin{bmatrix} A_1^1 & A_1^2 & \cdots & A_1^n \\ A_2^1 & A_2^2 & \cdots & A_2^n \\ \vdots & \vdots & \ddots & \vdots \\ A_m^1 & A_m^2 & \cdots & A_m^n \end{bmatrix}$$ **Equation 3-3**

$$O_i = \sum_{j=1}^{n} A_i^j \times F_j$$ **Equation 3-4**

where: $A_i^j \equiv$ order factors recognizing (F_j) relations to (O_i); $0 \leq A_i^j \leq 1$;

$F_j \equiv$ symbolic function representation

$O_i \equiv$ symbolic operation representation

(A_i^j) is unity when representing strong impact; and equals zero when representing nonexistent impact, from function (F_j) on the relevant operation (O_i).

The summation process presented by Equation 3-5 is a representation to functional accumulation to realize the intended operation.

$$O_i = A_i^1 \times F_1 + A_i^2 \times F_2 + A_i^3 \times F_3 + \cdots + A_i^n \times F_n$$ **Equation 3-5**

Equation 3-5 identifies the functions associated in delivering operation (O_i); the equation defines operation (O_i) as an accumulation of the mentioned functions with the associated order factors. This model doesn't inform about *"how"* the operation is delivered; it only informs about *"what"* functions are associated with delivering operation (O_i).

Using the functional structure presented in Figure 3-3, Equation 3-6 is a functional order representation to Figure 3-2 system; showing for instance operation O_1 to be an accumulation of a set of functions $\{F_1, F_2, F_4\}$ with coupling factors $\{A_1^1, A_1^2, A_1^4\}$ respectively.

$$\begin{Bmatrix} O_1 \\ O_2 \end{Bmatrix} = \begin{bmatrix} A_1^1 & A_1^2 & 0 & A_1^4 & 0 \\ A_2^1 & A_2^2 & A_2^3 & 0 & A_2^5 \end{bmatrix} \begin{Bmatrix} F_1 \\ F_2 \\ F_3 \\ F_4 \\ F_5 \end{Bmatrix} \qquad \textbf{Equation 3-6}$$

Functions/Components Coupling

After system components are identified, an assembly representation (without joints) can be developed. Components at this design stage are functional tasks that designed physical entities deliver to satisfy their functional requirements. Assuming a linear coupling model, the relationship between functions and components can be organized using the following representation;

$$\{F\} = \boldsymbol{FC_1} \times \{C^*\} \qquad \textbf{Equation 3-7}$$

where, $\{F\} \equiv$ vector representation of system functions;

$\{C^*\} \equiv$ vector representation of system components; components are considered functional tasks at this design stage.

$\boldsymbol{FC_1} \equiv n \times p$ matrix; Function-Component Coupling Matrix, for the first realized system physical representation, i.e. for first design iteration; (n) is number of system functions and (p) is number of system components

Expanding Equation 3-7:

$$\boldsymbol{FC_1} = \begin{bmatrix} B_1^1 & B_1^2 & \cdots & B_1^P \\ B_2^1 & B_2^2 & \cdots & B_2^P \\ \vdots & \vdots & \ddots & \vdots \\ B_n^1 & B_n^2 & \cdots & B_n^P \end{bmatrix} \qquad \textbf{Equation 3-8}$$

$$F_j = \sum_{k=1}^{p} B_j^k \times C_k \qquad \textbf{Equation 3-9}$$

where: B_j^k ≡ coupling factors between component (C_k) to function (F_j); $0 \leq B_j^k \leq 1$;

F_j ≡ symbolic function representation

$C^*{}_k$ ≡ symbolic component representation

(B_j^k) equals unity when representing strong coupling (hard coupling) and equals zero when representing nonexistent coupling between component $(C^*{}_k)$ and the relevant functions (F_j).

Equation 3-9 is a representation to the set of components associated in delivering the function (F_j). It defines operation (F_j) as an accumulation of the mentioned components $(C^*{}_k)$ tasks with associated coupling factors.

Figure 3-4 shows an assembly representation to the set of components designed to satisfy the functions identified in Figure 3-3; At this design stage, the physical joints connecting these components still have not been designed yet.

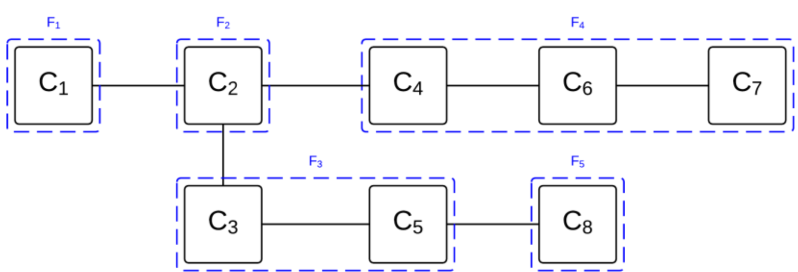

Figure 3-4: First component assembly structure to be realized

Using the assembly structure presented in Figure 3-4; Equation 3-10 captures the system coupling representations between functions and component; it shows for instance operation F_3 to be an accumulation of a set of components $\{C_3, C_5\}$ tasks; with coupling factors $\{B_3^3, B_3^5\}$ respectively.

$$\begin{Bmatrix} F_1 \\ F_2 \\ F_3 \\ F_4 \\ F_5 \end{Bmatrix} = \begin{bmatrix} B_1^1 & 0 & 0 & 0 & 0 & 0 & 0 & 0 \\ 0 & B_2^2 & 0 & 0 & 0 & 0 & 0 & 0 \\ 0 & 0 & B_3^3 & 0 & B_3^5 & 0 & 0 & 0 \\ 0 & 0 & 0 & B_4^4 & 0 & B_4^6 & B_4^7 & 0 \\ 0 & 0 & 0 & 0 & 0 & 0 & 0 & B_5^8 \end{bmatrix} \begin{Bmatrix} C_1 \\ C_2 \\ C_3 \\ C_4 \\ C_5 \\ C_6 \\ C_7 \\ C_8 \end{Bmatrix}$$

Equation 3-10

Operations/Components Functional Coupling

The first coupling relationship between system operations and system components $(\boldsymbol{OC_1})$, can be realized through the multiplication of $\boldsymbol{OF}$ from Equation 3-3 and $\boldsymbol{FC_1}$ from Equation 3-7; the coupling system is presented by Equation 3-11

$$\{O\} = \boldsymbol{OC_1} \times \{C^*\}$$

$$\boldsymbol{OC_1} = \boldsymbol{OF} \times \boldsymbol{FC_1}$$

Equation 3-11

where: $\boldsymbol{OC_1} \equiv m \times p$ matrix; Operation-Component Coupling Matrix for the first realized system physical representation; (m) is number of system operations and (p) is number of system components

$(\boldsymbol{OC_1})$ recognizes the operations requirements based on functional demand on components.

$$\boldsymbol{OC_1} = \begin{bmatrix} \theta_1^1 & \theta_1^2 & \cdots & \theta_1^p \\ \theta_2^1 & \theta_2^2 & \cdots & \theta_2^P \\ \vdots & \vdots & \ddots & \vdots \\ \theta_m^1 & \theta_m^2 & \cdots & \theta_m^P \end{bmatrix}$$ **Equation 3-12**

where: $\theta_i^k = \sum_{j=1}^{n} \left(A_i^j \times B_j^k \right)$ are operatins-components coupling factors; coupling operation (O_i) to set of components $\{C^*{}_k\}$; $0 \le \theta_i^k \le 1$.

The coupling factors $\left(\theta_i^k\right)$ are direct coupling between operations and components' tasks which in turn realize system required functions; the effect of components interactions and influence on each other is not taken into account by this system representation.

$$O_i = \sum_{k=1}^{p} \theta_i^k \times C^*{}_k$$

$$\theta_i^k = \sum_{j=1}^{n} A_i^j \times B_j^k$$ **Equation 3-13**

$$O_i = \sum_{k=1}^{p} \sum_{j=1}^{n} A_i^j \times B_j^k \times C^*{}_k$$

Expanding Equation 3-13 produces Equation 3-14 and Equation 3-15

$$O_i = \left(\sum_{j=1}^{n} A_i^j \times B_j^1 \right) \times C^*{}_1 + \left(\sum_{j=1}^{n} A_i^j \times B_j^2 \right) \times C^*{}_2 + \left(\sum_{j=1}^{n} A_i^j \times B_j^3 \right) \times C^*{}_3 + \cdots + \left(\sum_{j=1}^{n} A_i^j \times B_j^p \right) \times C^*{}_p$$ **Equation 3-14**

$$O_i = (A_i^1 \times B_1^1 + A_i^2 \times B_2^1 + \cdots + A_i^n \times B_n^1) \times C^*{}_1$$
$$+ (A_i^1 \times B_1^2 + A_i^2 \times B_2^2 + \cdots + A_i^n \times B_n^2) \times C^*{}_2$$
$$+ (A_i^1 \times B_1^3 + A_i^2 \times B_2^3 + \cdots + A_i^n \times B_n^3) \times C^*{}_3 + \cdots$$
$$+ \left(A_i^1 \times B_1^p + A_i^2 \times B_2^p + \cdots + A_i^n \times B_n^p\right) \times C^*{}_p$$

Equation 3-15

Considering the system represented by Figure 3-2, Figure 3-3 and Figure 3-4; by symbolically multiplying ($\boldsymbol{OF}$), from Equation 3-6 and ($\boldsymbol{FC_1}$), from Equation 3-10 we ca measure ($\boldsymbol{OC_1}$) as shown in Equation 3-16.

$$\boldsymbol{OC_1} = \begin{bmatrix} A_1^1 \times B_1^1 & A_1^2 \times B_2^2 & 0 & A_1^4 \times B_4^4 & 0 & A_1^4 \times B_4^6 & A_1^4 \times B_4^7 & 0 \\ A_2^1 \times B_1^1 & A_2^2 \times B_2^2 & A_2^3 \times B_3^3 & 0 & A_2^3 \times B_3^5 & 0 & 0 & A_2^5 \times B_5^8 \end{bmatrix}$$

Equation 3-16

Based on the matrix system presented by Equation 3-16 we can conclude the following:

1. looking horizontally at ($\boldsymbol{OC_1}$) matrix: the set of components: $\{C^*{}_1, C^*{}_2, C^*{}_4, C^*{}_6, C^*{}_7\}$ is coupled to operation-1, (O_1), and the set of components: $\{C^*{}_1, C^*{}_2, C^*{}_3, C^*{}_5, C^*{}_8\}$ is coupled to operation-2, (O_2).
2. looking vertically at ($\boldsymbol{OC_1}$) matrix: component-1, (C_1) for instance is involved in delivering two operations $\{O_1,\ O_2\}$ while component-7, (C_7) is involved in delivering just one operation $\{O_1\}$.
3. looking at ($\boldsymbol{OC_1}$) matrix we can recognize that the set of components: $\{C^*{}_3, C^*{}_5\}$ represents a subsystem because each have the same functional coupling parameter (A_2^3) and the set of components $\{C^*{}_4, C^*{}_6, C^*{}_7\}$ represents a subsystem because each have the same functional coupling parameter (A_1^4).

As the design process progresses to system embodiment phase, the system starts to have a 3D design form; and joints connecting components together get developed; by the end of this process, an assembly structure representation [14] can be developed as shown by Figure 3-5. The joints that connect these component might have physical form and might need to be included in the set of components influencing the performance of the system. That would lead to updating $(\boldsymbol{OC_1})$; for simplicity, at this point, the set of components will not be updated.

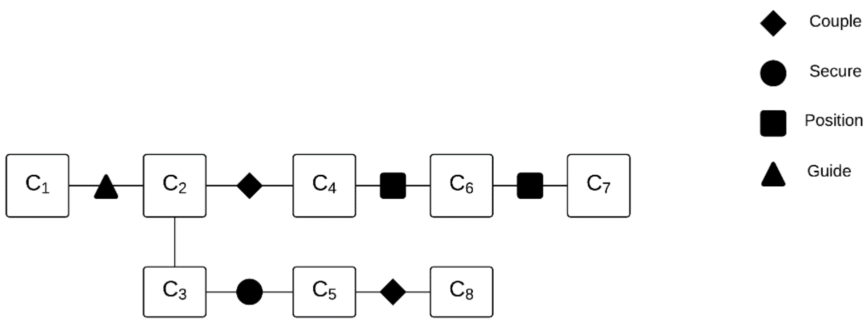

Figure 3-5: Assembly structure of the functional system presented in Figure 3-3

Components Interaction within System Boundaries

Interactions between components need to be recognized to understand their influence on each other; if components are structurally linked to each other, it is likely that they will be transferring stresses to each other when they contribute to system operations; *those stresses recognized should be relevant to failure mechanisms being addressed to be considered, modeled and analyzed for their influence on system reliability*.

Assuming a linear interaction model, the first realized interaction relationship between components can be realized through the system presented by Equation 3-17; this interaction matrix is based on system functional demand and response between components; the system designer should decide on including or excluding some of these interacions based on possibility of generating unnecessary stimuli between compoents; the system designer might decide to merge some of the influences together to reduce the number of parameters to be managed; for example if two components are neighbouring each other and sending or receiving system functional requirements to each other, their interactions can be merged into one interaction factor; these two influences, neighbourhood and functional demand, can also be seperated into two interaction matrices and managed independently.

$$\{C^*\} = \boldsymbol{I_1} \times \{C\} \qquad \textbf{Equation 3-17}$$

where, $\{C^*\} \equiv$ vector representation of system components; components as functional tasks.

$\{C\} \equiv$ vector representation of all system components; components are considered as physical entity behaviors.

$\boldsymbol{I_1} \equiv p \times p$ square matrix; Interaction Matrix for the first realized system physical representation, (p) is number of system components

Equation 3-18 is an expanded representation to $(\boldsymbol{I_1})$ in Equation 3-17. Components in this design perspective are considered as amalgamation of physical entity behaviors; i.e. different perspective than what was realized in section (0).

$$\boldsymbol{I_1} = \begin{bmatrix} I_1 & D_1^2 & D_1^2 & \dots & D_1^p \\ D_2^1 & I_2 & D_2^3 & \cdots & D_2^p \\ D_3^1 & D_3^2 & I_3 & \ddots & D_3^p \\ \vdots & \vdots & \vdots & & \vdots \\ D_p^1 & D_p^2 & D_p^2 & \cdots & I_p \end{bmatrix}$$ **Equation 3-18**

$$C^*{}_k = \sum_{l=1}^{p} D_k^l \times C_l$$ **Equation 3-19**

where: $D_k^l \equiv$ interaction stimuli factors from component (C_k) to components (C_l) and; $0 \leq D_k^l \leq 1$;

$I_k = D_k^k \equiv$ interaction stimuli factor from component (C_k) to itself; special representation. $0 \leq I_k \leq 1$;

$C^*{}_k$ & $C_l \equiv$ symbolic component representation

The stimulus perspective to interaction representation defines components as a set of stimuli sent to other system components triggered by their functional tasks; the interactions could be demand-based like the one presented by Equation 3-19 or indirect influences sent to other components such as mechanical stresses, heat, radiation, etc. These interactions can be captured with more than one interaction matrix and superimposed into one matrix at the end.

Equation 3-18 rows show the relevent component stimuli sent to system; the columns on the other hand, show the stimuli received from the system on the relevant component.

The interaction matrix developed for the system in Figure 3-4 is shown by Equation 3-20; the assumption made at this design stage is that the stimuli are two-way type; this assumption is more inclusive to capture all possible interactions.

$$\begin{Bmatrix} C^*{}_1 \\ C^*{}_2 \\ C^*{}_3 \\ C^*{}_4 \\ C^*{}_5 \\ C^*{}_6 \\ C^*{}_7 \\ C^*{}_8 \end{Bmatrix} = \begin{bmatrix} I_1 & D_1^2 & 0 & 0 & 0 & 0 & 0 & 0 \\ D_2^1 & I_2 & D_2^3 & D_2^4 & 0 & 0 & 0 & 0 \\ 0 & D_3^2 & I_3 & 0 & D_3^5 & 0 & 0 & 0 \\ 0 & D_4^2 & 0 & I_4 & 0 & D_4^6 & 0 & 0 \\ 0 & 0 & D_5^3 & 0 & I_5 & 0 & 0 & D_5^8 \\ 0 & 0 & 0 & D_6^4 & 0 & I_6 & D_6^7 & 0 \\ 0 & 0 & 0 & 0 & 0 & D_7^6 & I_7 & 0 \\ 0 & 0 & 0 & 0 & D_8^5 & 0 & 0 & I_8 \end{bmatrix} \begin{Bmatrix} C_1 \\ C_2 \\ C_3 \\ C_4 \\ C_5 \\ C_6 \\ C_7 \\ C_8 \end{Bmatrix}$$

Equation 3-20

$$\boldsymbol{I_1} = \begin{bmatrix} I_1 & D_1^2 & 0 & 0 & 0 & 0 & 0 & 0 \\ D_2^1 & I_2 & D_2^3 & D_2^4 & 0 & 0 & 0 & 0 \\ 0 & D_3^2 & I_3 & 0 & D_3^5 & 0 & 0 & 0 \\ 0 & D_4^2 & 0 & I_4 & 0 & D_4^6 & 0 & 0 \\ 0 & 0 & D_5^3 & 0 & I_5 & 0 & 0 & D_5^8 \\ 0 & 0 & 0 & D_6^4 & 0 & I_6 & D_6^7 & 0 \\ 0 & 0 & 0 & 0 & 0 & D_7^6 & I_7 & 0 \\ 0 & 0 & 0 & 0 & D_8^5 & 0 & 0 & I_8 \end{bmatrix}$$

Equation 3-21

Looking at the interaction system presented by Equation 3-20 one can recognize:

1. $\left(D_i^j\right)$ is an interaction stimulus factor for stimulus generated by component *(i)* functional task on component *(j)*.
2. the interaction stimulus factor of the system component on itself (I_k) is an indication of a component that is self-degrading or a subsystem that is beings reduced to one component, for example: treating an IC engine as one component entity in a system and recognizing the mechanical stresses impact produced by the engine vibration to its internal components yields (I_k).

Operations/Components Physical Coupling

The physical coupling relationship between operations and components can be recognized through superimposing the coupling relationships recognized at the current design stage i.e.: $\boldsymbol{OF}, \boldsymbol{FC_1}, \boldsymbol{I_1}$, to develop the coupling relationships between system operations and components; presented by Equation 3-22

$$\{O\} = \boldsymbol{OF} \times \boldsymbol{FC_1} \times \boldsymbol{I_1} \times \{C\}$$

$$\{O\} = \boldsymbol{OCI_1} \times \{C\}$$

Equation 3-22

The operation genereric coupling relationship with components is presented by the set of equations from Equation 3-23 to Equation 3-24

$$O_i = \sum_{l=1}^{p} \eta_i^l \times C_l$$

$$\eta_i^l = \sum_{k=1}^{p} \sum_{j=1}^{n} A_i^j \times B_j^k \times D_k^l$$

Equation 3-23

$$O_i = \sum_{l=1}^{p} \sum_{k=1}^{p} \sum_{j=1}^{n} A_i^j \times B_j^k \times D_k^l \times C_l$$

where: $\eta_i^l = \sum_{k=1}^{p} \sum_{j=1}^{n} A_i^j \times B_j^k \times D_k^l$ are coupling stimuli factors, they couple operation (O_i) to the set of component (C_i).

Expanding Equation 3-23 produces Equation 3-24;

$$O_i = \left(\sum_{k=1}^{p}\sum_{j=1}^{n} A_i^j \times B_j^k \times D_k^1\right) \times C_1 + \left(\sum_{k=1}^{p}\sum_{j=1}^{n} A_i^j \times B_j^k \times D_k^2\right) \times C_2 + \left(\sum_{k=1}^{p}\sum_{j=1}^{n} A_i^j \times B_j^k \times D_k^3\right) \times C_3 + \cdots + \left(\sum_{k=1}^{p}\sum_{j=1}^{n} A_i^j \times B_j^k \times D_k^p\right) \times C_p$$

Equation 3-24

The coupling stimuli factor (η_i^l) which is equal to $\left(\sum_{k=1}^{p}\sum_{j=1}^{n} A_i^j \times B_j^k \times D_k^l\right)$ represnets functional demad (A_i^j), functional-component task coupling (B_j^k) and stimulus received from other components on component (C_l); the row vector presented by Equation 3-24 represents the components affected by the delivery of (O_i).

$$\boldsymbol{OC_1} = \begin{bmatrix} A_1^1 \times B_1^1 & A_1^2 \times B_2^2 & 0 & A_1^4 \times B_4^4 & 0 & A_1^4 \times B_4^6 & A_1^4 \times B_4^7 & 0 \\ A_2^1 \times B_1^1 & A_2^2 \times B_2^2 & A_2^3 \times B_3^3 & 0 & A_2^3 \times B_3^5 & 0 & 0 & A_2^5 \times B_5^8 \end{bmatrix}$$

Equation 3-25

$$\boldsymbol{OCI_1} = \begin{bmatrix} A_1^2 \times B_2^2 \times D_2^1 + A_1^1 \times B_1^1 \times I_1 & A_1^1 \times B_1^1 \times D_1^2 + A_1^4 \times B_4^4 \times D_4^2 + A_1^2 \times B_2^2 \times I_2 & A_1^2 \times B_2^2 \times D_2^3 & A_1^2 \times B_2^2 \times D_2^4 + A_1^4 \times B_4^6 \times D_6^4 + A_1^4 \times B_4^4 \times I_4 & 0 & A_1^4 \times B_4^4 \times D_4^6 + A_1^4 \times B_4^7 \times D_7^6 + A_1^4 \times B_4^6 \times I_6 & A_1^4 \times B_4^6 \times D_6^7 + A_1^4 \times B_4^7 \times I_7 & 0 \\ A_2^2 \times B_2^2 \times D_2^1 + A_2^1 \times B_1^1 \times I_1 & A_2^1 \times B_1^1 \times D_1^2 + A_2^3 \times B_3^3 \times D_3^2 + A_2^2 \times B_2^2 \times I_2 & A_2^2 \times B_2^2 \times D_2^3 + A_2^3 \times B_3^5 \times D_5^3 + A_2^3 \times B_3^3 \times I_3 & A_2^2 \times B_2^2 \times D_2^4 & A_2^3 \times B_3^3 \times D_3^5 + A_2^5 \times B_5^8 \times D_8^5 + A_2^3 \times B_3^5 \times I_5 & 0 & 0 & A_2^3 \times B_3^5 \times D_5^8 + A_2^5 \times B_5^8 \times I_8 \end{bmatrix}$$

Equation 3-26

Considering Figure 3-3 and Figure 3-4, Equation 3-26 represents $(\boldsymbol{OCI_1})$ which was calculated based on Equation 3-22; $(\boldsymbol{OF})$, $(\boldsymbol{FC_1})$, $(\boldsymbol{I_1})$ are substituted from Equation 3-6, Equation 3-10 and Equation 3-21 respectively.

By evaluating Equation 3-26 system representation; we can recognize:

1. Components: $\{C_1, C_2, C_3, C_4, C_6, C_7\}$ are affected by the delivery of operation-1; as compared to the set: $\{C_1, C_2, C_4, C_6, C_7\}$ realized before physical interactions were taken into account.
2. Components: $\{C_1, C_2, C_3, C_4, C_5, C_8\}$ are affected by the delivery of operation-2 as compared to the set:$\{C_1, C_2, C_3, C_5, C_8\}$ realized before physical interactions were taken into account.
3. Operation-1 is affecting the set of components: $\{C_1, C_2, C_3, C_4, C_6, C_7\}$ by the set of coupling interactions: $\{A_1^2 \times B_2^2 \times D_2^1 + A_1^1 \times B_1^1 \times I_1, A_1^1 \times B_1^1 \times D_1^2 + A_1^4 \times B_4^4 \times D_4^2 + A_1^2 \times B_2^2 \times I_2, A_1^2 \times B_2^2 \times D_2^3, A_1^2 \times B_2^2 \times D_2^4 + A_1^4 \times B_4^6 \times D_6^4 + A_1^4 \times B_4^4 \times I_4, A_1^4 \times B_4^4 \times D_4^6 + A_1^4 \times B_4^7 \times D_7^6 + A_1^4 \times B_4^6 \times I_6, A_1^4 \times B_4^6 \times D_6^7 + A_1^4 \times B_4^7 \times I_7\}$. For instance operation-1 affects component-1 through the coupling parameter $(A_1^2 \times B_2^2 \times D_2^1 + A_1^1 \times B_1^1 \times I_1)$ which is a representation to the coupling coming from (operation-1, functions-2) through component-2 interaction: $(A_1^2 \times B_2^2 \times D_2^1)$; besides, the coupling coming from component-1 to itself through operation-1, function-1: $(A_1^1 \times B_1^1 \times I_1)$. Considering the set of components: $\{C_1, C_2, C_3, C_4, C_6, C_7\}$ to be associated in delivering operation-1 is more inclusive than using the set $\{C_1, C_2, C_4, C_6, C_7\}$; in this specific case (C_3) might not be directly involved in delivering (O_1) but it might be functioning as a structural support for other components that are directly involved in delivering (O_1) or its failure might lead to the failure of delivering (O_1). If the system analyst decided that (C_3) should not be affected by or affecting (O_1) he/she can substitute $D_2^3 = 0$ in the term $A_1^2 \times B_2^2 \times D_2^3$

4. The system representation, Equation 3-26, shows the components involved with delivering each of the required operations, but it doesn't describe *how* these operations are delivered. Another flow representation is need to describe the *"How"* factor.

Considering if joints need to be included in analyzing the system, we can recognize them as shown in Figure 3-6 where J_1 and J_2 are recognized as physical joints; with physical interactions couplings recognized by Equation 3-27.

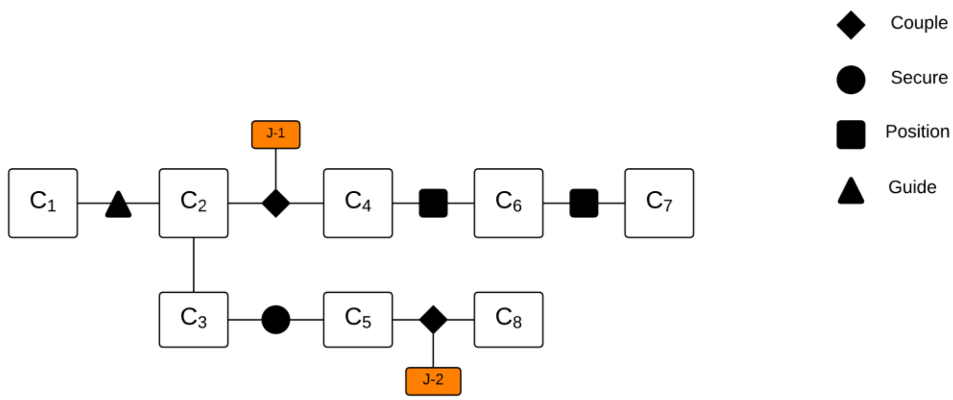

Figure 3-6: Assembly structure of the functional system presented in Figure 3-3, two joints, J₁ and J₂ are physically recognized

$$\begin{Bmatrix} C^*{}_1 \\ C^*{}_2 \\ C^*{}_3 \\ C^*{}_4 \\ C^*{}_5 \\ C^*{}_6 \\ C^*{}_7 \\ C^*{}_8 \\ J^*{}_1 \\ J^*{}_2 \end{Bmatrix} = \begin{bmatrix} I_1 & D_1^2 & 0 & 0 & 0 & 0 & 0 & 0 & 0 & 0 \\ D_2^1 & I_2 & D_2^3 & D_2^4 & 0 & 0 & 0 & 0 & D_2^{J_1} & 0 \\ 0 & D_3^2 & I_3 & 0 & D_3^5 & 0 & 0 & 0 & 0 & 0 \\ 0 & D_4^2 & 0 & I_4 & 0 & D_4^6 & 0 & 0 & D_4^{J_1} & 0 \\ 0 & 0 & D_5^3 & 0 & I_5 & 0 & 0 & D_5^8 & 0 & D_5^{J_2} \\ 0 & 0 & 0 & D_6^4 & 0 & I_6 & D_6^7 & 0 & 0 & 0 \\ 0 & 0 & 0 & 0 & 0 & D_7^6 & I_7 & 0 & 0 & 0 \\ 0 & 0 & 0 & 0 & D_8^5 & 0 & 0 & I_8 & 0 & D_8^{J_2} \\ 0 & D_{J_1}^2 & 0 & D_{J_1}^4 & 0 & 0 & 0 & 0 & I_{J_1} & 0 \\ 0 & 0 & 0 & 0 & D_{J_2}^5 & 0 & 0 & D_{J_2}^8 & 0 & I_{J_2} \end{bmatrix} \begin{Bmatrix} C_1 \\ C_2 \\ C_3 \\ C_4 \\ C_5 \\ C_6 \\ C_7 \\ C_8 \\ J_1 \\ J_2 \end{Bmatrix}$$

Equation 3-27

$$
\boldsymbol{I_2} = \begin{bmatrix}
I_1 & D_1^2 & 0 & 0 & 0 & 0 & 0 & 0 & 0 & 0 \\
D_2^1 & I_2 & D_2^3 & D_2^4 & 0 & 0 & 0 & 0 & D_2^{J_1} & 0 \\
0 & D_3^2 & I_3 & 0 & D_3^5 & 0 & 0 & 0 & 0 & 0 \\
0 & D_4^2 & 0 & I_4 & 0 & D_4^6 & 0 & 0 & D_4^{J_1} & 0 \\
0 & 0 & D_5^3 & 0 & I_5 & 0 & 0 & D_5^8 & 0 & D_5^{J_2} \\
0 & 0 & 0 & D_6^4 & 0 & I_6 & D_6^7 & 0 & 0 & 0 \\
0 & 0 & 0 & 0 & 0 & D_7^6 & I_7 & 0 & 0 & 0 \\
0 & 0 & 0 & 0 & D_8^5 & 0 & 0 & I_8 & 0 & D_8^{J_2} \\
0 & D_{J_1}^2 & 0 & D_{J_1}^4 & 0 & 0 & 0 & 0 & I_{J_1} & 0 \\
0 & 0 & 0 & 0 & D_{J_2}^5 & 0 & 0 & D_{J_2}^8 & 0 & I_{J_2}
\end{bmatrix}
$$

Equation 3-28

Due to the expansion of the set of components to include J_1 and J_2, updating $\boldsymbol{FC_1}$ to $\boldsymbol{FC_2}$ is required. The most inclusive approach is to assume the joint as a component that will be affected by the components being joined functions as shown in Figure 3-7.

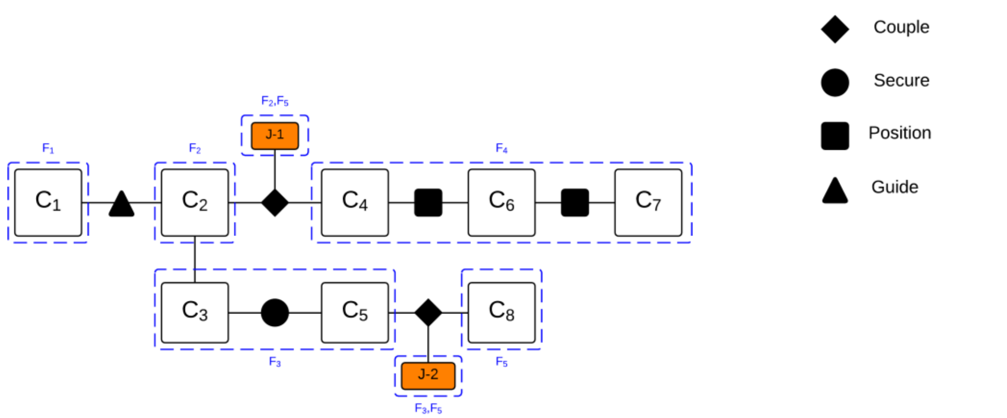

Figure 3-7: System joints and their associated functions

Updating $\boldsymbol{FC_1}$ to $\boldsymbol{FC_2}$ is shown in Equation 3-29 the system representation $\boldsymbol{OC}$ and $\boldsymbol{OCI}$ needs to be updated too

$$\begin{Bmatrix} F_1 \\ F_2 \\ F_3 \\ F_4 \\ F_5 \end{Bmatrix} = \begin{bmatrix} B_1^1 & 0 & 0 & 0 & 0 & 0 & 0 & 0 & 0 & 0 \\ 0 & B_2^2 & 0 & 0 & 0 & 0 & 0 & 0 & B_2^{J_1} & 0 \\ 0 & 0 & B_3^3 & 0 & B_3^5 & 0 & 0 & 0 & 0 & B_3^{J_2} \\ 0 & 0 & 0 & B_4^4 & 0 & B_4^6 & B_4^7 & 0 & B_4^{J_1} & 0 \\ 0 & 0 & 0 & 0 & 0 & 0 & 0 & B_5^8 & 0 & B_3^{J_2} \end{bmatrix} \begin{Bmatrix} C_1 \\ C_2 \\ C_3 \\ C_4 \\ C_5 \\ C_6 \\ C_7 \\ C_8 \\ J_1 \\ J_2 \end{Bmatrix}$$

Equation 3-29

Other types of direct or indirect interactions can be recognized and modeled, for example indirect interaction between C_5 and C_6, where C_5 is sending a stimulus to C_6 as shown in Figure 3-8, beside a two way stimulus interaction between C_7 and C_8. The interaction matrix for these two stimuli is shown by a separate representation in Equation 3-30.

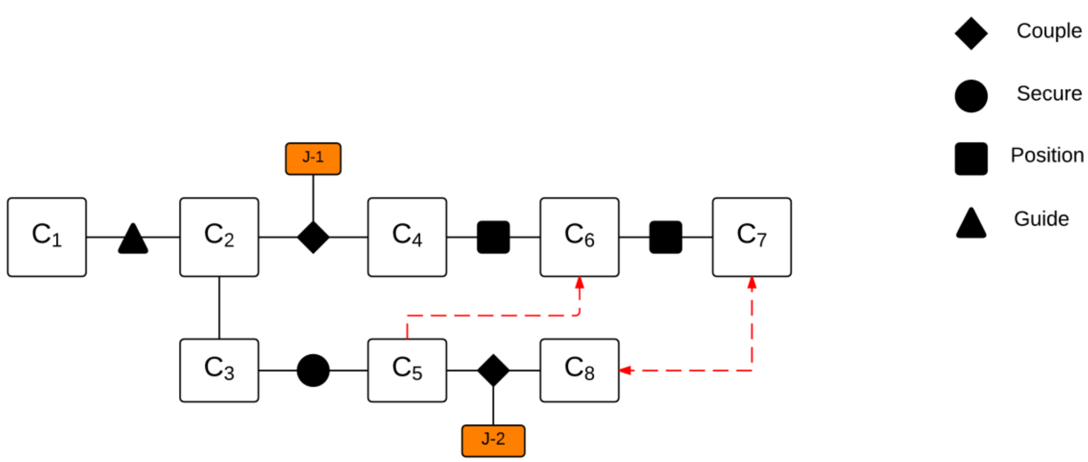

Figure 3-8: Assembly structural representation with two indirect actions between C_5, C_6 and C_7, C_8

$$I_3 = \begin{bmatrix} 0 & 0 & 0 & 0 & 0 & 0 & 0 & 0 & 0 & 0 \\ 0 & 0 & 0 & 0 & 0 & 0 & 0 & 0 & 0 & 0 \\ 0 & 0 & 0 & 0 & 0 & 0 & 0 & 0 & 0 & 0 \\ 0 & 0 & 0 & 0 & 0 & 0 & 0 & 0 & 0 & 0 \\ 0 & 0 & 0 & 0 & 0 & D_5^6 & 0 & 0 & 0 & 0 \\ 0 & 0 & 0 & 0 & 0 & 0 & 0 & 0 & 0 & 0 \\ 0 & 0 & 0 & 0 & 0 & 0 & 0 & D_7^8 & 0 & 0 \\ 0 & 0 & 0 & 0 & 0 & 0 & D_8^7 & 0 & 0 & 0 \\ 0 & 0 & 0 & 0 & 0 & 0 & 0 & 0 & 0 & 0 \\ 0 & 0 & 0 & 0 & 0 & 0 & 0 & 0 & 0 & 0 \end{bmatrix}$$ **Equation 3-30**

System Boundaries and External Environment

The external environment impact on the system lies on the inputs needed or stimuli from the environment and/or released to the environment; hence the environment can be modeled as a component with input and/or output stimuli. Following this process, many environments can be recognized and modeled if needed.

Operations Method of Delivery

The operational damage on components can be recognized by ($\boldsymbol{OCI}$) matrix; $\{O\} = \boldsymbol{OCI}\,\{C\}$, this matrix captures the operational, functional and physical interaction coupling relationships between operations and components within system environment. Relationship mapping from operations domain $\{O_i\}$ to components set domains $\{C_j^i\}$ can be defined as:

$$W^i: O_i \rightarrow \{C_1^i, C_2^i, C_3^i, \dots C_M^i\}$$ **Equation 3-31**

$$O_i \xrightarrow{W^i} \{C_1^i, C_2^i, C_3^i, \dots C_M^i\}$$ **Equation 3-32**

W^i is a mapping relationship between operations and components sets that identifies the components $\{C_j^i\}$ that are affected by the delivery of operations $\{O_i\}$; we are going to call this relationship Who/What -relationship or briefly *W-relationships*.

The reverse of W-relationships, relevant to components failure, is used to develop damage relationship. *D-relationships* will be used to relate components to operations that interface with them during the operational delivery process.

$$D^k: C_k \rightarrow \{O_1^k, O_2^k, O_3^k, \dots O_N^k\}$$ **Equation 3-33**

$$C_k \xrightarrow{D^k} \{O_1^k, O_2^k, O_3^k, \dots O_N^k\}$$ **Equation 3-34**

D^k is a mapping relationship between components and operations sets that identifies the operations $\{O_l^k\}$ that affect components $\{C_j\}$.

Damage accumulation using Miner's Rule will be used to assess the total resulting damage on components.

$$\Lambda_{C_k} = \sum\nolimits_{C_k} \Lambda_{O_i}^{C_k}$$ **Equation 3-35**

Λ_{C_k} is the total damage due to systems operations on component C_k; $\Lambda_{O_i}^{C_k}$ is the damage impact of operation O_i on component C_k.

On the system level, the process flow of operations delivery still need to identified, this can be modeled as a relationship, H^i, between O_i and the statement $(C_1^i \circ C_2^i \circ \dots \circ C_M^i)$;

$$H^i: O_i \rightarrow (C_1^i \circ C_2^i \circ C_3^i \circ \dots \circ C_M^i)$$ **Equation 3-36**

$$O_i \xrightarrow{H^i} \left(C_1^i \circ\ C_2^i \circ\ C_3^i \circ \ldots \circ C_M^i\right) \qquad \textbf{Equation 3-37}$$

H^i is a process relationship that identifies logical operations along the set $\{C_j^i\}$,i.e. $\left(C_1^i \circ\ C_2^i \circ\ C_3^i \circ \ldots \circ C_M^i\right)$, that delivers the operation (O_i). $(\circ)$ is a placeholder for a logical operator that belongs to the set $\{\cap,\cup\}$ and satisfies the operation (O_i) by-design; for example, Equation 3-37 is the short representation to the system shown by Equation 3-38:

$$\begin{gathered}
O_1 \xrightarrow{H^1} (C_1^1 \circ\ C_2^1 \circ\ C_3^1 \circ \ldots \circ C_A^1) \\
O_2 \xrightarrow{H^2} (C_1^2 \circ\ C_2^2 \circ\ C_3^2 \circ \ldots \circ C_B^2) \\
\vdots \\
O_m \xrightarrow{H^m} (C_1^m \circ\ C_2^m \circ\ C_3^m \circ \ldots \circ C_D^2)
\end{gathered} \qquad \textbf{Equation 3-38}$$

H^i is a logical relationship that identifies *how* the operations are logically delivered we are going to call this relationship How -relationship or briefly *H-relationships*.

For complicated systems, realization of subsystems make the process easier:

$$\begin{gathered}
O_i \xrightarrow{H^i} \left(S_1^i\{C_1^{i,1}, C_2^{i,1}, C_3^{i,1}, \ldots, C_A^{i,1}\} \circ S_2^i\{C_1^{i,2}, C_2^{i,2}, C_3^{i,2}, \ldots, C_B^{i,2}\}\right. \\
\left. \circ \ldots \circ S_m^i\{C_1^{i,m}, C_2^{i,m}, C_3^{i,m}, \ldots, C_D^{i,m}\}\right)
\end{gathered} \qquad \textbf{Equation 3-39}$$

where: S_j^i represents H-relationship over the set $\{C_k^{i,j}\}$; (k) is the domain of components satisfying portion of operation (O_i) by-design and recognized for having commonality between its members; for example: all components were designed to redundantly deliver portion of the operation, i.e. in-parallel subsystem.

$$S_j^i = O_j^i\ , portion\ of\ O_i \xrightarrow{H^i} \left(C_1^i \circ C_2^i \circ C_3^i \circ \dots \circ C_M^i\right)$$ **Equation 3-40**

$$S_j^i = H^i : O_j^i, portion\ of\ O_i \rightarrow \left(C_1^i \circ C_2^i \circ C_3^i \circ \dots \circ C_M^i\right)$$ **Equation 3-41**

$$S_j^i\left\{C_1^{i,j}, C_2^{i,j}, C_3^{i,j}, \dots, C_M^{i,j}\right\} = \left[O_j^i \xrightarrow{H^i} \left(C_1^i \circ C_2^i \circ C_3^i \circ \dots \circ C_M^i\right)\right]$$ **Equation 3-42**

$$S_j^i\left\{C_1^{i,j}, C_2^{i,j}, C_3^{i,j}, \dots, C_M^{i,j}\right\} = \left[H^i : O_j^i \rightarrow \left(C_1^i \circ C_2^i \circ C_3^i \circ \dots \circ C_M^i\right)\right]$$ **Equation 3-43**

An expanded version of Equation 3-39 is:

$$\begin{aligned}
O_1 &\xrightarrow{H^1} \left(S_1^1\left\{C_1^{1,1}, C_2^{1,1}, C_3^{1,1}, \dots, C_A^{1,1}\right\} \circ S_2^1\left\{C_1^{1,2}, C_2^{1,2}, C_3^{1,2}, \dots, C_B^{1,2}\right\} \circ \dots \right. \\
&\qquad \left. \circ\, S_q^1\left\{C_1^{1,q}, C_2^{1,q}, C_3^{1,q}, \dots, C_D^{1,q}\right\}\right) \\
O_2 &\xrightarrow{H^2} \left(S_1^2\left\{C_1^{2,1}, C_2^{2,1}, C_3^{2,1}, \dots, C_E^{2,1}\right\} \circ S_2^2\left\{C_1^{2,2}, C_2^{2,2}, C_3^{2,2}, \dots, C_F^{2,2}\right\} \circ \dots \right. \\
&\qquad \left. \circ\, S_r^2\left\{C_1^{2,r}, C_2^{2,r}, C_3^{2,r}, \dots, C_G^{2,r}\right\}\right) \\
&\vdots \\
O_m &\xrightarrow{H^m} \left(S_1^m\left\{C_1^{m,1}, C_2^{m,1}, C_3^{m,1}, \dots, C_U^{m,1}\right\} \circ S_2^m\left\{C_1^{m,2}, C_2^{m,2}, C_3^{m,2}, \dots, C_V^{m,2}\right\} \right. \\
&\qquad \left. \circ \dots \circ S_t^m\left\{C_1^{m,t}, C_2^{m,t}, C_3^{m,t}, \dots, C_Z^{m,t}\right\}\right)
\end{aligned}$$ **Equation 3-44**

3.2 Component Reliability

3.2.1 Component PoF Algorithm

The mechanical fatigue damage modeling will be used as an analogy base to outline and explain the mechanistic reliability processes. The durability of a component is assessed by knowing the number of cycles consumed of component's capacity to resist failure.

A deterministic mathematical model to assess the damage for one component under constant alternating mechanical stress (σ); is represented by the accumulated damage (Λ) model:

$$\Lambda = \frac{n}{N_f} \qquad \textbf{Equation 3-45}$$

where: $\Lambda \equiv$ accumulated damage at elapsed time (t^*)

$n \equiv$ accumulated stress cycles during elapsed time (t^*)

$N_f \equiv$ number of cycles to failure at alternating stress level (σ)

(N_f) is a function dependent on alternating stress (σ), the material (M) used for design and the form and geometry (G) of the component; $N_f = N_f(\sigma, M, G)$; hence;

$$\Lambda = \frac{n}{N_f(\sigma, M, G)} \qquad \textbf{Equation 3-46}$$

The Time to failure (TTF) of this component, under prescribed usage and material conditions is (t^*/Λ);

$$TTF = \frac{t^*}{\Lambda} = t^* \left(\frac{N_f(\sigma, M, G)}{n}\right) = \left(\frac{N_f(\sigma, M, G)}{\dot{n}}\right) \qquad \textbf{Equation 3-47}$$

where: $\dot{n} \equiv$ cycle rate, $\left(\frac{n}{t^*}\right)$, at constant alternating stress level (σ)

This equation captures the main causes to failure under fatigue loading, i.e.: usage time and cycles (t^*, n), operational stresses (σ), design material and geometry parameters (M, G)

3.2.2 Mechanistic Reliability

During the design phase, system designer should have specific life targets (T_g) for the system and system components. Reliability, $R(t)$, of a system or component during the design process could be called Design Phase Reliability and defined by:

$$R(t) = 1 - \Pr(TTF < T_g) \qquad \textbf{Equation 3-48}$$

The system designer normally aims for (TTF) to be greater than the life goal $\left(T_g\right)$; see Figure 3-9; the green hatched area is the reliability of the component and the blue hatched area is the probability $(TTF < T_g)$; where (T_g) is the life goal of this component under the predefined design conditions, Equation 3-49 represents the mechanical fatigue physics impact on component reliability.

$$R(t) = 1 - \Pr\left(\frac{N_f(\sigma, M, G)}{\dot{n}} < T_g\right) \qquad \textbf{Equation 3-49}$$

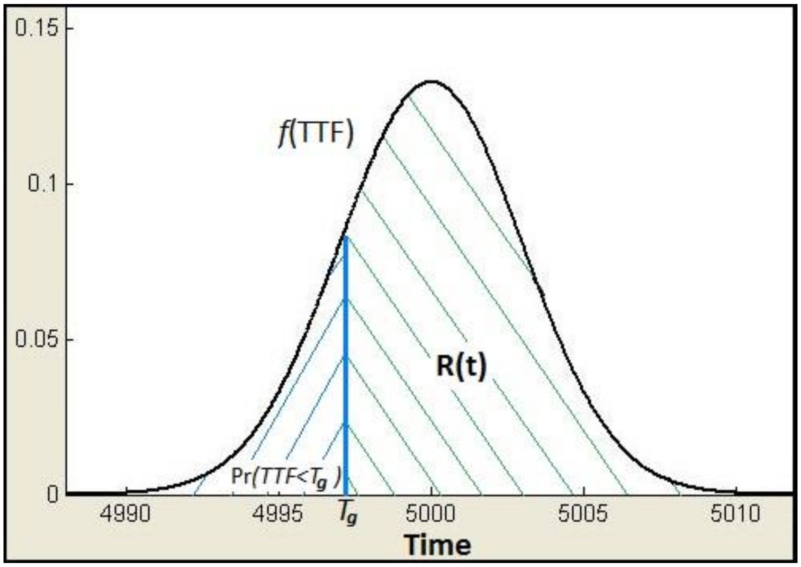

Figure 3-9: Probability density function of (TTF), $f(TTF)$; Design Phase Reliability $R(t)$ and Probability of $(TTF < Tg)$

Reliability is technically defined as, probability that a unit performs its intended function over a period of time without a failure under some specified conditions of use; in this research framework, reliability will be defined as: *probability that a unit delivers its intended operations over a period of time without a physics-based failure under some specified conditions of use*.

The reliability model presented in Equation 3-49 assumes the conditions of use to be the set $\{\sigma, n^*, M, G\}$ this PoF reliability model resolved within the context of system operations is sufficient to capture the definition of design phase mechanistic-based reliability.

3.2.3 Physics of the Damage Process

Mechanistic reliability is focusing on understanding the root cause of product failure events; it aims at developing relationship between the variables and parameters contributing to the failure event and the reliability of the product.

Considering mechanical fatigue as a base analogy; for a single component, the relationship between the number of cycles to failure and the alternating stress field, for low stress amplitudes can be condensed into Equation 3-50, [74]:

$$N_f = C_\sigma \, exp\left[A_\sigma \, ln\left(S_{amp}\right)\right] \qquad \textbf{Equation 3-50}$$

where: $C_\sigma = \exp\left[-\frac{\ln(\acute{S_f})}{b}\right]$

$A_\sigma = \frac{1}{b}$

$\acute{S_f} \equiv$ the fatigue strength coefficient

$b \equiv$ the stress fatigue exponent

$S_{amp} \equiv$ the stress amplitude

$N_f \equiv$ the number of cycles to failure

For a set of (σ, n), stress and number of stress cycles at time (t), Equation 3-45 becomes:

$$\Lambda = \frac{n}{N_f} = \frac{n}{C_\sigma \, exp\left[A_\sigma \, ln\left(S_{amp}\right)\right]} \qquad \textbf{Equation 3-51}$$

Indices can be added to refer to the damage from specific operation, (O_i):

$$\Lambda_i = \frac{n_i}{C_\sigma \, exp\left[A_\sigma \, ln\left(S_{amp_i}\right)\right]} \qquad \textbf{Equation 3-52}$$

For high stress amplitude, a fatigue model based on strain amplitudes is used. The true plastic strain (ϵ_p) will be used to assess the fatigue damage. The fatigue model represented above can be reconstructed as, [74]:

$$N_f = C_\epsilon \, exp\left[A_\epsilon \, ln\left(\epsilon_{amp}\right)\right] \qquad \textbf{Equation 3-53}$$

where: $C_\epsilon = exp\left[-\frac{ln(\epsilon_f')}{c}\right]$

$A_\epsilon = \frac{1}{c}$

$\epsilon_f{}' \equiv$ fatigue ductility coefficient

$c \equiv$ fatigue ductility exponent

$\epsilon_{amp} \equiv$ plastic strain amplitude

$N_f \equiv$ the number of cycles to failure

The damage for specific number of cycles (n) for the short life model is presented by Equation 3-54

$$\Lambda = \frac{n}{N_f} = \frac{n}{C_\epsilon \, exp\left[A_\epsilon \, ln\left(\epsilon_{amp_i}\right)\right]} \qquad \textbf{Equation 3-54}$$

For a specific operation (O_i):, the damage becomes:

$$\Lambda_i = \frac{n_i}{C_\epsilon \, exp\left[A_\epsilon \, ln\left(\epsilon_{amp_i}\right)\right]} \qquad \textbf{Equation 3-55}$$

Equation 3-52 and Equation 3-55 represent the mechanical fatigue damage behavior for steel-like materials; the damage created by a stress cycle that is less than the yield strength of the material need to be assessed using Equation 3-52, the damage created by a stress cycle that is greater than the yield strength of the material need to be assessed using Equation 3-55. A feasible data management process needs to be developed to address the statistics of the models parameters $C_\sigma, A_\sigma, C_\epsilon, A_\epsilon$ and the system usage inputs: $S_{amp_i}, \epsilon_{amp_i}, n_i(t)$.

3.2.4 Single Component Degradation: One Operation, Single Failure Mechanism Damage Modeling

A single component exposed to one fatigue failure mechanism caused by a constant alternating single stress field will exhibit the linear damage progression trend shown in Figure 3-10 and represented by Equation 3-46 for mechanical fatigue.

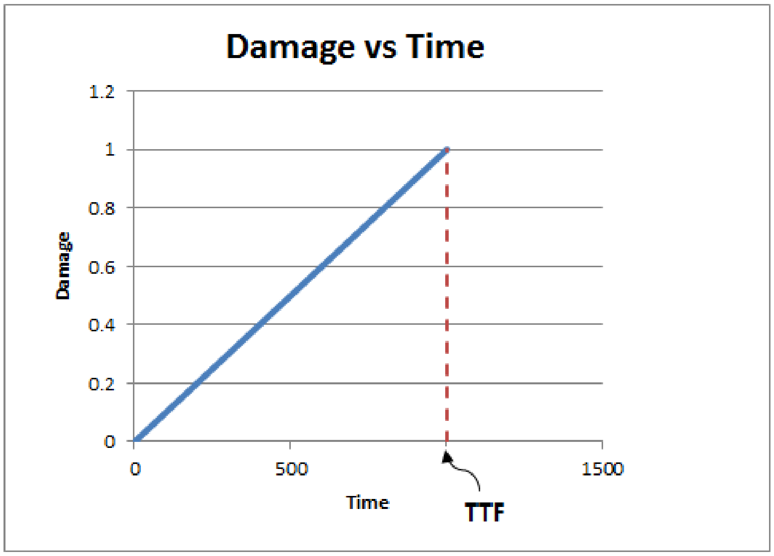

Figure 3-10: Damage progression due to a constant amplitude stress field, (TTF) is time to failure (equivalent to damage =1)

3.2.5 Single Component: Multiple Operations, Multiple Users, Single Failure Mechanism Damage Modeling

A component exposed to different operations will store the damage, created by an operation; according to Miner's rule. The total damage accumulated on a system component from a representative usage sample (a sample that captures all system usage operations with accurate operations percentage), over total sample elapsed time $\left(\sum_{i=1}^{m}(t^*)\right)$ is the summation over (i) for Λ_i^* as shown by Equation 3-56

$$\Lambda_T = \sum_{i=1}^{m} \Lambda_i^* = \sum_{i=1}^{m} \frac{n_i}{N_{f_i}} \qquad \textbf{Equation 3-56}$$

Where: $\Lambda_T \equiv$ total damage for the representative usage sample

$m \equiv$ number of operations performed by component

$\Lambda_i^* \equiv$ damage created by operation (O_i)

$n_i \equiv$ number of cycles accumulated at elapsed time (t^*) during operation (O_i)

$t = \sum_{i=1}^{m}(t^*) \equiv$ accumulative elapsed sample time (summation of operations elapsed times)

$N_{f_i} \equiv$ number of cycles to failure for stress level (σ_i) generated by operation (O_i)

Operations time duration could be stored in a vector $(\boldsymbol{u^j})$ that represents operation (O_i) usage time for a specific operator per unit time measurement, (for instance per T_g) the system design time goal, $(\boldsymbol{t}^{*\boldsymbol{j}})$ is presented by Equation 3-57:

$$\boldsymbol{t}^{*\boldsymbol{j}} = \begin{Bmatrix} Operation - 1\ duration \\ Operation - 2\ duration \\ \vdots \\ Operation - m\ duration \end{Bmatrix}^{j} = \begin{Bmatrix} {t^*}_1^j \\ {t^*}_2^j \\ {t^*}_3^j \\ \vdots \\ {t^*}_m^j \end{Bmatrix} \qquad \textbf{Equation 3-57}$$

where: $\boldsymbol{t}^{*\boldsymbol{j}} \equiv$ operator (j) usage for the set of (m) operations

For a set of system users, their usage time for a specific operation can be stored in the vector $(\boldsymbol{t}^*{}_{\boldsymbol{i}})$, presented by Equation 3-58

$$\boldsymbol{t}^*{}_{\boldsymbol{i}} = \{ {t^*}_i^1 \quad {t^*}_i^2 \quad {t^*}_i^3 \quad \cdots \quad {t^*}_i^h \} \qquad \textbf{Equation 3-58}$$

where: $\boldsymbol{t}^*{}_{\boldsymbol{i}} \equiv$ operation (i) time usage for the set of (h) operators

A sample of (h) users time-usage for a set of (m) operations can be stored in a matrix $(\boldsymbol{t}^*)$ as presented by Equation 3-59:

$$\boldsymbol{t}^* = \begin{bmatrix} t^{*1}_{1} & t^{*2}_{1} & \dots & t^{*h}_{1} \\ t^{*1}_{2} & t^{*2}_{2} & \dots & t^{*h}_{2} \\ \vdots & \vdots & \ddots & \vdots \\ t^{*1}_{m} & t^{*2}_{m} & \dots & t^{*h}_{m} \end{bmatrix} \qquad \textbf{Equation 3-59}$$

Equation 3-59 matrix needs to be converted to usage cycles per unit time measurement. Assuming the cycle rate per time usage is $\left(\dot{n}_i^j\right)$ for operation (O_i) for a specific operator (j), Equation 3-60 represents the vector format for $\dot{\boldsymbol{n}}^{\boldsymbol{j}}$

$$\dot{\boldsymbol{n}}^{\boldsymbol{j}} = \begin{Bmatrix} Operation - 1\ cycle\ rate \\ Operation - 2\ cycle\ rate \\ \vdots \\ Operation - m\ cycle\ rate \end{Bmatrix}^j = \begin{Bmatrix} \dot{n}_1^j \\ \dot{n}_2^j \\ \vdots \\ \dot{n}_m^j \end{Bmatrix} \qquad \textbf{Equation 3-60}$$

where: $\dot{\boldsymbol{n}}^{\boldsymbol{j}} \equiv$ operator (j) usage rate for the set of (m) operations

For a set of system users, their usage rate for a specific operation can be stored in the vector $(\boldsymbol{r_i})$, presented by Equation 3-61

$$\dot{\boldsymbol{n}}_{\boldsymbol{i}} = \{\dot{n}_i^1 \quad \dot{n}_i^2 \quad \dot{n}_i^3 \quad \cdots \quad \dot{n}_i^h\} \qquad \textbf{Equation 3-61}$$

where: $\dot{\boldsymbol{n}}_{\boldsymbol{i}} \equiv$ operation (i) rate of usage for the set of (h) operators

A sample of (h) users' usage rate for a set of (m) operations can be stored in a matrix $(\dot{\boldsymbol{n}})$ as shown by Equation 3-62:

$$\dot{\boldsymbol{n}} = \begin{bmatrix} \dot{n}_1^1 & \dot{n}_1^2 & \dots & \dot{n}_1^h \\ \dot{n}_2^1 & \dot{n}_2^2 & \dots & \dot{n}_2^h \\ \vdots & \vdots & \ddots & \vdots \\ \dot{n}_m^1 & \dot{n}_m^2 & \dots & \dot{n}_m^h \end{bmatrix} \qquad \textbf{Equation 3-62}$$

The number of usage cycles could be stored in a vector $(\boldsymbol{n}^{\boldsymbol{j}})$ that represents operations (O_i) number of cycles for a specific operator per unit time measurement, (for instance per T_g), as presented by Equation 3-63.

$$
\boldsymbol{n^j} = \begin{Bmatrix} Operation - 1\ number\ of\ cycle \\ Operation - 2\ number\ of\ cycle \\ \vdots \\ Operation - m\ number\ of\ cycle \end{Bmatrix}^j = \begin{Bmatrix} n_1 \\ n_2 \\ \vdots \\ n_m \end{Bmatrix}^j = \begin{Bmatrix} n_1^j \\ n_2^j \\ \vdots \\ n_m^j \end{Bmatrix} \qquad \textbf{Equation 3-63}
$$

A sample of (h) operators cycle usage vectors $\boldsymbol{n^j}$ can be stored in a matrix $\boldsymbol{n}$ as shown by Equation 3-64.

$$
\boldsymbol{n} = \begin{bmatrix} n_1^1 & n_1^2 & \dots & n_1^h \\ n_2^1 & n_2^2 & \dots & n_2^h \\ \vdots & \vdots & \ddots & \vdots \\ n_m^1 & n_m^2 & \dots & n_m^h \end{bmatrix} \qquad \textbf{Equation 3-64}
$$

The number of operations cycles is the multiplication of usage time by the usage rate, as shown by Equation 3-65

$$
\boldsymbol{n} = \begin{bmatrix} \dot{n}_1^1 t^{*1}_1 & \dot{n}_1^1 t^{*2}_1 & \dots & \dot{n}_1^1 t^{*h}_1 & \dot{n}_1^2 t^{*1}_1 & \dot{n}_1^2 t^{*2}_1 & \dots & \dot{n}_1^2 t^{*h}_1 & \dots & \dots & \dot{n}_1^h t^{*1}_1 & \dot{n}_1^h t^{*2}_1 & \dots & \dot{n}_1^h t^{*h}_1 \\ \dot{n}_2^1 t^{*1}_2 & \dot{n}_2^1 t^{*2}_2 & \dots & \dot{n}_2^1 t^{*h}_2 & \dot{n}_2^2 t^{*1}_2 & \dot{n}_2^2 t^{*2}_2 & \dots & \dot{n}_2^2 t^{*h}_2 & \dots & \dots & \dot{n}_2^h t^{*1}_2 & \dot{n}_2^h t^{*2}_2 & \dots & \dot{n}_2^h t^{*h}_2 \\ \vdots & \vdots & \ddots & \vdots & \vdots & \vdots & \ddots & \vdots & \vdots & \ddots & \vdots & \vdots & \ddots & \vdots \\ \dot{n}_m^1 t^{*1}_m & \dot{n}_m^1 t^{*2}_m & \dots & \dot{n}_m^1 t^{*h}_m & \dot{n}_m^2 t^{*1}_m & \dot{n}_m^2 t^{*2}_m & \dots & \dot{n}_m^2 t^{*h}_m & \dots & \dots & \dot{n}_m^h t^{*1}_m & \dot{n}_m^h t^{*2}_m & \dots & \dot{n}_m^h t^{*h}_m \end{bmatrix} \qquad \textbf{Equation 3-65}
$$

Operation (O_i) samples of (h) operators is the Kronecker tensor product of the usage rate vector $\left(\dot{n}_i^j\right)$ and usage time vector $\left(t^{*j}_i\right)$ for different operators, i.e. Kronecker tensor product of $\{\dot{n}_i^1 \quad \dot{n}_i^2 \quad \dot{n}_i^3 \quad \cdots \quad \dot{n}_i^h\}$ and $\{t^{*1}_i \quad t^{*2}_i \quad t^{*3}_i \quad \cdots \quad t^{*h}_i\}$ produces the sample set:

$[\{\dot{n}_i^1 t^{*1}_i \quad \dot{n}_i^1 t^{*2}_i \quad \dot{n}_i^1 t^{*3}_i \quad \cdots \quad \dot{n}_i^1 t^{*h}_i\} \quad \{\dot{n}_i^2 t^{*1}_i \quad \dot{n}_i^2 t^{*2}_i \quad \dot{n}_i^2 t^{*3}_i \quad \cdots \quad \dot{n}_i^2 t^{*h}_i\} \quad \cdots$

$\{\dot{n}_i^j t^{*1}_i \quad \dot{n}_i^j t^{*2}_i \quad \dot{n}_i^j t^{*3}_i \quad \cdots \quad \dot{n}_i^j t^{*h}_i\} \quad \cdots \quad \{\dot{n}_i^h t^{*1}_i \quad \dot{n}_i^h t^{*2}_i \quad \dot{n}_i^h t^{*3}_i \quad \cdots \quad \dot{n}_i^h t^{*h}_i\}]$;

internal brackets added for vector subset demonstration only, no relationship between vector subset elements. Another representation to Equation 3-65 is shown in Equation 3-66

$$\boldsymbol{n} = \begin{bmatrix} \dot{\boldsymbol{n}}_{\boldsymbol{1}} \otimes \boldsymbol{t}^{*}{}_{\boldsymbol{1}} \\ \dot{\boldsymbol{n}}_{\boldsymbol{2}} \otimes \boldsymbol{t}^{*}{}_{\boldsymbol{2}} \\ \dot{\boldsymbol{n}}_{\boldsymbol{3}} \otimes \boldsymbol{t}^{*}{}_{\boldsymbol{3}} \\ \vdots \\ \dot{\boldsymbol{n}}_{\boldsymbol{i}} \otimes \boldsymbol{t}^{*}{}_{\boldsymbol{i}} \\ \vdots \\ \dot{\boldsymbol{n}}_{\boldsymbol{m}} \otimes \boldsymbol{t}^{*}{}_{\boldsymbol{m}} \end{bmatrix}$$ **Equation 3-66**

Samples for operation (i) number of cycles vector is shown in Equation 3-67

$$\boldsymbol{n}_{\boldsymbol{i}} = \dot{\boldsymbol{n}}_{\boldsymbol{i}} \otimes \boldsymbol{t}^{*}{}_{\boldsymbol{i}}$$ **Equation 3-67**

In relation to mechanical fatigue, two material models are used for $\left(N_{f_i}\right)$, one for mechanical stress and strains below the yield strength of the material and another model for mechanical stress and strains above the yield strength of the material, presented by Equation 3-50 and Equation 3-53, i.e. $N_{f_i} = C_\sigma \, exp\left[A_\sigma \, ln\left(S_{amp_i}\right)\right]$, $N_{f_i} = C_\epsilon \, exp\left[A_\epsilon \, ln\left(\epsilon_{amp_i}\right)\right]$; the research will focus on the first model where cyclical stress amplitudes are below yield strength; the two main material parameters for this model are C_σ and A_σ, these two parameters are independent of component usage, the parameters can be presented in a matrix row set of material samples as shown by Equation 3-68 and Equation 3-69

$$\boldsymbol{A}_{\boldsymbol{\sigma}} = \{A_\sigma{}^1 \quad A_\sigma{}^2 \quad A_\sigma{}^3 \quad \cdots \quad A_\sigma{}^k \quad \cdots \quad A_\sigma{}^p\}$$ **Equation 3-68**

$$\boldsymbol{C}_{\boldsymbol{\sigma}} = \{C_\sigma{}^1 \quad C_\sigma{}^2 \quad C_\sigma{}^3 \quad \cdots \quad C_\sigma{}^k \quad \cdots \quad C_\sigma{}^p\}$$ **Equation 3-69**

The stress amplitudes for different operators for operation (O_i) can be stored in a vector matrix $\left(\boldsymbol{S}_{\boldsymbol{amp}_{\boldsymbol{i}}}\right)$ as shown by Equation 3-70

$$\boldsymbol{S}_{\boldsymbol{amp}_{\boldsymbol{i}}} = \left\{S_{amp_i}{}^1 \quad S_{amp_i}{}^2 \quad S_{amp_i}{}^3 \quad \cdots \quad S_{amp_i}{}^j \quad \cdots \quad S_{amp_i}{}^h\right\}$$ **Equation 3-70**

and for many operations, $\left(\boldsymbol{S_{amp_i}}\right)$ can be stored in $\left(\boldsymbol{S_{amp}}\right)$ matrix as shown by Equation 3-71.

$$\boldsymbol{S_{amp}} = \begin{bmatrix} {S_{amp}}_1^1 & {S_{amp}}_1^2 & \cdots & {S_{amp}}_1^j & \cdots & {S_{amp}}_1^h \\ {S_{amp}}_2^1 & {S_{amp}}_2^2 & \cdots & {S_{amp}}_2^j & \cdots & {S_{amp}}_2^h \\ \vdots & \vdots & \ddots & \vdots & \ddots & \vdots \\ {S_{amp}}_m^1 & {S_{amp}}_m^2 & \cdots & {S_{amp}}_m^j & \cdots & {S_{amp}}_m^h \end{bmatrix} \quad \textbf{Equation 3-71}$$

$\left(\boldsymbol{N_{f_i}}\right)$ is the number of cycles to failure for a specific stress amplitude $\left(\boldsymbol{S_{amp_i}}\right)$ produced by operation (O_i). All possible combinations of $\left(A_\sigma, C_\sigma, S_{amp_i}\right)$ results for $\left(\boldsymbol{N_{f_i}}\right)$ can be produced by the Kronecker multiplication of ($\boldsymbol{A_\sigma}$, $\boldsymbol{C_\sigma}$, $\boldsymbol{S_{amp_i}}$) as shown by Equation 3-72, the operations "ln" and "exp" are executed on individual vectors elements.

$$\boldsymbol{N_{f_i}} = \boldsymbol{C_\sigma} \otimes exp\left[\boldsymbol{A_\sigma} \otimes \ ln\left(\boldsymbol{S_{amp_i}}\right)\right] \quad \textbf{Equation 3-72}$$

Equation 3-72 produces the vector shown by Equation 3-73; with $(p^2 \times h)$ number of samples

$$\boldsymbol{N_{f_i}} = \left\{ {N_f}_i^1 \quad {N_f}_i^2 \quad {N_f}_i^3 \quad \cdots \quad {N_f}_i^l \quad \cdots \quad {N_f}_i^{p^2 \times h} \right\} \quad \textbf{Equation 3-73}$$

and the total damage produced by operation (O_i) can be presented by Equation 3-74

$$\boldsymbol{\Lambda_i^*} = \boldsymbol{n_i} \otimes \left(\frac{1}{\boldsymbol{C_\sigma} \otimes exp\left[\boldsymbol{A_\sigma} \otimes \ ln\left(\boldsymbol{S_{amp_i}}\right)\right]} \right) \quad \textbf{Equation 3-74}$$

Substituting Equation 3-67 into Equation 3-74 produces Equation 3-75

$$\boldsymbol{\Lambda_i^*} = \boldsymbol{\dot{n}_i} \otimes \boldsymbol{t^*}_i \otimes \left(\frac{1}{\boldsymbol{C_\sigma} \otimes exp\left[\boldsymbol{A_\sigma} \otimes \ ln\left(\boldsymbol{S_{amp_i}}\right)\right]} \right) \quad \textbf{Equation 3-75}$$

and Equation 3-75 produces the vector presented by Equation 3-76 with $(p^2 \times h^3)$ number of samples

$$\boldsymbol{\Lambda_i^*} = \{\Lambda_i^{*1} \quad \Lambda_i^{*2} \quad \Lambda_i^{*3} \quad \cdots \quad \Lambda_i^{*p^2 \times h^3}\} \qquad \textbf{Equation 3-76}$$

Equation 3-75 can be expanded to include design geometry factors (κ_g) which could be treated as a constant or statistical variable.

$$\boldsymbol{\Lambda_i^*} = \dot{\boldsymbol{n}}_{\boldsymbol{i}} \otimes \boldsymbol{t^*}_{\boldsymbol{i}} \otimes \left(\frac{1}{\boldsymbol{C_\sigma} \otimes exp\left[\boldsymbol{A_\sigma} \otimes \; ln\left(\kappa_g \boldsymbol{S_{amp_i}}\right)\right]} \right) \qquad \textbf{Equation 3-77}$$

Equation 3-77 shows (κ_s) as a constant scale to $\left(\boldsymbol{S_{amp_i}}\right)$; if (κ_s) is considered a statistical variable, a vector set of shape factors can be created and Kronecker multiplication between $\left(\boldsymbol{\kappa_g}\right)$ and $\left(\boldsymbol{S_{amp_i}}\right)$ need to be executed to produce $(q \times p^2 \times h^3)$ vector elements for $(\boldsymbol{\Lambda_i^*})$. (q) represents $\left(\boldsymbol{\kappa_g}\right)$ number of set elements. Considering instantaneous damage, the generic form of Equation 3-74 is presented in Equation 3-78.

$$\boldsymbol{\Lambda_i^*}(t^*|n, \sigma, M, G) = \dot{\boldsymbol{n}}_{\boldsymbol{i}} \otimes \boldsymbol{t^*}_{\boldsymbol{i}} \otimes \left(\frac{1}{\boldsymbol{C_\sigma} \otimes exp\left[\boldsymbol{A_\sigma} \otimes \; ln\left(\boldsymbol{\kappa_g} \otimes \boldsymbol{S_{amp_i}}\right)\right]} \right) \qquad \textbf{Equation 3-78}$$

A Matlab program, Appendix B.4, was developed to solve Equation 3-78 for every operation affecting components'' damage.

3.2.6 Damage Accumulation and Failure Paths

Several operations damage on a single component can be summed according to Miner's Rule, the main assumption of Miner's rule is that each operation damage is independent of all other operations damage; Figure 3-11 shows accumulated damage for three operations.

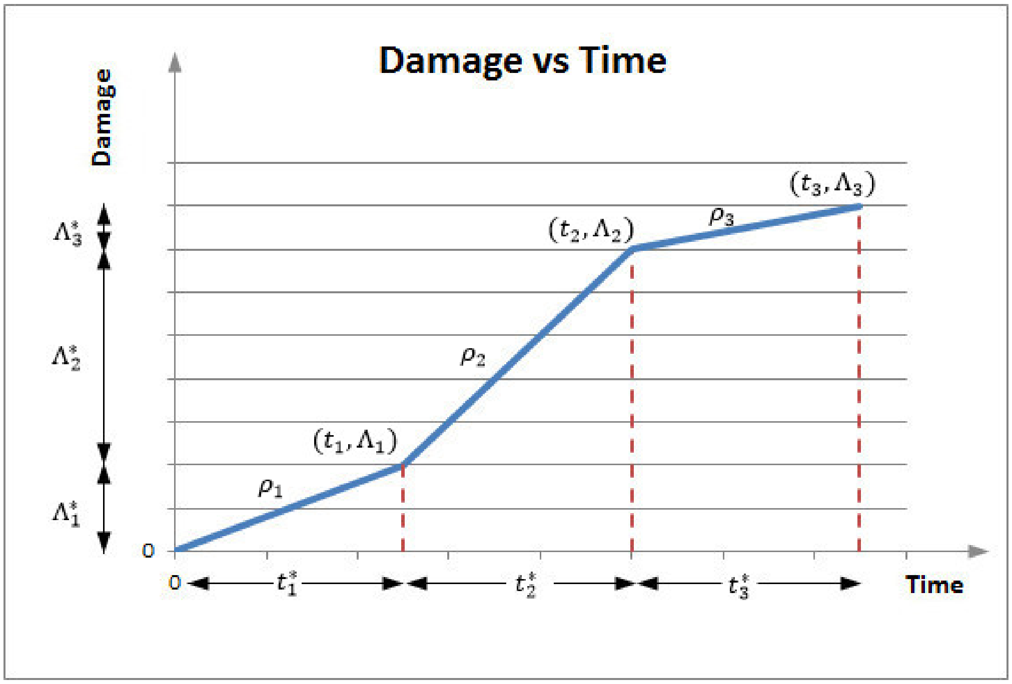

Figure 3-11: Accumulated damage for three operations

The accumulated time is the summation of each operation elapsed time. Due to the operations damage independency, each operation time can be treated as occurring and ending during a discrete time period; for example operation-1 is producing Λ_1^* damage, during elapsed time t_1^*. At the end of operation-1 the instantaneous time is t_1 and the accumulated damage is Λ_1 as shown by Equation 3-79 and Figure 3-11

$$t_1 = t_0 + t_1^* \,;\; (t_0 = 0) \rightarrow t_1 = t_1^* \qquad \textbf{Equation 3-79}$$

where: $t_0 \equiv$ initial time

$t_1^* \equiv$ operation-1 elapsed time; fraction of the total elapsed time (see Figure 3-11)

Equation 3-80 shows the relationship between operation damage and operation degradation

$$\Lambda_1^* = \rho_1 t_1^* \qquad \text{Equation 3-80}$$

where: $\Lambda_1^* \equiv$ damage generated by operation-1

$\rho_1 \equiv$ operation-1 degradation

Equation 3-81 shows the accumulated damage of the component at time (t_1)

$$\Lambda_1 = \Lambda_0 + \Lambda_1^* \,;\, (\Lambda_0 = 0) \rightarrow \Lambda_1 = \Lambda_1^* \qquad \text{Equation 3-81}$$

Substituting Equation 3-79 and Equation 3-81 variables to Equation 3-80 produces Equation 3-82

$$\Lambda_1 = \rho_1 t_1 \qquad \text{Equation 3-82}$$

Operations time can be stored in a vector matrix as shown by Equation 3-83 and Equation 3-84

$$\begin{Bmatrix} t_1 \\ t_2 \\ t_3 \\ \vdots \\ t_m \end{Bmatrix} = \begin{Bmatrix} t_0 + t_1^* \\ t_0 + t_1^* + t_2^* \\ t_0 + t_1^* + t_2^* + t_3^* \\ \vdots \\ t_0 + \sum_{j=1}^{m} t_j^* \end{Bmatrix} \qquad \text{Equation 3-83}$$

If $t_0 = 0$:

$$\begin{Bmatrix} t_1 \\ t_2 \\ t_3 \\ \vdots \\ t_m \end{Bmatrix} = \begin{Bmatrix} t_1^* \\ t_1^* + t_2^* \\ t_1^* + t_2^* + t_3^* \\ \vdots \\ \sum_{j=1}^{m} t_j^* \end{Bmatrix} \qquad \text{Equation 3-84}$$

And the same procedure can be applied to component accumulated damage; as shown by Equation 3-85 and Equation 3-86

$$\begin{Bmatrix} \mathit{\Lambda}_1 \\ \mathit{\Lambda}_2 \\ \mathit{\Lambda}_3 \\ \vdots \\ \mathit{\Lambda}_m \end{Bmatrix} = \begin{Bmatrix} \mathit{\Lambda}_0 + \mathit{\Lambda}_1^* \\ \mathit{\Lambda}_0 + \mathit{\Lambda}_1^* + \mathit{\Lambda}_2^* \\ \mathit{\Lambda}_0 + \mathit{\Lambda}_1^* + \mathit{\Lambda}_2^* + \mathit{\Lambda}_3^* \\ \vdots \\ \mathit{\Lambda}_0 + \sum_{j=1}^{m} \mathit{\Lambda}_j^* \end{Bmatrix}$$ **Equation 3-85**

If $\mathit{\Lambda}_0 = 0$:

$$\begin{Bmatrix} \Lambda_1 \\ \Lambda_2 \\ \Lambda_3 \\ \vdots \\ \Lambda_m \end{Bmatrix} = \begin{Bmatrix} \Lambda_1^* \\ \Lambda_1^* + \Lambda_2^* \\ \Lambda_1^* + \Lambda_2^* + \Lambda_3^* \\ \vdots \\ \sum_{j=1}^{m} \Lambda_j^* \end{Bmatrix}$$ **Equation 3-86**

Substituting the degradation model shown by Equation 3-82 produces the system shown by Equation 3-87

$$\begin{Bmatrix} \mathit{\Lambda}_1 \\ \mathit{\Lambda}_2 \\ \mathit{\Lambda}_3 \\ \vdots \\ \mathit{\Lambda}_{m-1} \\ \mathit{\Lambda}_m \end{Bmatrix} = \begin{bmatrix} \rho_1 & 0 & 0 & \cdots & 0 & 0 \\ (\rho_1 - \rho_2) & \rho_2 & 0 & \cdots & 0 & 0 \\ (\rho_1 - \rho_2) & (\rho_2 - \rho_3) & \rho_3 & \cdots & 0 & 0 \\ \vdots & \vdots & \vdots & \ddots & \vdots & \vdots \\ (\rho_1 - \rho_2) & (\rho_2 - \rho_3) & (\rho_3 - \rho_4) & \cdots & \rho_{m-1} & 0 \\ (\rho_1 - \rho_2) & (\rho_2 - \rho_3) & (\rho_3 - \rho_4) & & (\rho_{m-1} - \rho_m) & \rho_m \end{bmatrix} \begin{Bmatrix} t_1 \\ t_2 \\ t_3 \\ \vdots \\ t_{m-1} \\ t_m \end{Bmatrix}$$ **Equation 3-87**

$$\{\mathit{\Lambda}\} = \boldsymbol{\rho} \times \{t\}$$ **Equation 3-88**

where $\boldsymbol{\mathit{\Lambda}}$ ≡ accumulative damage per unit time measurement

$\boldsymbol{\rho}$ ≡ degradation matrix, Equation 3-89

$\{t\}$ ≡ operations accumulative time per unit time measurement

$$\boldsymbol{\rho} = \begin{bmatrix} \rho_1 & 0 & 0 & \cdots & 0 & 0 \\ (\rho_1 - \rho_2) & \rho_2 & 0 & \cdots & 0 & 0 \\ (\rho_1 - \rho_2) & (\rho_2 - \rho_3) & \rho_3 & \cdots & 0 & 0 \\ \vdots & \vdots & \vdots & \ddots & \vdots & \vdots \\ (\rho_1 - \rho_2) & (\rho_2 - \rho_3) & (\rho_3 - \rho_4) & \cdots & \rho_{m-1} & 0 \\ (\rho_1 - \rho_2) & (\rho_2 - \rho_3) & (\rho_3 - \rho_4) & & (\rho_{m-1} - \rho_m) & \rho_m \end{bmatrix}$$ **Equation 3-89**

Damage failure path vector is produced by dividing each element of $\{\Lambda\}$ by the lowest vector element, i.e the total accumulated damage of all operations due to their proportional usage. This produces, $\boldsymbol{P_D}$, the accumulative damage to failure; shown by Equation 3-90

$$\boldsymbol{P_D} = \begin{Bmatrix} \Lambda_1/\Lambda_m \\ \Lambda_2/\Lambda_m \\ \Lambda_3/\Lambda_m \\ \vdots \\ \Lambda_{m-1}/\Lambda_m \\ \Lambda_m/\Lambda_m \end{Bmatrix} = \begin{Bmatrix} \Lambda_1/\Lambda_m \\ \Lambda_2/\Lambda_m \\ \Lambda_3/\Lambda_m \\ \vdots \\ \Lambda_{m-1}/\Lambda_m \\ 1 \end{Bmatrix} \qquad \textbf{Equation 3-90}$$

where $\boldsymbol{P_D} \equiv$ cumulative damage to failure vector

$\Lambda_m = \Lambda_0 + \sum_{j=1}^{m} \Lambda_j^* \equiv$ damage summation for the representative usage sample; used as a scale factor, see Equation 3-85

The equivalent time-increments vector to $(\boldsymbol{P_D})$ can be generated by multiplying the inverse of the degradation matrix by $\{\boldsymbol{P_D}\}$.

$$\boldsymbol{P_T} = \boldsymbol{\rho}^{-1} \times \boldsymbol{P_D} \qquad \textbf{Equation 3-91}$$

where: $\boldsymbol{P_T} \equiv$ equivalent time increments vector to the accumulative damage to failure vector $\{\boldsymbol{P_D}\}$

Time to failure is the element at the bottom of $\boldsymbol{P_T}$ vector; i.e. $P_T(m)$; equivalent to an accumulative unity damage on $\boldsymbol{P_D}$ vector

$$TTF = P_T(m) \qquad \textbf{Equation 3-92}$$

where $TTF \equiv$ component time to failure

Plotting the vector $\boldsymbol{P_D}$ versus $\boldsymbol{P_T}$ produces the path to failure as shown by the example presented in Figure 3-12

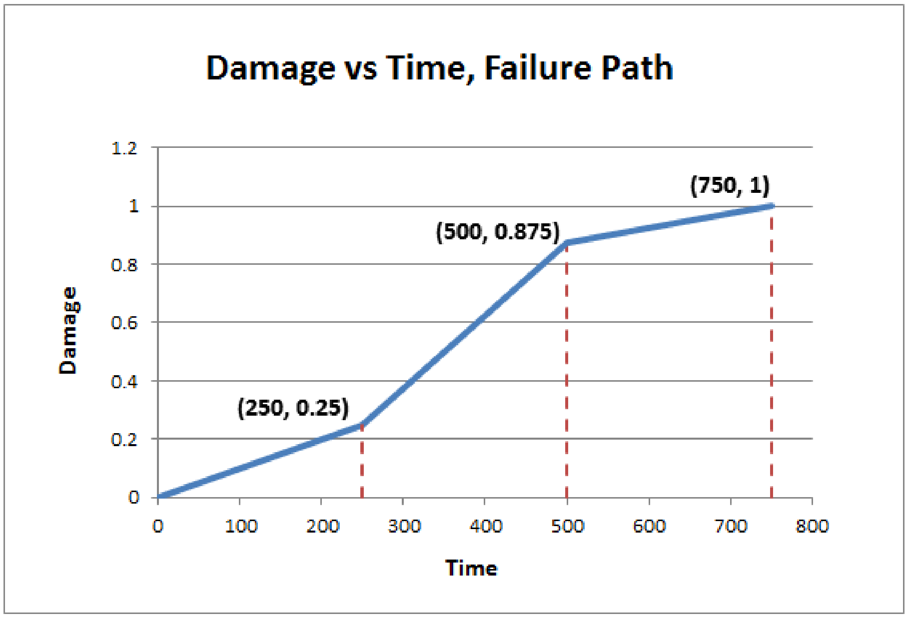

Figure 3-12: Component's path to failure ($\boldsymbol{P_T}, \boldsymbol{P_D}$) example

For the example shown by Figure 3-12: $(\boldsymbol{P_T})$ and $(\boldsymbol{P_D})$ are shown in Equation 3-90; when the damage reaches unity, failure occurs; i.e.TTF is, $\boldsymbol{P_T}(4)$, 750 hours as presented by Equation 3-93.

$$\boldsymbol{P_D} = \begin{Bmatrix} 0.25 \\ 0.875 \\ 1 \end{Bmatrix}; \quad \boldsymbol{P_T} = \begin{Bmatrix} 250 \\ 500 \\ 750 \end{Bmatrix} \qquad \textbf{Equation 3-93}$$

Equation 3-78 solves for the set of damage samples produced by one operation (O_i). For a set of more than one operation, the damage summation process for one sample was outlined by the set of equations: Equation 3-79 to Equation 3-91; to manage the damage path samples generated by more than one operation a data organization process to assure all possible damage paths are assessed and included is needed. Sample space for damage ratios and equivalent elapsed time need to be developed; Equation 3-94 shows the sample space for two vector $\boldsymbol{A}$ and $\boldsymbol{B}$ that would be developed for the accumulative damage process to be carried over the subsets $\{A_i, B_j\}$ as elaborated by the set of equations: Equation 3-79 to Equation 3-91.

$$S(\boldsymbol{A},\boldsymbol{B}) = \{\{A_1,B_1\},\{A_1,B_2\},\{A_1,B_3\},\dots,\{A_1,B_n\},$$
$$\{A_2,B_1\},\{A_2,B_2\},\{A_2,B_3\},\dots,\{A_2,B_n\},$$
$$\{A_3,B_1\},\{A_3,B_2\},\{A_3,B_3\},\dots,\{A_3,B_n\},$$
$$\dots,$$
$$\{A_m,B_1\},\{A_m,B_2\},\{A_m,B_3\},\dots,\{A_m,B_n\}\}$$

Equation 3-94

where: $\boldsymbol{A} \equiv n \times 1$ vector matrix

$\boldsymbol{B} \equiv m \times 1$ vector matrix

$S(\boldsymbol{A},\boldsymbol{B}) \equiv$ sample space of vector matrices $\boldsymbol{A}$ and $\boldsymbol{B}$; with $(m \times n)$ subsets

For (u) vectors with equal number of samples (m); the number of $S(\boldsymbol{A},\boldsymbol{B})$ subsets is equal to (m^u). For (u) vectors the short notation for sample space is presented by Equation 3-95.

$$\mathrm{S}_{i=1}^{u}(\boldsymbol{A_i}) = S(\boldsymbol{A_1},\boldsymbol{A_2},\boldsymbol{A_3}\dots,\boldsymbol{A_u})$$

Equation 3-95

where: $\boldsymbol{A_i} \equiv n_i \times 1$ vector matrix; n_i is a variable equal to each vector matrix number of elements; n_i varies from n_1 to n_u

$\mathrm{S}_{i=1}^{u} \equiv$ operator on set of vector matrices $(\boldsymbol{A_i})$; it generates sample space for vectors $i = 1$ to $i = u$; with: $\prod_1^u n_i = (n_1 \times n_2 \times n_3 \times \dots \times n_u)$ number of subsets

Equation 3-95 is expanded for demonstration in Equation 3-96; if the number of each matrix vector is the same, say (m), then $\mathrm{S}_{i=1}^{u}(\boldsymbol{A_i})$ will have (m^u) elments

$$S_{i=1}^{u}(\boldsymbol{A_i}) = \Big\{\{A_1^1, A_2^1, \dots, A_u^1\}, \{A_1^2, A_2^1, \dots, A_u^1\}, \dots, \{A_1^k, A_2^1, \dots, A_u^1\},$$
$$\{A_1^1, A_2^2, \dots, A_u^1\}, \{A_1^2, A_2^2, \dots, A_u^1\}, \dots, \{A_1^1, A_2^l, \dots, A_u^1\},$$
$$\dots,$$
$$\{A_1^k, A_2^l, \dots, A_u^1\}, \{A_1^k, A_2^l, \dots, A_u^2\}, \dots, \{A_1^k, A_2^l, \dots, A_u^m\}\Big\}$$

Equation 3-96

Figure 3-13 shows an example to 3 operations with 3 damage samples each on a single component; $S_{i=1}^{u}(\boldsymbol{A_i})$ produces, 3^3, =27 possible damage paths and TTF samples.

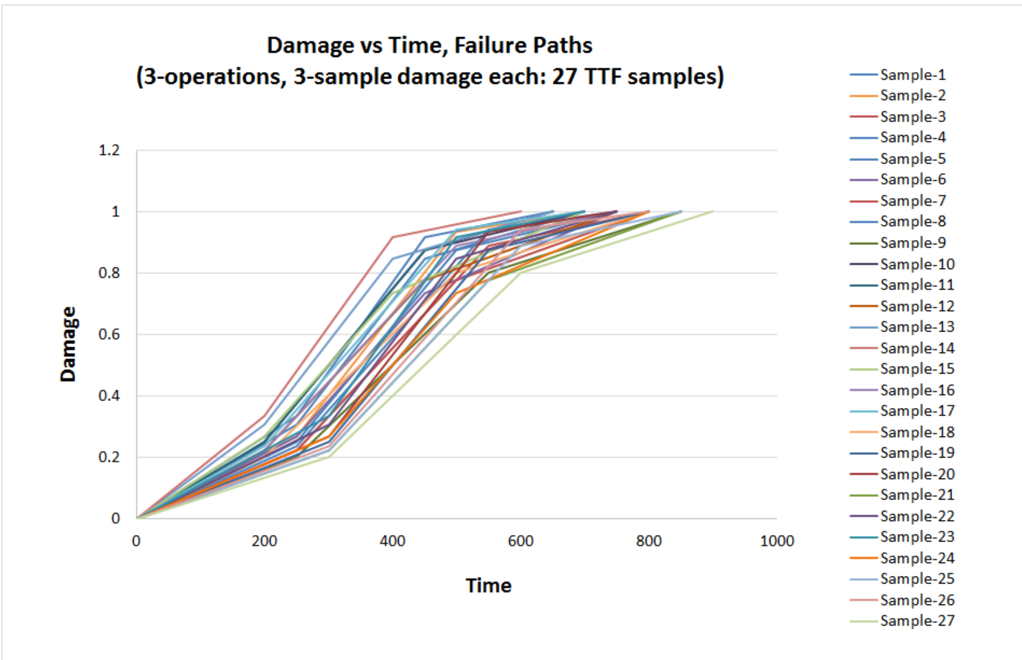

Figure 3-13: Example of 3-operations, 3-samples each; the resultant of $S_{i=1}^{u}(A_i)$ is $3^3 = 27$ TTF samples

Considering many users' samples, we can find the lower and upper envelop to all failure paths by sorting the operations' degradations in ascending order for the maximum TTF sample path as shown by Figure 3-14 we call this path the lower failure path (LFP); the same can be done to the minimum TTF damage path; we can sort the degradation in descending order to develop the upper failure path (UFP) as shown by Figure 3-15. All possible failure paths will be inside the envelope created by these two paths.

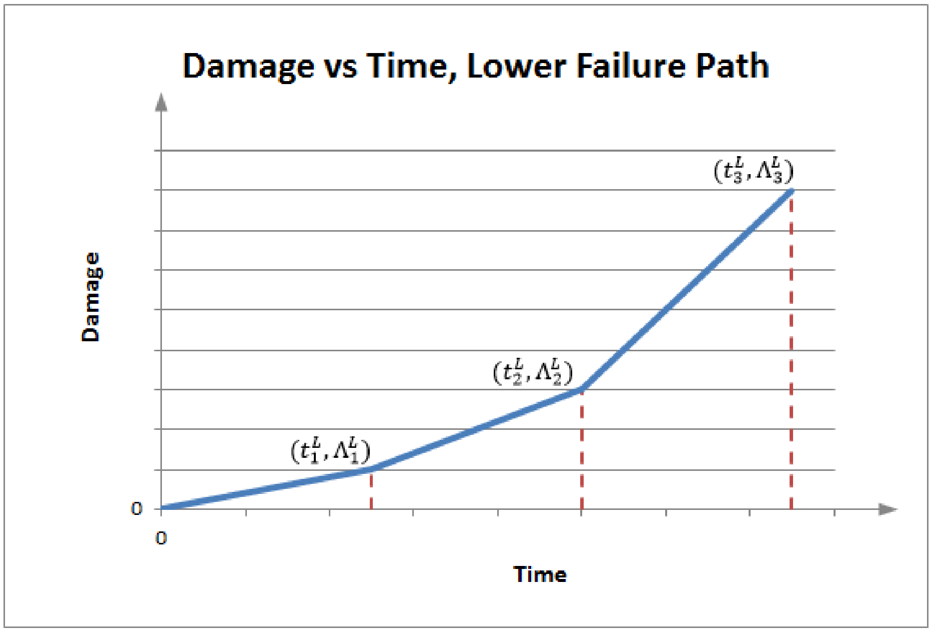

Figure 3-14: Lower Failure Path

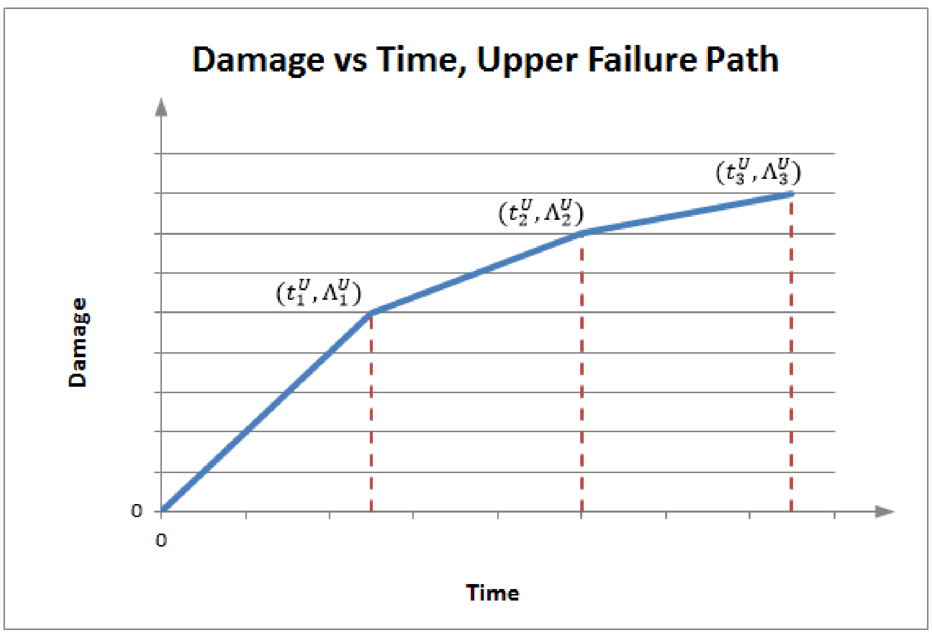

Figure 3-15: Upper Failure Path

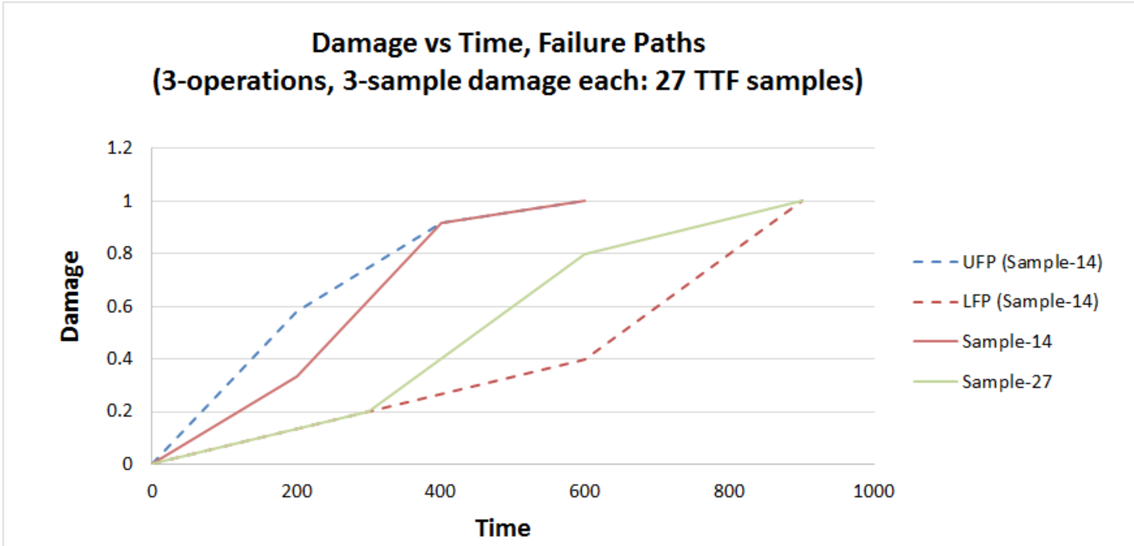

Figure 3-16: Example of UFP and LFP for the example presented by Figure 3-13, UFP and LFP is produced by sample 14 and sample 27 respectively

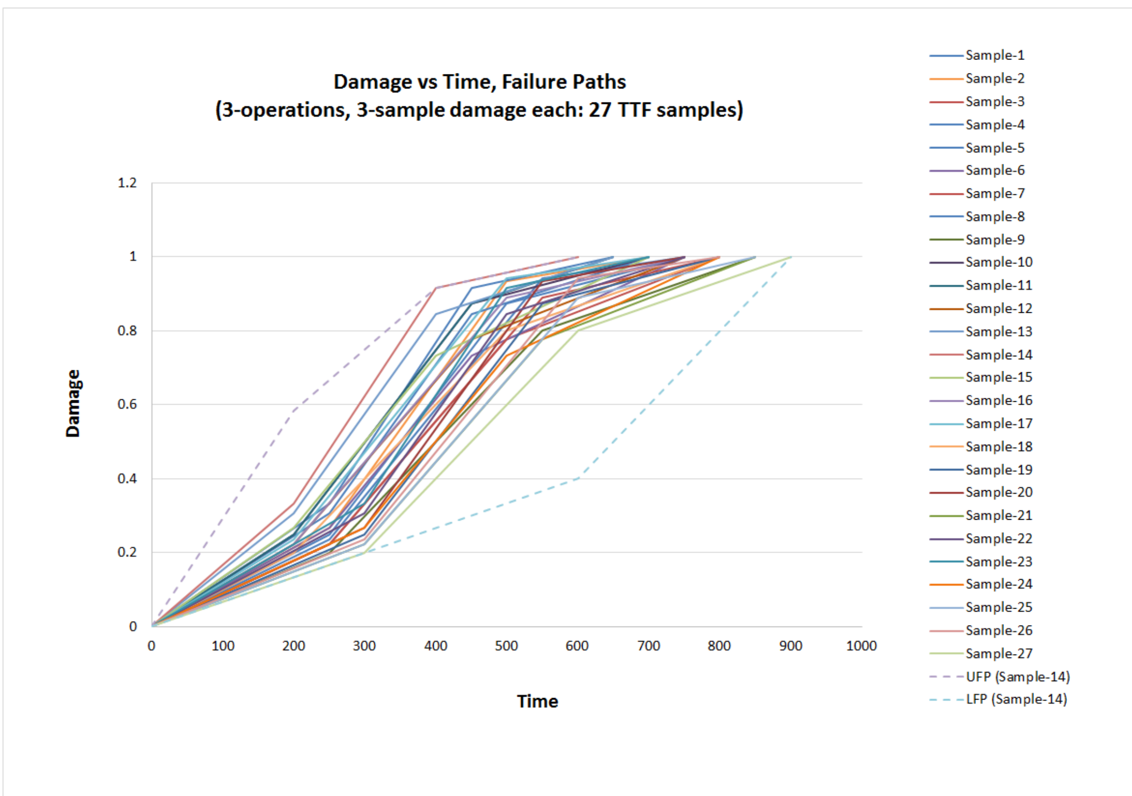

Figure 3-17: UFP, LFP and all other possible paths

By sorting TTF vector of all users' samples of usage in ascending order we can develop the vector $\boldsymbol{TTF_E^A}$, the median of $\boldsymbol{TTF_E}$ can be selected according to the method shown by Equation 3-97.

$$\widetilde{TTF_E} = \begin{cases} \boldsymbol{TTF_E^A}\left(\dfrac{\phi+1}{2}\right); & if\ (m)\ is\ an\ odd\ number \\ \dfrac{\boldsymbol{TTF_E^A}\left(\frac{\phi}{2}\right) + \boldsymbol{TTF_E^A}\left(\frac{\phi}{2}+1\right)}{2}; & if\ (m)\ is\ an\ even\ number \end{cases}$$ **Equation 3-97**

where: $\widetilde{TTF_E}$ ≡ median of time to failure vector

$\boldsymbol{TTF_E^A}$ ≡ ascendingly-sorted time to failure vector; i.e. from $\boldsymbol{TTF_E^A}$

$\boldsymbol{TTF_E^A}(i)$ ≡ ith row on $\boldsymbol{TTF_E^A}$ column vector, or ith column on $\boldsymbol{TTF_E^A}$ row vector

ϕ ≡ number of TTF samples

For one-operation damage model like the one presented by Equation 3-78 the number of TTF samples: $\phi = q \times p^2 \times h^3$; for mutliple (m) operations the number of TTF is: $\phi = (q \times p^2 \times h^3)^m$.

$$\phi = (q \times p^2 \times h^3)^m$$ **Equation 3-98**

where: ϕ ≡ number of TTF samples

h ≡ number of random users samples

p ≡ number of random design material samples

q ≡ number of random design geometry shape parameters samples

m ≡ number of system's operations

The mean of TTF is the algebraic average of the unsorted $\boldsymbol{TTF}$ vector as shown by Equation 3-99

$$\overline{TTF_E} = \sum_{i=1}^{\phi} \boldsymbol{TTF_E}(i)$$ Equation 3-99

where: $\overline{TTF_E} \equiv$ mean of time to failure vector

$\boldsymbol{TTF_E} \equiv$ unsorted time to failure vector

$\boldsymbol{TTF_E}(i) \equiv i$th row on $\boldsymbol{TTF_E}$ column vector, or ith column on $\boldsymbol{TTF_E}$ row vector

$\phi \equiv$ number of TTF samples

3.2.7 Multiple Failure Mechanisms Damage

For a single component, the damage created by many failure mechanism occurring at the same time can be recognized based on the damage location on the component. Figure 3-18 shows the categories of cumulative damage based on its location on the component

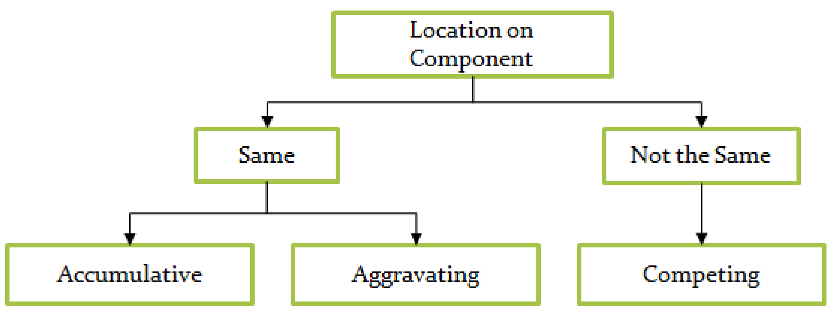

Figure 3-18: Component Damage: Categories

Cumulative damage is a type of damage that can be algebraically summed, i.e. two failure mechanisms damages can be summed to predict the effect of both over time; for example; thermal stresses and mechanical stresses generating fatigue failure affecting the same location on a component where the material doesn't exhibit phase shift due to increase in temperature.

Aggravated damage is a type of damage that cannot be algebraically summed; i.e. two failure mechanisms when they exist together on the same location of a component lead to aggravating the damage that could be produced by each separately; such behavior requires a new damage model to predict TTF produced by both stress agents working simultaneously; example: presence of mechanical fatigue and corrosion at the same location of a component.

When the location of stress agents on a component is not the same, competing damage can be considered; the TTF of this component will be determined by the failure mechanism that reaches unity first; for example: mechanical stress and corrosion that are affecting two different locations in a component.

Additive Failure Mechanisms Damages

Component additive failure mechanisms damage model can be used if:

1. Damage is generated by operations stress agents
2. The damage generated by failure mechanisms can be algebraically summed.

The damage accumulated over an elapsed time (t^*) can be modeled as following:

$$\Lambda_i(t^*) = \sum_{j=1}^{n} d_{FM_j}^{O_i}(t^*) \quad \textbf{Equation 3-100}$$

where: $\Lambda_i(t^*) \equiv$ component accumulated damage over an elapsed time (t^*) for operation (O_i)

$d_{FM_j}^{O_i}(t^*) \equiv$ damage accumulated at the end of operation (O_i) due to failure mechanism (FM_j).

Expanding the summation;

$$\Lambda_i(t^*) = \left[d_{FM_1}^{O_i}(t^*) + d_{FM_2}^{O_i}(t^*) + \cdots + d_{FM_n}^{O_i}(t^*)\right] \qquad \textbf{Equation 3-101}$$

Aggravating Failure Mechanisms Damages

The aggravating damage modeling assumes existence of a damage model that captures the presence of more than one stress agent; the damage modeling process is similar to the single failure mechanism process presented in section 3.2.5.

Competing Failure Mechanisms Damages

Competing failure mechanisms damage model can be used if failure mechanisms affect different locations on a component; the first location damage that reaches one fails first; damage generated from operation (O_i) can be modeled as shown by Equation 3-102:

$$\Lambda_i(t^*) = Max\left\{ d_{FM_j}^{O_i}(t^*)\right\}$$
$$= Max\left\{ d_{FM_1}^{O_i}(t^*), d_{FM_2}^{O_i}(t^*), \dots, d_{FM_n}^{O_i}(t^*)\right\} \qquad \textbf{Equation 3-102}$$

3.2.8 Component Mechanistic PoF Algorithm

Figure 3-38 shows the algorithm developed to assess the reliability of system components. Appendix B.1 shows the Matlab code developed to numerically solve the problem.

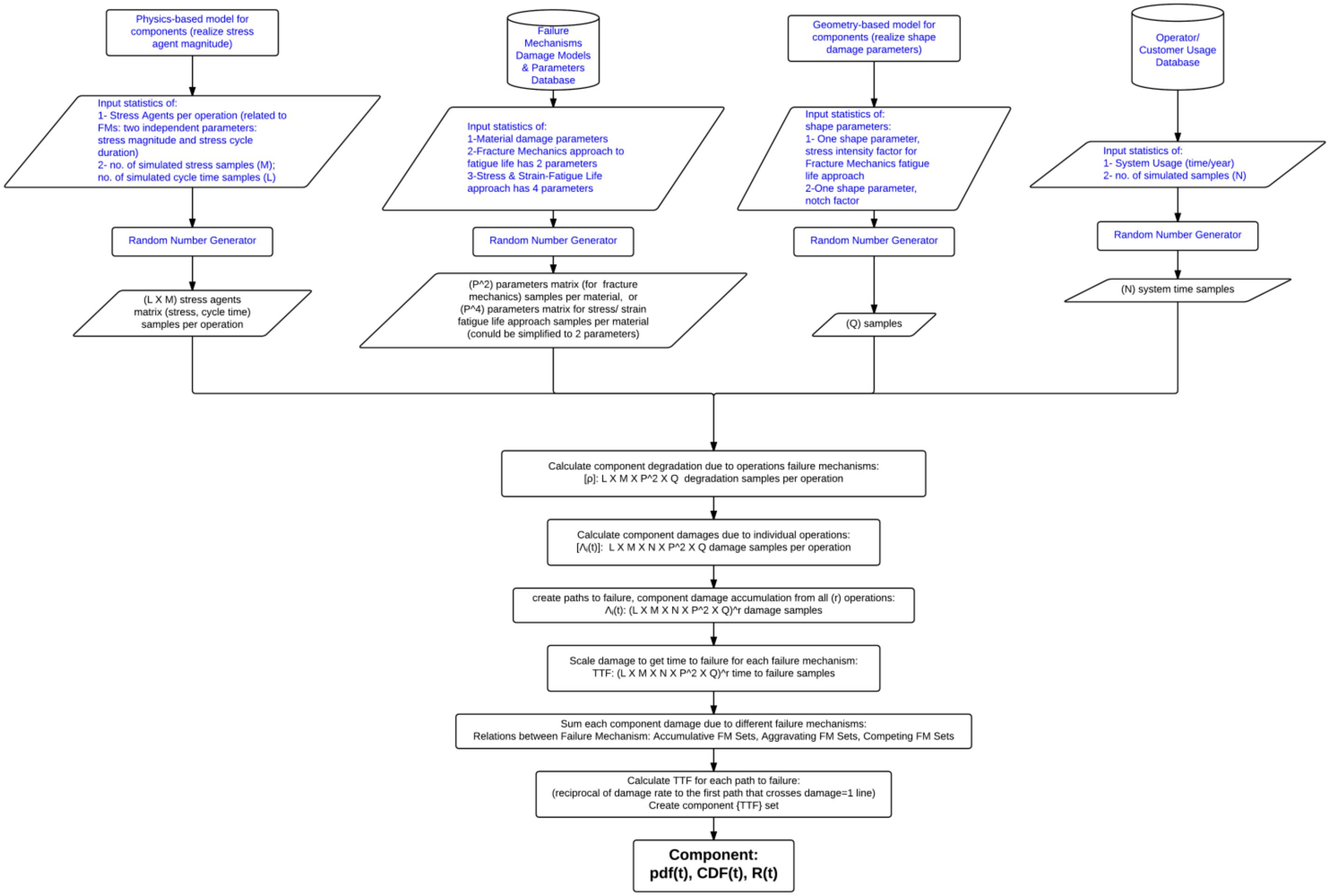

Figure 3-19: Component Mechanistic PoF Reliability Algorithm

3.3 System Reliability

The importance of a system component comes from its ability to keep the system running. The impact of a component failure on system operation can be analyzed by looking at the impact of the failure of that component on the other components damage progression and the impact on the overall system damage. In relation to the impact of the damage of one component on other components, we can recognize the two behaviors presented in Figure 3-20 and Figure 3-21; *this research will focus mainly on independent component damage models*.

Considering system damage we can define Synchronous Damage (Figure 3-20) as a representation to two independent damage progression trends that are not affected by each other. Asynchronous Damage (Figure 3-21) on the other hand represents a damage of a component that starts to progress at the event of a failure of another component, for example backup system components.

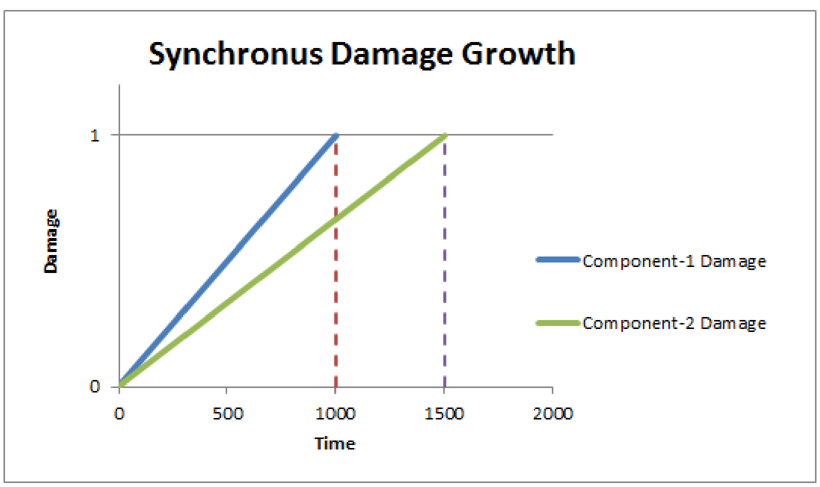

Figure 3-20: Two Components Synchronous Damage

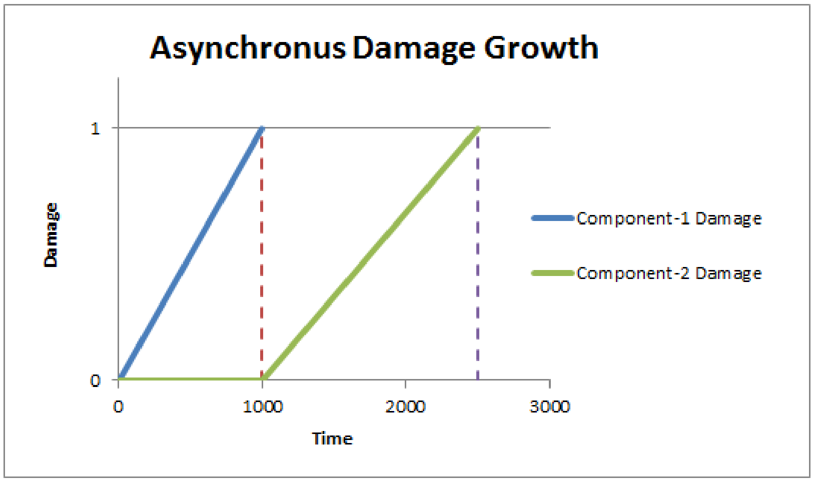

Figure 3-21: Two Components Asynchronous Damage

3.3.1 System Damage – Synchronous Degradation

The system damage behavior for synchronous-damage components can be modeled after the impact of the first component failure and/or the last component failure; there are two types of synchronous damage behaviors:

1. Synchronous-1: where the failure of the first component within a system or subsystem leads to system failure; this is typical of components that deliver portion of a function within a functional system or subsystem. **SYNC1** will be used as abbreviation for this type.
2. Synchronous-2: where the failure of the last component within a system or subsystem leads to system failure: this is typical of components that work together to deliver system functionality. **SYNC2** will be used as abbreviation for this system.

For **SYNC1** system damage behavior, the maximum damage model represents the system damage behavior; represented by Equation 3-103; the system instantaneous damage is the maximum of components instantaneous damages. Figure 3-22 shows this behavior for a system of two components. System time-to-failure, as shown by Equation 3-104, would be the minimum of the components individual TTF; for **SYNC1**:

$$\Lambda_{sys}(t) = Max\{\Lambda_i(t)\}$$ **Equation 3-103**

where, $\{\Lambda_i(t)\}$ represents a set of $\Lambda(t)$ for the individual components that compose the system.

$$TTF_{sys} = Min\{TTF_i\}$$ **Equation 3-104**

where, $\{TTF_i\}$ represents a set of TTF for the individual components that compose the system.

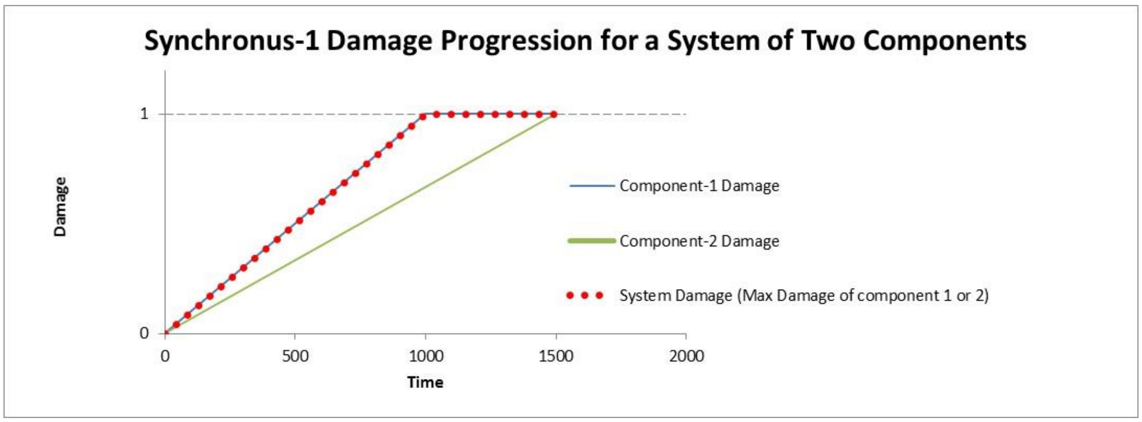

Figure 3-22: Synchronous-1 System Damage Behavior

Figure 3-23 shows simulation of TTF and failure probability of the two **SYNC1** system described by Figure 3-22. Appendix B.11 presents a Matlab program that performs the (TTF) simulation of any number of components affected by **SYNC1** damage behavior.

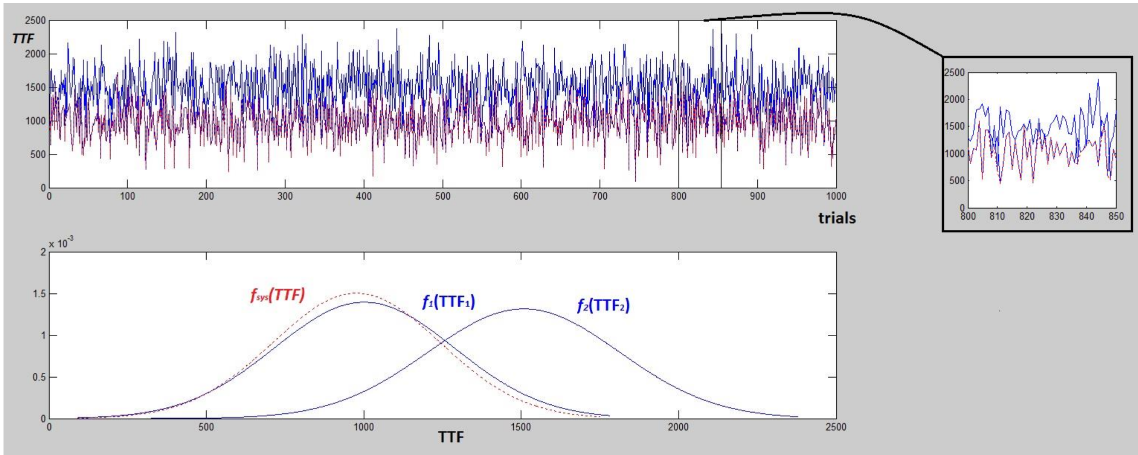

Figure 3-23: System Failure Probability Simulation Results; Max Damage Model of Two Synchronous-Damage Components

For **SYNC2** system damage behavior, the minimum damage model represents the system damage behavior; represented by Equation 3-105, the system instantaneous damage is the minimum of components instantaneous damage. Figure 3-24 shows this behavior for a system of two components. System time-to-failure, as shown by Equation 3-106, would be the minimum of the components individual TTF; for **SYNC2** degradation:

$$\Lambda_{sys}(t) = Min\{\Lambda_i(t)\} \qquad \textbf{Equation 3-105}$$

where, $\{\Lambda_i(t)\}$ represents a set of $\Lambda(t)$ for the individual components that compose the system.

$$TTF_{sys} = Max\{TTF_i\} \qquad \textbf{Equation 3-106}$$

where, $\{TTF_i\}$ represents a set of TTF for the individual components that compose the system.

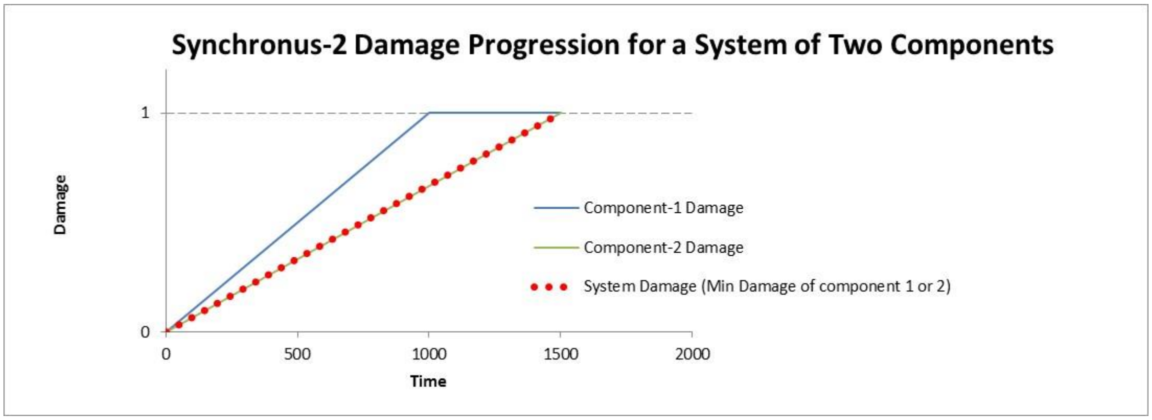

Figure 3-24: Synchronous-2 System Damage Behavior

Figure 3-25 shows simulation of TTF and failure probability of the two **SYNC2** system described by Figure 3-24. Appendix B.12 presents a Matlab program that performs the (TTF) simulation of any number of components affected by **SYNC2** damage behavior.

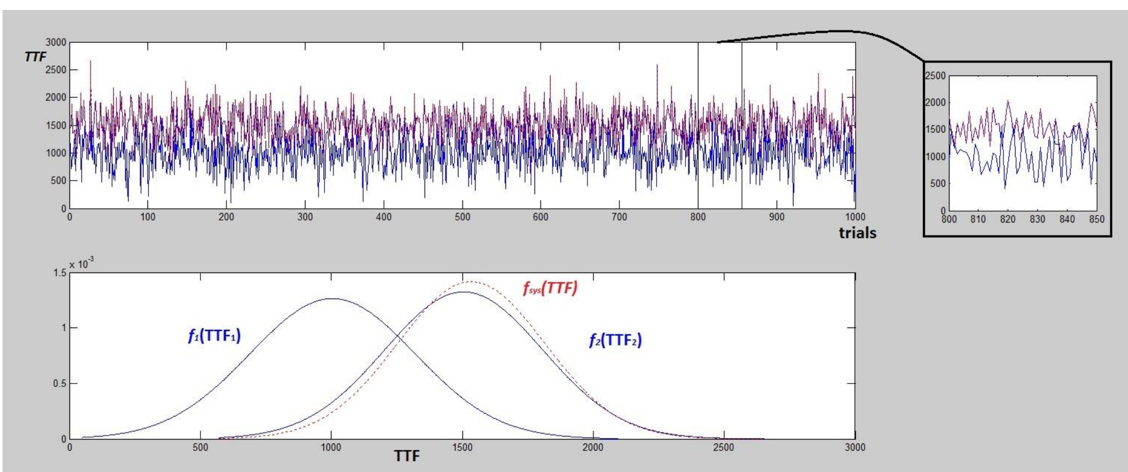

Figure 3-25: System Failure Probability Simulation Results; Min Damage Model of Two Synchronous-Damage Components

3.3.2 System Damage – Asynchronous Degradation

For asynchronous-damage components; the system wouldn't fail until all components fail. Each component, independently, would be able to deliver the functionality of the system. The average system damage path can be represented with Equation 3-107. Figure 3-26 shows this behavior for a system of two components. System time-to-failure, as shown by Equation 3-108 would be the algebraic sum of individual components TTF; for **ASYNC** degradation:

$$\Lambda_{sys}(t) = \left(\frac{\prod \rho_i}{\sum \rho_i}\right) t \qquad \textbf{Equation 3-107}$$

where: $\rho_i \equiv$ degradations of the individual components that compose the system.

$$TTF_{sys} = \sum_{i=1}^{n} \{TTF_i\} \qquad \textbf{Equation 3-108}$$

where: $\{TTF_i\} \equiv$ set of TTF for the individual components that compose the system.

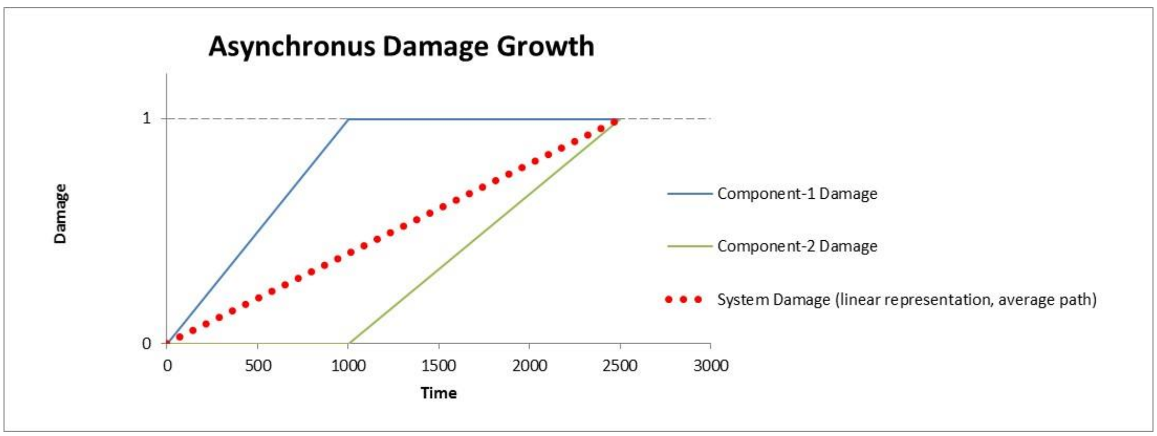

Figure 3-26: Asynchronous System Damage

Figure 3-27 shows simulation of TTF and failure probability of the two ASYNC system described by Figure 3-26. Appendix B.13 presents a Matlab program that performs the (TTF) simulation of any number of components affected by A**SYNC** damage behavior.

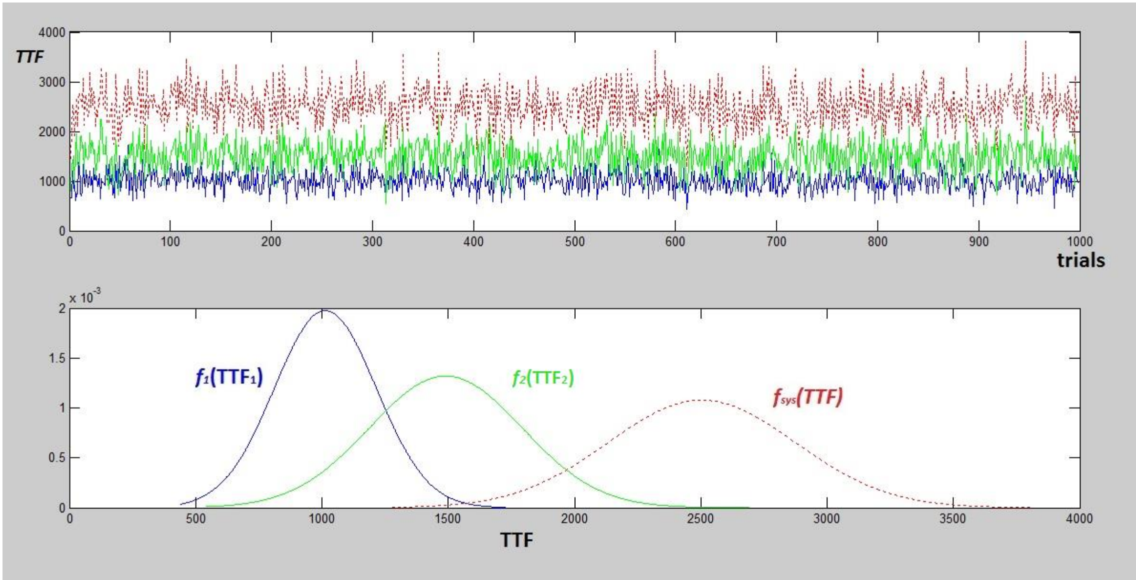

Figure 3-27: System Failure Probability Simulation Results; Damage Model of Two Asynchronous-Damage Components

3.3.3 System Damage and TTF Statements

The system damage statement describes the system damage behavior by leveraging W-and H-relationship statements and using the operators set {**SYNC1, SYNC2, ASYNC**} as descriptors. Equation 3-109 shows a system damage statement to five subsystems.

$$\Lambda_{SYS} = \mathbf{SYNC1}\left(\Lambda_{S_1}, \mathbf{ASYNC}\left(\Lambda_{S_5}, \mathbf{SYNC1}\left(\Lambda_{S_2}, \mathbf{ASYNC}(\Lambda_{S_3}, \Lambda_{S_4})\right)\right)\right) \quad \textbf{Equation 3-109}$$

System TTF statement, on the other hand, uses the system damage statement to assess the time to failure of the system. It uses the operator (ProbSpace) to generate set of sets of all possible combinations of the subsystems' TTF; before executing the operators set {**SYNC1, SYNC2, ASYNC**} as described in section (3.3.1) and section(3.3.2) on (ProbSpace) created probability domain. Equation 3-110 shows the equivalent system TTF statement of Equation 3-109.

$$TTF_{SYS} = \mathbf{SYNC1}\big(\text{ProbSpace}\big\{TTF_{S_1}, \mathbf{ASYNC}\big(\text{ProbSpace}\,\big\{TTF_{S_5}, \mathbf{SYNC1}\big(\text{ProbSpace}\big\{TTF_{S_2}, \mathbf{ASYNC}\big(\text{ProbSpace}\big\{TTF_{S_3}, TTF_{S_5}\big\}\big)\big\}\big)\big\}\big)\big\}\big) \quad \textbf{Equation 3-110}$$

3.4 System Availability Assessment

Considering a repairable component with linear degradation and repair behavior; a failure and repair cycle represents the damage behavior during the time interval starting at the end of the previous repair event and ending at the beginning of damage progression of the next failure event; if the component is repaired and put back on service to immediately start accumulating damage at the end time of repair it can, graphically, be represented by Figure 3-28. This behavior can mathematically be modeled using the formulation presented by Equation 3-111 and Equation 3-114:

$$for: (m-1)(TTF+TTR) \leq t_f \leq (m-1)(TTF+TTR)+(TTF) \rightarrow$$

$$0 \leq \Lambda(t) \leq 1 \quad \textbf{Equation 3-111}$$

$$\Lambda(t) = \frac{t_f}{TTF} - \frac{(m-1)(TTF+TTR)}{TTF}$$

where: $m \equiv$ Cycle number

$TTF \equiv$ component time to failure

$TTR \equiv$ component time to repair

$t_f \equiv$ time during damage progression phase

The reverse model for $t_f(\Lambda)$ is

$$t_f(\Lambda) = TTF.\Lambda + (m-1)(TTF + TTR) \quad \textbf{Equation 3-112}$$

The linear repair process which follows the occurrence of a failure event can mathematically be modeled as:

$$for: (m-1)(TTF + TTR) + (TTF) < t_r < m(TTF + TTR) \rightarrow \Lambda(t) \leq 1, \Lambda(t) \geq 0$$

$$\Lambda(t) = \frac{m(TTF + TTR) - t_r}{TR} \quad \textbf{Equation 3-113}$$

The reverse model for $t_r(d)$ is

$$t_r(\Lambda) = m(TTF + TTR) - TTR.\Lambda \quad \textbf{Equation 3-114}$$

Figure 3-28 shows a generic mth failure/repair cycle of a single component.

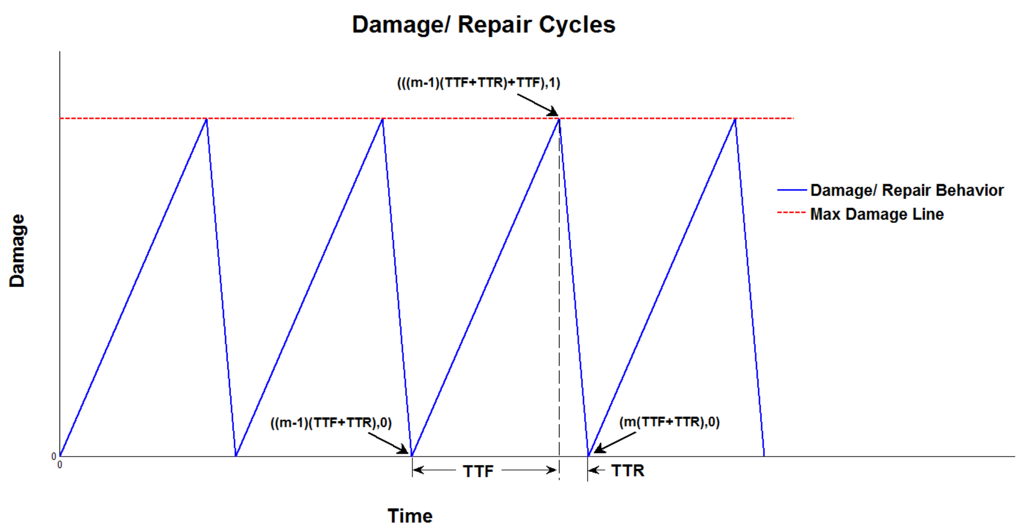

Figure 3-28: Damage/ repair nth damage cycle; damage line is represented by Equation 3-113, repair line is presented by Equation 3-114

Considering modeling the damage behavior of a system of repairable components requires functional components to be available when the damage is below unity, the graphical representation of the repairable component shown by Figure 3-28 will be substituted by the graphical representation shown by Figure 3-29

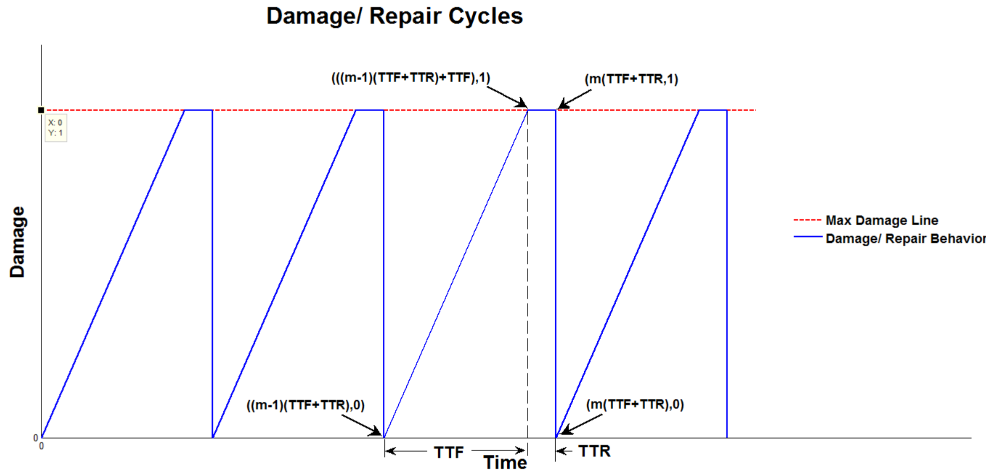

Figure 3-29: Damage/ repair m^th damage cycle; damage line is represented by Equation 3-113, repair line is presented by Equation 3-114

The characteristics for curves representing damage are the slope ρ_d and the intercept C_d

$$C_d = -\rho_d(m-1)(TTF+TTR) \qquad \textbf{Equation 3-115}$$

where: $C_d \equiv$ intercept of the damage line for the mth component failure/repair cycle

$\rho_d \equiv$ degradation (damage rate) of the damage line for the mth component failure/repair cycle

The characteristics for the repair lines shown by Figure 3-28 are the slope ρ_r and intercept C_r

$$C_r = 1-\rho_r\big((m-1)(TTF+TTR)+TTF\big) \qquad \textbf{Equation 3-116}$$

where: $C_r \equiv$ intercept of the repair line for the mth component failure/repair cycle

$\rho_r \equiv$ restoration (repair rate) of the repair line for the m[th] component failure/repair cycle

The models presented by Equation 3-115 and Equation 3-116 for calculating the intercepts of the failure and repair lines takes into account that degradation and restoration could be a function of (m); the impact of failure on some systems might lead to higher degradation on the subsequent repair cycles. In this research the degradation and restoration will be assumed to stay constant during repair cycles.

3.4.1 Synchronous Repairable Subsystems

Synchronous damage is described in section 3.3.1; an example of two Synchronous damage type component system, where the two components are accumulating damage simultaneously, will exhibit the damage behavior shown by Figure 3-30.

A repairable system of these two components would have a maximum accumulated damage as presented by Figure 3-31; this system damage behavior will be referred to as Synchronous-1; **SYNC1** damage model is a representation to a system damage behavior where a failure of a component would lead to the failure of the whole system. It can be observed from Figure 3-31 that the damage behavior of component-2 is affected by component-1 during the first repair period where the damage of component-2 stayed at the same level as before when component-1 failed.

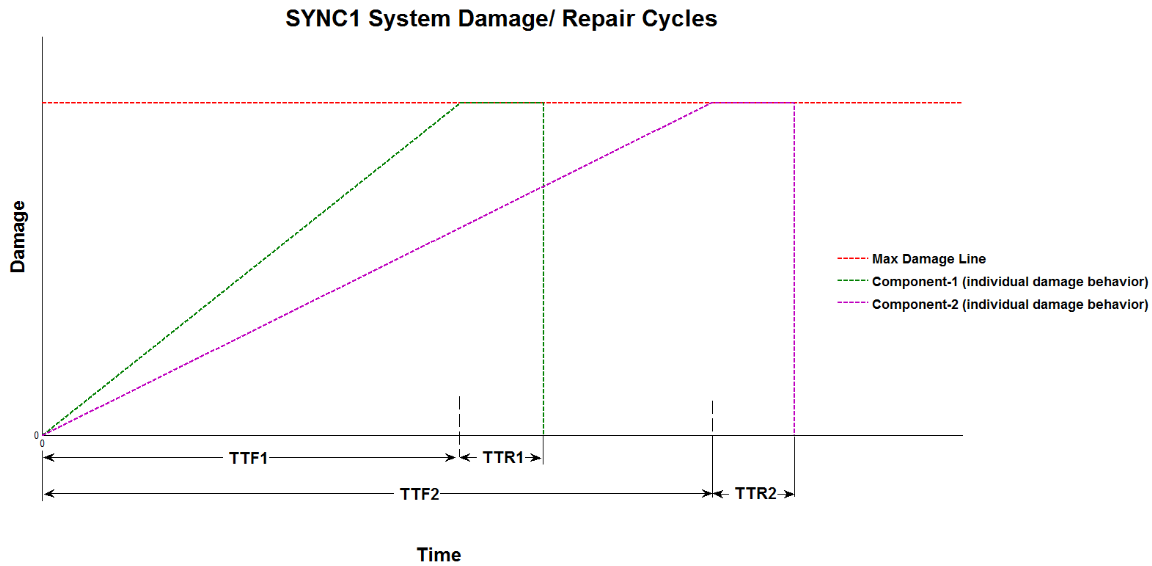

Figure 3-30: Two Synchronous repairable components

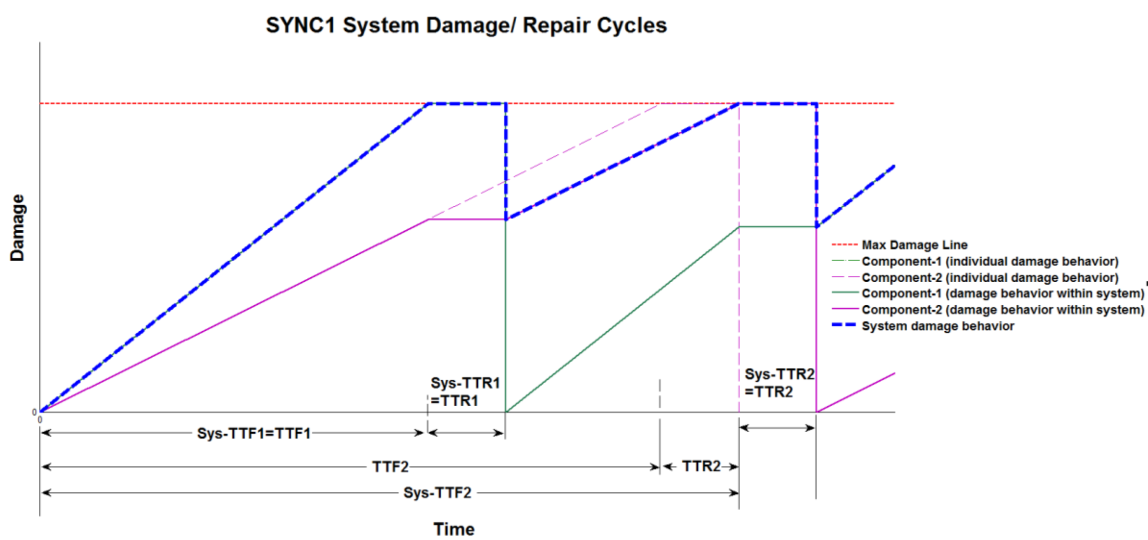

Figure 3-31: SYNC1 System damage behavior of two components

A repairable system of the two components shown by Figure 3-30 would have a minimum accumulated damage as presented by Figure 3-32 ; this system damage behavior will be referred to as Synchronous-2; **SYNC2** damage model is a representation to a system damage behavior where component functionality is backed-up by another one, so the failure of the system happens when both of the two components fail at the same time.

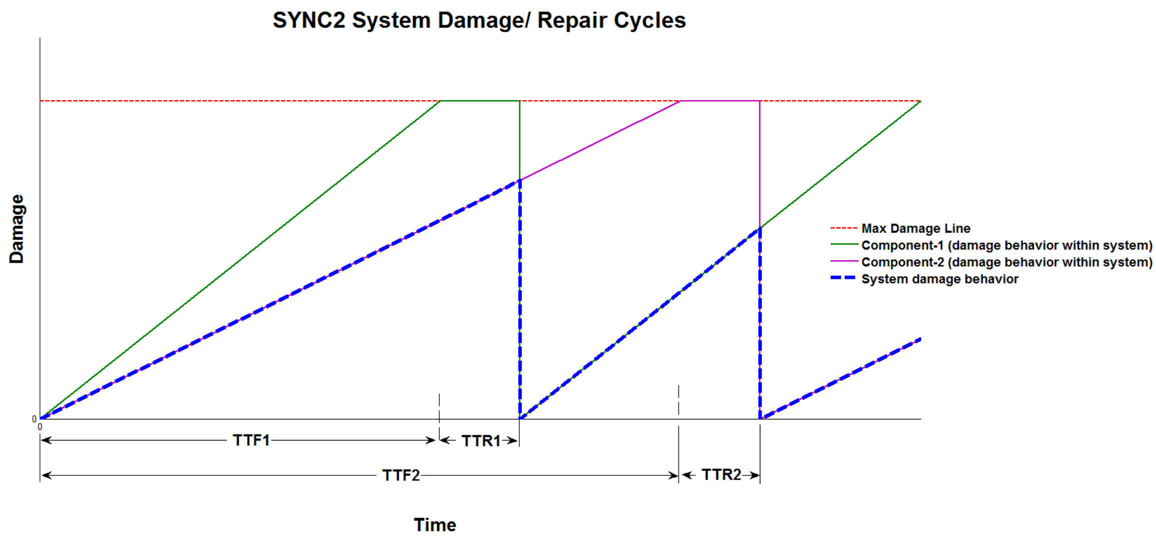

Figure 3-32: SYNC2 System damage behavior of two components

A system damage behavior that is presented with plots similar to Figure 3-31 and/or Figure 3-32 allows design engineers to make decisions about maintenance intervals and the levels of component reliability needed. Figure 3-33 and Figure 3-34 show complete Synchronous systems cycle, **SYNC1** & **SYNC2**, where system damage starts at zero and ends at zero. At the end of a complete system damage cycle, the functional value of the system is essentially zero; more repairs to the system doesn't add functional value and replacing it with a new one might be a better choice.

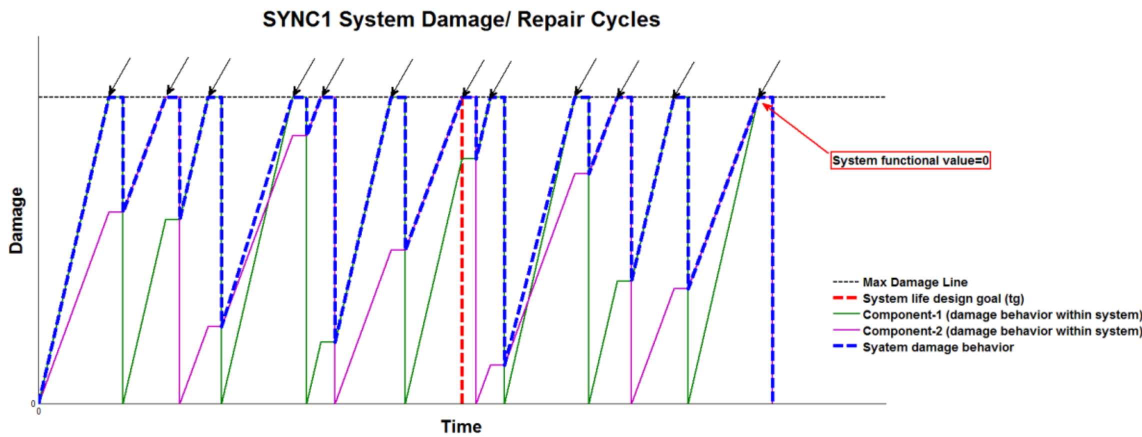

Figure 3-33: SYNC1 Damage model of two components; plot shows system failure events (highlighted by arrows), besides the time when system functional value reaches zero

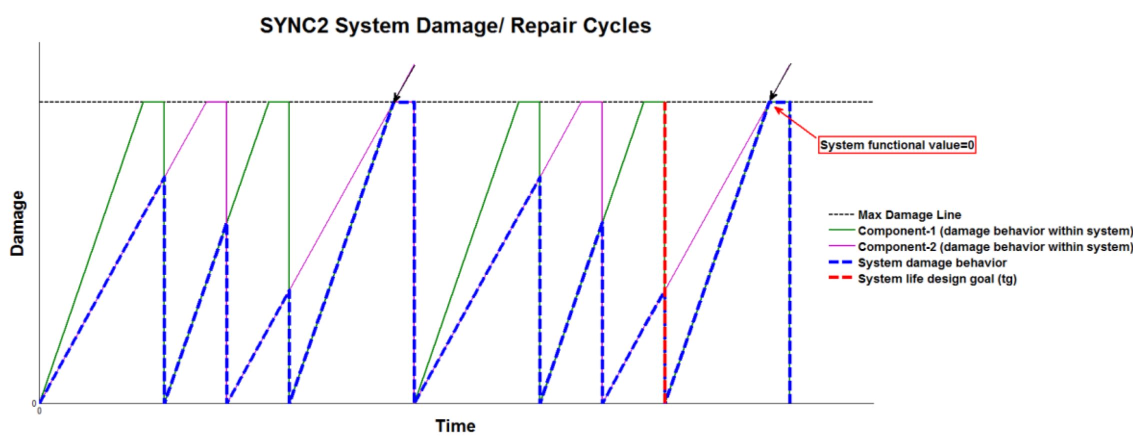

Figure 3-34: SYNC2 Damage model of two components; plot shows system failure events (highlighted by arrows), besides the time when system functional value reaches zero

3.4.2 Asynchronous Repairable Subsystems

Asynchronous damage is described in section 3.3.2; an example of two Asynchronous damage type component system, where the two components are accumulating damage sequentially, will exhibit the damage behavior shown by Figure 3-35.

A repairable system of these two components would have a maximum accumulated damage as presented by Figure 3-36; this system damage behavior will be referred to as Asynchronous-1; **ASYNC** damage model is a representation to a system damage behavior where all components has to fail for the system to fail. It can be observed from Figure 3-36 that the damage behavior of component-2 starts at the time component-1 fails. The system transition from component-1 to component-2 has not effect on system functionality.

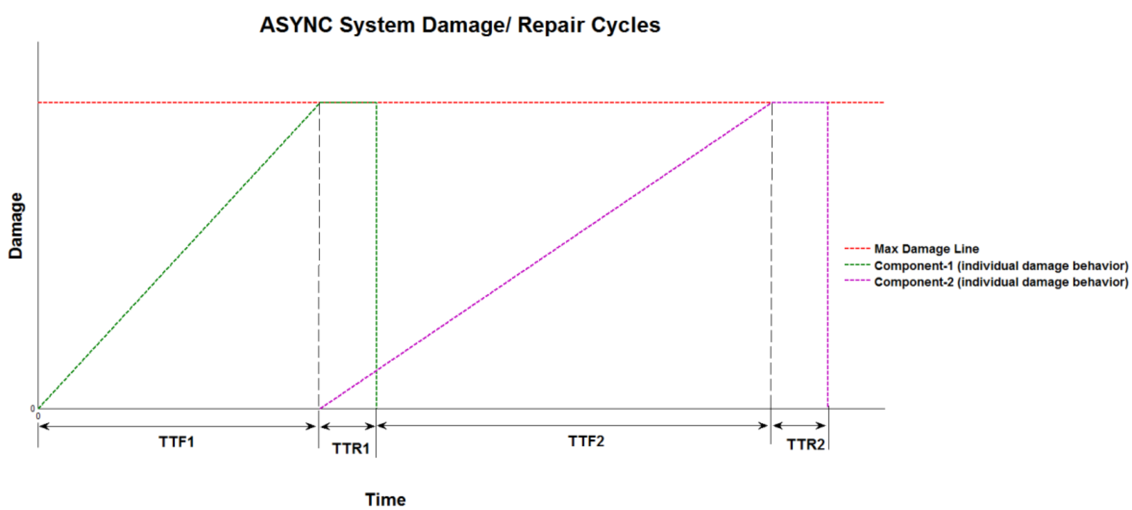

Figure 3-35: Two Asynchronous-damage repairable components: linear damage progression behavior

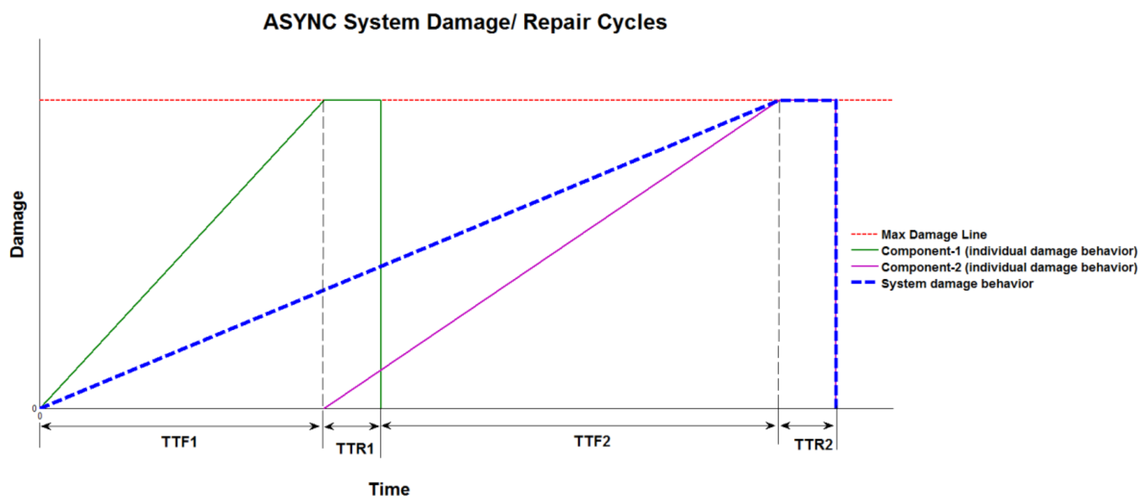

Figure 3-36: ASYNC System damage behavior of two components

3.5 Reliability Process Overview

Figure 3-37 shows how the mechanistic reliability evaluation process is integrated with Systematic Design. Axiomatic Design was utilized for design synthesis as outlined in section 3.1. Figure 3-38 shows the synthesis of the design reliability validation algorithm in a flowchart; the color-coded table on the middle shows the field type or process the activity belongs to. The flowchart outlines two phases of the design process; the first phase, at the top of the flow chart, provides an assessment to components and their associated system before joints and system assembly structure were realized; the lower portion is showing the reliability evaluation process with joints and a system assembly structure. It's apparent that the two processes are similar and it can be repeated when new realization about the system design is recognized.

The synthesis of the MDRV process, as shown by Figure 3-38, shows the following attributes and steps:

- Design Synthesis; with the following steps:
    - Identify (or update) system operations
    - Construct (or update) functional structure
    - Develop (or update) ($\boldsymbol{OF}$) matrix
    - Construct (or update) Assembly structure
    - Develop (or update) ($\boldsymbol{FC}$) matrix; Multiply $\boldsymbol{OF} \times \boldsymbol{FC}$ to produce – (or update) ($\boldsymbol{OC}$) matrix
- Output of the Design Synthesis; interpreted by system analyst, is:
    - W-Relationships
- System experts' interpretation to W-relationships to produce:
    - D- relationships
    - H-relationships
- Evaluate component reliability by executing the mechanistic reliability algorithm on components (using D-relationships) and damage model parameters
- Develop system damage statement TTF statement (using H-relationships)
- Evaluate system reliability

This process runs in a looping cycle; the process needs to be rerun whenever new information or design relaizaition has been identified. Each of the five attributes highlighted by the color codes are independent of each other and resemble MDRV framework main elements.

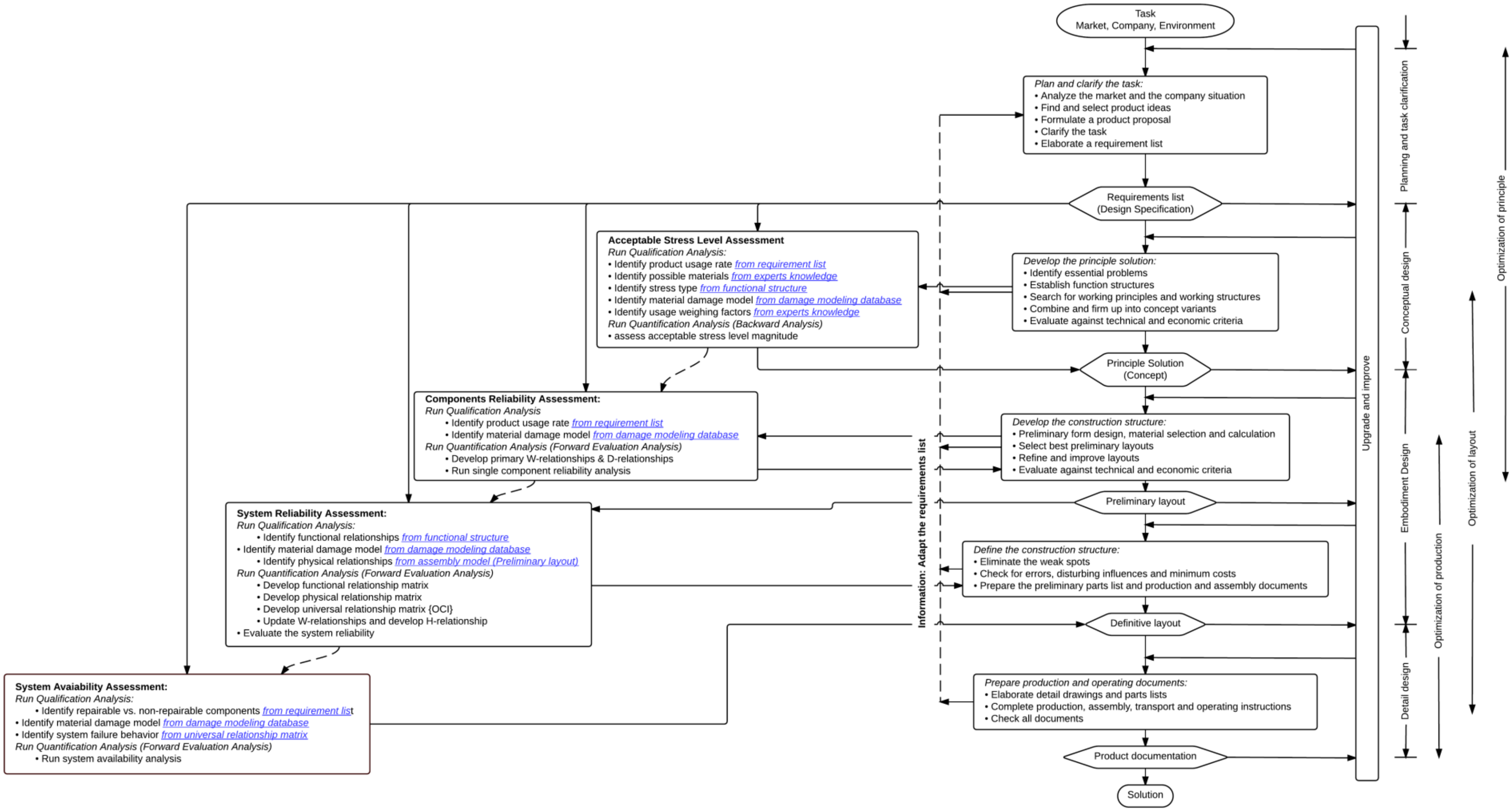

Figure 3-37: Integration of the Mechanistic Reliability Evaluation to Systematic Design

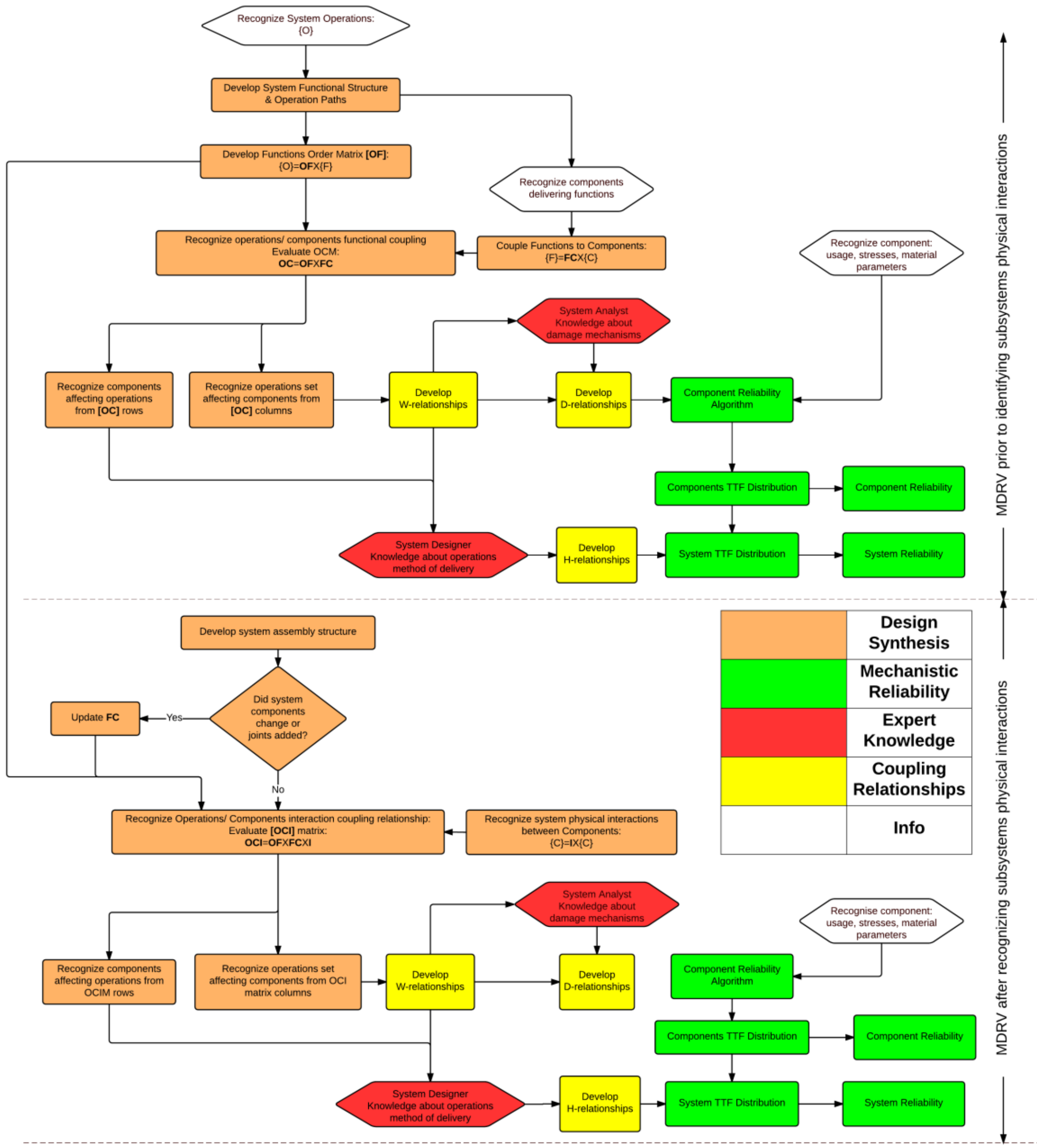

Figure 3-38: Synthesis of the mechanistic reliability process (before and after components interactions recognized)

Chapter 4 Methodology Demonstration

In this chapter, the mechanistic-based design-integrated reliability validation framework will be implemented to a generic example to explore the capabilities, potential and limitations of the framework. The knowledge and processes outlined in Chapter 3 will be exercised; starting from, design synthesis processes (section 3.1) and followed by a system reliability assessment demonstration for the generic example (section 4.2).The reliability assessment procedure will focus on system reliability; detailed integration of component mechanistic reliability to design is presented in Chapter 5- (Case Study). Observations will be highlighted during implementation of the framework and summary of lessons learned (section 4.3) will be provided at the end of the chapter.

4.1 System Synthesis:

Synthesizing design of a generic system, using the knowledge and processes outlined in section 3.1 will be exercised in this section. The system example starts from a conceptual functional structure and progresses until a system assembly structure is realized. The design synthesis process will extract, structure and formulized the required information and relationships needed to validate the system reliability.

4.1.1 System Design Phase-1: Conceptual Design

(Figure 4-1) shows a functional structure for a mechanical system that was designed to meet the four operations presented in Figure 4-2

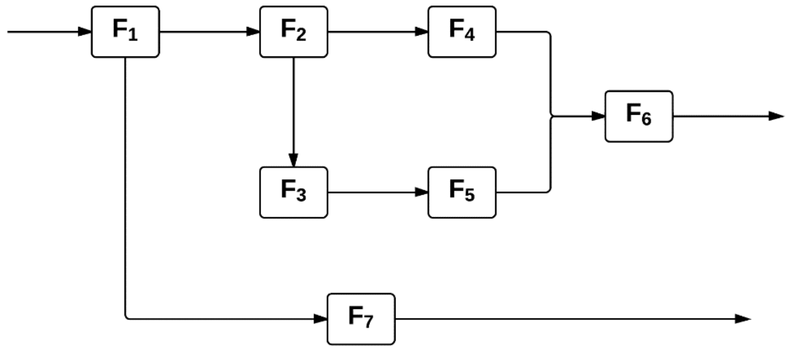

Figure 4-1: Functional structure for a mechanical system example

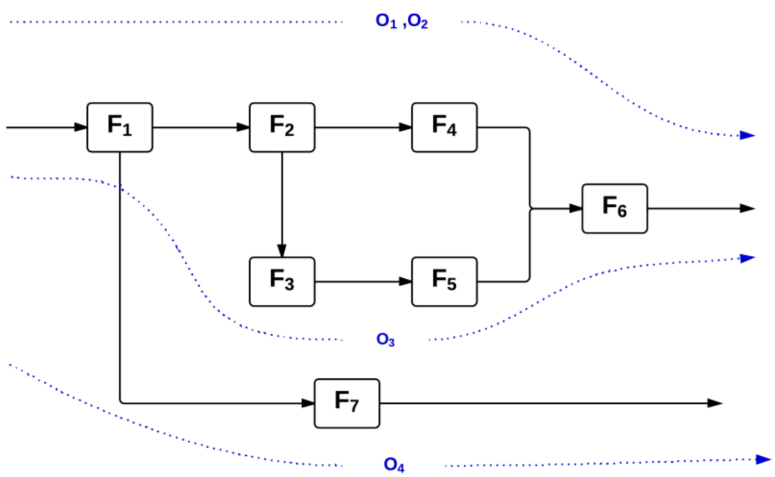

Figure 4-2: Functional structure with operations that will be executed

The operations-functions coupling relationships from Figure 4-2 are modeled with a linear system presented in Equation 4-1 and Equation 4-2;

$$\{O\} = \boldsymbol{OF} \times \{F\} \qquad \text{Equation 4-1}$$

$$\begin{Bmatrix} O_1 \\ O_2 \\ O_3 \\ O_4 \end{Bmatrix} = \begin{bmatrix} A_1^1 & A_1^2 & 0 & A_1^4 & 0 & A_1^6 & 0 \\ A_2^1 & A_2^2 & 0 & A_2^4 & 0 & A_2^6 & 0 \\ A_3^1 & A_3^2 & A_3^3 & 0 & A_3^5 & A_3^6 & 0 \\ A_4^1 & 0 & 0 & 0 & 0 & 0 & A_4^7 \end{bmatrix} \begin{Bmatrix} F_1 \\ F_2 \\ F_3 \\ F_4 \\ F_5 \\ F_6 \\ F_7 \end{Bmatrix}$$

Equation 4-2

$$\boldsymbol{OF} = \begin{bmatrix} A_1^1 & A_1^2 & 0 & A_1^4 & 0 & A_1^6 & 0 \\ A_2^1 & A_2^2 & 0 & A_2^4 & 0 & A_2^6 & 0 \\ A_3^1 & A_3^2 & A_3^3 & 0 & A_3^5 & A_3^6 & 0 \\ A_4^1 & 0 & 0 & 0 & 0 & 0 & A_4^7 \end{bmatrix}$$

Equation 4-3

The following assembly structural model was developed as a first conceptual solution to satisfy the functional structure presented by Figure 4-2.

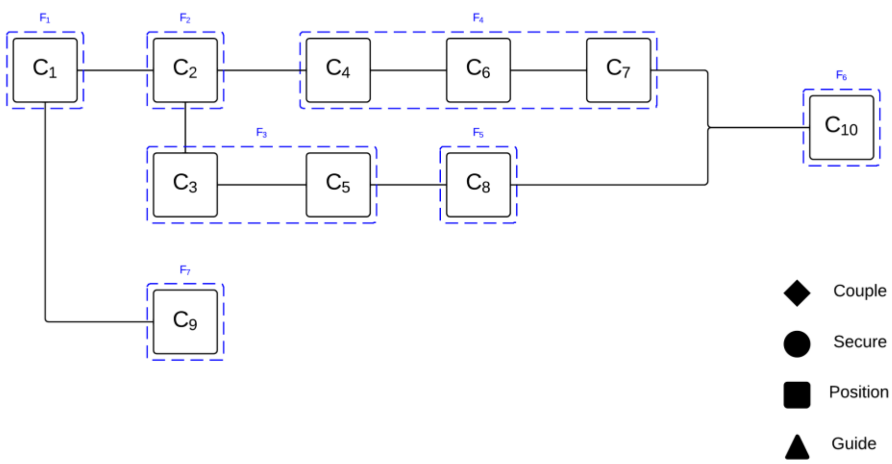

Figure 4-3: Assembly Structure; Components realization

Using the assembly structure shown by Figure 4-3, functions-components coupling relationships are developed and presented by Equation 4-4 and Equation 4-5.

$$\{F\} = \boldsymbol{FC_1}\{C^*\}$$ **Equation 4-4**

$$\begin{Bmatrix} F_1 \\ F_2 \\ F_3 \\ F_4 \\ F_5 \\ F_6 \\ F_7 \end{Bmatrix} = \begin{bmatrix} B_1^1 & 0 & 0 & 0 & 0 & 0 & 0 & 0 & 0 & 0 \\ 0 & B_2^2 & 0 & 0 & 0 & 0 & 0 & 0 & 0 & 0 \\ 0 & 0 & B_3^3 & 0 & B_3^5 & 0 & 0 & 0 & 0 & 0 \\ 0 & 0 & 0 & B_4^4 & 0 & B_4^6 & B_4^7 & 0 & 0 & 0 \\ 0 & 0 & 0 & 0 & 0 & 0 & 0 & B_5^8 & 0 & 0 \\ 0 & 0 & 0 & 0 & 0 & 0 & 0 & 0 & 0 & B_6^{10} \\ 0 & 0 & 0 & 0 & 0 & 0 & 0 & 0 & B_7^9 & 0 \end{bmatrix} \begin{Bmatrix} C^*{}_1 \\ C^*{}_2 \\ C^*{}_3 \\ C^*{}_4 \\ C^*{}_5 \\ C_6 \\ C^*{}_7 \\ C^*{}_8 \\ C^*{}_9 \\ C^*{}_{10} \end{Bmatrix}$$ **Equation 4-5**

$$\boldsymbol{FC_1} = \begin{bmatrix} B_1^1 & 0 & 0 & 0 & 0 & 0 & 0 & 0 & 0 & 0 \\ 0 & B_2^2 & 0 & 0 & 0 & 0 & 0 & 0 & 0 & 0 \\ 0 & 0 & B_3^3 & 0 & B_3^5 & 0 & 0 & 0 & 0 & 0 \\ 0 & 0 & 0 & B_4^4 & 0 & B_4^6 & B_4^7 & 0 & 0 & 0 \\ 0 & 0 & 0 & 0 & 0 & 0 & 0 & B_5^8 & 0 & 0 \\ 0 & 0 & 0 & 0 & 0 & 0 & 0 & 0 & 0 & B_6^{10} \\ 0 & 0 & 0 & 0 & 0 & 0 & 0 & 0 & B_7^9 & 0 \end{bmatrix}$$ **Equation 4-6**

The operations-components functional dependencies can be realized through multiplication of $\boldsymbol{OF}$ and $\boldsymbol{FC_1}$ as shown by Equation 4-7.

$$\{O\} = \boldsymbol{OC_1} \times \{C^*\}$$

$$\boldsymbol{OC_1} = \boldsymbol{OF} \times \boldsymbol{FC_1}$$ **Equation 4-7**

At this stage of the design, the obvious component interactions that can be observed from the structural model shown in Figure 4-3 would be “neighborhood-based interactions”; these interactions need to create stresses (i.e. stimulus) that causes or influence damaging effects between components to be included in a neighborhood-interaction matrix. In relation to mechanical fatigue damage, the stress under consideration is mechanical stress. Neighborhood-interactions are presented for the ten components system in Equation 4-8, Equation 4-9 and Equation 4-10; $(\boldsymbol{I_1^N})$ represents the first realized neighborhood interactions. The components' vector superscript index is needed to identify the context of interaction; the superscript used for the interaction matrix is to realize the type of interaction.

$$\{C^*\}^N = \boldsymbol{I_1^N} \times \{C\}^N \qquad \textbf{Equation 4-8}$$

$$\begin{Bmatrix} C^*_1 \\ C^*_2 \\ C^*_3 \\ C^*_4 \\ C^*_5 \\ C^*_6 \\ C^*_7 \\ C^*_8 \\ C^*_9 \\ C^*_{10} \end{Bmatrix}^N = \begin{bmatrix} I_1 & D_1^2 & 0 & 0 & 0 & 0 & 0 & 0 & D_1^9 & 0 \\ D_2^1 & I_2 & D_2^3 & D_2^4 & 0 & 0 & 0 & 0 & 0 & 0 \\ 0 & D_3^2 & I_3 & 0 & D_3^5 & 0 & 0 & 0 & 0 & 0 \\ 0 & D_4^2 & 0 & I_4 & 0 & D_4^6 & 0 & 0 & 0 & 0 \\ 0 & 0 & D_5^3 & 0 & I_5 & 0 & 0 & D_5^8 & 0 & 0 \\ 0 & 0 & 0 & D_6^4 & 0 & I_6 & D_6^7 & 0 & 0 & 0 \\ 0 & 0 & 0 & 0 & 0 & D_7^6 & I_7 & 0 & 0 & D_7^{10} \\ 0 & 0 & 0 & 0 & D_8^5 & 0 & 0 & I_8 & 0 & D_8^{10} \\ D_9^1 & 0 & 0 & 0 & 0 & 0 & 0 & 0 & I_9 & 0 \\ 0 & 0 & 0 & 0 & 0 & 0 & D_{10}^7 & D_{10}^8 & 0 & I_{10} \end{bmatrix} \begin{Bmatrix} C_1 \\ C_2 \\ C_3 \\ C_4 \\ C_5 \\ C_6 \\ C_7 \\ C_8 \\ C_9 \\ C_{10} \end{Bmatrix}^N \qquad \textbf{Equation 4-9}$$

$$\boldsymbol{I_1^N} = \begin{bmatrix} I_1 & D_1^2 & 0 & 0 & 0 & 0 & 0 & 0 & D_1^9 & 0 \\ D_2^1 & I_2 & D_2^3 & D_2^4 & 0 & 0 & 0 & 0 & 0 & 0 \\ 0 & D_3^2 & I_3 & 0 & D_3^5 & 0 & 0 & 0 & 0 & 0 \\ 0 & D_4^2 & 0 & I_4 & 0 & D_4^6 & 0 & 0 & 0 & 0 \\ 0 & 0 & D_5^3 & 0 & I_5 & 0 & 0 & D_5^8 & 0 & 0 \\ 0 & 0 & 0 & D_6^4 & 0 & I_6 & D_6^7 & 0 & 0 & 0 \\ 0 & 0 & 0 & 0 & 0 & D_7^6 & I_7 & 0 & 0 & D_7^{10} \\ 0 & 0 & 0 & 0 & D_8^5 & 0 & 0 & I_8 & 0 & D_8^{10} \\ D_9^1 & 0 & 0 & 0 & 0 & 0 & 0 & 0 & I_9 & 0 \\ 0 & 0 & 0 & 0 & 0 & 0 & D_{10}^7 & D_{10}^8 & 0 & I_{10} \end{bmatrix} \qquad \textbf{Equation 4-10}$$

For the first system design, $\left(\boldsymbol{I_1} = \boldsymbol{I_1^N}\right)$; i.e. the only realized interactions, so far are neighborhood-based ones. Multiplication of $\boldsymbol{OF}$, $\boldsymbol{FC_1}$ and $\boldsymbol{I_1}$ leads to the first realized operations-component coupling ($\boldsymbol{OCI_1}$); as presented by Equation 4-11 and Equation 4-14.

$$\{O\} = \boldsymbol{OCI_1}\{C\}$$

$$\boldsymbol{OCI_1} = \boldsymbol{OF} \times \boldsymbol{FC_1} \times \boldsymbol{I_1}$$

Equation 4-11

Equation 4-14 functional dependency parameters, recognize the subsystems presented in Equation 4-12

$$S_1 = \{C_1\}$$

$$S_2 = \{C_2\}$$

$$S_3 = \{C_4, C_6, C_7\};\ \ (\{A_1^4, A_2^4\}\ common\ functions)$$

$$S_4 = \{C_3, C_5\};\ \ (\{A_3^3\}\ common\ function)$$

$$S_5 = \{C_8\}$$

$$S_6 = \{C_9\}$$

$$S_7 = \{C_{10}\}$$

Equation 4-12

The functional dependencies between operations and components at phase-1of the system design is:

$$\boldsymbol{OC_1} = \begin{bmatrix} A_1^1 \times B_1^1 & A_1^2 \times B_2^2 & 0 & A_1^4 \times B_4^4 & 0 & A_1^4 \times B_4^6 & A_1^4 \times B_4^7 & 0 & 0 & A_1^6 \times B_6^{10} \\ A_2^1 \times B_1^1 & A_2^2 \times B_2^2 & 0 & A_2^4 \times B_4^4 & 0 & A_2^4 \times B_4^6 & A_2^4 \times B_4^7 & 0 & 0 & A_2^6 \times B_6^{10} \\ A_3^1 \times B_1^1 & A_3^2 \times B_2^2 & A_3^3 \times B_3^3 & 0 & A_3^3 \times B_3^5 & 0 & 0 & A_3^5 \times B_5^8 & 0 & A_3^6 \times B_6^{10} \\ A_4^1 \times B_1^1 & 0 & 0 & 0 & 0 & 0 & 0 & 0 & A_4^7 \times B_7^9 & 0 \end{bmatrix} \quad \textbf{Equation 4-13}$$

Components coupling with operations is presented with:

$$\boldsymbol{OCI_1} = \left[\begin{matrix} A_1^2 \times B_2^2 \times D_2^1 + A_1^1 \times B_1^1 \times I_1 & A_1^1 \times B_1^1 \times D_1^2 + A_1^4 \times B_4^4 \times D_4^2 + A_1^2 \times B_2^2 \times I_2 & A_1^2 \times B_2^2 \times D_2^3 & A_1^2 \times B_2^2 \times D_2^4 + A_1^4 \times B_4^6 \times D_6^4 + A_1^4 \times B_4^4 \times I_4 \\ A_2^2 \times B_2^2 \times D_2^1 + A_2^1 \times B_1^1 \times I_1 & A_2^1 \times B_1^1 \times D_1^2 + A_2^4 \times B_4^4 \times D_4^2 + A_2^2 \times B_2^2 \times I_2 & A_2^2 \times B_2^2 \times D_2^3 & A_2^2 \times B_2^2 \times D_2^4 + A_2^4 \times B_4^6 \times D_6^4 + A_2^4 \times B_4^4 \times I_4 \\ A_3^2 \times B_2^2 \times D_2^1 + A_3^1 \times B_1^1 \times I_1 & A_3^1 \times B_1^1 \times D_1^2 + A_3^3 \times B_3^3 \times D_3^2 + A_3^2 \times B_2^2 \times I_2 & A_3^2 \times B_2^2 \times D_2^3 + A_3^3(B_5^3 \times D_5^3 + B_3^3 \times I_3) & A_3^2 \times B_2^2 \times D_2^4 \\ A_4^7 \times B_7^9 \times D_9^1 + A_4^1 \times B_1^1 \times I_1 & A_4^1 \times B_1^1 \times D_1^2 & 0 & 0 \end{matrix}\right.$$

$$\cdots \begin{matrix} 0 & A_1^4(B_4^4 \times D_4^6 + B_4^7 \times D_7^6 + B_4^6 \times I_6^6) & A_1^6 \times B_6^{10} \times D_{10}^7 + A_1^4(B_4^6 \times D_6^7 + B_4^7 \times I_7) & A_1^6 \times B_6^{10} \times D_{10}^8 \\ 0 & A_2^4(B_4^4 \times D_4^6 + B_4^7 \times D_7^6 + B_4^6 \times I_6^6) & A_2^6 \times B_6^{10} \times D_{10}^7 + A_2^4(B_4^6 \times D_6^7 + B_4^7 \times I_7) & A_2^6 \times B_6^{10} \times D_{10}^8 \\ A_3^5 \times B_5^8 \times D_8^5 + A_3^3(B_3^3 \times D_3^5 + B_3^5 \times I_5) & 0 & A_3^6 \times B_6^{10} \times D_{10}^7 & A_3^3 \times B_6^{10} \times D_5^8 + A_3^6 \times B_6^{10} \times D_{10}^8 + A_3^5 \times B_5^8 \times I_8 \\ 0 & 0 & 0 & 0 \end{matrix} \cdots \quad \textbf{Equation 4-14}$$

$$\cdots \left.\begin{matrix} A_1^1 \times B_1^1 \times D_1^9 & A_1^4 \times B_4^7 \times D_7^{10} + A_1^6 \times B_6^{10} \times I_{10} \\ A_2^1 \times B_1^1 \times D_1^9 & A_2^4 \times B_4^7 \times D_7^{10} + A_2^6 \times B_6^{10} \times I_{10} \\ A_3^1 \times B_1^1 \times D_1^9 & A_3^5 \times B_5^8 \times D_8^{10} + A_3^6 \times B_6^{10} \times I_{10} \\ A_4^1 \times B_1^1 \times D_1^9 + A_4^7 \times B_7^9 \times I_9 & 0 \end{matrix}\right]$$

If interactions between components are not considered:

$$\boldsymbol{OCI_1} = \begin{bmatrix} A_1^1 \times B_1^1 \times I_1 & A_1^2 \times B_2^2 \times I_2 & 0 & A_1^4 \times B_4^4 \times I_4 & 0 & A_1^4 \times B_4^6 \times I_6^6 & A_1^4 \times B_4^7 \times I_7 & 0 & 0 & A_1^6 \times B_6^{10} \times I_{10} \\ A_2^1 \times B_1^1 \times I_1 & A_2^2 \times B_2^2 \times I_2 & 0 & A_2^4 \times B_4^4 \times I_4 & 0 & A_2^4 \times B_4^6 \times I_6^6 & A_2^4 \times B_4^7 \times I_7 & 0 & 0 & A_2^6 \times B_6^{10} \times I_{10} \\ A_3^1 \times B_1^1 \times I_1 & A_3^2 \times B_2^2 \times I_2 & A_3^3 \times B_3^3 \times I_3 & 0 & A_3^3 \times B_3^5 \times I_5 & 0 & 0 & A_3^5 \times B_5^8 \times I_8 & 0 & A_3^6 \times B_6^{10} \times I_{10} \\ A_4^1 \times B_1^1 \times I_1 & 0 & 0 & 0 & 0 & 0 & 0 & 0 & A_4^7 \times B_7^9 \times I_9 & 0 \end{bmatrix} \quad \textbf{Equation 4-15}$$

4.1.2 System Design Phase-2: Realizing Environments

System boundaries and external environments are realized and embedded in the system representation shown in Figure 4-4.

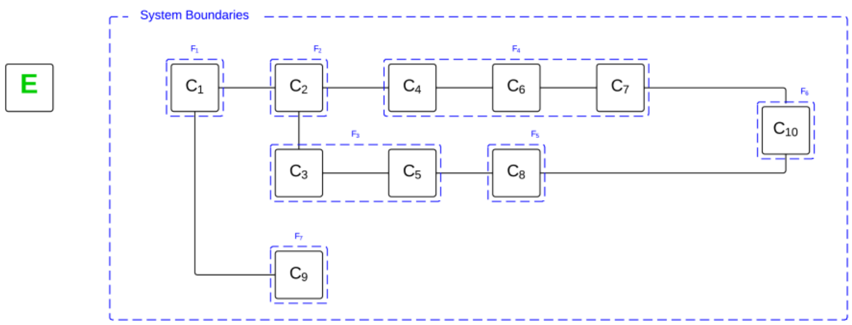

Figure 4-4: System boundary beside one environment, (E), is realized

External environment-based interactions can be captured and modeled as shown in Figure 4-5; the arrows show the flow of stimulus. The environment and component C_1 have two-directional impact on each other; components C_2 and C_9 has one-directional impact on the environment.

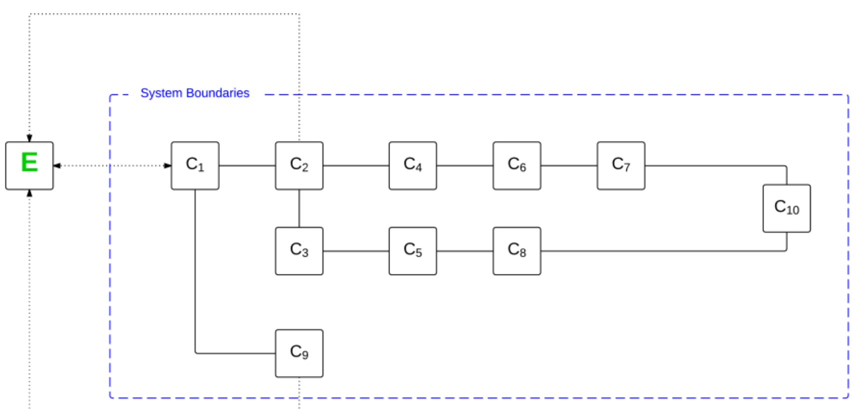

Figure 4-5: System interactions with environment, first layer of realization

The environment is also recognized as a component, (E), that is needed to satisfy functions: F_1, F_6, F_7.,(Figure 4-6). An updated $(\boldsymbol{FC})$ is presented in Equation 4-16 and Equation 4-17.

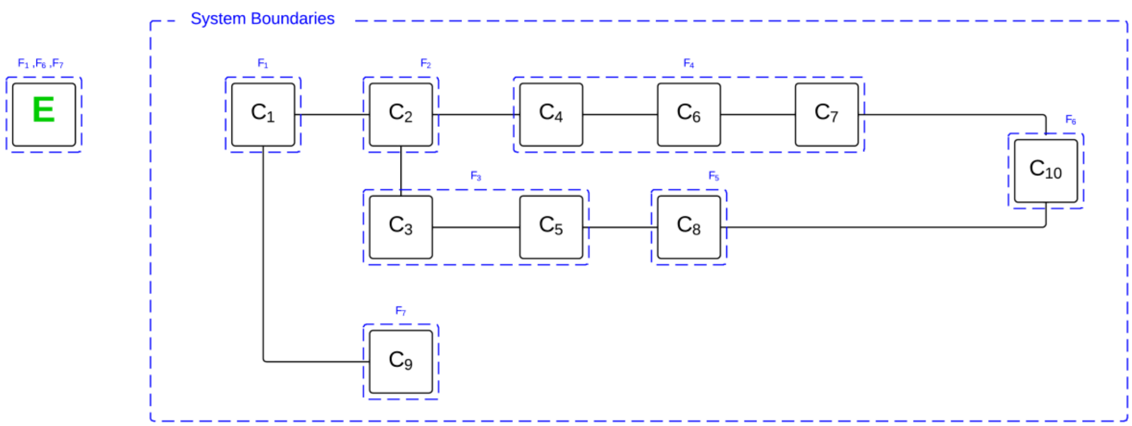

Figure 4-6: Realizing environment functional influence

$$\begin{Bmatrix} F_1 \\ F_2 \\ F_3 \\ F_4 \\ F_5 \\ F_6 \\ F_7 \end{Bmatrix} = \begin{bmatrix} \Omega_1^1 & B_1^1 & 0 & 0 & 0 & 0 & 0 & 0 & 0 & 0 & 0 \\ 0 & 0 & B_2^2 & 0 & 0 & 0 & 0 & 0 & 0 & 0 & 0 \\ 0 & 0 & 0 & B_3^3 & 0 & B_3^5 & 0 & 0 & 0 & 0 & 0 \\ 0 & 0 & 0 & 0 & B_4^4 & 0 & B_4^6 & B_4^7 & 0 & 0 & 0 \\ 0 & 0 & 0 & 0 & 0 & 0 & 0 & 0 & B_5^8 & 0 & 0 \\ \Omega_6^1 & 0 & 0 & 0 & 0 & 0 & 0 & 0 & 0 & 0 & B_6^{10} \\ \Omega_7^1 & 0 & 0 & 0 & 0 & 0 & 0 & 0 & 0 & B_7^9 & 0 \end{bmatrix} \begin{Bmatrix} E \\ C_1 \\ C_2 \\ C_3 \\ C_4 \\ C_5 \\ C_6 \\ C_7 \\ C_8 \\ C_9 \\ C_{10} \end{Bmatrix}$$

Equation 4-16

$$\boldsymbol{FC_2} = \begin{bmatrix} \Omega_1^1 & B_1^1 & 0 & 0 & 0 & 0 & 0 & 0 & 0 & 0 & 0 \\ 0 & 0 & B_2^2 & 0 & 0 & 0 & 0 & 0 & 0 & 0 & 0 \\ 0 & 0 & 0 & B_3^3 & 0 & B_3^5 & 0 & 0 & 0 & 0 & 0 \\ 0 & 0 & 0 & 0 & B_4^4 & 0 & B_4^6 & B_4^7 & 0 & 0 & 0 \\ 0 & 0 & 0 & 0 & 0 & 0 & 0 & 0 & B_5^8 & 0 & 0 \\ \Omega_6^1 & 0 & 0 & 0 & 0 & 0 & 0 & 0 & 0 & 0 & B_6^{10} \\ \Omega_7^1 & 0 & 0 & 0 & 0 & 0 & 0 & 0 & 0 & B_7^9 & 0 \end{bmatrix}$$

Equation 4-17

The environment-interaction matrix at this design realization stage is presented in Equation 4-22

$$\{C^*\}^E = \boldsymbol{I_4^E} \times \{C\}^E$$

Equation 4-18

$$\begin{Bmatrix} E^* \\ C^*{}_1 \\ C^*{}_2 \\ C^*{}_3 \\ C^*{}_4 \\ C^*{}_5 \\ C^*{}_6 \\ C^*{}_7 \\ C^*{}_8 \\ C^*{}_9 \\ C^*{}_{10} \end{Bmatrix}^E = \begin{bmatrix} I_E & D_E^1 & D_E^2 & 0 & 0 & 0 & 0 & 0 & 0 & D_E^9 & 0 \\ D_1^E & 0 & 0 & 0 & 0 & 0 & 0 & 0 & 0 & 0 & 0 \\ D_2^E & 0 & 0 & 0 & 0 & 0 & 0 & 0 & 0 & 0 & 0 \\ 0 & 0 & 0 & 0 & 0 & 0 & 0 & 0 & 0 & 0 & 0 \\ 0 & 0 & 0 & 0 & 0 & 0 & 0 & 0 & 0 & 0 & 0 \\ 0 & 0 & 0 & 0 & 0 & 0 & 0 & 0 & 0 & 0 & 0 \\ 0 & 0 & 0 & 0 & 0 & 0 & 0 & 0 & 0 & 0 & 0 \\ 0 & 0 & 0 & 0 & 0 & 0 & 0 & 0 & 0 & 0 & 0 \\ 0 & 0 & 0 & 0 & 0 & 0 & 0 & 0 & 0 & 0 & 0 \\ D_9^E & 0 & 0 & 0 & 0 & 0 & 0 & 0 & 0 & 0 & 0 \\ 0 & 0 & 0 & 0 & 0 & 0 & 0 & 0 & 0 & 0 & 0 \end{bmatrix} \begin{Bmatrix} E \\ C_1 \\ C_2 \\ C_3 \\ C_4 \\ C_5 \\ C_6 \\ C_7 \\ C_8 \\ C_9 \\ C_{10} \end{Bmatrix}^E$$

Equation 4-19

$$
\boldsymbol{I}_2^E = \begin{bmatrix}
I_E & D_E^1 & 0 & 0 & 0 & 0 & 0 & 0 & 0 & 0 & 0 \\
D_1^E & 0 & 0 & 0 & 0 & 0 & 0 & 0 & 0 & 0 & 0 \\
D_2^E & 0 & 0 & 0 & 0 & 0 & 0 & 0 & 0 & 0 & 0 \\
0 & 0 & 0 & 0 & 0 & 0 & 0 & 0 & 0 & 0 & 0 \\
0 & 0 & 0 & 0 & 0 & 0 & 0 & 0 & 0 & 0 & 0 \\
0 & 0 & 0 & 0 & 0 & 0 & 0 & 0 & 0 & 0 & 0 \\
0 & 0 & 0 & 0 & 0 & 0 & 0 & 0 & 0 & 0 & 0 \\
0 & 0 & 0 & 0 & 0 & 0 & 0 & 0 & 0 & 0 & 0 \\
0 & 0 & 0 & 0 & 0 & 0 & 0 & 0 & 0 & 0 & 0 \\
D_9^E & 0 & 0 & 0 & 0 & 0 & 0 & 0 & 0 & 0 & 0 \\
0 & 0 & 0 & 0 & 0 & 0 & 0 & 0 & 0 & 0 & 0
\end{bmatrix}
$$

Equation 4-20

Expanding the system universal interaction matrix to include the environment-interaction matrix leads to the systems presented by Equation 4-22 and Equation 4-23.

$$
\boldsymbol{I_2} = \boldsymbol{I_2^E} + \boldsymbol{I_1}
$$

Equation 4-21

$$
\begin{Bmatrix} E^* \\ C^*{}_1 \\ C^*{}_2 \\ C^*{}_3 \\ C^*{}_4 \\ C^*{}_5 \\ C^*{}_6 \\ C^*{}_7 \\ C^*{}_8 \\ C^*{}_9 \\ C^*{}_{10} \end{Bmatrix} = \begin{bmatrix}
I_E & D_E^1 & 0 & 0 & 0 & 0 & 0 & 0 & 0 & 0 & 0 \\
D_1^E & I_1 & D_1^2 & 0 & 0 & 0 & 0 & 0 & 0 & D_1^9 & 0 \\
D_2^E & D_2^1 & I_2 & D_2^3 & D_2^4 & 0 & 0 & 0 & 0 & 0 & 0 \\
0 & 0 & D_3^2 & I_3 & 0 & D_3^5 & 0 & 0 & 0 & 0 & 0 \\
0 & 0 & D_4^2 & 0 & I_4 & 0 & D_4^6 & 0 & 0 & 0 & 0 \\
0 & 0 & 0 & D_5^3 & 0 & I_5 & 0 & 0 & D_5^8 & 0 & 0 \\
0 & 0 & 0 & 0 & D_6^4 & 0 & I_6 & D_6^7 & 0 & 0 & 0 \\
0 & 0 & 0 & 0 & 0 & 0 & D_7^6 & I_7 & 0 & 0 & D_7^{10} \\
0 & 0 & 0 & 0 & 0 & D_8^5 & 0 & 0 & I_8 & 0 & D_8^{10} \\
D_9^E & D_9^1 & 0 & 0 & 0 & 0 & 0 & 0 & 0 & I_9 & 0 \\
0 & 0 & 0 & 0 & 0 & 0 & 0 & D_{10}^7 & D_{10}^8 & 0 & I_{10}
\end{bmatrix} \begin{Bmatrix} E \\ C_1 \\ C_2 \\ C_3 \\ C_4 \\ C_5 \\ C_6 \\ C_7 \\ C_8 \\ C_9 \\ C_{10} \end{Bmatrix}
$$

Equation 4-22

$$
\boldsymbol{I_2} = \begin{bmatrix}
I_E & D_E^1 & 0 & 0 & 0 & 0 & 0 & 0 & 0 & 0 & 0 \\
D_1^E & I_1 & D_1^2 & 0 & 0 & 0 & 0 & 0 & 0 & D_1^9 & 0 \\
D_2^E & D_2^1 & I_2 & D_2^3 & D_2^4 & 0 & 0 & 0 & 0 & 0 & 0 \\
0 & 0 & D_3^2 & I_3 & 0 & D_3^5 & 0 & 0 & 0 & 0 & 0 \\
0 & 0 & D_4^2 & 0 & I_4 & 0 & D_4^6 & 0 & 0 & 0 & 0 \\
0 & 0 & 0 & D_5^3 & 0 & I_5 & 0 & 0 & D_5^8 & 0 & 0 \\
0 & 0 & 0 & 0 & D_6^4 & 0 & I_6 & D_6^7 & 0 & 0 & 0 \\
0 & 0 & 0 & 0 & 0 & 0 & D_7^6 & I_7 & 0 & 0 & D_7^{10} \\
0 & 0 & 0 & 0 & 0 & D_8^5 & 0 & 0 & I_8 & 0 & D_8^{10} \\
D_9^E & D_9^1 & 0 & 0 & 0 & 0 & 0 & 0 & 0 & I_9 & 0 \\
0 & 0 & 0 & 0 & 0 & 0 & 0 & D_{10}^7 & D_{10}^8 & 0 & I_{10}
\end{bmatrix}
$$

Equation 4-23

Updating $\boldsymbol{OC}$ at this stage of design realization is presented by Equation 4-24 and Equation 4-26.

$$\boldsymbol{OCI_2} = \boldsymbol{OF} \times \boldsymbol{FC_2} \times \boldsymbol{I_2}$$

Equation 4-24

Equation 4-26 recognizes the subsystems presented by Equation 4-25.

$$S_E = \{E\}$$

$$S_1 = \{C_1\}$$

$$S_2 = \{C_2\}$$

$$S_3 = \{C_4, C_6, C_7\}$$

$$S_4 = \{C_3, C_5\}$$

$$S_5 = \{C_8\}$$

$$S_6 = \{C_9\}$$

$$S_7 = \{C_{10}\}$$

Equation 4-25

The functional dependencies between operations and components at phase-2 of the system design is:

$$\boldsymbol{OC_2} = \begin{bmatrix} A_1^1 \times \Omega_1^1 + A_1^6 \times \Omega_6^1 & A_1^1 \times B_1^1 & A_1^2 \times B_2^2 & 0 & A_1^4 \times B_4^4 & 0 & A_1^4 \times B_4^6 & A_1^4 \times B_4^7 & 0 & 0 & A_1^6 \times B_6^{10} \\ A_2^1 \times \Omega_1^1 + A_2^6 \times \Omega_6^1 & A_2^1 \times B_1^1 & A_2^2 \times B_2^2 & 0 & A_2^4 \times B_4^4 & 0 & A_2^4 \times B_4^6 & A_2^4 \times B_4^7 & 0 & 0 & A_2^6 \times B_6^{10} \\ A_3^1 \times \Omega_1^1 + A_3^6 \times \Omega_6^1 & A_3^1 \times B_1^1 & A_3^2 \times B_2^2 & A_3^3 \times B_3^3 & 0 & A_3^3 \times B_3^5 & 0 & 0 & A_3^5 \times B_5^8 & 0 & A_3^6 \times B_6^{10} \\ A_4^1 \times \Omega_1^1 + A_4^7 \times \Omega_7^1 & A_4^1 \times B_1^1 & 0 & 0 & 0 & 0 & 0 & 0 & 0 & A_4^7 \times B_7^9 & 0 \end{bmatrix}$$

Equation 4-26

If environmental impacts are not included, $\boldsymbol{OC_2}$ becomes:

$$\boldsymbol{OC_2} = \begin{bmatrix} A_1^6 \times \Omega_6^1 & A_1^1 \times B_1^1 & A_1^2 \times B_2^2 & 0 & A_1^4 \times B_4^4 & 0 & A_1^4 \times B_4^6 & A_1^4 \times B_4^7 & 0 & 0 & A_1^6 \times B_6^{10} \\ A_2^6 \times \Omega_6^1 & A_2^1 \times B_1^1 & A_2^2 \times B_2^2 & 0 & A_2^4 \times B_4^4 & 0 & A_2^4 \times B_4^6 & A_2^4 \times B_4^7 & 0 & 0 & A_2^6 \times B_6^{10} \\ A_3^6 \times \Omega_6^1 & A_3^1 \times B_1^1 & A_3^2 \times B_2^2 & A_3^3 \times B_3^3 & 0 & A_3^3 \times B_3^5 & 0 & 0 & A_3^5 \times B_5^8 & 0 & A_3^6 \times B_6^{10} \\ A_4^7 \times \Omega_7^1 & A_4^1 \times B_1^1 & 0 & 0 & 0 & 0 & 0 & 0 & 0 & A_4^7 \times B_7^9 & 0 \end{bmatrix}$$

Equation 4-27

Components coupling with operations at phase-2 is presented with the following system:

$$\boldsymbol{OCI_2} = \left[\begin{matrix} (A_1^1 \times \Omega_1^1 + A_1^6 \times \Omega_6^1)I_E + A_1^1 \times B_1^1 \times D_1^E + A_1^2 \times B_2^2 \times D_2^E & (A_1^1 \times \Omega_1^1 + A_1^6 \times \Omega_6^1)D_E^1 + A_1^2 \times B_2^2 \times D_2^1 + A_1^1 \times B_1^1 \times I_1 & A_1^1 \times B_1^1 \times D_1^2 + A_1^4 \times B_4^4 \times D_4^2 + A_1^2 \times B_2^2 \times I_2 \\ (A_2^1 \times \Omega_1^1 + A_2^6 \times \Omega_6^1)I_E + A_2^1 \times B_1^1 \times D_1^E + A_2^2 \times B_2^2 \times D_2^E & (A_2^1 \times \Omega_1^1 + A_2^6 \times \Omega_6^1)D_E^1 + A_2^2 \times B_2^2 \times D_2^1 + A_2^1 \times B_1^1 \times I_1 & A_2^1 \times B_1^1 \times D_1^2 + A_2^4 \times B_4^4 \times D_4^2 + A_2^2 \times B_2^2 \times I_2 \\ (A_3^1 \times \Omega_1^1 + A_3^6 \times \Omega_6^1)I_E + A_3^1 \times B_1^1 \times D_1^E + A_3^2 \times B_2^2 \times D_2^E & (A_3^1 \times \Omega_1^1 + A_3^6 \times \Omega_6^1)D_E^1 + A_3^2 \times B_2^2 \times D_2^1 + A_3^1 \times B_1^1 \times I_1 & A_3^1 \times B_1^1 \times D_1^2 + A_3^3 \times B_3^3 \times D_3^2 + A_3^2 \times B_2^2 \times I_2 \\ (A_4^1 \times \Omega_1^1 + A_4^7 \times \Omega_7^1)I_E + A_4^1 \times B_1^1 \times D_1^E + A_4^7 \times B_7^9 \times D_2^E & (A_4^1 \times \Omega_1^1 + A_4^7 \times \Omega_7^1)D_E^1 + A_4^7 \times B_7^9 \times D_9^1 + A_4^1 \times B_1^1 \times I_1 & A_4^1 \times B_1^1 \times D_1^2 \end{matrix}\right. \cdots$$

$$\cdots \begin{matrix} A_1^2 \times B_2^2 \times D_2^3 & A_1^2 \times B_2^2 \times D_2^4 + A_1^4 \times B_4^6 \times D_6^4 + A_1^4 \times B_4^4 \times I_4 & 0 & A_1^4(B_4^4 \times D_4^6 + B_4^7 \times D_7^6 + B_4^6 \times I_6^6) \\ A_2^2 \times B_2^2 \times D_2^3 & A_2^2 \times B_2^2 \times D_2^4 + A_2^4 \times B_4^6 \times D_6^4 + A_2^4 \times B_4^4 \times I_4 & 0 & A_2^4(B_4^4 \times D_4^6 + B_4^7 \times D_7^6 + B_4^6 \times I_6^6) \\ A_3^2 \times B_2^2 \times D_2^3 + A_3^3(B_5^3 \times D_5^3 + B_3^3 \times I_3) & A_3^2 \times B_2^2 \times D_2^4 & A_3^5 \times B_5^8 \times D_8^5 + A_3^3(B_3^3 \times D_3^5 + B_3^5 \times I_5) & 0 \\ 0 & 0 & 0 & 0 \end{matrix} \cdots$$

Equation 4-28

$$\cdots \left.\begin{matrix} A_1^6 \times B_6^{10} \times D_{10}^7 + A_1^4(B_4^6 \times D_6^7 + B_4^7 \times I_7) & A_1^6 \times B_6^{10} \times D_{10}^8 & A_1^1 \times B_1^1 \times D_1^9 & A_1^4 \times B_4^7 \times D_7^{10} + A_1^6 \times B_6^{10} \times I_{10} \\ A_2^6 \times B_6^{10} \times D_{10}^7 + A_2^4(B_4^6 \times D_6^7 + B_4^7 \times I_7) & A_2^6 \times B_6^{10} \times D_{10}^8 & A_2^1 \times B_1^1 \times D_1^9 & A_2^4 \times B_4^7 \times D_7^{10} + A_2^6 \times B_6^{10} \times I_{10} \\ A_3^6 \times B_6^{10} \times D_{10}^7 & A_3^3 \times B_6^{10} \times D_5^8 + A_3^6 \times B_6^{10} \times D_{10}^8 + A_3^5 \times B_5^8 \times I_8 & A_3^1 \times B_1^1 \times D_1^9 & A_3^5 \times B_5^8 \times D_8^{10} + A_3^6 \times B_6^{10} \times I_{10} \\ 0 & 0 & A_4^1 \times B_1^1 \times D_1^9 + A_4^7 \times B_7^9 \times I_9 & 0 \end{matrix}\right]$$

4.1.3 System Design Phase-3: Embodiment Design

Adding Joints

At the embodiment stage of system design, physical joints can be developed and the system can have a realized physical shape, which is presented by the assembly structure in Figure 4-7; this representation can be in the form of a CAD model.

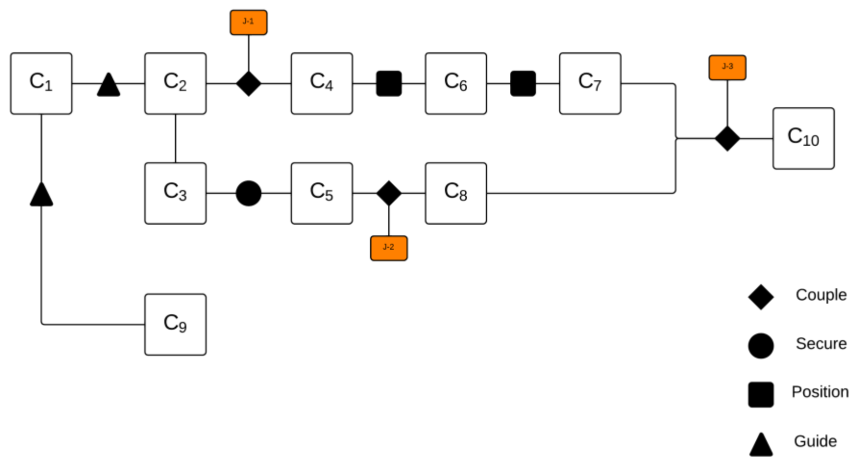

Figure 4-7: System assembly structure

Including the environment as a component is presented in Figure 4-8. Special recognition was given to representing environment stimulus. Dotted arrows specially recognized environmental interactions; all interactions that are not neighborhood-based can be presented similarly.

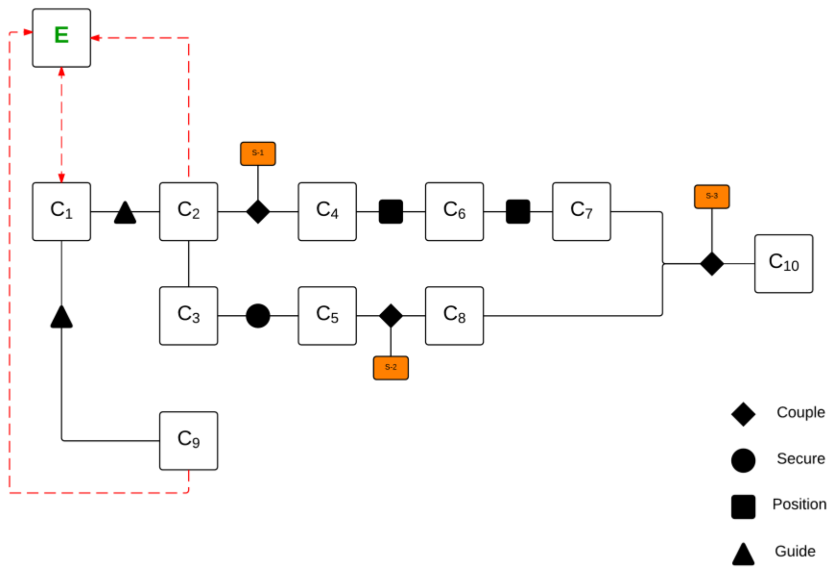

Figure 4-8: System components and environment interactions

Graphical presentation to functional coupling caused by the addition of joints: $\{J_1, J_2, J_3\}$ to the mechanical system is presented in Figure 4-9. An update to $(\boldsymbol{FC})$ to take into account the system expansion by adding structural joints is presented in Equation 4-29.

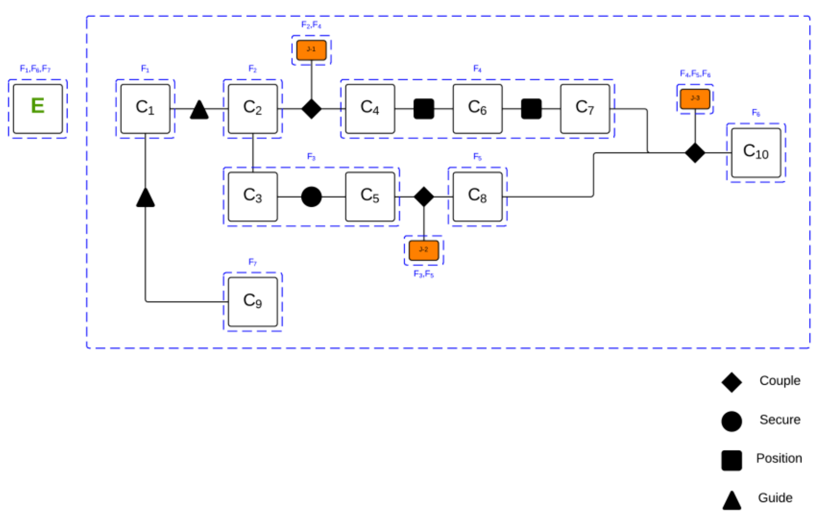

Figure 4-9: Update to functional, structural interrelations to the system after adding joints

$$
\begin{Bmatrix} F_1 \\ F_2 \\ F_3 \\ F_4 \\ F_5 \\ F_6 \\ F_7 \end{Bmatrix} =
\begin{bmatrix}
\Omega_1^1 & B_1^1 & 0 & 0 & 0 & 0 & 0 & 0 & 0 & 0 & 0 & 0 & 0 & 0 \\
0 & 0 & B_2^2 & 0 & 0 & 0 & 0 & 0 & 0 & 0 & 0 & B_2^{J_1} & 0 & 0 \\
0 & 0 & 0 & B_3^3 & 0 & B_3^5 & 0 & 0 & 0 & 0 & 0 & 0 & B_3^{J_2} & 0 \\
0 & 0 & 0 & 0 & B_4^4 & 0 & B_4^6 & B_4^7 & 0 & 0 & 0 & B_4^{J_1} & 0 & B_4^{J_3} \\
0 & 0 & 0 & 0 & 0 & 0 & 0 & 0 & B_5^8 & 0 & 0 & 0 & B_5^{J_2} & B_5^{J_3} \\
\Omega_6^1 & 0 & 0 & 0 & 0 & 0 & 0 & 0 & 0 & 0 & B_6^{10} & 0 & 0 & B_6^{J_3} \\
\Omega_7^1 & 0 & 0 & 0 & 0 & 0 & 0 & 0 & 0 & B_7^9 & 0 & 0 & 0 & 0
\end{bmatrix}
\begin{Bmatrix} E \\ C_1 \\ C_2 \\ C_3 \\ C_4 \\ C_5 \\ C_6 \\ C_7 \\ C_8 \\ C_9 \\ C_{10} \\ J_1 \\ J_2 \\ J_3 \end{Bmatrix}
$$

Equation 4-29

$$
\boldsymbol{FC_3} =
\begin{bmatrix}
\Omega_1^1 & B_1^1 & 0 & 0 & 0 & 0 & 0 & 0 & 0 & 0 & 0 & 0 & 0 & 0 \\
0 & 0 & B_2^2 & 0 & 0 & 0 & 0 & 0 & 0 & 0 & 0 & B_2^{J_1} & 0 & 0 \\
0 & 0 & 0 & B_3^3 & 0 & B_3^5 & 0 & 0 & 0 & 0 & 0 & 0 & B_3^{J_2} & 0 \\
0 & 0 & 0 & 0 & B_4^4 & 0 & B_4^6 & B_4^7 & 0 & 0 & 0 & B_4^{J_1} & 0 & B_4^{J_3} \\
0 & 0 & 0 & 0 & 0 & 0 & 0 & 0 & B_5^8 & 0 & 0 & 0 & B_5^{J_2} & B_5^{J_3} \\
\Omega_6^1 & 0 & 0 & 0 & 0 & 0 & 0 & 0 & 0 & 0 & B_6^{10} & 0 & 0 & B_6^{J_3} \\
\Omega_7^1 & 0 & 0 & 0 & 0 & 0 & 0 & 0 & 0 & B_7^9 & 0 & 0 & 0 & 0
\end{bmatrix}
$$

Equation 4-30

Updating the interaction matrix is needed due to the addition of three joints: $\{J_1, J_2, J_3\}$ to the system assembly structure; Equation 4-31 and Equation 4-32.shows the updates.

$$
\begin{Bmatrix} E^* \\ C^*{}_1 \\ C^*{}_2 \\ C^*{}_3 \\ C^*{}_4 \\ C^*{}_5 \\ C^*{}_6 \\ C^*{}_7 \\ C^*{}_8 \\ C^*{}_9 \\ C^*{}_{10} \\ J^*{}_1 \\ J^*{}_2 \\ J^*{}_3 \end{Bmatrix} =
\begin{bmatrix}
I_E & D_E^1 & 0 & 0 & 0 & 0 & 0 & 0 & 0 & 0 & 0 & 0 & 0 & 0 \\
D_1^E & I_1 & D_1^2 & 0 & 0 & 0 & 0 & 0 & 0 & D_1^9 & 0 & 0 & 0 & 0 \\
D_2^E & D_2^1 & I_2 & D_2^3 & D_2^4 & 0 & 0 & 0 & 0 & 0 & 0 & D_2^{J_1} & 0 & 0 \\
0 & 0 & D_3^2 & I_3 & 0 & D_3^5 & 0 & 0 & 0 & 0 & 0 & 0 & 0 & 0 \\
0 & 0 & D_4^2 & 0 & I_4 & 0 & D_4^6 & 0 & 0 & 0 & 0 & D_4^{J_1} & 0 & 0 \\
0 & 0 & 0 & D_5^3 & 0 & I_5 & 0 & 0 & D_5^8 & 0 & 0 & 0 & D_5^{J_2} & 0 \\
0 & 0 & 0 & 0 & D_6^4 & 0 & I_6 & D_6^7 & 0 & 0 & 0 & 0 & 0 & 0 \\
0 & 0 & 0 & 0 & 0 & 0 & D_7^6 & I_7 & 0 & 0 & D_7^{10} & 0 & 0 & D_7^{J_3} \\
0 & 0 & 0 & 0 & 0 & D_8^5 & 0 & 0 & I_8 & 0 & D_8^{10} & 0 & D_8^{J_2} & D_8^{J_3} \\
D_9^E & D_9^1 & 0 & 0 & 0 & 0 & 0 & 0 & 0 & I_9 & 0 & 0 & 0 & 0 \\
0 & 0 & 0 & 0 & 0 & 0 & 0 & D_{10}^7 & D_{10}^8 & 0 & I_{10} & 0 & 0 & D_{10}^{J_3} \\
0 & 0 & D_{J_1}^2 & 0 & D_{J_1}^4 & 0 & 0 & 0 & 0 & 0 & 0 & I_{J_1} & 0 & 0 \\
0 & 0 & 0 & 0 & 0 & D_{J_2}^5 & 0 & 0 & D_{J_2}^8 & 0 & 0 & 0 & I_{J_2} & 0 \\
0 & 0 & 0 & 0 & 0 & 0 & 0 & D_{J_3}^7 & D_{J_3}^8 & 0 & D_{J_3}^{10} & 0 & 0 & I_{J_3}
\end{bmatrix}
\begin{Bmatrix} E \\ C_1 \\ C_2 \\ C_3 \\ C_4 \\ C_5 \\ C_6 \\ C_7 \\ C_8 \\ C_9 \\ C_{10} \\ J_1 \\ J_2 \\ J_3 \end{Bmatrix}
$$

Equation 4-31

$$
\boldsymbol{I_3} = \begin{bmatrix}
I_E & D_E^1 & 0 & 0 & 0 & 0 & 0 & 0 & 0 & 0 & 0 & 0 & 0 & 0 \\
D_1^E & I_1 & D_1^2 & 0 & 0 & 0 & 0 & 0 & 0 & D_1^9 & 0 & 0 & 0 & 0 \\
D_2^E & D_2^1 & I_2 & D_2^3 & D_2^4 & 0 & 0 & 0 & 0 & 0 & 0 & D_2^{J_1} & 0 & 0 \\
0 & 0 & D_3^2 & I_3 & 0 & D_3^5 & 0 & 0 & 0 & 0 & 0 & 0 & 0 & 0 \\
0 & 0 & D_4^2 & 0 & I_4 & 0 & D_4^6 & 0 & 0 & 0 & 0 & D_4^{J_1} & 0 & 0 \\
0 & 0 & 0 & D_5^3 & 0 & I_5 & 0 & 0 & D_5^8 & 0 & 0 & 0 & D_5^{J_2} & 0 \\
0 & 0 & 0 & 0 & D_6^4 & 0 & I_6 & D_6^7 & 0 & 0 & 0 & 0 & 0 & 0 \\
0 & 0 & 0 & 0 & 0 & 0 & D_7^6 & I_7 & 0 & 0 & D_7^{10} & 0 & 0 & D_7^{J_3} \\
0 & 0 & 0 & 0 & 0 & D_8^5 & 0 & 0 & I_8 & 0 & D_8^{10} & 0 & D_8^{J_2} & D_8^{J_3} \\
D_9^E & D_9^1 & 0 & 0 & 0 & 0 & 0 & 0 & 0 & I_9 & 0 & 0 & 0 & 0 \\
0 & 0 & 0 & 0 & 0 & 0 & 0 & D_{10}^7 & D_{10}^8 & 0 & I_{10} & 0 & 0 & D_{10}^{J_3} \\
0 & 0 & D_{J_1}^2 & 0 & D_{J_1}^4 & 0 & 0 & 0 & 0 & 0 & 0 & I_{J_1} & 0 & 0 \\
0 & 0 & 0 & 0 & 0 & D_{J_2}^5 & 0 & 0 & D_{J_2}^8 & 0 & 0 & 0 & I_{J_2} & 0 \\
0 & 0 & 0 & 0 & 0 & 0 & 0 & D_{J_3}^7 & D_{J_3}^8 & 0 & D_{J_3}^{10} & 0 & 0 & I_{J_3}
\end{bmatrix}
$$

Equation 4-32

Updating $(\boldsymbol{OC})$ and $(\boldsymbol{OCI})$, to capture interaction matrix $(\boldsymbol{I_3})$ effects, is presented in Equation 4-34 and Equation 4-35.

$$\boldsymbol{OCI_3} = \boldsymbol{OF} \times \boldsymbol{FC_3} \times \boldsymbol{I_3}$$

Equation 4-33

The functional dependencies between operations and components at phase-3 of the system design is:

$$\boldsymbol{OC_3} = \begin{bmatrix} A_1^1 \times \Omega_1^1 + A_1^6 \times \Omega_6^1 & A_1^1 \times B_1^1 & A_1^2 \times B_2^2 & 0 & A_1^4 \times B_4^4 & 0 & A_1^4 \times B_4^6 & A_1^4 \times B_4^7 & 0 & 0 & A_1^6 \times B_6^{10} & A_1^2 \times B_2^{J_1} + A_1^4 \times B_4^{J_1} & 0 & A_1^4 \times B_4^{J_3} + A_1^6 \times B_6^{J_3} \\ A_2^1 \times \Omega_1^1 + A_2^6 \times \Omega_6^1 & A_2^1 \times B_1^1 & A_2^2 \times B_2^2 & 0 & A_2^4 \times B_4^4 & 0 & A_2^4 \times B_4^6 & A_2^4 \times B_4^7 & 0 & 0 & A_2^6 \times B_6^{10} & A_2^2 \times B_2^{J_1} + A_2^4 \times B_4^{J_1} & 0 & A_2^6 \times B_4^{J_3} + A_2^6 \times B_6^{J_3} \\ A_3^1 \times \Omega_1^1 + A_3^6 \times \Omega_6^1 & A_3^1 \times B_1^1 & A_3^2 \times B_2^2 & A_3^3 \times B_3^3 & 0 & A_3^3 \times B_3^5 & 0 & 0 & A_3^5 \times B_5^8 & 0 & A_3^6 \times B_6^{10} & A_3^2 \times B_2^{J_1} & A_3^3 \times B_3^{J_2} + A_3^5 \times B_5^{J_2} & A_3^4 \times B_4^{J_3} + A_3^4 \times B_6^{J_3} \\ A_4^1 \times \Omega_1^1 + A_4^7 \times \Omega_7^1 & A_4^1 \times B_1^1 & 0 & 0 & 0 & 0 & 0 & 0 & 0 & A_4^7 \times B_7^9 & 0 & 0 & 0 & 0 \end{bmatrix}$$

Equation 4-34

$$\boldsymbol{OCI_3} = \left[\begin{matrix} (A_1^1 \times \Omega_1^1 + A_1^6 \times \Omega_6^1)I_E + A_1^1 \times B_1^1 \times D_1^E + A_1^2 \times B_2^2 \times D_2^E & (A_1^1 \times \Omega_1^1 + A_1^6 \times \Omega_6^1)D_E^1 + A_1^2 \times B_2^2 \times D_2^1 + A_1^1 \times B_1^1 \times I_1 \\ (A_2^1 \times \Omega_1^1 + A_2^6 \times \Omega_6^1)I_E + A_2^1 \times B_1^1 \times D_1^E + A_2^2 \times B_2^2 \times D_2^E & (A_2^1 \times \Omega_1^1 + A_2^6 \times \Omega_6^1)D_E^1 + A_2^2 \times B_2^2 \times D_2^1 + A_2^1 \times B_1^1 \times I_1 \\ (A_3^1 \times \Omega_1^1 + A_3^6 \times \Omega_6^1)I_E + A_3^1 \times B_1^1 \times D_1^E + A_3^2 \times B_2^2 \times D_2^E & (A_3^1 \times \Omega_1^1 + A_3^6 \times \Omega_6^1)D_E^1 + A_3^2 \times B_2^2 \times D_2^1 + A_3^1 \times B_1^1 \times I_1 \\ (A_4^1 \times \Omega_1^1 + A_4^7 \times \Omega_7^1)I_E + A_4^1 \times B_1^1 \times D_1^E + A_4^7 \times B_7^9 \times D_2^E & (A_4^1 \times \Omega_1^1 + A_4^7 \times \Omega_7^1)D_E^1 + A_4^7 \times B_7^9 \times D_9^1 + A_4^1 \times B_1^1 \times I_1 \end{matrix}\right. \cdots$$

$$\cdots \begin{matrix} \left(A_1^2 \times B_2^{J_1} + A_1^4 \times B_4^{J_1}\right)D_{J_1}^2 + A_1^1 \times B_1^1 \times D_1^2 + A_1^4 \times B_4^4 \times D_4^2 + A_1^2 \times B_2^2 \times I_2 & A_1^2 \times B_2^2 \times D_2^3 \\ \left(A_2^2 \times B_2^{J_1} + A_2^4 \times B_4^{J_1}\right)D_{J_1}^2 + A_2^1 \times B_1^1 \times D_1^2 + A_2^4 \times B_4^4 \times D_4^2 + A_2^2 \times B_2^2 \times I_2 & A_2^2 \times B_2^2 \times D_2^3 \\ A_3^2 \times B_2^{J_1} \times D_{J_1}^2 + A_3^1 \times B_1^1 \times D_1^2 + A_3^3 \times B_3^3 \times D_3^2 + A_3^2 \times B_2^2 \times I_2 & A_3^2 \times B_2^2 \times D_2^3 + A_3^3\left(B_3^5 \times D_5^3 + B_3^3 \times I_3\right) \\ A_4^1 \times B_1^1 \times D_1^2 & 0 \end{matrix} \cdots$$

$$\cdots \begin{matrix} \left(A_1^2 \times B_2^{J_1} + A_1^4 \times B_4^{J_1}\right)D_{J_1}^4 + A_1^2 \times B_2^2 \times D_2^4 + A_1^4 \times B_4^6 \times D_6^4 + A_1^4 \times B_4^4 \times I_4 & 0 & A_1^4(B_4^4 \times D_4^6 + B_4^7 \times D_7^6 + B_4^6 \times I_6^6) \\ \left(A_2^2 \times B_2^{J_1} + A_2^4 \times B_4^{J_1}\right)D_{J_1}^4 + A_2^2 \times B_2^2 \times D_2^4 + A_2^4 \times B_4^6 \times D_6^4 + A_2^4 \times B_4^4 \times I_4 & 0 & A_2^4(B_4^4 \times D_4^6 + B_4^7 \times D_7^6 + B_4^6 \times I_6^6) \\ A_3^2 \times B_2^{J_1} \times D_{J_1}^4 + A_3^2 \times B_2^2 \times D_2^4 & \left(A_3^3 \times B_3^{J_2} + A_3^5 \times B_5^{J_2}\right)D_{J_2}^5 + A_3^5 \times B_5^8 \times D_8^5 + A_3^3\left(B_3^3 \times D_3^5 + B_3^5 \times I_5\right) & 0 \\ 0 & 0 & 0 \end{matrix} \cdots$$

$$\cdots \begin{matrix} \left(A_1^4 \times B_4^{J_3} + A_1^6 \times B_6^{J_3}\right)D_{J_3}^7 + A_1^6 \times B_6^{10} \times D_{10}^7 + A_1^4(B_4^6 \times D_6^7 + B_4^7 \times I_7) & \left(A_1^4 \times B_4^{J_3} + A_1^6 \times B_6^{J_3}\right)D_{J_3}^8 + A_1^6 \times B_6^{10} \times D_{10}^8 \\ \left(A_2^4 \times B_4^{J_3} + A_2^6 \times B_6^{J_3}\right)D_{J_3}^7 + A_2^6 \times B_6^{10} \times D_{10}^7 + A_2^4(B_4^6 \times D_6^7 + B_4^7 \times I_7) & \left(A_2^4 \times B_4^{J_3} + A_2^6 \times B_6^{J_3}\right)D_{J_3}^8 + A_2^6 \times B_6^{10} \times D_{10}^8 \\ \left(A_3^5 \times B_5^{J_3} + A_3^6 \times B_6^{J_3}\right)D_{J_3}^7 + A_3^6 \times B_6^{10} \times D_{10}^7 & \left(A_3^3 \times B_3^{J_2} + A_3^5 \times B_5^{J_2}\right)D_{J_2}^8 + \left(A_3^5 \times B_5^{J_3} + A_3^6 \times B_6^{J_3}\right)D_{J_3}^8 + A_3^3 \times B_3^5 \times D_5^8 + A_3^6 \times B_6^{10} \times D_{10}^8 + A_3^5 \times B_5^8 \times I_8 \\ 0 & 0 \end{matrix} \cdots$$

$$\cdots \begin{matrix} A_1^1 \times B_1^1 \times D_1^9 & \left(A_1^4 \times B_4^{J_3} + A_1^6 \times B_6^{J_3}\right)D_{J_3}^{10} + A_1^4 \times B_4^7 \times D_7^{10} + A_1^6 \times B_6^{10} \times I_{10} & A_1^2 \times B_2^2 \times D_2^{J_1} + A_1^4 \times B_4^4 \times D_4^{J_1} + \left(A_1^2 \times B_2^{J_1} + A_1^4 \times B_4^{J_1}\right)I_{J_1} \\ A_2^1 \times B_1^1 \times D_1^9 & \left(A_2^4 \times B_4^{J_3} + A_2^6 \times B_6^{J_3}\right)D_{J_3}^{10} + A_2^4 \times B_4^7 \times D_7^{10} + A_2^6 \times B_6^{10} \times I_{10} & A_2^2 \times B_2^2 \times D_2^{J_1} + A_2^4 \times B_4^4 \times D_4^{J_1} + \left(A_2^2 \times B_2^{J_1} + A_2^4 \times B_4^{J_1}\right)I_{J_1} \\ A_3^1 \times B_1^1 \times D_1^9 & \left(A_3^5 \times B_5^{J_3} + A_3^6 \times B_6^{J_3}\right)D_{J_3}^{10} + A_3^5 \times B_5^8 \times D_8^{10} + A_3^6 \times B_6^{10} \times I_{10} & A_3^2 \times B_2^2 \times D_2^{J_1} + A_3^2 \times B_2^{J_1} \times I_{J_1} \\ A_4^1 \times B_1^1 \times D_1^9 + A_4^7 \times B_7^9 \times I_9 & 0 & 0 \end{matrix} \cdots$$

$$\cdots \left.\begin{matrix} 0 & A_1^6 \times B_6^{10} \times D_{10}^{J_3} + A_1^4 \times B_4^7 \times D_7^{J_3} + \left(A_1^4 \times B_4^{J_3} + A_1^6 \times B_6^{J_3}\right)I_{J_3} \\ 0 & A_2^6 \times B_6^{10} \times D_{10}^{J_3} + A_2^4 \times B_4^7 \times D_7^{J_3} + \left(A_2^6 \times B_4^{J_3} + A_2^6 \times B_6^{J_3}\right)I_{J_3} \\ \left(A_3^3 \times B_3^{J_2} + A_3^5 \times B_5^{J_2}\right)I_{J_2} + A_3^3 \times B_3^5 \times D_5^{J_2} + A_3^5 \times B_5^8 \times D_8^{J_2} & A_3^6 \times B_6^{10} \times D_{10}^{J_3} + A_3^4 \times B_4^7 \times D_7^{J_3} + \left(A_3^4 \times B_4^{J_3} + A_3^4 \times B_6^{J_3}\right)I_{J_3} \\ 0 & 0 \end{matrix}\right]$$

Equation 4-35

Equation 4-34 recognizes the subsystems presented in Equation 4-25

$$\begin{gathered} S_E = \{E\} \\ S_1 = \{C_1\} \\ S_2 = \{C_2\} \\ S_3 = \{C_4, C_6, C_7\} \\ S_4 = \{C_3, C_5\} \\ S_5 = \{C_8\} \\ S_6 = \{C_9\} \\ S_7 = \{C_{10}\} \\ S_8 = \{J_1\} \\ S_9 = \{J_2\} \\ S_{10} = \{J_3\} \end{gathered}$$

Equation 4-36

Indirect Stimulus between Components

One additional mechanical stress (indirect stimulus) between (C_8) and (C_4) was recognized at a late stage of the embodiment design; the interaction was captured and presented in Figure 4-10. Components' stimulus interaction matrix is modeled by Equation 4-37, Equation 4-38 and Equation 4-39.

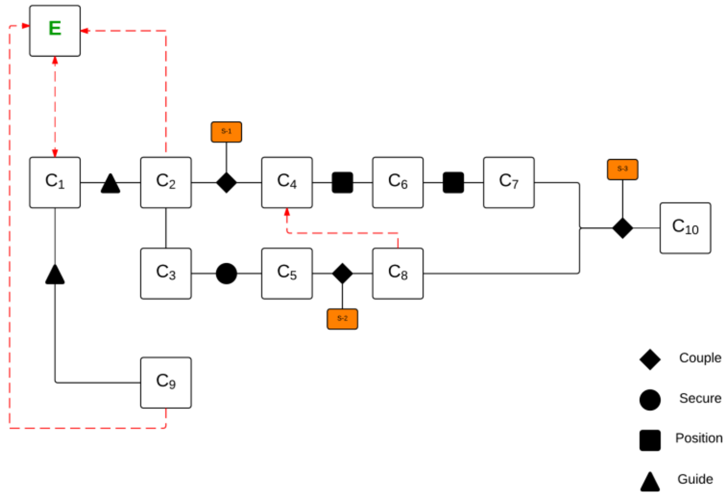

Figure 4-10: Updated assembly structure with stimulus

$$\{C^*\}^S = \boldsymbol{I}_4^{CS}\{C\}^S$$ **Equation 4-37**

$$\begin{Bmatrix} E^* \\ C^*{}_1 \\ C^*{}_2 \\ C^*{}_3 \\ C^*{}_4 \\ C^*{}_5 \\ C^*{}_6 \\ C^*{}_7 \\ C^*{}_8 \\ C^*{}_9 \\ C^*{}_{10} \\ J^*{}_1 \\ J^*{}_2 \\ J^*{}_3 \end{Bmatrix}^S = \begin{bmatrix} 0 & 0 & 0 & 0 & 0 & 0 & 0 & 0 & 0 & 0 & 0 & 0 & 0 & 0 \\ 0 & 0 & 0 & 0 & 0 & 0 & 0 & 0 & 0 & 0 & 0 & 0 & 0 & 0 \\ 0 & 0 & 0 & 0 & 0 & 0 & 0 & 0 & 0 & 0 & 0 & 0 & 0 & 0 \\ 0 & 0 & 0 & 0 & 0 & 0 & 0 & 0 & 0 & 0 & 0 & 0 & 0 & 0 \\ 0 & 0 & 0 & 0 & 0 & 0 & 0 & 0 & 0 & 0 & 0 & 0 & 0 & 0 \\ 0 & 0 & 0 & 0 & 0 & 0 & 0 & 0 & 0 & 0 & 0 & 0 & 0 & 0 \\ 0 & 0 & 0 & 0 & 0 & 0 & 0 & 0 & 0 & 0 & 0 & 0 & 0 & 0 \\ 0 & 0 & 0 & 0 & 0 & 0 & 0 & 0 & 0 & 0 & 0 & 0 & 0 & 0 \\ 0 & 0 & 0 & 0 & G_8^4 & 0 & 0 & 0 & 0 & 0 & 0 & 0 & 0 & 0 \\ 0 & 0 & 0 & 0 & 0 & 0 & 0 & 0 & 0 & 0 & 0 & 0 & 0 & 0 \\ 0 & 0 & 0 & 0 & 0 & 0 & 0 & 0 & 0 & 0 & 0 & 0 & 0 & 0 \\ 0 & 0 & 0 & 0 & 0 & 0 & 0 & 0 & 0 & 0 & 0 & 0 & 0 & 0 \\ 0 & 0 & 0 & 0 & 0 & 0 & 0 & 0 & 0 & 0 & 0 & 0 & 0 & 0 \\ 0 & 0 & 0 & 0 & 0 & 0 & 0 & 0 & 0 & 0 & 0 & 0 & 0 & 0 \end{bmatrix} \begin{Bmatrix} E \\ C_1 \\ C_2 \\ C_3 \\ C_4 \\ C_5 \\ C_6 \\ C_7 \\ C_8 \\ C_9 \\ C_{10} \\ J_1 \\ J_2 \\ J_3 \end{Bmatrix}^S$$ **Equation 4-38**

$$\boldsymbol{I_4^{CS}} = \begin{bmatrix} 0 & 0 & 0 & 0 & 0 & 0 & 0 & 0 & 0 & 0 & 0 & 0 & 0 & 0 \\ 0 & 0 & 0 & 0 & 0 & 0 & 0 & 0 & 0 & 0 & 0 & 0 & 0 & 0 \\ 0 & 0 & 0 & 0 & 0 & 0 & 0 & 0 & 0 & 0 & 0 & 0 & 0 & 0 \\ 0 & 0 & 0 & 0 & 0 & 0 & 0 & 0 & 0 & 0 & 0 & 0 & 0 & 0 \\ 0 & 0 & 0 & 0 & 0 & 0 & 0 & 0 & 0 & 0 & 0 & 0 & 0 & 0 \\ 0 & 0 & 0 & 0 & 0 & 0 & 0 & 0 & 0 & 0 & 0 & 0 & 0 & 0 \\ 0 & 0 & 0 & 0 & 0 & 0 & 0 & 0 & 0 & 0 & 0 & 0 & 0 & 0 \\ 0 & 0 & 0 & 0 & 0 & 0 & 0 & 0 & 0 & 0 & 0 & 0 & 0 & 0 \\ 0 & 0 & 0 & 0 & G_8^4 & 0 & 0 & 0 & 0 & 0 & 0 & 0 & 0 & 0 \\ 0 & 0 & 0 & 0 & 0 & 0 & 0 & 0 & 0 & 0 & 0 & 0 & 0 & 0 \\ 0 & 0 & 0 & 0 & 0 & 0 & 0 & 0 & 0 & 0 & 0 & 0 & 0 & 0 \\ 0 & 0 & 0 & 0 & 0 & 0 & 0 & 0 & 0 & 0 & 0 & 0 & 0 & 0 \\ 0 & 0 & 0 & 0 & 0 & 0 & 0 & 0 & 0 & 0 & 0 & 0 & 0 & 0 \\ 0 & 0 & 0 & 0 & 0 & 0 & 0 & 0 & 0 & 0 & 0 & 0 & 0 & 0 \end{bmatrix}$$ **Equation 4-39**

The updated universal interaction matrix is shown by Equation 3-24

$$\boldsymbol{I_4} = \begin{bmatrix} I_E & D_E^1 & 0 & 0 & 0 & 0 & 0 & 0 & 0 & 0 & 0 & 0 & 0 & 0 \\ D_1^E & I_1 & D_1^2 & 0 & 0 & 0 & 0 & 0 & 0 & D_1^9 & 0 & 0 & 0 & 0 \\ D_2^E & D_2^1 & I_2 & D_2^3 & D_2^4 & 0 & 0 & 0 & 0 & 0 & 0 & D_2^{J_1} & 0 & 0 \\ 0 & 0 & D_3^2 & I_3 & 0 & D_3^5 & 0 & 0 & 0 & 0 & 0 & 0 & 0 & 0 \\ 0 & 0 & D_4^2 & 0 & I_4 & 0 & D_4^6 & 0 & 0 & 0 & 0 & D_4^{J_1} & 0 & 0 \\ 0 & 0 & 0 & D_5^3 & 0 & I_5 & 0 & 0 & D_5^8 & 0 & 0 & 0 & D_5^{J_2} & 0 \\ 0 & 0 & 0 & 0 & D_6^4 & 0 & I_6 & D_6^7 & 0 & 0 & 0 & 0 & 0 & 0 \\ 0 & 0 & 0 & 0 & 0 & 0 & D_7^6 & I_7 & 0 & 0 & D_7^{10} & 0 & 0 & D_7^{J_3} \\ 0 & 0 & 0 & 0 & G_8^4 & D_8^5 & 0 & 0 & I_8 & 0 & D_8^{10} & 0 & D_8^{J_2} & D_8^{J_3} \\ D_9^E & D_9^1 & 0 & 0 & 0 & 0 & 0 & 0 & 0 & I_9 & 0 & 0 & 0 & 0 \\ 0 & 0 & 0 & 0 & 0 & 0 & 0 & D_{10}^7 & D_{10}^8 & 0 & I_{10} & 0 & 0 & D_{10}^{J_3} \\ 0 & 0 & D_{J_1}^2 & 0 & D_{J_1}^4 & 0 & 0 & 0 & 0 & 0 & 0 & I_{J_1} & 0 & 0 \\ 0 & 0 & 0 & 0 & 0 & D_{J_2}^5 & 0 & 0 & D_{J_2}^8 & 0 & 0 & 0 & I_{J_2} & 0 \\ 0 & 0 & 0 & 0 & 0 & 0 & 0 & D_{J_3}^7 & D_{J_3}^8 & 0 & D_{J_3}^{10} & 0 & 0 & I_{J_3} \end{bmatrix}$$ **Equation 4-40**

MDRV framework captures the damage stimulus synthesis using interaction matrices: $\boldsymbol{I_1}, \boldsymbol{I_2}, \boldsymbol{I_3}$, and $\boldsymbol{I_4}$,during different development phases of the system design. The relationships between operations and components for the finalized design form are presented by Equation 4-41 and Equation 4-42. At this stage of the design ($\boldsymbol{OC_4} = \boldsymbol{OC_3}$); the operations-components functional coupling relationships did not get affected ($\boldsymbol{FC_4} = \boldsymbol{FC_3}$).

$$\boldsymbol{OCI_4} = \boldsymbol{OF} \times \boldsymbol{FC_3} \times \boldsymbol{I_4}$$ **Equation 4-41**

$$
\boldsymbol{OCI_4} = \left[\begin{matrix}
(A_1^1 \times \Omega_1^1 + A_1^6 \times \Omega_6^1)I_E + A_1^1 \times B_1^1 \times D_1^E + A_1^2 \times B_2^2 \times D_2^E & (A_1^1 \times \Omega_1^1 + A_1^6 \times \Omega_6^1)D_E^1 + A_1^2 \times B_2^2 \times D_2^1 + A_1^1 \times B_1^1 \times I_1 \\
(A_2^1 \times \Omega_1^1 + A_2^6 \times \Omega_6^1)I_E + A_2^1 \times B_1^1 \times D_1^E + A_2^2 \times B_2^2 \times D_2^E & (A_2^1 \times \Omega_1^1 + A_2^6 \times \Omega_6^1)D_E^1 + A_2^2 \times B_2^2 \times D_2^1 + A_2^1 \times B_1^1 \times I_1 \\
(A_3^1 \times \Omega_1^1 + A_3^6 \times \Omega_6^1)I_E + A_3^1 \times B_1^1 \times D_1^E + A_3^2 \times B_2^2 \times D_2^E & (A_3^1 \times \Omega_1^1 + A_3^6 \times \Omega_6^1)D_E^1 + A_3^2 \times B_2^2 \times D_2^1 + A_3^1 \times B_1^1 \times I_1 \\
(A_4^1 \times \Omega_1^1 + A_4^7 \times \Omega_7^1)I_E + A_4^1 \times B_1^1 \times D_1^E + A_4^7 \times B_7^9 \times D_2^E + A_4^7 \times B_7^9 \times D_9^E & (A_4^1 \times \Omega_1^1 + A_4^7 \times \Omega_7^1)D_E^1 + A_4^7 \times B_7^9 \times D_9^1 + A_4^1 \times B_1^1 \times I_1
\end{matrix}\right. \quad \cdots
$$

$$
\cdots \quad \begin{matrix}
\left(A_1^2 \times B_2^{J_1} + A_1^4 \times B_4^{J_1}\right)D_{J_1}^2 + A_1^1 \times B_1^1 \times D_1^2 + A_1^4 \times B_4^4 \times D_4^2 + A_1^2 \times B_2^2 \times I_2 & A_1^2 \times B_2^2 \times D_2^3 \\
\left(A_2^2 \times B_2^{J_1} + A_2^4 \times B_4^{J_1}\right)D_{J_1}^2 + A_2^1 \times B_1^1 \times D_1^2 + A_2^4 \times B_4^4 \times D_4^2 + A_2^2 \times B_2^2 \times I_2 & A_2^2 \times B_2^2 \times D_2^3 \\
A_3^2 \times B_2^{J_1} \times D_{J_1}^2 + A_3^1 \times B_1^1 \times D_1^2 + A_3^3 \times B_3^3 \times D_3^2 + A_3^2 \times B_2^2 \times I_2 & A_3^2 \times B_2^2 \times D_2^3 + A_3^3(B_3^5 \times D_5^3 + B_3^3 \times I_3) \\
A_4^1 \times B_1^1 \times D_1^2 & 0
\end{matrix} \quad \cdots
$$

$$
\cdots \quad \begin{matrix}
\left(A_1^2 \times B_2^{J_1} + A_1^4 \times B_4^{J_1}\right)D_{J_1}^4 + A_1^2 \times B_2^2 \times D_2^4 + A_1^4 \times B_4^6 \times D_6^4 + A_1^4 \times B_4^4 \times I_4 & 0 & A_1^4(B_4^4 \times D_4^6 + B_4^7 \times D_7^6 + B_4^6 \times I_6^6) \\
\left(A_2^2 \times B_2^{J_1} + A_2^4 \times B_4^{J_1}\right)D_{J_1}^4 + A_2^2 \times B_2^2 \times D_2^4 + A_2^4 \times B_4^6 \times D_6^4 + A_2^4 \times B_4^4 \times I_4 & 0 & A_2^4(B_4^4 \times D_4^6 + B_4^7 \times D_7^6 + B_4^6 \times I_6^6) \\
A_3^2 \times B_2^{J_1} \times D_{J_1}^4 + A_3^2 \times B_2^2 \times D_2^4 + A_3^5 \times B_5^8 \times G_8^4 & \left(A_3^3 \times B_3^{J_2} + A_3^5 \times B_5^{J_2}\right)D_{J_2}^5 + A_3^5 \times B_5^8 \times D_8^5 + A_3^3(B_3^3 \times D_3^5 + B_3^5 \times I_5) & 0 \\
0 & 0 & 0
\end{matrix} \quad \cdots
$$

Equation 4-42

$$
\cdots \quad \begin{matrix}
\left(A_1^4 \times B_4^{J_3} + A_1^6 \times B_6^{J_3}\right)D_{J_3}^7 + A_1^6 \times B_6^{10} \times D_{10}^7 + A_1^4(B_4^6 \times D_6^7 + B_4^7 \times I_7) & \left(A_1^4 \times B_4^{J_3} + A_1^6 \times B_6^{J_3}\right)D_{J_3}^8 + A_1^6 \times B_6^{10} \times D_{10}^8 \\
\left(A_2^4 \times B_4^{J_3} + A_2^6 \times B_6^{J_3}\right)D_{J_3}^7 + A_2^6 \times B_6^{10} \times D_{10}^7 + A_2^4(B_4^6 \times D_6^7 + B_4^7 \times I_7) & \left(A_2^4 \times B_4^{J_3} + A_2^6 \times B_6^{J_3}\right)D_{J_3}^8 + A_2^6 \times B_6^{10} \times D_{10}^8 \\
\left(A_3^5 \times B_5^{J_3} + A_3^6 \times B_6^{J_3}\right)D_{J_3}^7 + A_3^6 \times B_6^{10} \times D_{10}^7 & \left(A_3^3 \times B_3^{J_2} + A_3^5 \times B_5^{J_2}\right)D_{J_2}^8 + \left(A_3^5 \times B_5^{J_3} + A_3^6 \times B_6^{J_3}\right)D_{J_3}^8 + A_3^3 \times B_3^5 \times D_5^8 + A_3^6 \times B_6^{10} \times D_{10}^8 + A_3^5 \times B_5^8 \times I_8 \\
0 & 0
\end{matrix} \quad \cdots
$$

$$
\cdots \quad \begin{matrix}
A_1^1 \times B_1^1 \times D_1^9 & \left(A_1^4 \times B_4^{J_3} + A_1^6 \times B_6^{J_3}\right)D_{J_3}^{10} + A_1^4 \times B_4^7 \times D_7^{10} + A_1^6 \times B_6^{10} \times I_{10} & A_1^2 \times B_2^2 \times D_2^{J_1} + A_1^4 \times B_4^4 \times D_4^{J_1} + \left(A_1^2 \times B_2^{J_1} + A_1^4 \times B_4^{J_1}\right)I_{J_1} \\
A_2^1 \times B_1^1 \times D_1^9 & \left(A_2^4 \times B_4^{J_3} + A_2^6 \times B_6^{J_3}\right)D_{J_3}^{10} + A_2^4 \times B_4^7 \times D_7^{10} + A_2^6 \times B_6^{10} \times I_{10} & A_2^2 \times B_2^2 \times D_2^{J_1} + A_2^4 \times B_4^4 \times D_4^{J_1} + \left(A_2^2 \times B_2^{J_1} + A_2^4 \times B_4^{J_1}\right)I_{J_1} \\
A_3^1 \times B_1^1 \times D_1^9 & \left(A_3^5 \times B_5^{J_3} + A_3^6 \times B_6^{J_3}\right)D_{J_3}^{10} + A_3^5 \times B_5^8 \times D_8^{10} + A_3^6 \times B_6^{10} \times I_{10} & A_3^2 \times B_2^2 \times D_2^{J_1} + A_3^2 \times B_2^{J_1} \times I_{J_1} \\
A_4^1 \times B_1^1 \times D_1^9 + A_4^7 \times B_7^9 \times I_9 & 0 & 0
\end{matrix} \quad \cdots
$$

$$
\cdots \quad \left.\begin{matrix}
0 & A_1^6 \times B_6^{10} \times D_{10}^{J_3} + A_1^4 \times B_4^7 \times D_7^{J_3} + \left(A_1^4 \times B_4^{J_3} + A_1^6 \times B_6^{J_3}\right)I_{J_3} \\
0 & A_2^6 \times B_6^{10} \times D_{10}^{J_3} + A_2^4 \times B_4^7 \times D_7^{J_3} + \left(A_2^6 \times B_4^{J_3} + A_2^6 \times B_6^{J_3}\right)I_{J_3} \\
\left(A_3^3 \times B_3^{J_2} + A_3^5 \times B_5^{J_2}\right)I_{J_2} + A_3^3 \times B_3^5 \times D_5^{J_2} + A_3^5 \times B_5^8 \times D_8^{J_2} & A_3^6 \times B_6^{10} \times D_{10}^{J_3} + A_3^4 \times B_4^7 \times D_7^{J_3} + \left(A_3^4 \times B_4^{J_3} + A_3^4 \times B_6^{J_3}\right)I_{J_3} \\
0 & 0
\end{matrix}\right]
$$

4.2 Reliability Assessment:

The focus of the reliability assessment in this section will be on assessing the system synthesis developed during the previous design phases, Chapter 5- (Case Study) will focus on MRDV integration to components design.

4.2.1 Component Reliability: Design Phase-1

At this phase of the design state initial W-relationships can be realized, using Equation 4-13, the following relationships are realized:

$$O_1 \xrightarrow{W^1} \{C_1, C_2, C_4, C_6, C_7, C_{10}\}$$

$$O_2 \xrightarrow{W^2} \{C_1, C_2, C_4, C_6, C_7, C_{10}\}$$

$$O_3 \xrightarrow{W^3} \{C_1, C_3, C_5, C_8, C_{10}\}$$

$$O_4 \xrightarrow{W^4} \{C_1, C_9\}$$

Equation 4-43

H-relationships would be defined by the system designer; a system operational descriptive model will outline these relationships in more details, logical description is presented in Equation 4-44:

$$O_1 \xrightarrow{H^1} (C_1 \cap C_2 \cap (C_4 \cup C_6 \cup C_7) \cap C_{10})$$

$$O_2 \xrightarrow{H^2} (C_1 \cap C_2 \cap (C_4 \cup C_6 \cup C_7) \cap C_{10})$$

$$O_3 \xrightarrow{H^3} (C_1 \cap (C_3 \cap C_5) \cap C_8 \cap C_{10})$$

$$O_4 \xrightarrow{H^4} (C_1 \cap C_9)$$

Equation 4-44

Using Equation 4-14, the following damage relationships can realized

$$
\begin{aligned}
&C_1 \xrightarrow{d^1} \{O_1, O_2, O_3, O_4\} \\
&C_2 \xrightarrow{d^2} \{O_1, O_2, O_3, O_4\} \\
&C_3 \xrightarrow{d^3} \{O_2\} \\
&C_4 \xrightarrow{d^4} \{O_1, O_2\} \\
&C_5 \xrightarrow{d^5} \{O_3\} \\
&C_6 \xrightarrow{d^6} \{O_1, O_2\} \\
&C_7 \xrightarrow{d^7} \{O_1, O_2\} \\
&C_8 \xrightarrow{d^8} \{ O_3\} \\
&C_9 \xrightarrow{d^9} \{O_4\} \\
&C_{10} \xrightarrow{d^{10}} \{O_1, O_2, O_3\}
\end{aligned}
$$

Equation 4-45

The following TTF distributions can be realized from Equation 4-45 system of relationships

$$
\begin{aligned}
&TTF_{C_1} \xrightarrow{d^1} \{\Lambda_{C_1}^{O_1}, \Lambda_{C_1}^{O_2}, \Lambda_{C_1}^{O_3}, \Lambda_{C_1}^{O_4}\} \\
&TTF_{C_2} \xrightarrow{d^2} \{\Lambda_{C_2}^{O_1}, \Lambda_{C_2}^{O_2}, \Lambda_{C_2}^{O_3}, \Lambda_{C_2}^{O_4}\} \\
&TTF_{C_3} \xrightarrow{d^3} \{\Lambda_{C_3}^{O_2}\} \\
&TTF_{C_4} \xrightarrow{d^4} \{\Lambda_{C_4}^{O_1}, \Lambda_{C_4}^{O_2}\}
\end{aligned}
$$

Equation 4-46

$$TTF_{C_5} \xrightarrow{d^5} \{\Lambda_{C_5}^{O_3}\}$$

$$TTF_{C_6} \xrightarrow{d^6} \{\Lambda_{C_6}^{O_1}, \Lambda_{C_6}^{O_2}\}$$

$$TTF_{C_7} \xrightarrow{d^7} \{\Lambda_{C_7}^{O_1}, \Lambda_{C_7}^{O_2}\}$$

$$TTF_{C_8} \xrightarrow{d^8} \{\Lambda_{C_8}^{O_3}\}$$

$$TTF_{C_9} \xrightarrow{d^9} \{\Lambda_{C_9}^{O_4}\}$$

$$TTF_{C_{10}} \xrightarrow{d^{10}} \{\Lambda_{C_{10}}^{O_1}, \Lambda_{C_{10}}^{O_2}, \Lambda_{C_{10}}^{O_3}\}$$

where: $TTF_{C_\mathrm{i}} \equiv$ Time to failure of component (C_i)

$\Lambda_{C_i}^{O_j} \equiv$ damage of component (C_i) caused by operation (O_j)

The system operational reliability statement is presented in Equation 4-47 where (t) represents time variable, (O) represents operations logical statement and $\{M\}$ represents materials set used for design.

$$R(t) = R(t|O_1 \cap O_2 \cap O_3 \cap O_4, \{M\}) \qquad \textbf{Equation 4-47}$$

The reliability statement shows all operations are equally important to the system user. The stress distributions on components are presented in Table 4-1; the stress cycle duration is presented in Table 4-2; material damage model parameters are presented in Table 4-3 and system annual usage is presented in Table 4-4.

Table 4-1: Components Stress Distribution, pdf distribution for different operations

Component	Stress (MPa)			
	O_1	O_2	O_3	O_4
C_1	LN(3.91,0.0500)	LN(4.57,0.0998)	LN(4.25,0.0699)	LN(4.20,0.0799)
C_2	LN(4.53,0.0599)	LN(4.29,0.0500)	LN(3.22,0.0400)	LN(3.49,0.0599)
C_3			LN(4.09,0.0998)	
C_4	LN(4.02,0.0799)	LN(3.87,0.0699)		
C_5			LN(3.99,0.0799)	
C_6	LN(4.78,0.0799)	LN(3.91,0.0500)		
C_7	LN(4.22,0.0699)	LN(4.46,0.0898)		
C_8			LN(3.85,0.0898)	
C_9				LN(3.63,0.0898)
C_{10}	LN(4.72,0.0699)	LN(4.29,0.0699)	LN(4.47,0.0898)	

Table 4-2: Stress cycle duration; pdf distribution for different operations

Stress Cycle Duration (hrs)			
O_1	O_2	O_3	O_4
LN(-0.92,0.0200)	LN(-0.11,0.0300)	LN(-4.61,0.0400)	LN(-2.30,0.0100)

Table 4-3: Material Fatigue Properties: Two parameters are needed, pdf distribution

Fatigue Strength Coefficient (MPa)	σ'_f	LN(6.55,0.0100)
Fatigue Strength Exponent	b	-LN(-2.15,0.0100)
Fatigue Ductility Coefficient	ε'_f	LN(-2.00,0.0100)
Fatigue Ductility Exponent	c	-LN(-0.90,0.0100)

Table 4-4: System Usage; pdf distribution for different operations

Operations	System Usage (Hrs/yr)
O_1	LN(4.61,0.0100)
O_2	LN(5.52,0.0150)
O_3	LN(5.77,0.0100)
O_4	LN(5.98,0.0100)

The data from Table 4-1 Table 4-2, Table 4-3 and Table 4-4 were used as inputs to Component Reliability Assessment Matlab code (Appendix B.1): the TTF outputs are presented in Table 4-5. Figure 4-11 shows some of the Matlab code outputs for one of the components. Figure 4-12 presents the Lognormal Maximum Likelihood Estimation to TTF reliability function.

Table 4-5: Component TTF distribution and Reliability at design time goal

Component	TTF (Hrs.)		Reliability at (Tg=5E6 Hrs)
	E(TTF)	Distribution	
C_1	1.0883E7	LN(16.0518,0.5493)	0.8731
C_2	1.2957E8	LN(18.6604,0.1968)	1.0000
C_3	9.8095E8	LN(20.6486,0.3329)	1.000
C_4	2.9797E9	LN(21.7899,0.2246)	1.000
C_5	7.5375E9	LN(21.8764,1.3166)	1.0000
C_6	5.4016E6	LN(15.4045,0.4422)	0.4815
C_7	7.0247E7	LN(17.9073,0.5661)	1.000
C_8	1.2474E10	LN(23.1356, 0.4717)	1.0000
C_9	1.5590E10	LN(23.4660, 0.0875)	1.0000
C_{10}	1.0958E6	LN(13.5061,0.8954)	0.0161

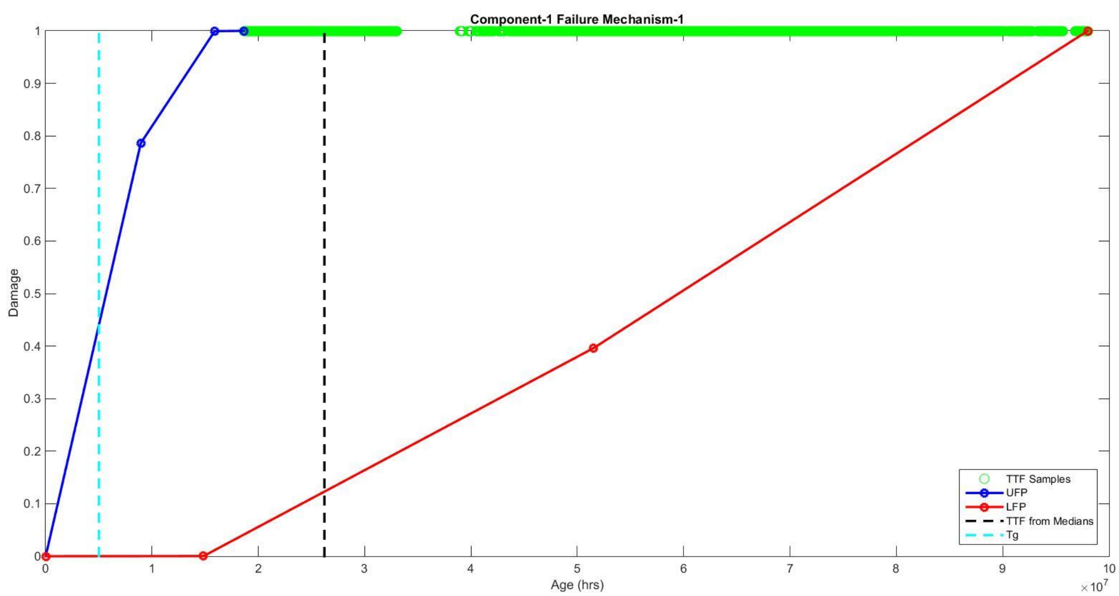

Figure 4-11: Mechanistic Reliability Algorithm Outputs

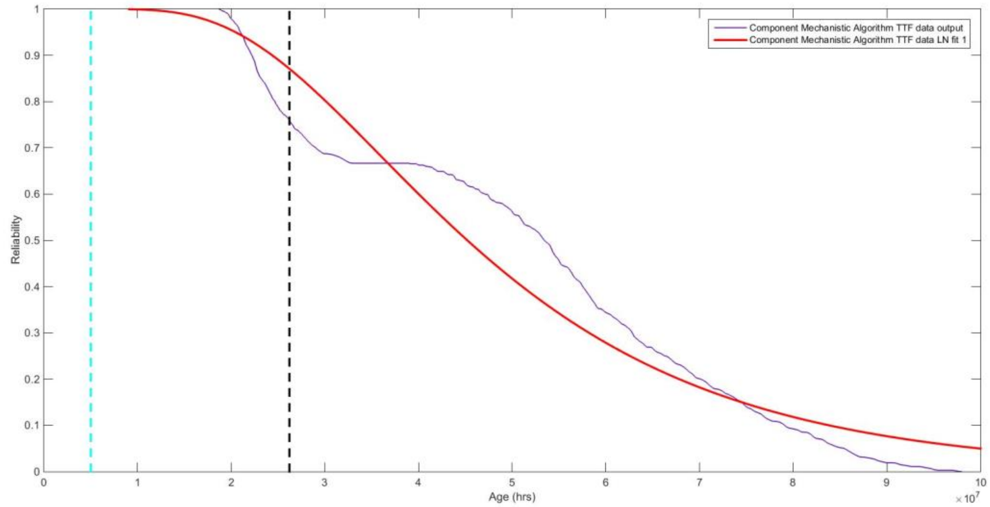

Figure 4-12: TTF Reliability Function vs Lognormal MLE Reliability

4.2.2 System Reliability: Design Phase-1

Equation 4-12 recognizes the sets presented in Equation 4-48 as subsystems candidates because they deliver the same set of functions. The following subsystems are realized by system analyst:

$$\begin{gathered} S_1 = \{C_1\} \\ S_2 = \{C_2\} \\ S_3 = \{C_4, C_6, C_7\} \\ S_4 = \{C_3, C_5\} \\ S_5 = \{C_8\} \\ S_6 = \{C_9\} \\ S_7 = \{C_{10}\} \end{gathered} \tag{Equation 4-48}$$

This method can be helpful for the system analyst to realize subsystems, for the system designer this is a trivial activity. Using Equation 4-44, the subsystem resultant damages can be realized from components damages interrelationship, as shown by Equation 4-49 :

$$\Lambda_{S_1} = \Lambda_{C_1}$$
$$\Lambda_{S_2} = \Lambda_{C_2}$$
$$\Lambda_{S_3} = \mathbf{SYNC2}(\Lambda_{C_4}, \Lambda_{C_6}, \Lambda_{C_7})$$
$$\Lambda_{S_4} = \mathbf{SYNC2}(\Lambda_{C_3}, \Lambda_{C_5}) \qquad \textbf{Equation 4-49}$$
$$\Lambda_{S_5} = \Lambda_{C_8}$$
$$\Lambda_{S_6} = \Lambda_{C_9}$$
$$\Lambda_{S_7} = \Lambda_{C_{10}}$$

where: $\Lambda_{S_\mathrm{i}} \equiv$ subsystem (S_i) damage

$\Lambda_{C_\mathrm{i}} \equiv$ component (C_i) damage

System damage statement can be assembled from subsystems damage relationships as shown in Equation 4-53:

$$\Lambda_{O_1}^{SYS} = \mathbf{SYNC1}(\Lambda_{C_1}, \Lambda_{C_2}, \Lambda_{C_{10}})$$
$$\Lambda_{O_2}^{SYS} = \mathbf{SYNC1}(\mathbf{SYNC2}(\Lambda_{C_4}, \Lambda_{C_6}, \Lambda_{C_7}), \Lambda_{C_{10}})$$
$$\Lambda_{O_3}^{SYS} = \mathbf{SYNC1}(\Lambda_{C_1}, \Lambda_{C_2}, \mathbf{SYNC2}(\Lambda_{C_3}, \Lambda_{C_5}), \Lambda_{C_8}, \Lambda_{C_{10}}) \qquad \textbf{Equation 4-50}$$
$$\Lambda_{O_4}^{SYS} = \mathbf{SYNC1}(\Lambda_{C_1}, \Lambda_{C_9})$$

$$\Lambda_{O_1 \cap O_2}^{SYS} = \mathbf{SYNC1}(\Lambda_{C_1}, \Lambda_{C_2}, \mathbf{SYNC2}(\Lambda_{C_4}, \Lambda_{C_6}, \Lambda_{C_7}), \Lambda_{C_{10}})$$
$$\Lambda_{O_3}^{SYS} = \mathbf{SYNC1}(\Lambda_{C_1}, \Lambda_{C_2}, \mathbf{SYNC2}(\Lambda_{C_3}, \Lambda_{C_5}), \Lambda_{C_8}, \Lambda_{C_{10}}) \qquad \textbf{Equation 4-51}$$
$$\Lambda_{O_4}^{SYS} = \mathbf{SYNC1}(\Lambda_{C_1}, \Lambda_{C_9})$$

$$\Lambda_{SYS} = \Lambda^{SYS}_{(O_1 \cap O_2) \cap O_3 \cap O_3}$$

$$\Lambda_{SYS} = \mathbf{SYNC1}\left(\Lambda_{C_1}, \mathbf{ASYNC}\left(\Lambda_{C_9}, \mathbf{SYNC1}\left(\Lambda_{C_2}, \mathbf{ASYNC}\left(\mathbf{SYNC2}\left(\Lambda_{C_4}, \Lambda_{C_6}, \Lambda_{C_7}\right), \mathbf{SYNC1}\left(\mathbf{SYNC2}\left(\Lambda_{C_3}, \Lambda_{C_5}\right), \Lambda_{C_8}\right)\right), \Lambda_{C_{10}}\right)\right)\right)$$ **Equation 4-52**

System damage statements can also be developed from subsystems realized by Equation 4-49

$$\Lambda_{SYS} = \mathbf{SYNC1}\left(\Lambda_{S_1}, \mathbf{ASYNC}\left(\Lambda_{S_6}, \mathbf{SYNC1}\left(\Lambda_{S_2}, \mathbf{ASYNC}\left(\Lambda_{S_3}, \mathbf{SYNC1}\left(\Lambda_{S_4}, \Lambda_{S_5}\right)\right), \Lambda_{S_7}\right)\right)\right)$$ **Equation 4-53**

Probability spaces for subsystems composed of more than one component need to be created before assessing their TTF.

$$TTF_{S_1} = TTF_{C_1}$$

$$TTF_{S_2} = TTF_{C_2}$$

$$TTF_{S_3} = \mathbf{SYNC2}\left(\text{ProbSpace}\left\{TTF_{C_4}, TTF_{C_6}, TTF_{C_7}\right\}\right)$$

$$TTF_{S_4} = \mathbf{SYNC2}\left(\text{ProbSpace}\left\{TTF_{C_3}, TTF_{C_5}\right\}\right)$$ **Equation 4-54**

$$TTF_{S_5} = TTF_{C_8}$$

$$TTF_{S_6} = TTF_{C_9}$$

$$TTF_{S_7} = TTF_{C_{10}}$$

where: $TTF_{S_i} \equiv$ Time to failure set of subsystem (S_i); set of random TTF samples generated from a known time to failure distribution

$TTF_{C_i} \equiv$ Time to failure set of component (C_i); set of random TTF samples generated from a known time to failure distribution

ProbSpace ≡ an operator on sets of random numbers, it generates set of sets of all possible combinations of input sets elements.

$$TTF_{SYS} = \mathbf{SYNC1}\Big(\text{ProbSpace}\Big\{TTF_{C_1}, \mathbf{ASYNC}\Big(\text{ProbSpace}\Big\{TTF_{C_9}, \mathbf{SYNC1}\Big(\text{ProbSpace}\Big\{TTF_{C_2}, \mathbf{ASYNC}\Big(\text{ProbSpace}\Big\{\mathbf{SYNC2}\Big(\text{ProbSpace}\big\{TTF_{C_4}, TTF_{C_6}, TTF_{C_7}\big\}\Big), \mathbf{SYNC1}\Big(\text{ProbSpace}\Big\{TTF_{C_8}, \mathbf{SYNC2}\Big(\text{ProbSpace}\big\{TTF_{C_3}, TTF_{C_5}\big\}\Big)\Big\}\Big)\Big\}\Big), TTF_{C_{10}}\Big\}\Big)\Big\}\Big)\Big\}\Big) \quad \textbf{Equation 4-55}$$

A graphical representation, as shown in Figure 4-13, can better organize and elaborate these relationships. Each (ProbSpace) node create sets inputs to **SYNC1**, **SYNC2** or **ASYNC** operators.

Based on the initial system, Figure 4-13, reliability representation the TTF density function was evaluated as LN (16.0640, 0.4789); the reliability of this system at 5,000,000 hours is 0.9090.

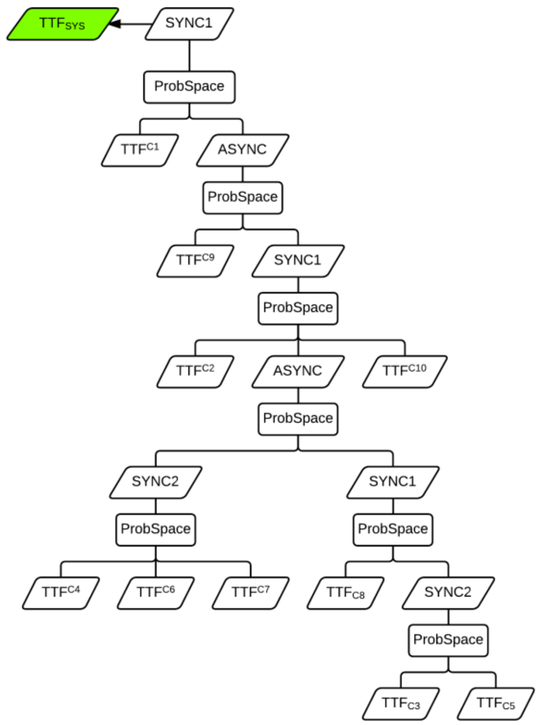

Figure 4-13: Graphical representation to component/system TTF functional-based relationships

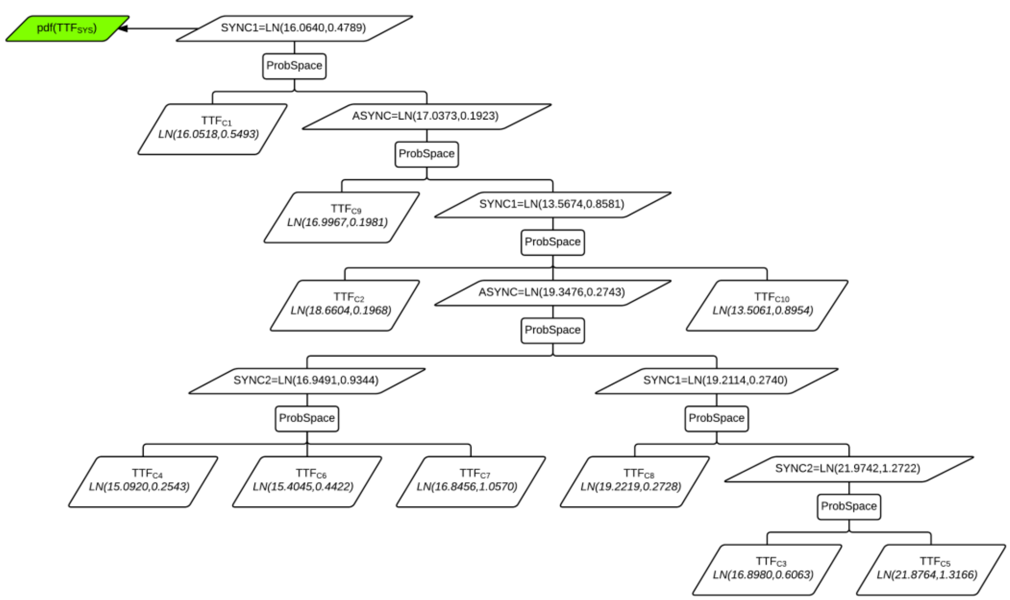

Figure 4-14: Design Phase-1: System TTF Reliability Analysis

4.2.3 Component Reliability: Design Phase-2 & 3

At this phase of the design process, W-relationships can be modified to include the design synthesis expansion caused by the realization of environments and the addition of joints; using Equation 4-34, the following relationships are realized:

$$O_1 \xrightarrow{W^1} \{E, C_1, C_2, C_4, C_6, C_7, C_{10}, J_1, J_3\}$$

$$O_2 \xrightarrow{W^2} \{E, C_1, C_2, C_4, C_6, C_7, C_{10}, J_1, J_3\}$$

$$O_3 \xrightarrow{W^3} \{E, C_1, C_2, C_3, C_5, C_8, C_{10}, J_1, J_2, J_3\}$$

$$O_4 \xrightarrow{W^4} \{E, C_1, C_9\}$$

Equation 4-56

The fatigue damage relations (Equation 4-57) are used to recognize the damaging operations affecting each component. $(d^{i,j})$ is a relation, coupling components (i) with the relevant damaging operations causing failure mechanism (j); for the example below (Equation 4-57) the (j) notation was omitted because one failure mechanism is being assessed.

$$E \xrightarrow{d^{\mathrm{E}}} \{O_1, O_2, O_3, O_4\}$$

$$C_1 \xrightarrow{d^1} \{O_1, O_2, O_3, O_4\}$$

$$C_2 \xrightarrow{d^2} \{O_1, O_2, O_3, O_4\}$$

$$C_3 \xrightarrow{d^3} \{O_1, O_2, O_3\}$$

$$C_4 \xrightarrow{d^4} \{O_1, O_2, O_3\}$$

$$C_5 \xrightarrow{d^5} \{O_3\}$$

Equation 4-57

$$C_6 \xrightarrow{d^6} \{O_1, O_2\}$$

$$C_7 \xrightarrow{d^7} \{O_1, O_2, O_3\}$$

$$C_8 \xrightarrow{d^8} \{O_1, O_2, O_3\}$$

$$C_9 \xrightarrow{d^9} \{O_1, O_2, O_3, O_4\}$$

$$C_{10} \xrightarrow{d^{10}} \{O_1, O_2, O_3\}$$

$$J_1 \xrightarrow{d^{11}} \{O_1, O_2\}$$

$$J_2 \xrightarrow{d^{12}} \{O_3\}$$

$$J_3 \xrightarrow{d^{13}} \{O_1, O_2, O_3\}$$

Time to failure distribution for component (i), TTF^{C_i} , is realized from the damage generated from the set of operations affecting (C_i) as shown in Equation 4-58.

$$TTF_{C_1} \xrightarrow{d^1} \left\{\Lambda_{C_1}^{O_1}, \Lambda_{C_1}^{O_2}, \Lambda_{C_1}^{O_3}, \Lambda_{C_1}^{O_4}\right\}$$

$$TTF_{C_2} \xrightarrow{d^2} \left\{\Lambda_{C_2}^{O_1}, \Lambda_{C_2}^{O_2}, \Lambda_{C_2}^{O_3}, \Lambda_{C_2}^{O_4}\right\}$$

$$TTF_{C_3} \xrightarrow{d^3} \left\{\Lambda_{C_3}^{O_1}, \Lambda_{C_3}^{O_2}, \Lambda_{C_3}^{O_3}\right\}$$

$$TTF_{C_4} \xrightarrow{d^4} \left\{\Lambda_{C_4}^{O_1}, \Lambda_{C_4}^{O_2}, \Lambda_{C_4}^{O_3}\right\}$$

Equation 4-58

$$TTF_{C_5} \xrightarrow{d^5} \left\{\Lambda_{C_5}^{O_3}\right\}$$

$$TTF_{C_6} \xrightarrow{d^6} \left\{\Lambda_{C_6}^{O_1}, \Lambda_{C_6}^{O_2}\right\}$$

$$TTF_{C_7} \xrightarrow{d^7} \left\{\Lambda_{C_7}^{O_1}, \Lambda_{C_7}^{O_2}, \Lambda_{C_7}^{O_3}\right\}$$

$$TTF_{C_8} \xrightarrow{d^8} \left\{\Lambda_{C_8}^{O_1}, \Lambda_{C_8}^{O_2}, \Lambda_{C_8}^{O_3}\right\}$$

$$TTF_{C_9} \xrightarrow{d^9} \{\Lambda_{C_9}^{O_1}, \Lambda_{C_9}^{O_2}, \Lambda_{C_9}^{O_3}, \Lambda_{C_9}^{O_4}\}$$

$$TTF_{C_{10}} \xrightarrow{d^{10}} \{\Lambda_{C_{10}}^{O_1}, \Lambda_{C_{10}}^{O_2}, \Lambda_{C_{10}}^{O_3}\}$$

$$TTF_{J_1} \xrightarrow{d^{11}} \{\Lambda_{S_1}^{O_1}, \Lambda_{S_1}^{O_2}\}$$

$$TTF_{J_2} \xrightarrow{d^{12}} \{\Lambda_{S_2}^{O_3}\}$$

$$TTF_{J_3} \xrightarrow{d^{13}} \{\Lambda_{S_3}^{O_1}, \Lambda_{S_3}^{O_2}, \Lambda_{S_3}^{O_3}\}$$

The updated stress probability distributions are presented in Table 4-6, the stress cycle duration is presented in Table 4-2.

Table 4-6: Stress amplitudes for system components; pdf distribution for system operations

Component	Stress (MPa)			
	O_1	O_2	O_3	O_4
C_1	LN(3.91,0.0500)	LN(4.57,0.0998)	LN(4.25,0.0699)	LN(4.20,0.0799)
C_2	LN(4.53,0.0599)	LN(4.29,0.0500)	LN(3.22,0.0400)	LN(3.49,0.0599)
C_3	LN(3.61,0.0699)	LN(4.46,0.0500)	LN(4.09,0.0998)	
C_4	LN(4.02,0.0799)	LN(3.87,0.0699)	LN(4.34,0.0350)	
C_5			LN(3.99,0.0799)	
C_6	LN(4.78,0.0799)	LN(3.91,0.0500)		
C_7	LN(4.22,0.0699)	LN(4.46,0.0898)	LN(4.03,0.1295)	
C_8	LN(4.17,0.0699)	LN(3.64,0.0699)	LN(3.85,0.0898)	
C_9	LN(4.52,0.0500)	LN(3.33,0.0699)	LN(4.16,0.0200)	LN(3.63,0.0898)
C_{10}	LN(4.72,0.0699)	LN(4.29,0.0699)	LN(4.47,0.0898)	
J_1	LN(4.60,0.0699)	LN(4.87,0.0400)		
J_2			LN(4.49,0.0998)	
J_3	LN(4.38,0.0799)	LN(4.25,0.0699)	LN(4.50,0.0599)	

The data from Table 4-6, Table 4-7, Table 4-2, Table 4-3 and Table 4-4 were used as inputs to Component Reliability Assessment Matlab code (Appendix B.1): the TTF outputs are presented in Table 4-7.

Table 4-7: Component TTF distribution and Reliability at design time goal

Component	TTF (Hrs.)		Reliability at (Tg=5E6 Hrs)
	E(TTF)	Distribution	
C_1	1.0883E7	LN(16.0518,0.5493)	0.8731
C_2	1.2957E8	LN(18.6604,0.1968)	1.0000
C_3	2.6214E7	LN(16.8980,0.6063)	0.9924
C_4	3.7019E6	LN(15.0920,0.2543)	0.0952
C_5	7.5375E9	LN(21.8764,1.3166)	1.0000
C_6	5.4016E6	LN(15.4045,0.4422)	0.4815
C_7	3.6187E7	LN(16.8456,1.0570)	0.9105
C_8	2.3127E8	LN(19.2219,0.2728)	1.0000
C_9	2.4552E7	LN(16.9967,0.1981)	1.0000
C_{10}	1.0958E6	LN(13.5061,0.8954)	0.0161
J_1	9.2202E7	LN(18.2892,0.3170)	1.0000
J_2	2.2306E6	LN(14.5961,0.2082)	3.4269E-05
J_3	9.6156E5	LN(13.6705,0.4599)	6.8242E-05

4.2.4 System Reliability: Design Phase-2 & 3

Equation 4-34 recognizes the following sets, (Equation 4-59), as subsystems candidates: $\{C_2, C_{10}\}$ $\{C_4, C_6, C_7\}$ and $\{C_3, C_5, C_8\}$ because they deliver the same set of functions; the following subsystems are realized by system analyst:

$$S_1 = \{C_1\}$$

$$S_2 = \{C_2\}$$

$$S_3 = \{C_4, C_6, C_7\}$$

$$S_4 = \{C_3, C_5, C_8\} \qquad \textbf{Equation 4-59}$$

$$S_5 = \{C_9\}$$

$$S_6 = \{C_{10}\}$$

Using Equation 4-59, the subsystem resultant damages can be realized from components damages interrelationship, as shown by Equation 4-49

$$\Lambda_{S_6} = \Lambda_{C_{10}}$$

$$\Lambda_{S_5} = \Lambda_{C_9}$$

$$\Lambda_{S_4} = \mathbf{SYNC2}(\Lambda_{C_3}, \Lambda_{C_5}, \Lambda_{C_8})$$

$$\Lambda_{S_3} = \mathbf{SYNC2}(\Lambda_{C_4}, \Lambda_{C_6}, \Lambda_{C_7})$$

$$\Lambda_{S_2} = \Lambda_{C_2}$$

$$\Lambda_{S_1} = \Lambda_{C_1}$$

Equation 4-60

System damage statement can be assembled from subsystems damage relationships starting with recognizing Asynchronous damage relationships as shown in Equation 4-61:

$$\Lambda_{SYS} = \mathbf{SYNC1}\left(\Lambda_{S_1}, \mathbf{ASYNC}\left(\Lambda_{S_5}, \mathbf{SYNC1}\left(\Lambda_{S_2}, \mathbf{ASYNC}\left(\Lambda_{S_3}, \Lambda_{S_4}\right), \Lambda_{S_6}\right)\right)\right)$$

Equation 4-61

The system damage statement can be extended to the component level using Equation 4-60 statements and projecting that knowledge into Equation 4-61 to produce Equation 4-62

$$\Lambda_{SYS} = \mathbf{SYNC1}\Bigg(\Lambda_{C_1}, \mathbf{ASYNC}\Bigg(\Lambda_{C_9}, \mathbf{SYNC1}\left(\Lambda_{C_2}, \mathbf{ASYNC}\left(\mathbf{SYNC2}(\Lambda_{C_4}, \Lambda_{C_6}, \Lambda_{C_7}), \mathbf{SYNC2}(\Lambda_{C_3}, \Lambda_{C_5}, \Lambda_{C_8})\right), \Lambda_{C_{10}}\right)\Bigg)\Bigg)$$

Equation 4-62

Probability spaces (ProbSpace) for subsystems composed of more than one component need to be created before assessing their TTF.

$$TTF_{S_1} = TTF_{C_1}$$

$$TTF_{S_2} = TTF_{C_2}$$

$$TTF_{S_3} = \mathbf{SYNC2}\left(\text{ProbSpace}\left\{TTF_{C_4}, TTF_{C_6}, TTF_{C_7}\right\}\right)$$

$$TTF_{S_4} = \mathbf{SYNC2}\left(\text{ProbSpace}\left\{TTF_{C_3}, TTF_{C_5}, TTF_{C_8}\right\}\right)$$

$$TTF_{S_5} = TTF_{C_9}$$

$$TTF_{S_6} = TTF_{C_{10}}$$

Equation 4-63

$$\begin{aligned} &TTF_{\text{SYS}} \\ &= \mathbf{SYNC1}\Big(\text{ProbSpace}\Big\{TTF_{C_1}, \mathbf{ASYNC}\Big(\text{ProbSpace}\Big\{TTF_{C_9}, \\ &\mathbf{SYNC1}\Big(\text{ProbSpace}\Big\{TTF_{C_2}, \\ &\mathbf{ASYNC}\Big(\text{ProbSpace}\Big\{\mathbf{SYNC2}\left(\text{ProbSpace}\left\{TTF_{C_4}, TTF_{C_6}, TTF_{C_7}\right\}\right), \\ &\mathbf{SYNC2}\left(\text{ProbSpace}\left\{TTF_{C_3}, TTF_{C_5}, TTF_{C_8}\right\}\right)\Big\}\Big), TTF_{C_{10}}\Big\}\Big)\Big\}\Big)\Big\}\Big) \end{aligned}$$

Equation 4-64

Figure 4-13 shows graphical representation to the damage system presented by Equation 3-54 and Equation 3-55; joints are not included in this chart; After joints were added to the system, Figure 4-16, the TTF density function was found to be LN (16.0313, 0.4968); and the reliability of this system at 5,000,000 hours is 0.8889.

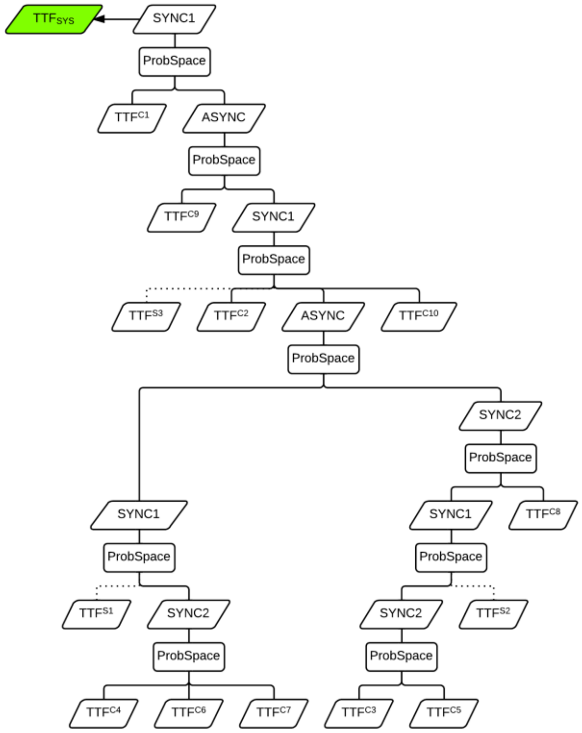

Figure 4-15: Graphical representation to component/system TTF structural-based relationships; i.e. joints are included

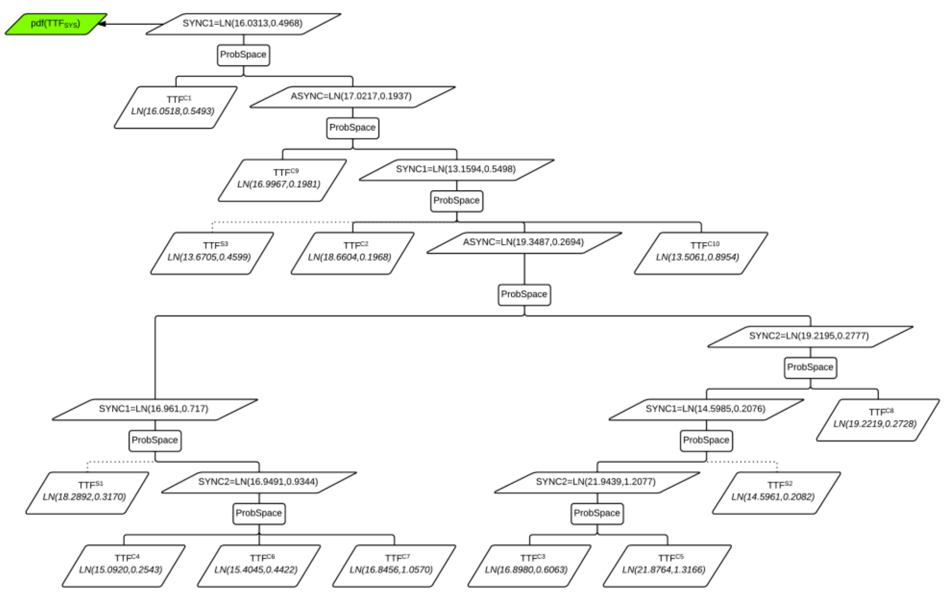

Figure 4-16: System with joints TTF Analysis

4.3 Summary and Lessons Learned

The design entity went through many iterations, as it progressed from conceptual design to embodiment. The following steps were followed for every design iteration ($\boldsymbol{i}$):

- Identify (or update) system operations
- Construct (or update) functional structure
- Develop ($\boldsymbol{OF_i}$) matrix
- Construct (or update) Assembly structure
- Develop ($\boldsymbol{FC_i}$) matrix
- Multiply $\boldsymbol{OF_i} \times \boldsymbol{FC_i}$ to produce -or update) ($\boldsymbol{OC_i}$) matrix
- Identify subsystems from ($\boldsymbol{OC_i}$) (*to be used for system reliability assessment*) and develop W-relationships
- System Designer develops H-relationships
- Construct (or update) Assembly structure with assembly constraints, joints, environments, and components indirect/ direct stimulus
- Develop ($\boldsymbol{I^N}$), ($\boldsymbol{I^E}$), ($\boldsymbol{I^{CS}}$) and update: $\boldsymbol{I_i} = \boldsymbol{I^N} + \boldsymbol{I^E} + \boldsymbol{I^{CS}}$
- Multiply $\boldsymbol{OF_i} \times \boldsymbol{FC_i} \times \boldsymbol{I_i}$ to produce(or update) ($\boldsymbol{OCI_i}$) matrix
- Identify components/operations couplings from ($\boldsymbol{OCI_i}$) columns (*to be used for component's reliability*) and develop d-relationships
- Evaluate component reliability by executing the mechanistic reliability algorithm on components using (d-relationships) and damage model parameters
- Develop system damage statement TTF statement (*from H-relationships*)
- Evaluate system reliability (*using system TTF statement*)

W and H-relationships were very important to develop the damage relationships which lead to calculate time-to-failure (TTF) for components and assess the system reliability.

System damage statements were very important to clarify the damage interrelationships between subsystems and to describe components’ damage propagation to cause system failure. The graphical representation to system TTF statement allowed clear view to show the impact of each component TTF distribution on system reliability.

It was noticed a drop in system reliability due to the addition of joints. This section did not assess component reliability confidence bounds (will be demonstrated in Chapter 5).

The design synthesis process is time consuming and prone to error while building design matrices and executing the symbolic matrix multiplications; developing a Graphical User Interface (GUI) to the matlab script would reduce the effort and the likelihood of making mistakes.

The component reliability assessment algorithm (Appendix B.1) run time (especially with more than two operations) was too long to solve for component’s TTF; it’s recommended to use an equivalent damage stress approximation process when applicable (Appendix A.1 & Appendix B.3) to reduce simulation run time.

Confidence bounds were not assessed for the components analyzed in this section; Chapter 5 covers assessment of confidence bounds using bootstrap resampling on a case study model. Due to the lack of data, the results of a system reliability assessment was not compared to field TTF data in this research.

Chapter 5 Case Study

5.1 Background:

An internal combustion engine intake-manifold was used to further study the capabilities and limitations of MDRV. The manifold structure supports an air-turbocharger; mounted on it through a bolted-joint. The internal combustion engine is used to power an off-road equipment vehicle. The vehicle is exposed to 25 different operations, representing averaged customer usage of the equipment. The mechanical vibration created by the IC engine, besides vehicle response to dynamic excitations created by the external environment, while executing main system operations; creates dynamic mechanical stresses on the manifold structure that leads to mechanical fatigue failure over time. The case study will focus on assessing the reliability of the manifold structure using MDRV methodology and compare the results to field data. MDRV will start at the conceptual design phase and will progress to embodiment design to demonstrate the integration of the mechanistic process to the design process.

During the embodiment design phase, finite element models for the manifold structure were created to assess the mechanical stress/ time response. 25 time samples, representing the system dynamic behavior were used to derive the FEA model. The engine manifold problem was treated as a base-excitation vibration problem. Accelerometers mounted on the engine block were used to generate the average base displacement/ time data to feed to FEM. High-stress areas on the manifold structure were identified for further TTF and reliability assessments. Demonstration to the final design expected reliability and comparison to field data is presented at the end of this chapter;

besides, a summary of lessons learned during implementing MDRV to this design project.

5.2 Implementation during Conceptual Design Phase

5.2.1 Functional Structure Development

Development of a functional structure during the conceptual design provides the reliability analyst a start point to assess the system and components reliability goals. Figure 5-1 and Figure 5-2 show different stages of the conceptual design process, only the top level functional structure for power transmission is shown on these two figures. Figure 5-3 shows a more detailed engine model. A complete vehicle functional structure is larger and more detailed than presented here.

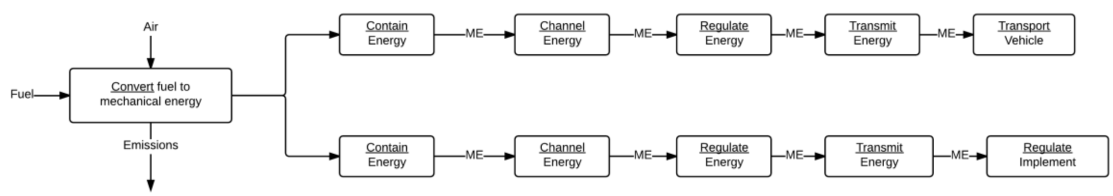

Figure 5-1: Top level functional structure of an off-road construction equipment

An expanded functional structure with equipment operations is presented in Figure 5-4 and Figure 5-5 below. Equation 5-1 shows the operations/ functions order: $\{O\} = \boldsymbol{OF} \times \{F\}$.

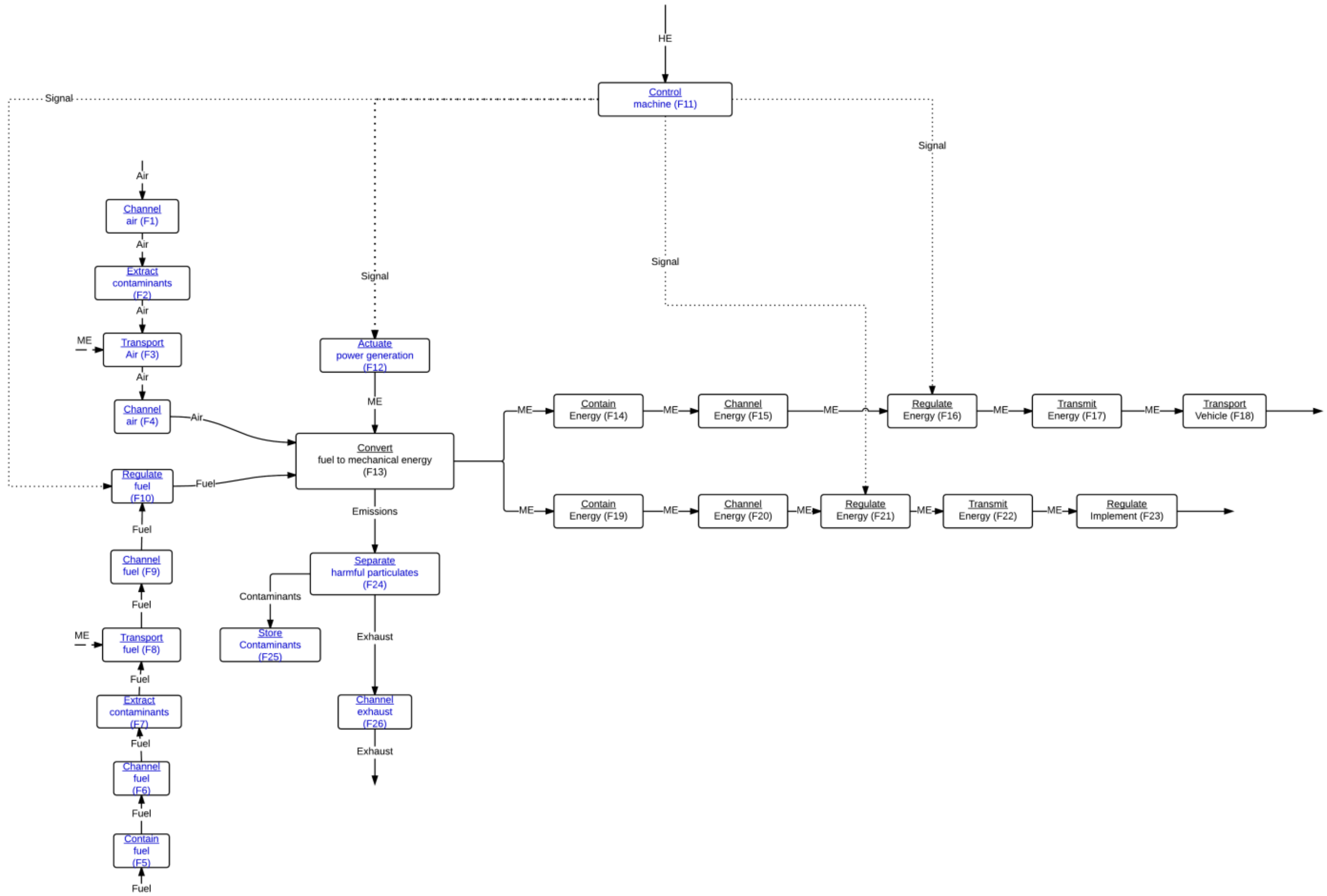

Figure 5-2: Functional structure model for off-road construction equipment with detailed engine air intake and fuel delivery sub-models

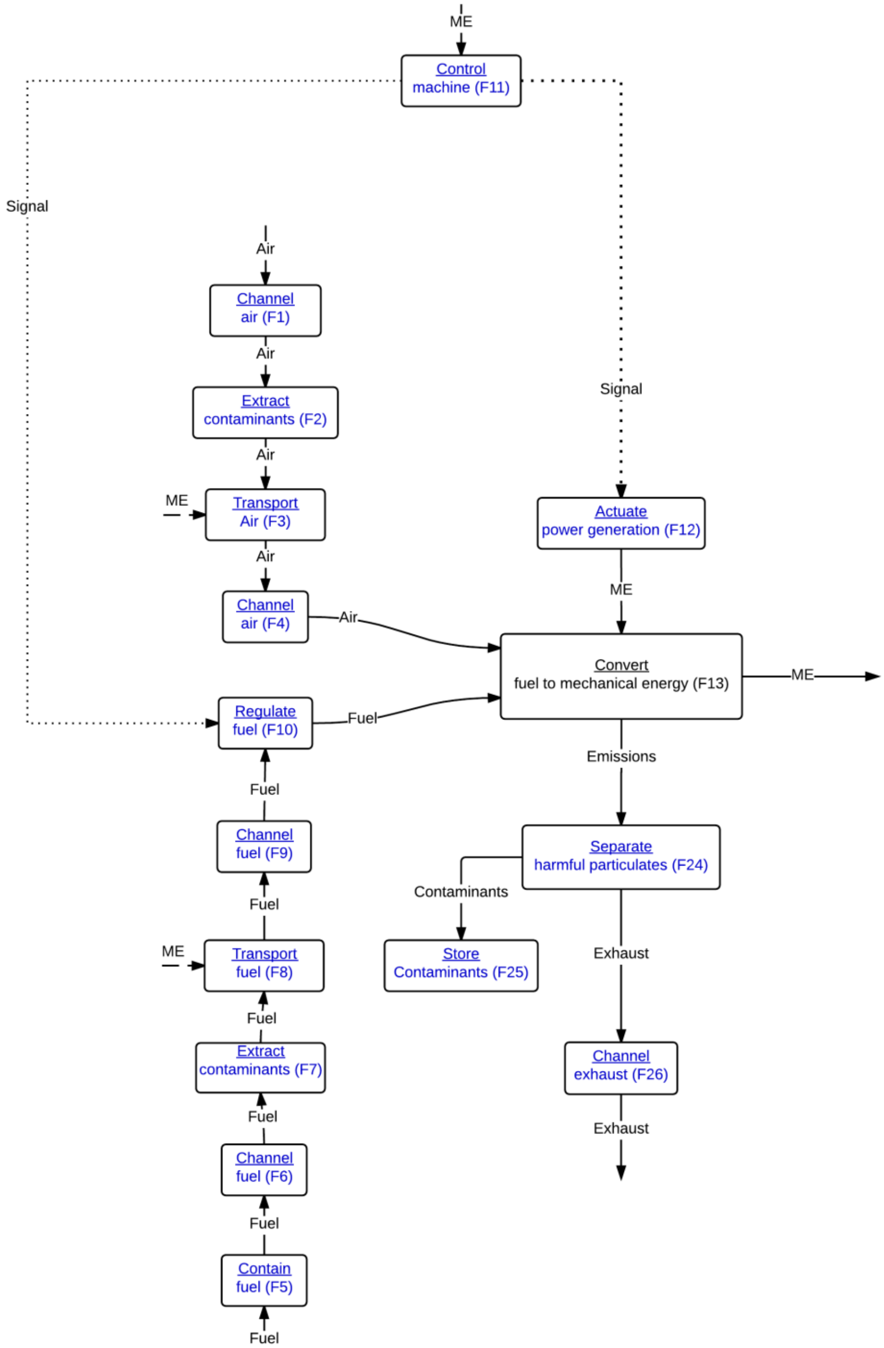

Figure 5-3: Engine system functional structure

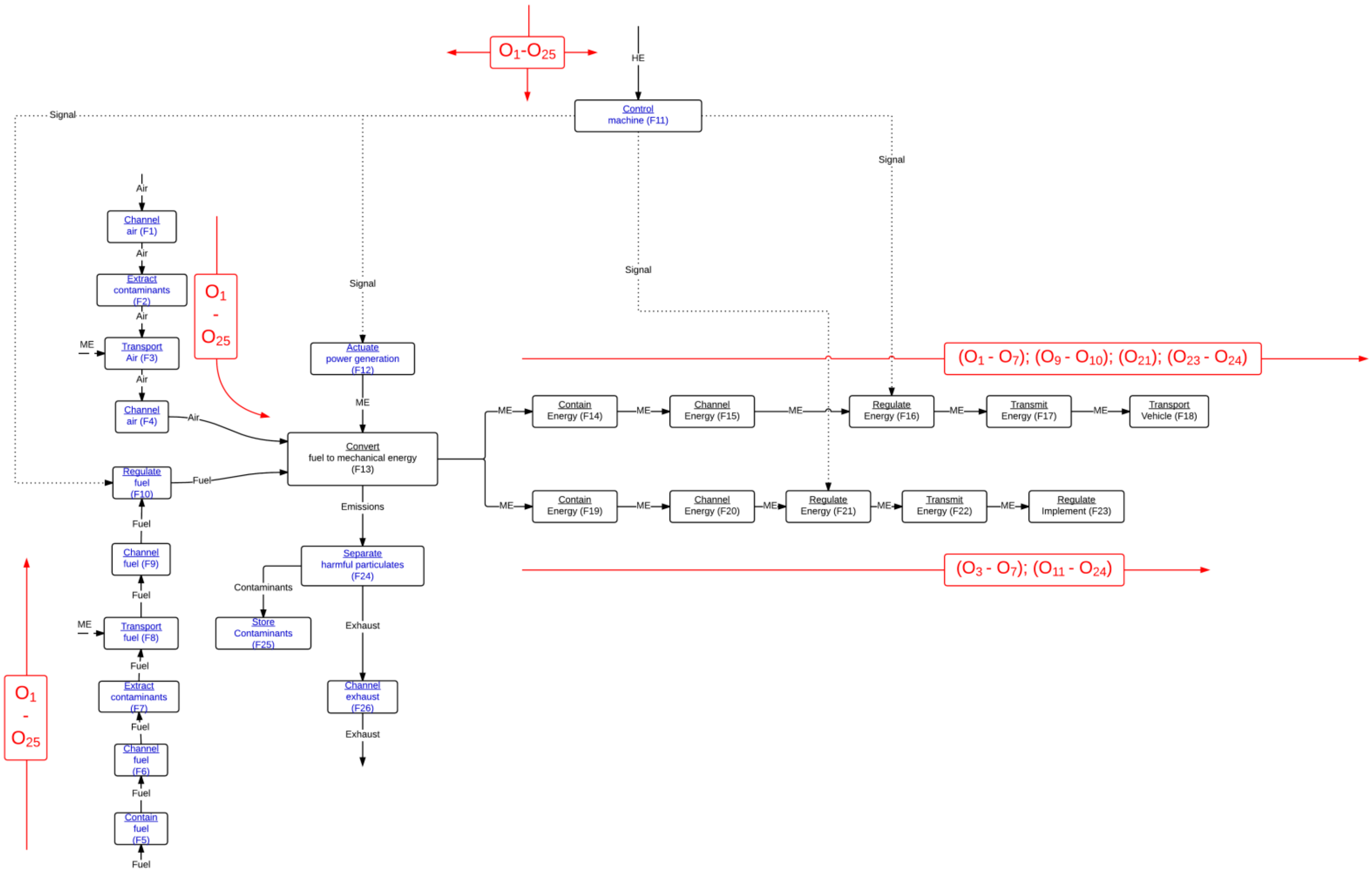

Figure 5-4: Vehicle functional structure with operation paths demonstrated

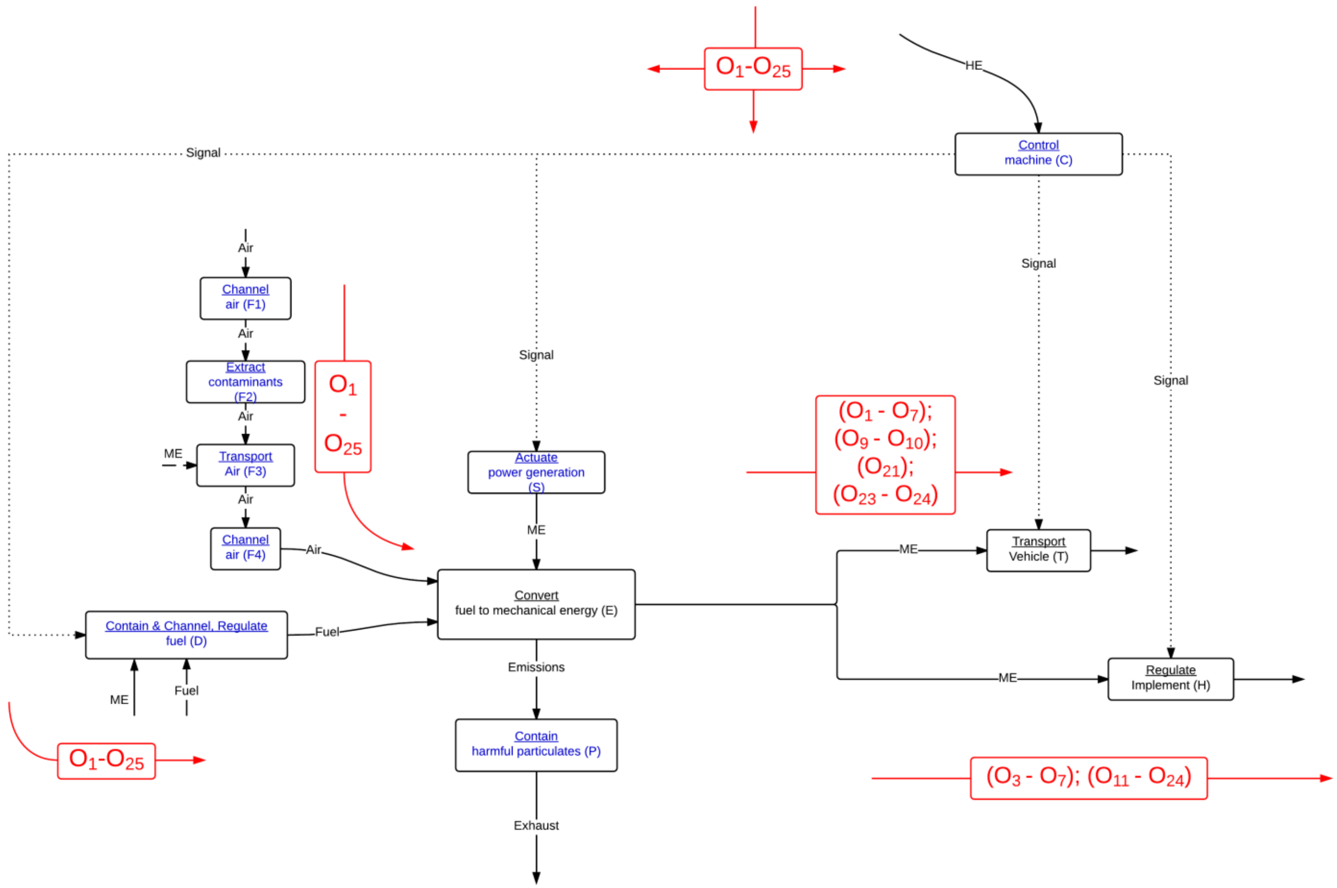

Figure 5-5: Vehicle functional structure with operations representation; condensed form

$$
\begin{Bmatrix} O_1 \\ O_2 \\ O_3 \\ O_4 \\ O_5 \\ O_6 \\ O_7 \\ O_8 \\ O_9 \\ O_{10} \\ O_{11} \\ O_{12} \\ O_{13} \\ O_{14} \\ O_{15} \\ O_{16} \\ O_{17} \\ O_{18} \\ O_{19} \\ O_{20} \\ O_{21} \\ O_{22} \\ O_{23} \\ O_{24} \\ O_{25} \end{Bmatrix}
=
\begin{bmatrix}
A_1^1 & A_1^2 & A_1^3 & A_1^4 & A_1^5 & A_1^6 & A_1^7 & A_1^8 & A_1^9 & 0 & 0 \\
A_2^1 & A_2^2 & A_2^3 & A_2^4 & A_2^5 & A_2^6 & A_2^7 & A_2^8 & A_2^9 & 0 & 0 \\
A_3^1 & A_3^2 & A_3^3 & A_3^4 & A_3^5 & A_3^6 & A_3^7 & A_3^8 & A_3^9 & A_3^{10} & 0 \\
A_4^1 & A_4^2 & A_4^3 & A_4^4 & A_4^5 & A_4^6 & A_4^7 & A_4^8 & A_4^9 & A_4^{10} & 0 \\
A_5^1 & A_5^2 & A_5^3 & A_5^4 & A_5^5 & A_5^6 & A_5^7 & A_5^8 & A_5^9 & A_5^{10} & 0 \\
A_6^1 & A_6^2 & A_6^3 & A_6^4 & A_6^5 & A_6^6 & A_6^7 & A_6^8 & A_6^9 & A_6^{10} & 0 \\
A_7^1 & A_7^2 & A_7^3 & A_7^4 & A_7^5 & A_7^6 & A_7^7 & A_7^8 & A_7^9 & A_7^{10} & 0 \\
A_8^1 & A_8^2 & A_8^3 & A_8^4 & A_8^5 & A_8^6 & A_8^7 & A_8^8 & 0 & 0 & 0 \\
A_9^1 & A_9^2 & A_9^3 & A_9^4 & A_9^5 & A_9^6 & A_9^7 & A_9^8 & A_9^9 & 0 & 0 \\
A_{10}^1 & A_{10}^2 & A_{10}^3 & A_{10}^4 & A_{10}^5 & A_{10}^6 & A_{10}^7 & A_{10}^8 & A_{10}^9 & 0 & 0 \\
A_{11}^1 & A_{11}^2 & A_{11}^3 & A_{11}^4 & A_{11}^5 & A_{11}^6 & A_{11}^7 & A_{11}^8 & 0 & A_{11}^{10} & 0 \\
A_{12}^1 & A_{12}^2 & A_{12}^3 & A_{12}^4 & A_{12}^5 & A_{12}^6 & A_{12}^7 & A_{12}^8 & 0 & A_{12}^{10} & 0 \\
A_{13}^1 & A_{13}^2 & A_{13}^3 & A_{13}^4 & A_{13}^5 & A_{13}^6 & A_{13}^7 & A_{13}^8 & 0 & A_{13}^{10} & 0 \\
A_{14}^1 & A_{14}^2 & A_{14}^3 & A_{14}^4 & A_{14}^5 & A_{14}^6 & A_{14}^7 & A_{14}^8 & 0 & A_{14}^{10} & 0 \\
A_{15}^1 & A_{15}^2 & A_{15}^3 & A_{15}^4 & A_{15}^5 & A_{15}^6 & A_{15}^7 & A_{15}^8 & 0 & A_{15}^{10} & 0 \\
A_{16}^1 & A_{16}^2 & A_{16}^3 & A_{16}^4 & A_{16}^5 & A_{16}^6 & A_{16}^7 & A_{16}^8 & 0 & A_{16}^{10} & 0 \\
A_{17}^1 & A_{17}^2 & A_{17}^3 & A_{17}^4 & A_{17}^5 & A_{17}^6 & A_{17}^7 & A_{17}^8 & 0 & A_{17}^{10} & 0 \\
A_{18}^1 & A_{18}^2 & A_{18}^3 & A_{18}^4 & A_{18}^5 & A_{18}^6 & A_{18}^7 & A_{18}^8 & 0 & A_{18}^{10} & 0 \\
A_{19}^1 & A_{19}^2 & A_{19}^3 & A_{19}^4 & A_{19}^5 & A_{19}^6 & A_{19}^7 & A_{19}^8 & 0 & A_{19}^{10} & 0 \\
A_{20}^1 & A_{20}^2 & A_{20}^3 & A_{20}^4 & A_{20}^5 & A_{20}^6 & A_{20}^7 & A_{20}^8 & 0 & A_{20}^{10} & 0 \\
A_{21}^1 & A_{21}^2 & A_{21}^3 & A_{21}^4 & A_{21}^5 & A_{21}^6 & A_{21}^7 & A_{21}^8 & A_{21}^9 & A_{21}^{10} & 0 \\
A_{22}^1 & A_{22}^2 & A_{22}^3 & A_{22}^4 & A_{22}^5 & A_{22}^6 & A_{22}^7 & A_{22}^8 & 0 & A_{22}^{10} & 0 \\
A_{23}^1 & A_{23}^2 & A_{23}^3 & A_{23}^4 & A_{23}^5 & A_{23}^6 & A_{23}^7 & A_{23}^8 & A_{23}^9 & A_{23}^{10} & 0 \\
A_{24}^1 & A_{24}^2 & A_{24}^3 & A_{24}^4 & A_{24}^5 & A_{24}^6 & A_{24}^7 & A_{24}^8 & A_{24}^9 & A_{24}^{10} & 0 \\
A_{25}^1 & A_{25}^2 & A_{25}^3 & A_{25}^4 & A_{25}^5 & A_{25}^6 & A_{25}^7 & A_{25}^8 & 0 & 0 & 0
\end{bmatrix}
\begin{Bmatrix} F_1 \\ F_2 \\ F_3 \\ F_4 \\ D \\ C \\ S \\ E \\ T \\ H \\ P \end{Bmatrix}
$$

Equation 5-1

5.2.2 Identify Product Usage

The vehicle expected customer usage is demonstrated in Table 5-1 and Table 5-2. Two types of operations are identified: continuous operations (take long time duration to be executed), and discrete operations: (short time duration events). Driving a vehicle to and from job-sites is an example to continuous operation, while abrupt vehicle stopping is a discrete operation.

Table 5-1: Vehicle Usage: Continuous Operations (percentage usage per hour)

Continuous Operations	Median Percentage Usage (per hour)	Coefficient of Variation
Operation-1	16%	20%
Operation-2	4%	15%
Operation-3	35%	13%
Operation-4	8%	17%
Operation-5	2%	10%
Operation-6	10%	12%
Operation-7	10%	17%
Operation-8	15%	13%

Table 5-2: Vehicle Usage: Discrete Operations (events per hour)

Discrete Operations	Median Events Rate (per hour)	Coefficient of Variation
Operation-9	0.125	15%
Operation-10	0.125	30%
Operation-11	0.5	14%
Operation-12	0.5	20%
Operation-13	2	22%
Operation-14	1.5	15%
Operation-15	0.25	33%
Operation-16	0.25	21%
Operation-17	1	30%
Operation-18	0.25	15%
Operation-19	0.25	17%
Operation-20	0.1	33%
Operation-21	0.005	26%
Operation-22	0.005	17%
Operation-23	0.005	18%
Operation-24	0.005	19%
Operation-25	0.25	13%

5.2.3 Product Usage Distribution

At this stage of the design process the customer usage known is just system hourly usage as documented in Table 5-3 and Table 5-4 below. Stress cycles cannot be identified at this stage of the design without developing components design forms. It's recommended at this phase of the design to recognize stress cycles as a design goal.

Table 5-3: Vehicle Usage: Continuous Operations Design Goals

Continuous Operations	Median Percentage Usage (per hour)	Coefficient of Variation	Median Usage -10 years (hrs)	Std Dev (hrs)
Operation-1	16%	20%	4672	934
Operation-2	4%	15%	1168	175
Operation-3	35%	13%	10220	1329
Operation-4	8%	17%	2336	397
Operation-5	2%	10%	584	58
Operation-6	10%	12%	2920	350
Operation-7	10%	17%	2920	496
Operation-8	15%	13%	4380	569
	Total Time (hrs)=	6%	29200	1877

Table 5-4: Vehicle Usage: Discrete Operations Design Goals

Discrete Operations	Median Events Rate (per hour)	Coefficient of Variation	Events count-10 years (hrs)	Std Dev (hrs)
Operation-9	0.125	15%	3650	548
Operation-10	0.125	30%	3650	1095
Operation-11	0.5	14%	14600	2044
Operation-12	0.5	20%	14600	2920
Operation-13	2	22%	58400	12848
Operation-14	1.5	15%	43800	6570
Operation-15	0.25	33%	7300	2409
Operation-16	0.25	21%	7300	1533
Operation-17	1	30%	29200	8760
Operation-18	0.25	15%	7300	1095
Operation-19	0.25	17%	7300	1241
Operation-20	0.1	33%	2920	964
Operation-21	0.005	26%	146	38
Operation-22	0.005	17%	146	25
Operation-23	0.005	18%	146	26
Operation-24	0.005	19%	146	28
Operation-25	0.25	13%	7300	949
	Total (events)=	8%	207904	17661

5.2.4 Material Identification:

For steel components, SAE J1099 [75] material database will be used with emphasis given to SAE1099-0030 cast steel sample, which will further be used to design the manifold structure. The material mechanical property standard deviations were assessed from a different cast steel sample: SAE1099-0050A, which is expected to have the same material variation at the long life side of the fatigue curve. The standard deviations from SAE1099-0050A samples are acceptable to be used to assess (A_{σ}) and (C_{σ}) but not suitable to assess (A_{ϵ}) and (C_{ϵ}) due to the difference in material ductility. Table 5-5 shows the material properties for SAE1099-0030 cast steel.

In general, more than one material failure characteristic properties would be present to address the list of possible failure mechanisms, shown in Table 3-1. Damaging stresses would be any type of force driver to produce failure; they are not limited to mechanical-type stresses.

Table 5-5: SAE 1099, 0030 cast steel sample properties

SAE J1099 properties		(Median)	(std dev %)
Monotonic Properties			
Brinnnel Hardness #	BHN	137	7%
Yield Strength (MPa)	σys 0.2%	303	14%
Ultimate Tensile Strength (MPa)	UTS	496	12%
Reduction in area after fracture (%)	RA%	46%	16%
Monotonic Strength Coefficient (MPa)	K	NA	
Monotonic Strain Hardening Exponent	n	NA	
Modulus of Elasticity (MPa)	E	207000	0.45%
Engineering strain at Yield	ey	0.003464	7%
True strain at Yield	εy	0.003458	7%
True Fracture Ductility	εf	0.616186	18%
Cyclic Properties			
Fatigue Strength Coefficient (MPa)	σ'f	655	17%
Fatigue Strength Exponent	b	-0.083	11%

Fatigue Ductility Coefficient	ε'f	0.28	66%
Fatigue Ductility Exponent	c	-0.552	15%
Cyclical Strength Coefficient (MPa)	K'	738	17%
Cyclical Strain Hardening Exponent	n'	0.136	10%
Cyclical Modulus of Elasticity (MPa)	E'	207000	0.45%

5.2.5 Identification of Damaging Stresses

From the functional structure presented in Figure 5-2 the only type of damaging stresses, identified from the transfer of mechanical energy, are mechanical stresses. Functional structures are not good representations of "*how*" the functional goals are being delivered. Assembly stresses, environmental stresses or stresses generated due to energy conversion processes are not captured during this phase of the design.

At this stage of the design process, it's recommended to develop stress targets for relevant failure mechanisms and use those targets as guidance to meet the reliability goals of the design. These stress targets are also valuable when selecting subsystems from external sources/ suppliers; they provide a quick check whether a component or a subsystem can withstand system operational demands at the component level or not. The system usage, presented in Table 5-3, was used to derive the cycle goals for the manifold. Considering variable cycle rate for different notch factors (k_f), Table 5-6 shows the stress goals for median SAE1099-003 cast steel material properties using Equation 5-2

$$S_{amp} = \exp\left(\left(\frac{1}{A_\sigma}\right)\ln\left(\frac{N_f}{C_\sigma}\right)\right) \qquad \textbf{Equation 5-2}$$

A Matlab computer code, Appendix B.2, is used to run statistical simulations using the median and standard deviation properties shown in Table 5-5. 50 samples of each parameter affecting (A_σ) and (C_σ), namely the fatigue strength coefficient: (σ_f') and fatigue strength exponent: (b), were used to run statistical simulation to generate 2500 samples of stress amplitudes for each of the cycle targets shown in Table 5-6. Lognormal density and reliability distributions were generated from the statistical simulation results. Figure 5-6 and Figure 5-7 show the PDF and $R(t)$ results generated for 58400 cycles' usage goal. Figure 5-8 shows stress amplitudes probability density functions for different cycle goals.

Table 5-6: Stress Goal Analysis using median SAE1099 0030 Properties

Cycles per hour		1	10	100	1000	10000	1E+05	1E+06
Nf as a cycle goal (100% damage, n=Nf)		29200	3E+05	3E+06	3E+07	3E+08	3E+09	3E+10
Nf as a cycle goal (50% damage, n=0.5Nf)		58400	6E+05	6E+06	6E+07	6E+08	6E+09	6E+10
Stress amplitudes goal at 50% damage	K_f=1	263	218	180	148	123	101	84
	K_f=1.5	176	145	120	99	82	68	56
	K =2	132	109	90	74	61	51	42
	K_f=3	88	73	60	49	41	34	28

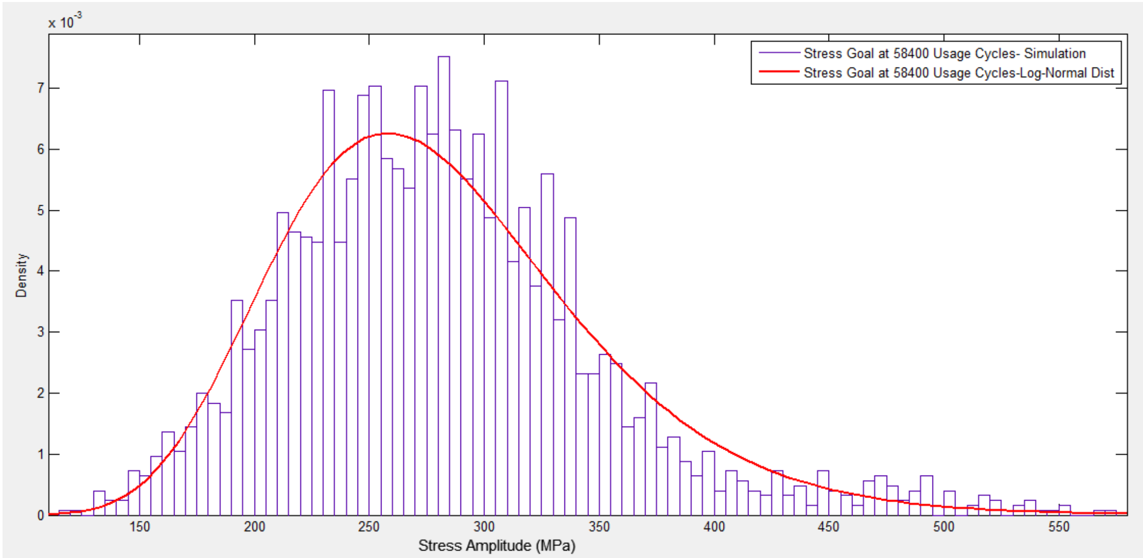

Figure 5-6: Statistical simulation results and Lognormal probability density generated for 58400 cycles stress amplitude goals

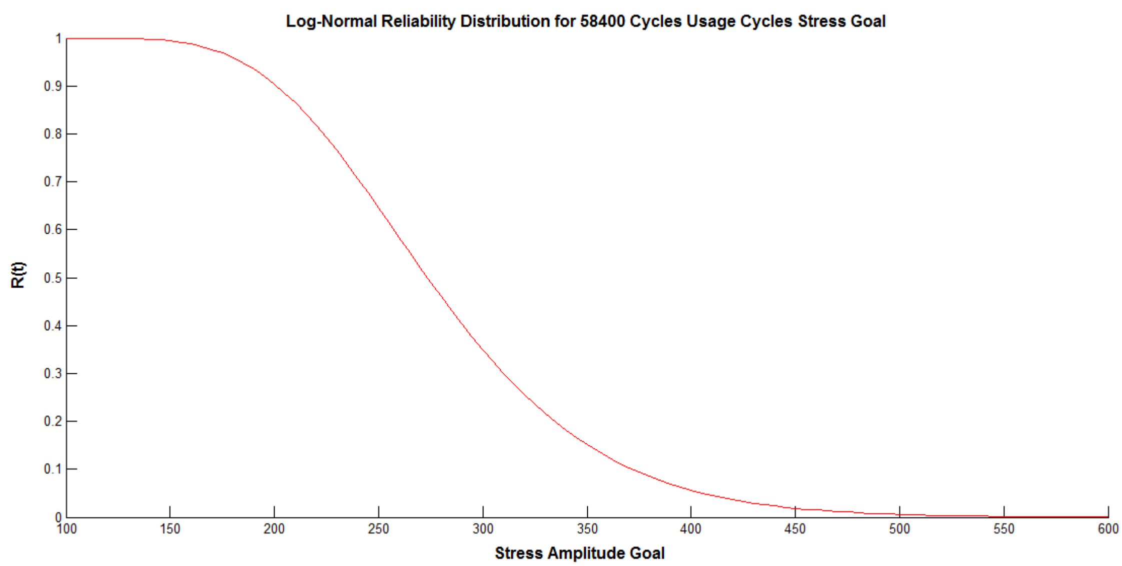

Figure 5-7: Lognormal reliability distribution for 58400 cycles usage stress goals

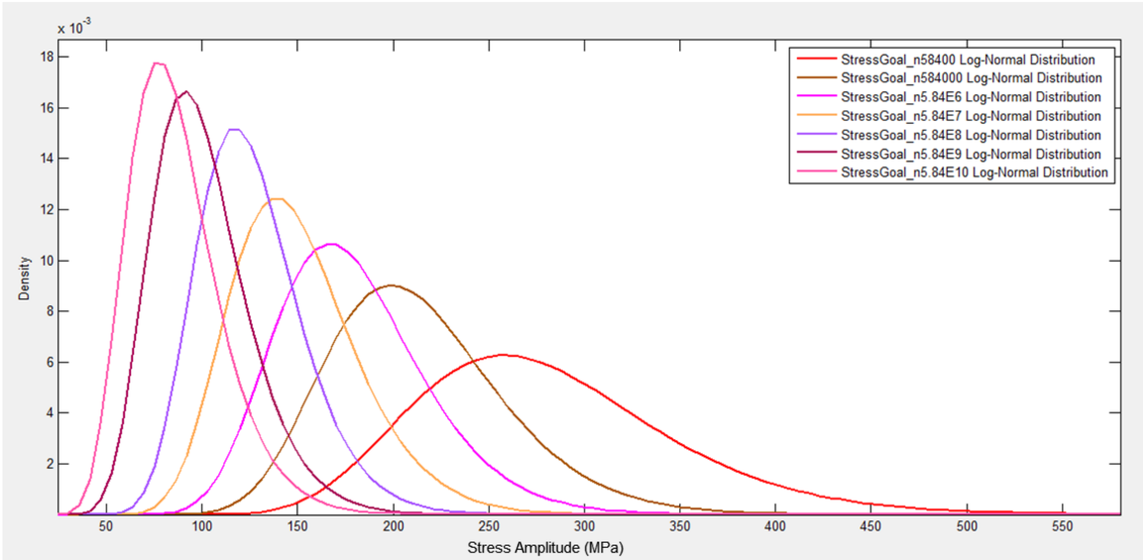

Figure 5-8: Probability density functions for variable cycles/ stress usage goals

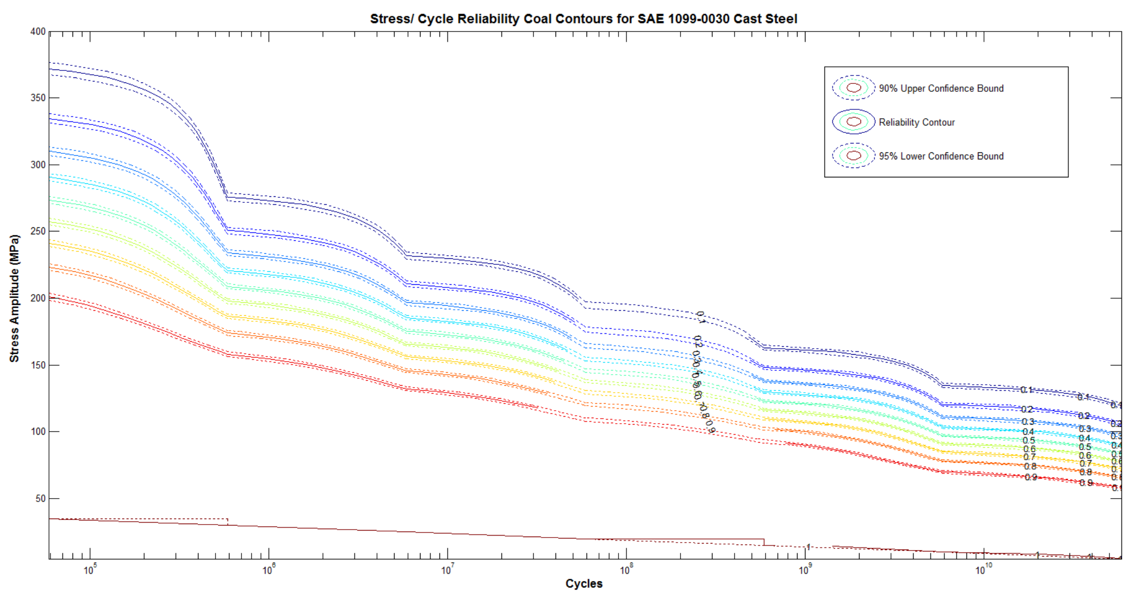

Figure 5-9: Reliability target contours for variable mechanical stress and cycle goals

The reliability distribution curves can be compiled with stress and cycle goals to produce a three-variable contour plot. These contour plots can be used to design for different known cycles, stress amplitudes or reliability targets. Figure 5-9 shows a reliability contour plot for SAE1099-003 steel cast material. Figure 5-10 shows how reliability goals would be used for an engine-mounted structure. For the intake-manifold case: cycles summation for 10yrs usage for a 2000 rpm engine speed is: (μ, c_v)=(3.5E9, 6.43%) cycles, *produced from* Table 5-3 and Table 5-4, with 3.795E9 cycles for the 90th percentile user. The stress goal for (K_f=1) is 74 MPa; for (K_f=1.5) the stress goals would approximately be (74/1.5)= 49MPa for 90% reliability goal,. Figure 5-11 shows, graphically, the process of identifying the stress target for 90% reliability goals.

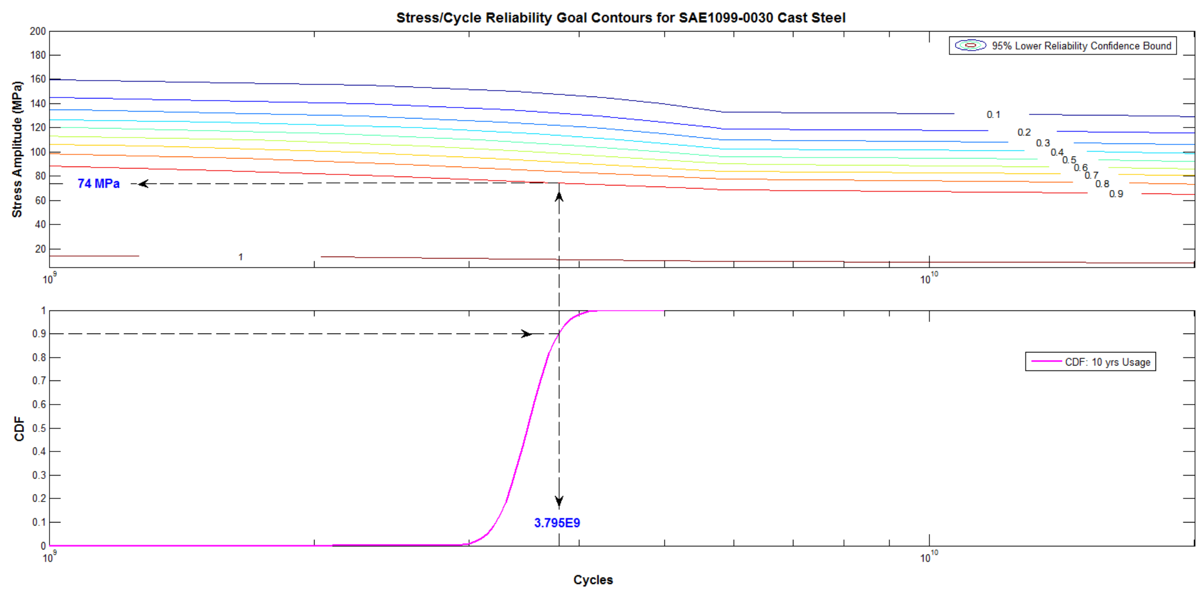

Figure 5-10: 90% reliability stress goal for SAE1099-003 cast steel material for 90th percentile usage population

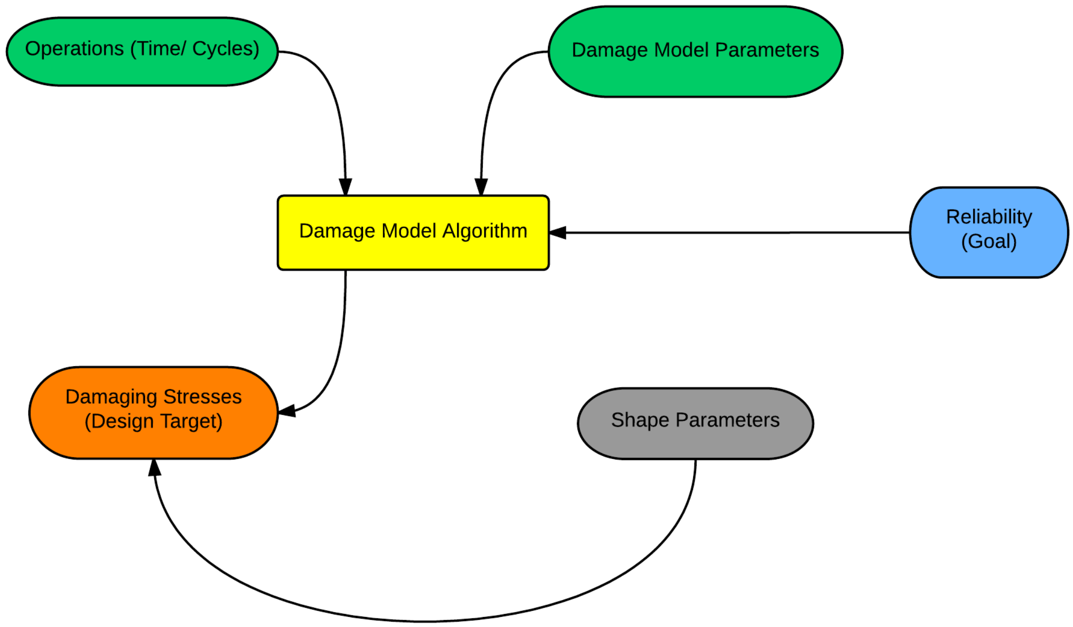

Figure 5-11: Design stress targets: emergence out of component-MDRV during conceptual design phase

5.3 Implementation during Embodiment Design

5.3.1 Assembly Structure Development

Figure 5-12 shows the assembly structure for the vehicle main systems; since the main focus of this case study is the assessment of the manifold structure, there is no need for adding modeling details that doesn’t affect the reliability assessment of the manifold structure. Figure 5-13 shows the assembly structure with the functional goals for every component or subsystem presented in Figure 5-12. Equation 5-3 and Table 5-7 show the functional/ components coupling relationships and the function-component coupling matrix ($\boldsymbol{FC}$). Table 5-8 shows the system interaction matrix ($\boldsymbol{I}$).

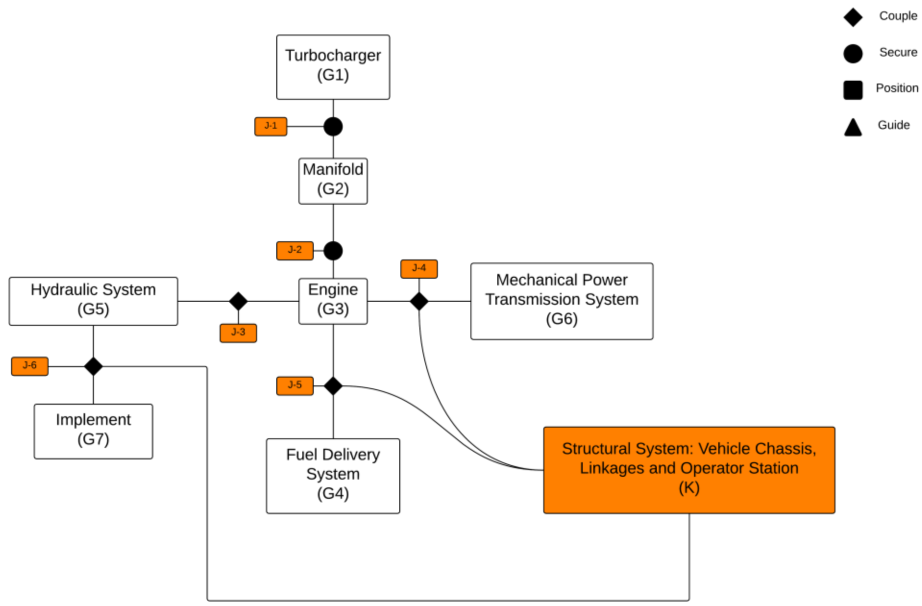

Figure 5-12: Assembly Structure for Main Vehicle Systems

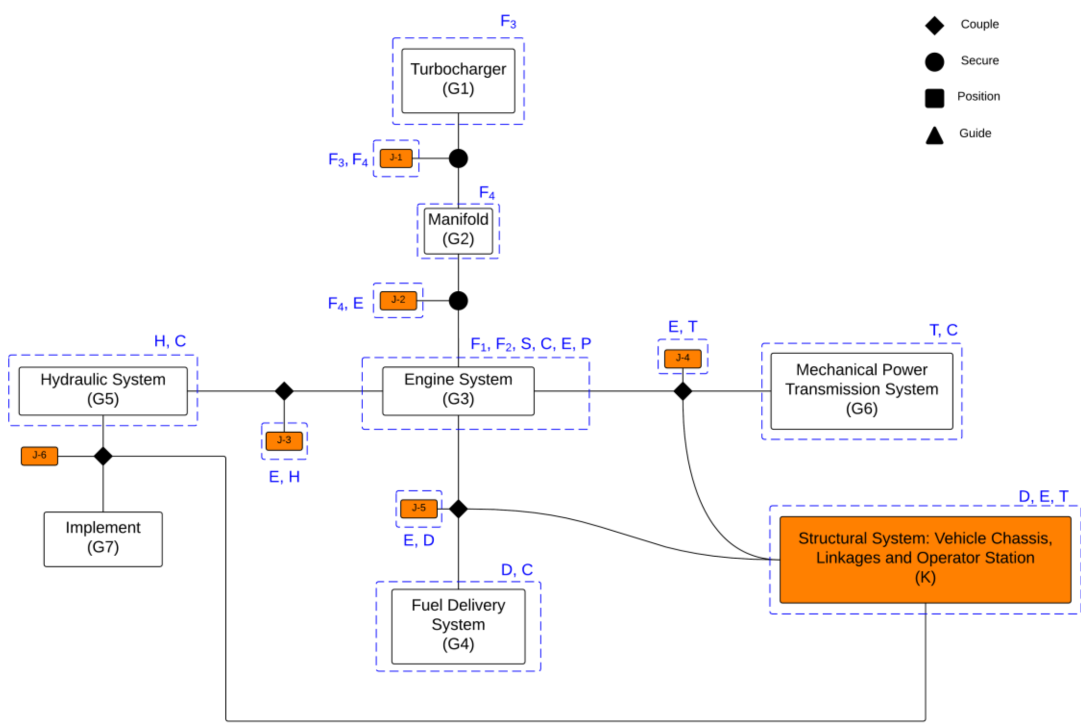

Figure 5-13: Assembly Structure for Main Vehicle Systems with Realized Subsystems Functions

$$\begin{Bmatrix} F_1 \\ F_2 \\ F_3 \\ F_4 \\ D \\ C \\ S \\ E \\ T \\ H \\ P \end{Bmatrix} = \begin{bmatrix} 0 & 0 & B_1^3 & 0 & 0 & 0 & 0 & B_1^8 & B_1^9 & 0 & 0 & 0 \\ 0 & 0 & B_2^3 & 0 & 0 & 0 & 0 & 0 & 0 & 0 & 0 & 0 \\ B_3^1 & 0 & 0 & 0 & 0 & 0 & 0 & B_3^8 & 0 & 0 & 0 & 0 \\ 0 & B_4^2 & 0 & 0 & 0 & 0 & 0 & 0 & 0 & 0 & 0 & 0 \\ 0 & 0 & 0 & B_5^4 & 0 & 0 & B_5^7 & 0 & 0 & 0 & 0 & B_5^{12} \\ 0 & 0 & B_6^3 & B_6^4 & B_6^5 & B_6^6 & 0 & 0 & 0 & 0 & 0 & 0 \\ 0 & 0 & B_7^3 & 0 & 0 & 0 & 0 & 0 & 0 & 0 & 0 & 0 \\ 0 & 0 & B_8^3 & 0 & 0 & 0 & B_8^7 & 0 & B_8^9 & B_8^{10} & B_8^{11} & B_8^{12} \\ 0 & 0 & 0 & 0 & 0 & B_9^6 & B_9^7 & 0 & 0 & 0 & 0 & 0 \\ 0 & 0 & 0 & 0 & B_{10}^5 & 0 & 0 & 0 & 0 & B_{10}^{10} & 0 & 0 \\ 0 & 0 & B_{11}^3 & 0 & 0 & 0 & 0 & 0 & 0 & 0 & 0 & 0 \end{bmatrix} \begin{Bmatrix} G^*{}_1 \\ G^*{}_2 \\ G^*{}_3 \\ G^*{}_4 \\ G^*{}_5 \\ G^*{}_6 \\ K^* \\ J^*{}_1 \\ J^*{}_2 \\ J^*{}_3 \\ J^*{}_4 \\ J^*{}_5 \end{Bmatrix}$$

Equation 5-3

Table 5-7: FC Matrix of the Off-road Vehicle in Table Format

	Components											
Functions	$G^*{}_1$	$G^*{}_2$	$G^*{}_3$	$G^*{}_4$	$G^*{}_5$	$G^*{}_6$	K^*	$J^*{}_1$	$J^*{}_2$	$J^*{}_3$	$J^*{}_4$	$J^*{}_5$
F_1	0	0	B_1^3	0	0	0	0	B_1^8	B_1^9	0	0	0
F_2	0	0	B_2^3	0	0	0	0	0	0	0	0	0
F_3	B_3^1	0	0	0	0	0	0	B_3^8	0	0	0	0
F_4	0	B_4^2	0	0	0	0	0	0	0	0	0	0
D	0	0	0	B_5^4	0	0	B_5^7	0	0	0	0	B_5^{12}
C	0	0	B_6^3	B_6^4	B_6^5	B_6^6	0	0	0	0	0	0
S	0	0	B_7^3	0	0	0	0	0	0	0	0	0
E	0	0	B_8^3	0	0	0	B_8^7	0	B_8^9	B_8^{10}	B_8^{11}	B_8^{12}
T	0	0	0	0	0	B_9^6	B_9^7	0	0	0	B_9^{11}	0
H	0	0	0	0	B_{10}^5	0	0	0	0	B_{10}^{10}	0	0
P	0	0	B_{11}^3	0	0	0	0	0	0	0	0	0

$$
\begin{Bmatrix} G^*{}_1 \\ G^*{}_2 \\ G^*{}_3 \\ G^*{}_4 \\ G^*{}_5 \\ G^*{}_6 \\ K^* \\ J^*{}_1 \\ J^*{}_2 \\ J^*{}_3 \\ J^*{}_4 \\ J^*{}_5 \end{Bmatrix} = \begin{bmatrix}
I_1 & D_1^2 & 0 & 0 & 0 & 0 & 0 & D_1^8 & 0 & 0 & 0 & 0 \\
D_2^1 & I_2 & D_2^3 & 0 & 0 & 0 & 0 & D_2^8 & D_2^9 & 0 & 0 & 0 \\
0 & D_3^2 & I_3 & D_3^4 & D_3^5 & D_3^6 & D_3^7 & 0 & D_3^9 & D_3^{10} & D_3^{11} & D_3^{12} \\
0 & 0 & D_4^3 & I_4 & 0 & 0 & D_4^7 & 0 & 0 & 0 & 0 & D_4^{12} \\
0 & 0 & D_5^3 & 0 & I_5 & 0 & 0 & 0 & 0 & D_5^{10} & 0 & 0 \\
0 & 0 & D_6^3 & 0 & 0 & I_6 & D_6^7 & 0 & 0 & 0 & D_6^{11} & 0 \\
0 & 0 & D_7^3 & D_7^4 & 0 & D_7^6 & I_7 & 0 & 0 & 0 & D_7^{11} & D_7^{12} \\
D_8^1 & D_8^2 & 0 & 0 & 0 & 0 & 0 & I_8 & 0 & 0 & 0 & 0 \\
0 & D_9^2 & D_9^3 & 0 & 0 & 0 & 0 & 0 & I_9 & 0 & 0 & 0 \\
0 & 0 & D_{10}^3 & 0 & D_{10}^5 & 0 & 0 & 0 & 0 & I_{10} & 0 & 0 \\
0 & 0 & D_{11}^3 & 0 & 0 & D_{11}^6 & D_{11}^7 & 0 & 0 & 0 & I_{11} & 0 \\
0 & 0 & D_{12}^3 & D_{12}^4 & 0 & 0 & D_7^{12} & 0 & 0 & 0 & 0 & I_{13}
\end{bmatrix} \begin{Bmatrix} G_1 \\ G_2 \\ G_3 \\ G_4 \\ G_5 \\ G_6 \\ K \\ J_1 \\ J_2 \\ J_3 \\ J_4 \\ J_5 \end{Bmatrix}
$$

Equation 5-4

Table 5-8: Interaction Matrix of the Off-road Vehicle in Table Format

	Components (physical entity)											
Components (tasks)	G_1	G_2	G_3	G_4	G_5	G_6	K	J_1	J_2	J_3	J_4	J_5
$G^*{}_1$	I_1	D_1^2	0	0	0	0	0	D_1^8	0	0	0	0
$G^*{}_2$	D_2^1	I_2	D_2^3	0	0	0	0	D_2^8	D_2^9	0	0	0
$G^*{}_3$	0	D_3^2	I_3	D_3^4	D_3^5	D_3^6	D_3^7	0	D_3^9	D_3^{10}	D_3^{11}	D_3^{12}
$G^*{}_4$	0	0	D_4^3	I_4	0	0	D_4^7	0	0	0	0	D_4^{12}
$G^*{}_5$	0	0	D_5^3	0	I_5	0	0	0	0	D_5^{10}	0	0
$G^*{}_6$	0	0	D_6^3	0	0	I_6	D_6^7	0	0	0	D_6^{11}	0
K^*	0	0	D_7^3	D_7^4	0	D_7^6	I_7	0	0	0	D_7^{11}	D_7^{12}
$J^*{}_1$	D_8^1	D_8^2	0	0	0	0	0	I_8	0	0	0	0
$J^*{}_2$	0	D_9^2	D_9^3	0	0	0	0	0	I_9	0	0	0
$J^*{}_3$	0	0	D_{10}^3	0	D_{10}^5	0	0	0	0	I_{10}	0	0
$J^*{}_4$	0	0	D_{11}^3	0	0	D_{11}^6	D_{11}^7	0	0	0	I_{11}	0
$J^*{}_5$	0	0	D_{12}^3	D_{12}^4	0	0	D_{12}^7	0	0	0	0	I_{12}

Matlab Symbolic Toolbox was used to multiply, $(\boldsymbol{FC})$ and $(\boldsymbol{I})$ to produce the $(\boldsymbol{OCI})$ matrix; which shows that, all of the engine subsystems are affected by the 25 vehicle operations; In relation to the hydraulic system and power transmission, the impact of all of the 25 operations is not accurate, the merger of all of their components into one subsystem; besides, the assumption that these two systems has physical interactions with each other leads to this conclusion. In general some of the hydraulics system components might not be affected by the functionality delivered by the mechanical power transmission system.

If the system analyst is interested in one specific subsystem or component's reliability; he needs to sufficiently capture all of its functionalities and interactions besides the functionality and interactions of its surrounding components and environments.

$$O_i|_1^{25} \xrightarrow{W^i} \{C_1, C_2, C_3, \dots C_{12}\} \qquad \textbf{Equation 5-5}$$

$$O_i|_1^{25} \xrightarrow{H^i} \{C_1 \cap\ C_2 \cap\ C_3, \dots \cap C_{12}\} \qquad \textbf{Equation 5-6}$$

Considering the $(\boldsymbol{OCI})$ column relevant to the intake-manifold, shown in Figure 5-14, it's obvious that the manifold reliability has impact on all operations; it is influenced by its neighboring relationship with the engine, turbocharger and the joints connecting to both sides. No other interactions, besides physical neighboring, were identified in this model; to accurately test the manifold reliability it will be required to test the whole subsystem presented in Figure 5-14.

```
D32*(A11*B13 + A12*B23 + A16*B63 + A17*B73 + A18*B83) + D82*(A11*B18 + A13*B38) + D92*(A11*B19 + A18*B89) + A13*B31*D12 + A14*B42*I2
D32*(A21*B13 + A22*B23 + A26*B63 + A27*B73 + A28*B83) + D82*(A21*B18 + A23*B38) + D92*(A21*B19 + A28*B89) + A23*B31*D12 + A24*B42*I2
D32*(A31*B13 + A32*B23 + A36*B63 + A37*B73 + A38*B83) + D82*(A31*B18 + A33*B38) + D92*(A31*B19 + A38*B89) + A33*B31*D12 + A34*B42*I2
D32*(A41*B13 + A42*B23 + A46*B63 + A47*B73 + A48*B83) + D82*(A41*B18 + A43*B38) + D92*(A41*B19 + A48*B89) + A43*B31*D12 + A44*B42*I2
D32*(A51*B13 + A52*B23 + A56*B63 + A57*B73 + A58*B83) + D82*(A51*B18 + A53*B38) + D92*(A51*B19 + A58*B89) + A53*B31*D12 + A54*B42*I2
D32*(A61*B13 + A62*B23 + A66*B63 + A67*B73 + A68*B83) + D82*(A61*B18 + A63*B38) + D92*(A61*B19 + A68*B89) + A63*B31*D12 + A64*B42*I2
D32*(A71*B13 + A72*B23 + A76*B63 + A77*B73 + A78*B83) + D82*(A71*B18 + A73*B38) + D92*(A71*B19 + A78*B89) + A73*B31*D12 + A74*B42*I2
D32*(A81*B13 + A82*B23 + A86*B63 + A87*B73 + A88*B83) + D82*(A81*B18 + A83*B38) + D92*(A81*B19 + A88*B89) + A83*B31*D12 + A84*B42*I2
D32*(A91*B13 + A92*B23 + A96*B63 + A97*B73 + A98*B83) + D82*(A91*B18 + A93*B38) + D92*(A91*B19 + A98*B89) + A93*B31*D12 + A94*B42*I2
D32*(A101*B13 + A102*B23 + A106*B63 + A107*B73 + A108*B83) + D82*(A101*B18 + A103*B38) + D92*(A101*B19 + A108*B89) + A103*B31*D12 + A104*B42*I2
D32*(A111*B13 + A112*B23 + A116*B63 + A117*B73 + A118*B83) + D82*(A111*B18 + A113*B38) + D92*(A111*B19 + A118*B89) + A113*B31*D12 + A114*B42*I2
D32*(A121*B13 + A122*B23 + A126*B63 + A127*B73 + A128*B83) + D82*(A121*B18 + A123*B38) + D92*(A121*B19 + A128*B89) + A123*B31*D12 + A124*B42*I2
D32*(A131*B13 + A132*B23 + A136*B63 + A137*B73 + A138*B83) + D82*(A131*B18 + A133*B38) + D92*(A131*B19 + A138*B89) + A133*B31*D12 + A134*B42*I2
D32*(A141*B13 + A142*B23 + A146*B63 + A147*B73 + A148*B83) + D82*(A141*B18 + A143*B38) + D92*(A141*B19 + A148*B89) + A143*B31*D12 + A144*B42*I2
D32*(A151*B13 + A152*B23 + A156*B63 + A157*B73 + A158*B83) + D82*(A151*B18 + A153*B38) + D92*(A151*B19 + A158*B89) + A153*B31*D12 + A154*B42*I2
D32*(A161*B13 + A162*B23 + A166*B63 + A167*B73 + A168*B83) + D82*(A161*B18 + A163*B38) + D92*(A161*B19 + A168*B89) + A163*B31*D12 + A164*B42*I2
D32*(A171*B13 + A172*B23 + A176*B63 + A177*B73 + A178*B83) + D82*(A171*B18 + A173*B38) + D92*(A171*B19 + A178*B89) + A173*B31*D12 + A174*B42*I2
D32*(A181*B13 + A182*B23 + A186*B63 + A187*B73 + A188*B83) + D82*(A181*B18 + A183*B38) + D92*(A181*B19 + A188*B89) + A183*B31*D12 + A184*B42*I2
D32*(A191*B13 + A192*B23 + A196*B63 + A197*B73 + A198*B83) + D82*(A191*B18 + A193*B38) + D92*(A191*B19 + A198*B89) + A193*B31*D12 + A194*B42*I2
D32*(A201*B13 + A202*B23 + A206*B63 + A207*B73 + A208*B83) + D82*(A201*B18 + A203*B38) + D92*(A201*B19 + A208*B89) + A203*B31*D12 + A204*B42*I2
D32*(A211*B13 + A212*B23 + A216*B63 + A217*B73 + A218*B83) + D82*(A211*B18 + A213*B38) + D92*(A211*B19 + A218*B89) + A213*B31*D12 + A214*B42*I2
D32*(A221*B13 + A222*B23 + A226*B63 + A227*B73 + A228*B83) + D82*(A221*B18 + A223*B38) + D92*(A221*B19 + A228*B89) + A223*B31*D12 + A224*B42*I2
D32*(A231*B13 + A232*B23 + A236*B63 + A237*B73 + A238*B83) + D82*(A231*B18 + A233*B38) + D92*(A231*B19 + A238*B89) + A233*B31*D12 + A234*B42*I2
D32*(A241*B13 + A242*B23 + A246*B63 + A247*B73 + A248*B83) + D82*(A241*B18 + A243*B38) + D92*(A241*B19 + A248*B89) + A243*B31*D12 + A244*B42*I2
D32*(A251*B13 + A252*B23 + A256*B63 + A257*B73 + A258*B83) + D82*(A251*B18 + A253*B38) + D92*(A251*B19 + A258*B89) + A253*B31*D12 + A254*B42*I2
```

Figure 5-14: Manifold $OCIM$ relevant column, first number index is the row number and the second is the column number for example A197 is A_{19}^{7} (relating operation-19 and component-7)

5.3.2 Intake Manifold Form Design

The body forces passing through the manifold structure is produced by the dynamics response of the turbocharger inertia due to the engine base excitation. Figure 5-15 and Figure 5-16 show two schematic projections to the manifold problem; Since the dominant vibration amplitudes are occurring along the lateral and vertical engine directions, i.e. (Y, Z) plane, we can simplify the loading passing through the manifold as a bending behavior influences by a dynamic set $(\Gamma_y g, \Gamma_z g)$ acceleration field $\left(\overrightarrow{A_{T,(y,z)}}\right)$ centered around the turbocharger center of gravity, i.e.: $\overrightarrow{A_{T,(y,z)}} = \Gamma_y g \hat{j} + \Gamma_z g \hat{k}$. The dynamic responses of internal combustion engines are typically measured by accelerometers mounted on the engine block. The (x) moment reaction at the joint connecting the manifold to the engine block is presented in Equation 5-7.

$$M_{xx} = m_T g\left(\Gamma_y L_z + \Gamma_z L_y\right) \quad \textbf{Equation 5-7}$$

where: M_{xx} ≡ resultant x-moment at the joint connecting the manifold to the engine block

m_T ≡ distributed tube sharing of turbocharger mass, see Table 5-9

g ≡ gravity

Γ_y ≡ dynamic y-direction factor (gravity scaling)

Γ_z ≡ dynamic z-direction factor (gravity scaling)

L_y ≡ turbocharger center of gravity distance to manifold center line joint with engine block, see Figure 5-15

L_z ≡ turbocharger center of gravity distance to manifold joint face with engine block, see Figure 5-15

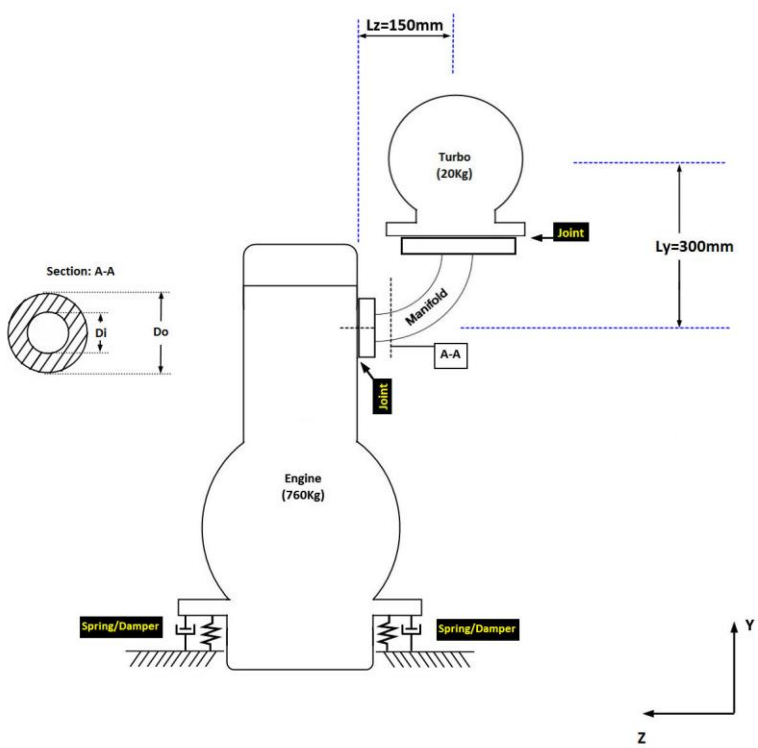

Figure 5-15: Schematic Representation to Manifold and Components Affecting its Design (Y-Z) Plane

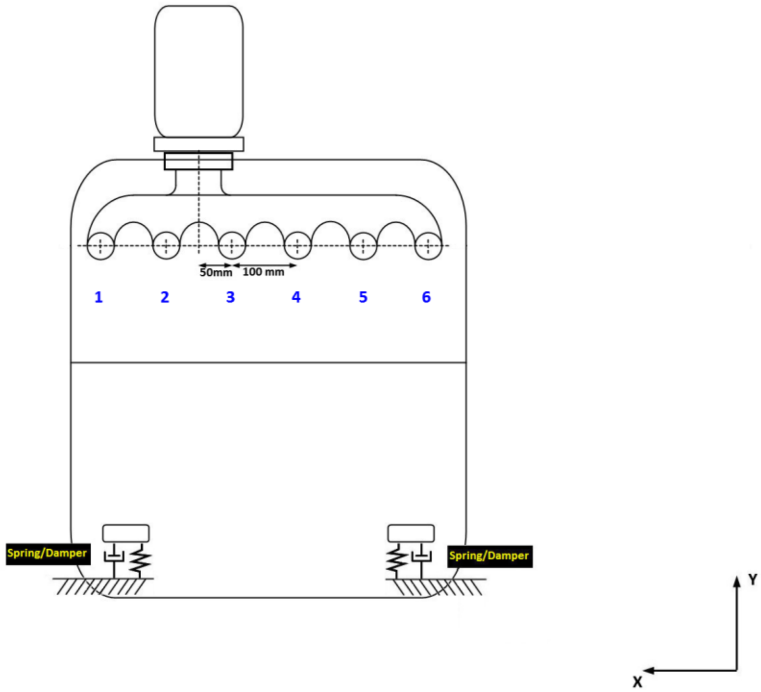

Figure 5-16: Schematic Representation to Manifold and Components Affecting its Design (X-Y) Plane

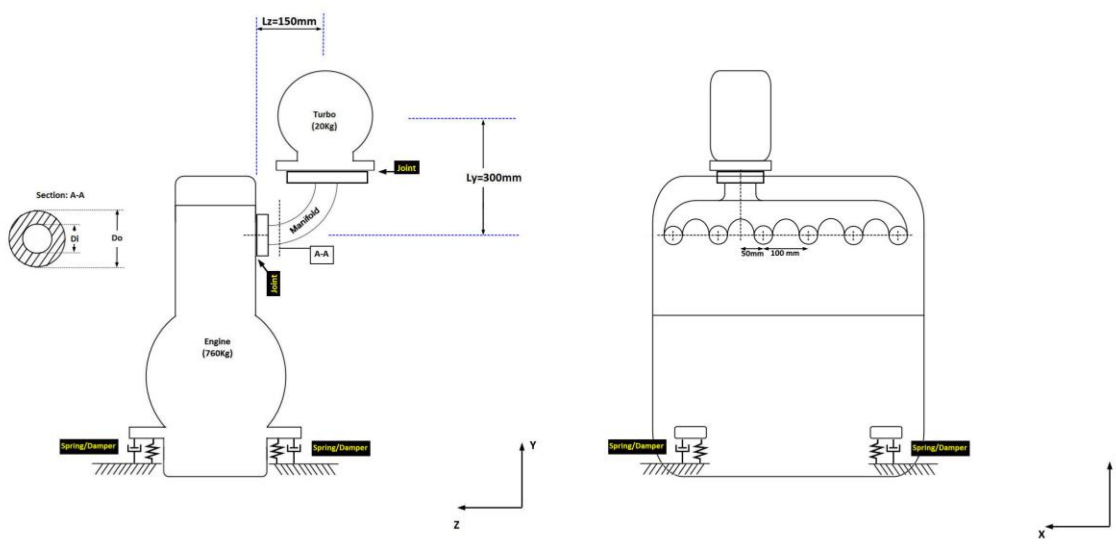

Figure 5-17: Schematic Representation to Manifold and Components Affecting its Design

Table 5-9: Distribution of Turbocharger Mass (used for load sharing calculations)

Tube number (see Figure 5-16)	X-Distance from Turbo (mm)	Mass Distribution Ratio Inversely Proportional with Distance (X)
1	150	11.08%
2	50	33.23%
3	50	33.23%
4	150	11.08%
5	250	6.65%
6	350	4.75%

The mass distribution presented in Table 5-9 shows tube-2 and 3 to be carrying more loading than others; their mass share (6.65Kg), or 33.23% of 20 Kg, will be used for designing each tube cross section.

Designing for a circular tube section for the manifold under bending stresses (Equation 5-8 and Equation 5-9); taking into account the stress concentration generated by the manifold/engine interface; a fatigue notch factor of 1.5 and 2 will be used to assess the stress concentration effects on fatigue; $\left(k_f = 1.5\right), (k_t = 2)$ will be used as design goal for the manifold shape.

$$\sigma_{xx} = \frac{M_{xx}\left({}^{D_o}\!/_2\right)}{\frac{\pi}{64}\left({D_o}^4 - {D_i}^4\right)} \quad \textbf{Equation 5-8}$$

$$\sigma_{xx} = \frac{32\ M_{xx} D_o}{\pi\left({D_o}^4 - {D_i}^4\right)} \quad \textbf{Equation 5-9}$$

where: $\sigma_{xx} \equiv$ bending stress at the outer upper fiber on the tube section

$D_o \equiv$ tube outer diameter, see section presented in Figure 5-15

$D_i \equiv$ tube inner diameter, see section presented in Figure 5-15

Considering there is a requirement for 40 mm internal diameter for optimum air flow to the engine, the problem unknowns become the: external tube diameter, (D_o), and two dynamic factors (Γ_y, Γ_z).

Rewriting Equation A-7 and considering $\frac{32\, M_{xx}}{\pi \sigma_{xx}} = c$, Equation 5-9 is generated,

$$D_o{}^4 - cD_o - D_i{}^4 = 0 \qquad \textbf{Equation 5-10}$$

Solving Equation 5-10, numerically for (D_o), knowing: $(D_i = 40mm)$; for 90% reliability goal; and variable (Γ_y, Γ_z) acceleration field matrix from 1 to 20; yields the domain of solution $(\Gamma_y, \Gamma_z, D_o)$ presented in Figure 5-18. Detailed engineering analyses to dynamic force responses, section sizing and numerical modeling executed to solve for the manifold external diameter problem is present in (Appendix A.3).

The averaged acceleration amplitudes around the engine/manifold joint is: $\overrightarrow{A_{T,(x,y,z)}} = 5.2g\hat{\imath} + 3.3g\hat{\jmath} + 8.9g\hat{k}$; (see Appendix A.3 for details). Using $(\Gamma_y = 3.3, \Gamma_z = 8.9)$, an external diameter of 44.6 mm would be sufficient for 90% reliability at 10 years age; provided the assumptions used for the analysis were correct. Figure 5-19 shows how the 44.6 mm was selected.

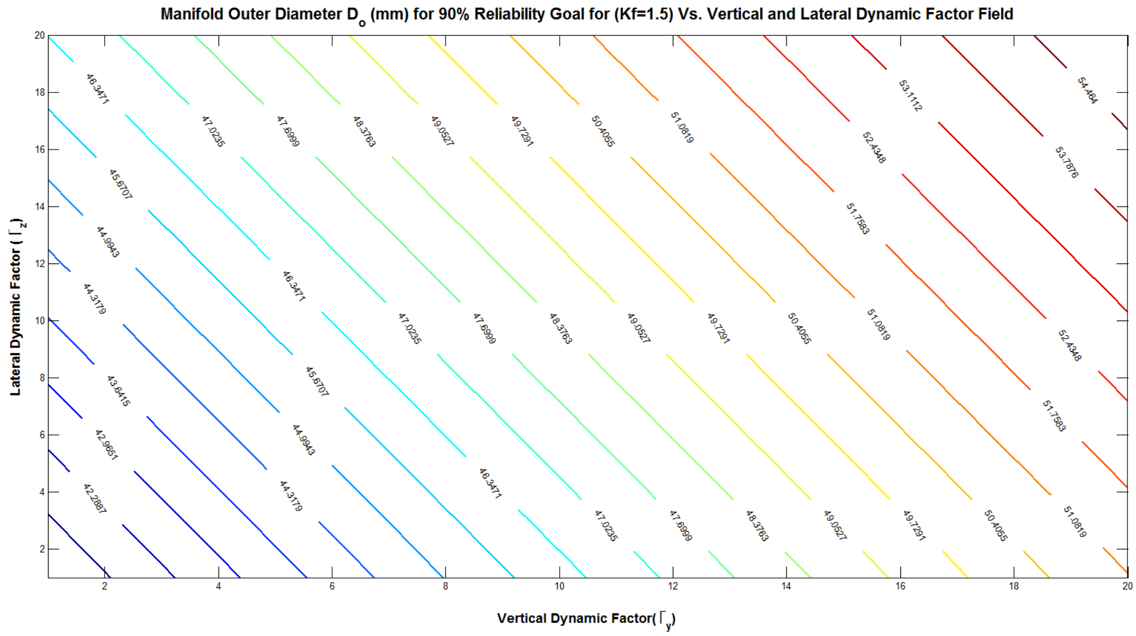

Figure 5-18: Manifold Outer Diameter to satisfy 90% Reliability Goal for (k_f=1.5) versus Vertical and Lateral Dynamic Factors Loading

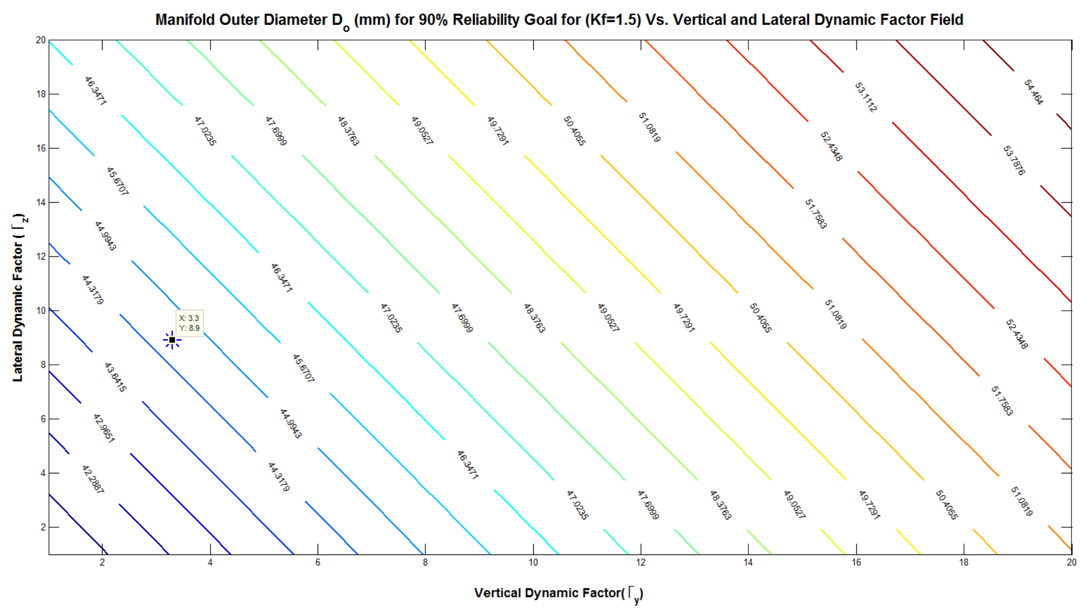

Figure 5-19: Manifold Outer Diameter Target Field for 90% Reliability Vs Averaged Manifold Loading (Shown as a point asterisk)

At this stage of the embodiment, Figure 5-20 shows the process followed to identify an initial design form for the manifold outer diameter. The process can also be manipulated similarly to identify materials characteristics or design operational thresholds.

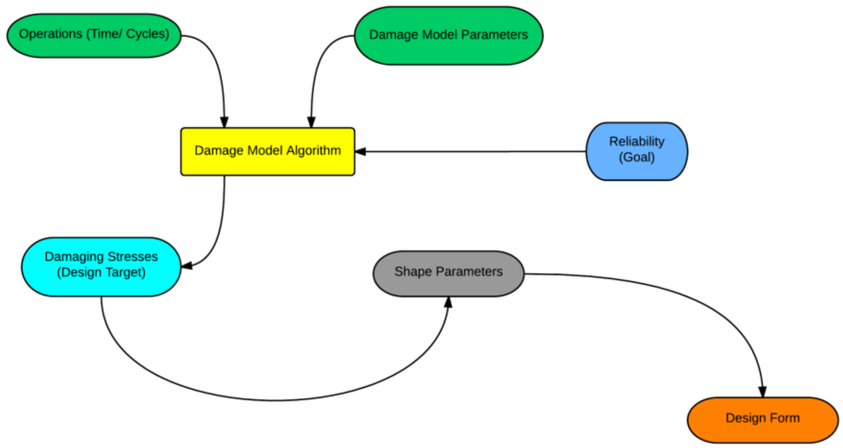

Figure 5-20: Design form emergence out of the component Mechanistic Reliability process at the start of the embodiment design phase

5.3.3 Finite Element Model

The first manifold design iteration, with 45mm outer diameter tubes, was developed using Pro/E, a three dimensional CAD software. Due to the proprietary of the information related to the design, the manifold design form will not be presented but the reliability analysis process will be outlined. Following the realization of design form, stress analysis using finite element analyses was performed; Abaqus-CAE software was used to assess the mechanical stresses on the manifold structure. (Appendix A.3) presents more details about the FEA modeling procedure. Table 5-10 and Table 5-11 show the accelerometer sample durations used for continuous and discrete operations.

Table 5-10: Sample Durations of Accelerometer Data used for Continuous Operations

Continuous Operations	
Operation	Sample duration (sec)
O1	19.2
O2	4.8
O3	42
O4	9.6
O5	2.4
O6	12
O7	12
O8	18
SUM	120

Table 5-11: Sample Durations of Accelerometer Data used for Discrete Operations

Discrete Operations		
Operation	Sample duration (sec)	Counts
O9	9	1 event
O10	9	1 event
O11	4	1 event
O12	4	1 event
O13	10	1 event
O14	1.5	1 event
O15	1.5	1 event
O16	1.5	1 event
O17	1.5	1 event
O18	4.5	1 event
O19	2	1 event
O20	5	1 event
O21	20	1 event
O22	1.5	1 event
O23	1.5	1 event
O24	2	1 event
O25	7.5	1 event

Seven virtual gauges were identified; one location (Gauge-A), consistently, had the highest stress response amplitudes and was identified as the lowest life area; further damage and reliability analyses were performed on this location.

5.3.4 Reliability Assessment during Embodiment Design

Rainflow counting for Gauge-A dynamic stress response of 120-seconds time sample of all 25 vehicle operations is shown in Figure 5-21. Cycle counts were hidden for information confidentiality. Every four bins were merged into one equivalent damaging stress range with an equivalent cycle summation. Stochastic simulation using Matlab code (Appendix B.3) was used to produce the equivalent median stress and standard deviation. The process was repeated twice to produce one equivalent stress range for the 25 vehicle operations as shown in Table 5-12.

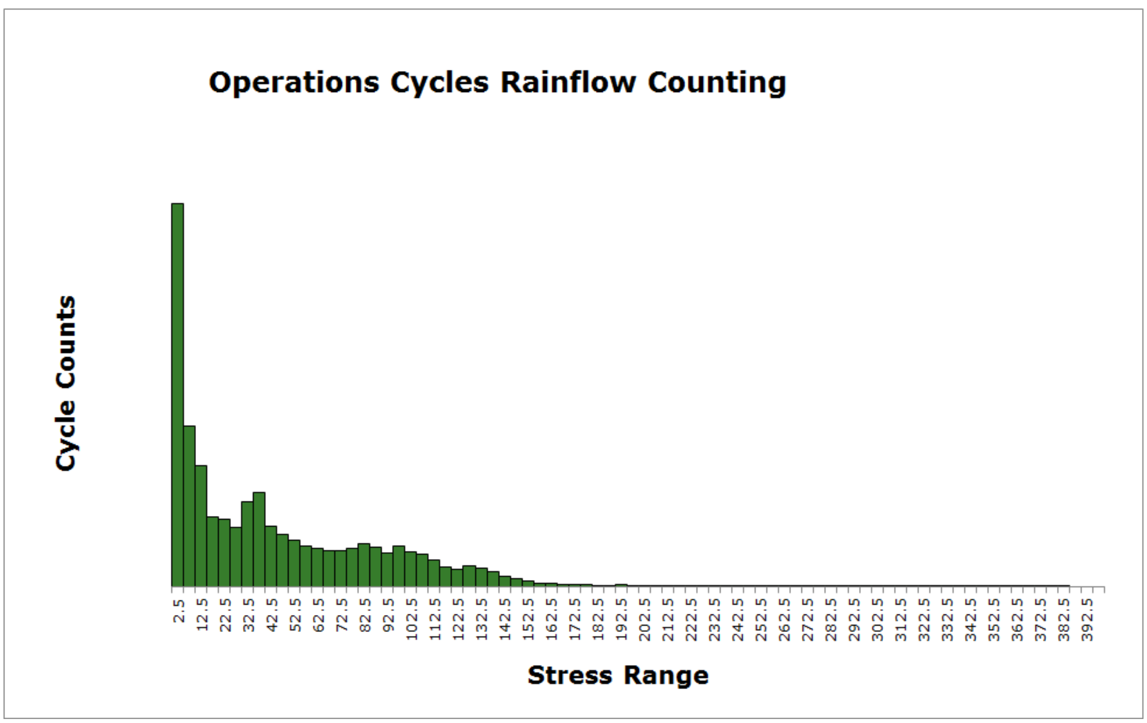

Figure 5-21: Vehicle operations rainflow cycle counting for Gauge-A on manifold structure

Table 5-12: Equivalent stress generated for vehicle operations; process repeated three times

<table>
<tr><th rowspan="2">BIN SUM Cycles</th><th colspan="3">Equivalent Stress</th><th rowspan="2">BIN SUM</th><th colspan="3">Equivalent Stress</th><th rowspan="2">BIN SUM</th><th colspan="3">Equivalent Stress</th></tr>
<tr><th>median,</th><th>mean,</th><th>Std dev%</th><th>median,</th><th>mean,</th><th>Std dev%</th><th>median,</th><th>mean,</th><th>Std dev%</th></tr>
<tr><td>9926</td><td>8</td><td>8</td><td>0.1698</td><td rowspan="4">18832</td><td rowspan="4">34</td><td rowspan="4">35</td><td rowspan="4">0.1539</td><td rowspan="20">24372</td><td rowspan="20">109</td><td rowspan="20">110</td><td rowspan="20">0.0792</td></tr>
<tr><td>4138</td><td>19</td><td>20</td><td>0.1449</td></tr>
<tr><td>2719</td><td>29</td><td>30</td><td>0.1821</td></tr>
<tr><td>2050</td><td>40</td><td>41</td><td>0.1523</td></tr>
<tr><td>2141</td><td>52</td><td>53</td><td>0.1176</td><td rowspan="4">5085</td><td rowspan="4">74</td><td rowspan="4">74</td><td rowspan="4">0.0912</td></tr>
<tr><td>1559</td><td>60</td><td>62</td><td>0.1706</td></tr>
<tr><td>990</td><td>72</td><td>74</td><td>0.141</td></tr>
<tr><td>395</td><td>86</td><td>86</td><td>0.1233</td></tr>
<tr><td>144</td><td>93</td><td>94</td><td>0.1247</td><td rowspan="4">341</td><td rowspan="4">117</td><td rowspan="4">118</td><td rowspan="4">0.0914</td></tr>
<tr><td>92</td><td>104</td><td>108</td><td>0.1571</td></tr>
<tr><td>56</td><td>118</td><td>119</td><td>0.1214</td></tr>
<tr><td>49</td><td>128</td><td>131</td><td>0.1446</td></tr>
<tr><td>36</td><td>137</td><td>140</td><td>0.1459</td><td rowspan="4">104</td><td rowspan="4">160</td><td rowspan="4">161</td><td rowspan="4">0.0787</td></tr>
<tr><td>27</td><td>151</td><td>153</td><td>0.1168</td></tr>
<tr><td>27</td><td>159</td><td>160</td><td>0.115</td></tr>
<tr><td>14</td><td>172</td><td>174</td><td>0.1381</td></tr>
<tr><td>9</td><td>187</td><td>185</td><td>0.1368</td><td rowspan="4">9.06</td><td rowspan="4">193</td><td rowspan="4">191</td><td rowspan="4">0.1406</td></tr>
<tr><td>0.018</td><td>192</td><td>196</td><td>0.1242</td></tr>
<tr><td>0.009</td><td>205</td><td>204</td><td>0.1261</td></tr>
<tr><td>0.003</td><td>214</td><td>218</td><td>0.1289</td></tr>
</table>

The equivalent stress, for 24372 cycles per 120 seconds was found to have a mean=110MPa, median=109MPa and coefficient of variation percentage=7.92%. Majority of the manifold stress responses were due to engine vibrations and dynamic responses affected by the natural frequency of the manifold structure. The statistical variation for the stress cycle duration was assumed minimal and neglected. The mechanistic reliability subroutine with 110 MPa mean equivalent stress besides the material property distribution (Table 5-5) were used to generated TTF distributions. Figure 5-22, Figure 5-23, Figure 5-24 show 50 samples randomly generated inputs for stress amplitude (see Table 5-12), annual usage in hours (see Table 5-3) , and (A_σ, C_σ)

material properties (see Table 5-5), to the component mechanistic reliability assessment algorithm.

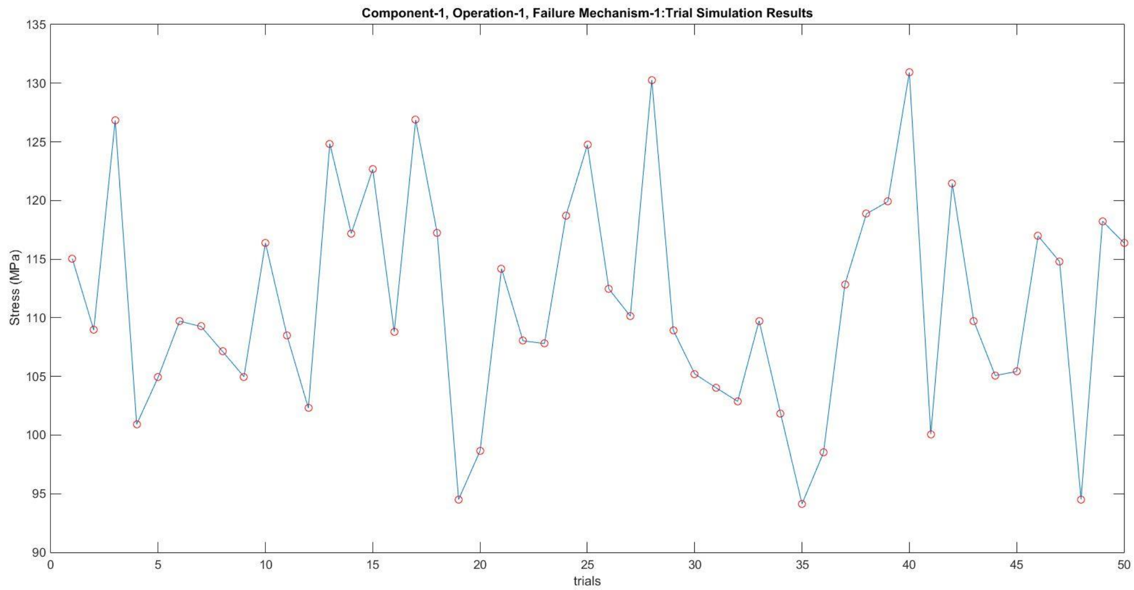

Figure 5-22: Random Stress Amplitude Input for First Design Iteration (50 samples)

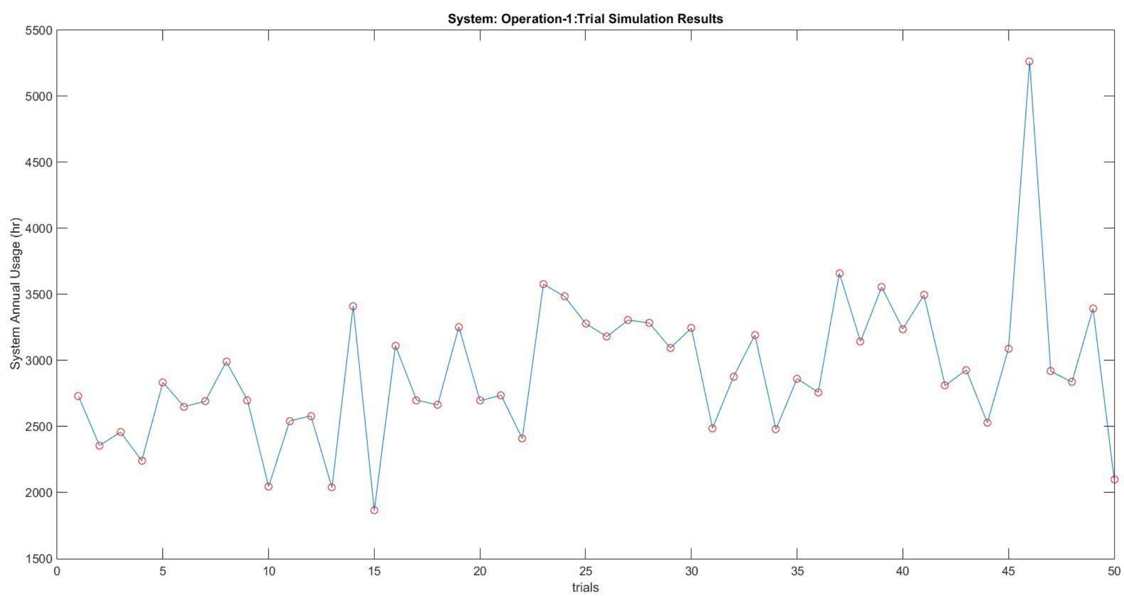

Figure 5-23: Random annual engine usage: input for first design iteration (50 samples)

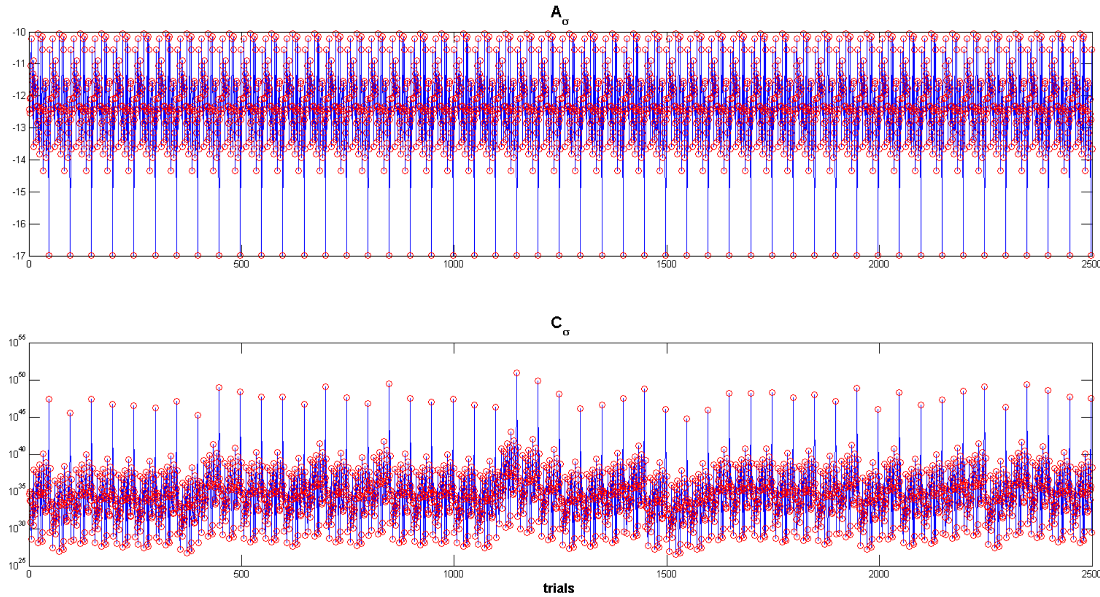

Figure 5-24: A_σ and C_σ Material damage constants

The component mechanistic algorithm TTF output is shown in Figure 5-25 with its corresponding reliability function (0 to 50000hrs) shown in Figure 5-26 along with the reliability goal and design life target lines. It's obvious that the first design iteration doesn't meet the life target (29200hrs) at 90% reliability goal.

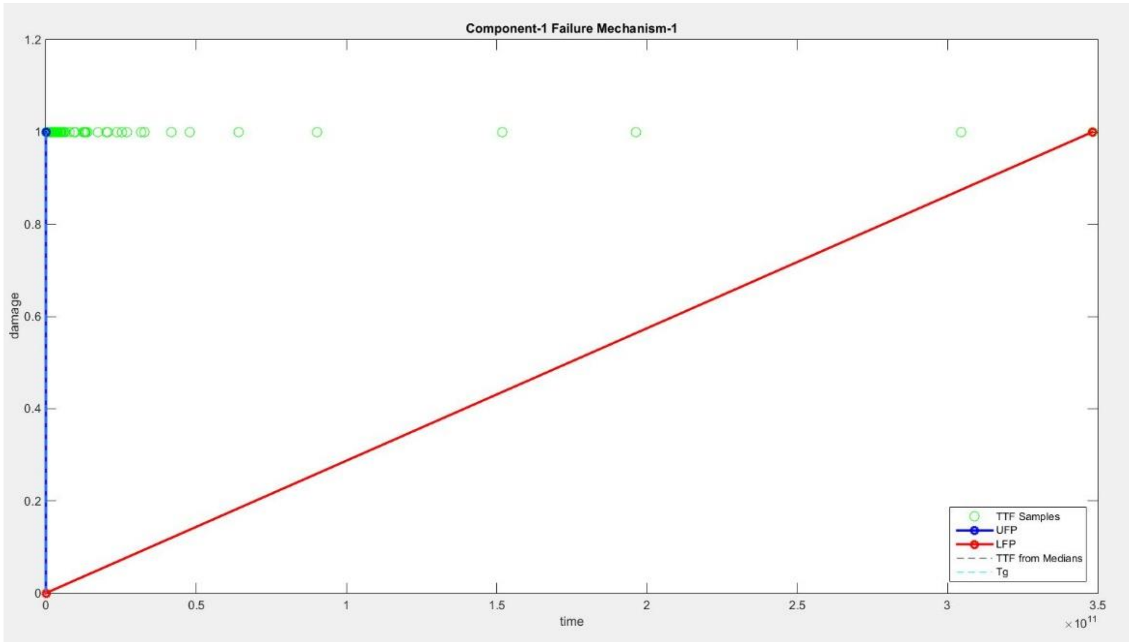

Figure 5-25: TTF Output vs Life Goal and Upper and Lower Damage Path for 1-operation equivalent damage

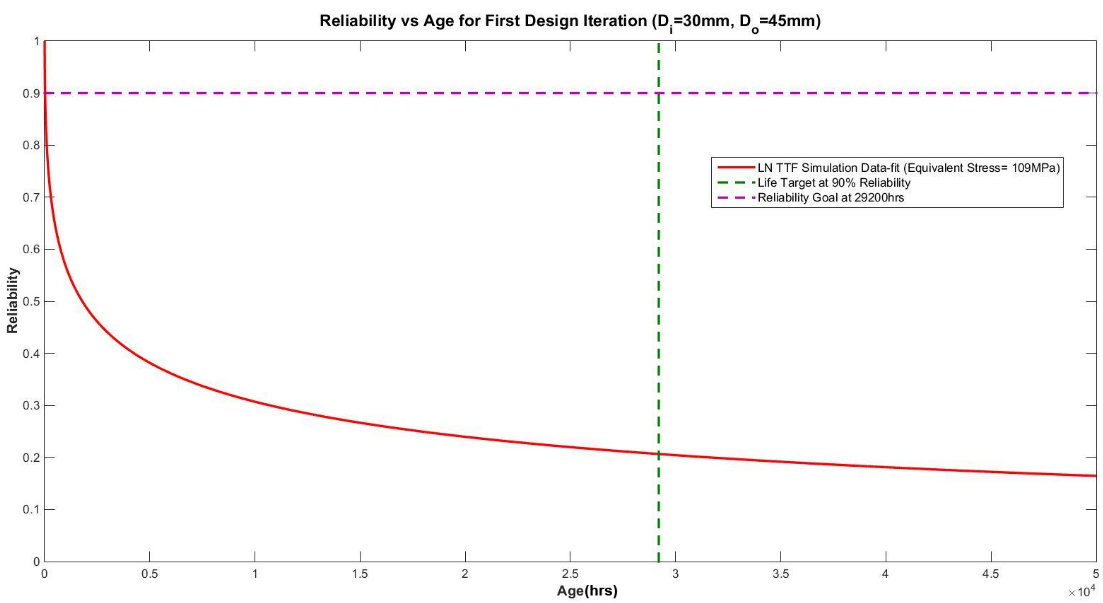

Figure 5-26: Reliability Function in Comparison to Life Target at 90% Reliability

The equivalent stress amplitude was reduced three times by 20% each to improve the reliability of the new design at the targeted life. The fourth design iteration ($D_o = 49.2mm$) as shown in Figure 5-27 passes the reliability goal line. Figure 5-28 shows the reliability improvements during the embodiment design of the intake manifold. Figure 5-29 presents reliability 95th percentile confidence assessment using Bootstrap resampling technique, with 100 reliability curves each generated from ($25^4 = 390625\,\text{TTF}$) samples. The final design iteration reliability is equal to 0.93 with $(0.02, -0.01)$ confidence bound

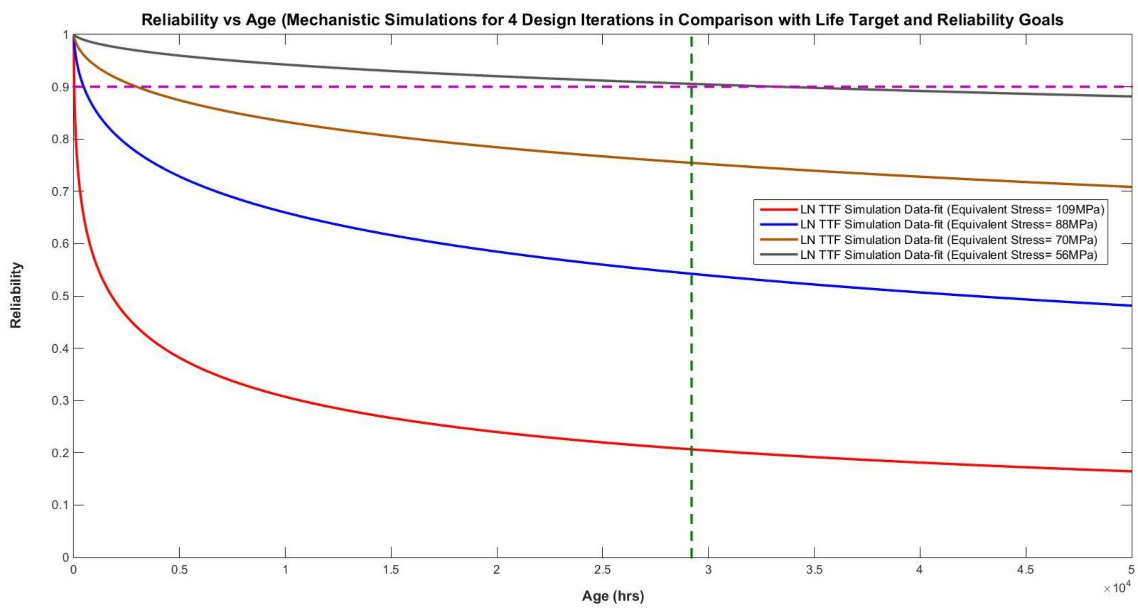

Figure 5-27: Reliability simulation of all design iterations, stress is dropped at 20% rate from an iteration to the next one

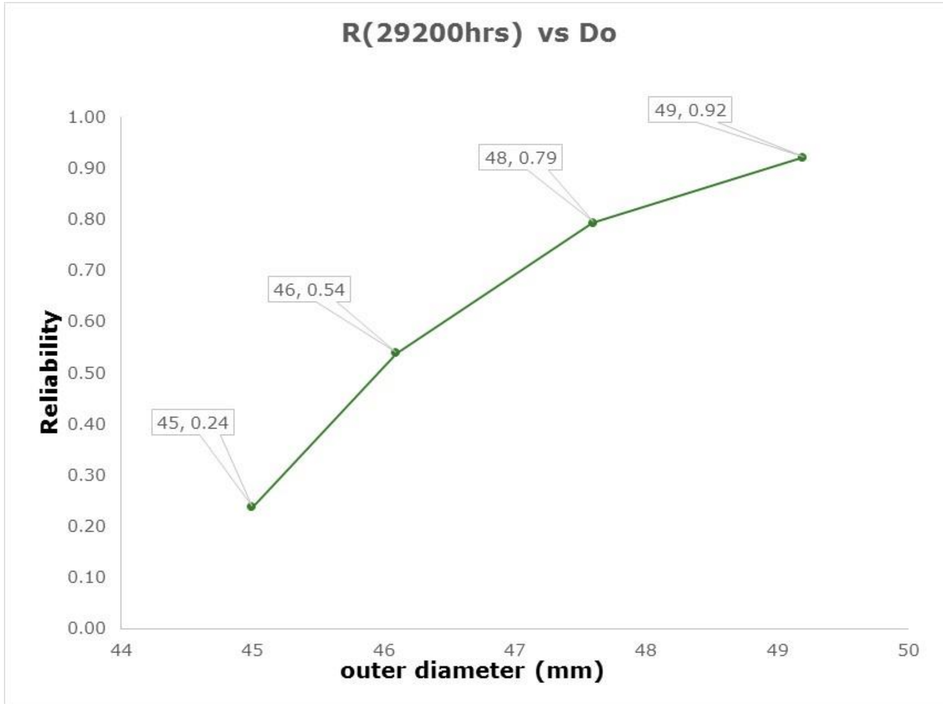

Figure 5-28: Reliability improvement due to design modifications of the manifold outer diameter during embodiment design phase

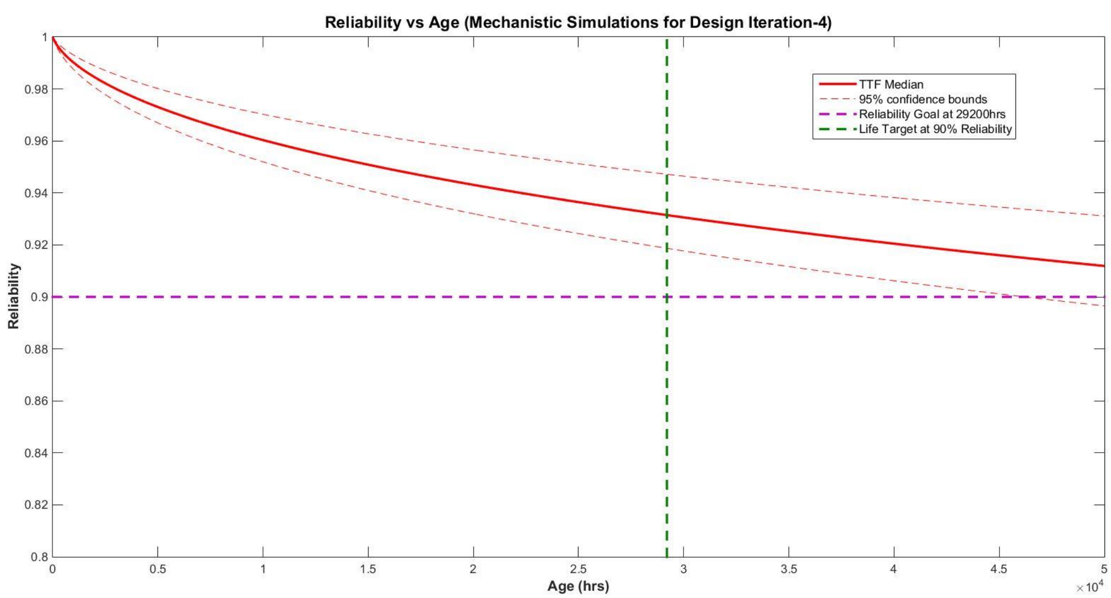

Figure 5-29: Reliability confidence assessment using Bootstrap resampling

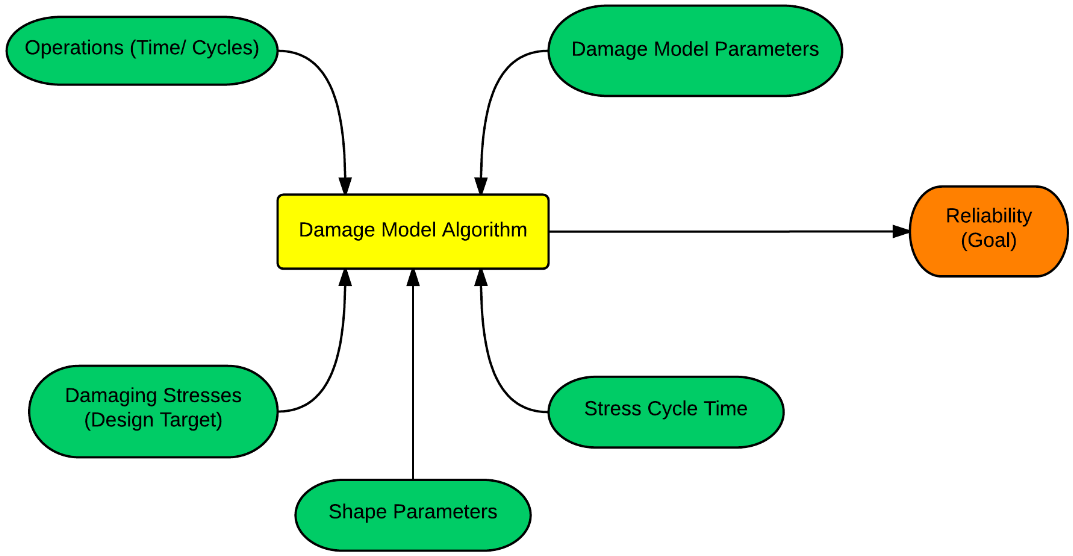

Figure 5-30: Mechanistic reliability assessment at the embodiment design phase

5.4 Mechanistic Reliability Model: Comparison to Field Data and Validation of the Approach

Figure 3-29 shows a comparison of reliability functions from mechanistic simulation and filed data for a manifold on a different product engine. The comparison shows the mechanistic reliability model is conservative in assessing reliability at the early life hours, but as the component ages the mechanistic reliability model becomes more accurate, Figure 5-32 shows the long life portion of the reliability curves.

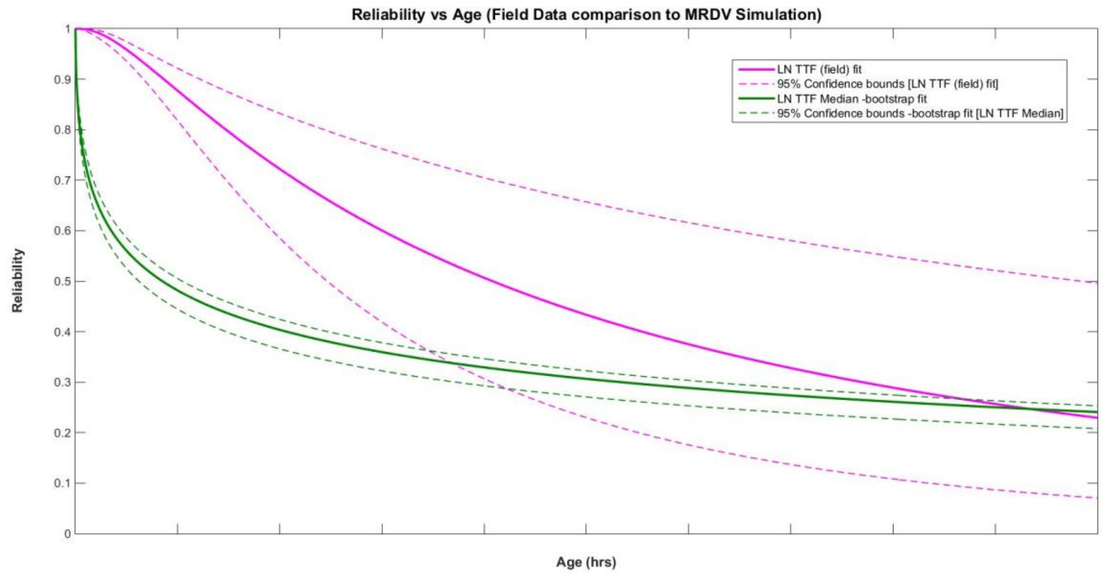

Figure 5-31: MRDV Reliability Simulation vs Field Reliability

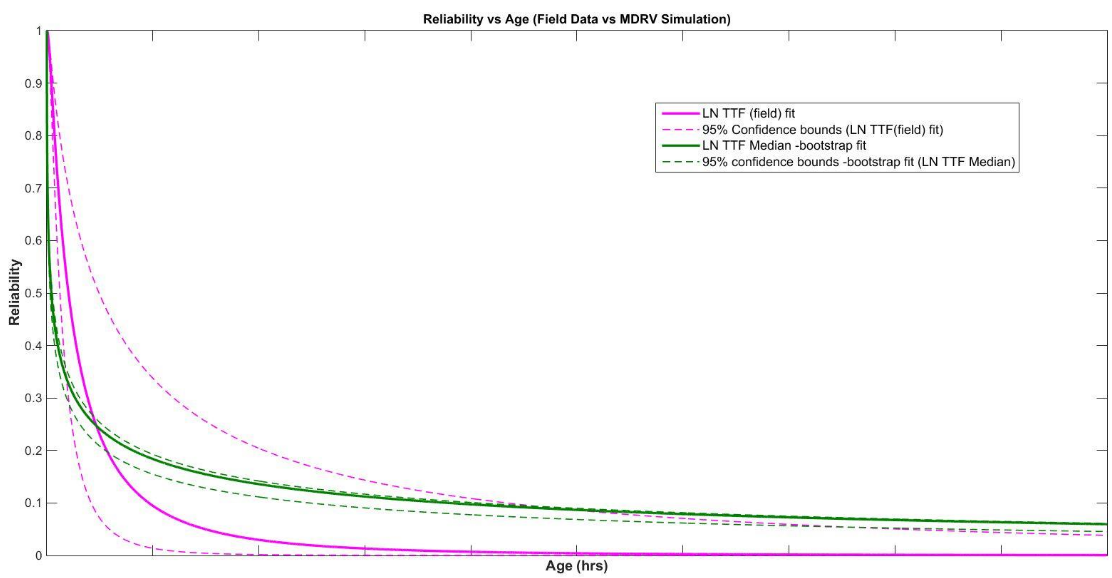

Figure 5-32: MRDV Reliability Simulation vs Field Reliability, long-life

5.5 Summary and Lessons Learned

Customer usage, operational stresses and material damage models are the minimum amount of information that needs to be available during the conceptual design phase to develop primary design form that could meet specific reliability targets for a component under development. System operations modeling helped to identify the operations that directly or indirectly impacted the manifold structure; the H-relationships did not have influence on the reliability assessment of system components.

Functional structures are not good representations of "*how*" the functional goals are being delivered. Stresses generated by energy flows can be recognized but assembly stresses, environmental stresses or stresses generated due to energy conversion processes are not recognizable (for example thermal stresses generated due to energy conversion from thermal latent energy to mechanical energy in internal combustion engines would not be recognizable by functional structure.).

During the conceptual design phase the stress goal was easily developed for single failure mechanism; for multiple failure mechanisms the process doesn't have that capability due to absence of design form; i.e. evaluating damage interactions needs a design form.

In this case study, one failure mechanism, (mechanical fatigue due to engine vibration and turbocharger inertial response), was the main focus of design analysis. In a generic mechanical system situation, all of the mechanical failure mechanisms presented in Table 3-1 need to be assessed, *individually*, during the conceptual design phase; and, following the multi-failure mode damage accumulation processes, section (3.2.7), after a design form is realized.

Including reliability goals to design components at the conceptual design phase provides a clear path to economical solutions, the steps were very clear but the design form problem framing and hand calculations took significant amount of time.

During the design process, MDRV allows for design parameters to be studied and assess their significance on design forms, for example the effect of the fatigue notch factor on the manifold outer diameter $\left(\text{from } k_f = 1.5 \text{ to } 2\right)$, as presented in Figure 5-33, is about 1 mm difference on low dynamic factors and about 4 mm on high dynamic factors, so it might not be numerically feasible to treat it as a statistical variable.

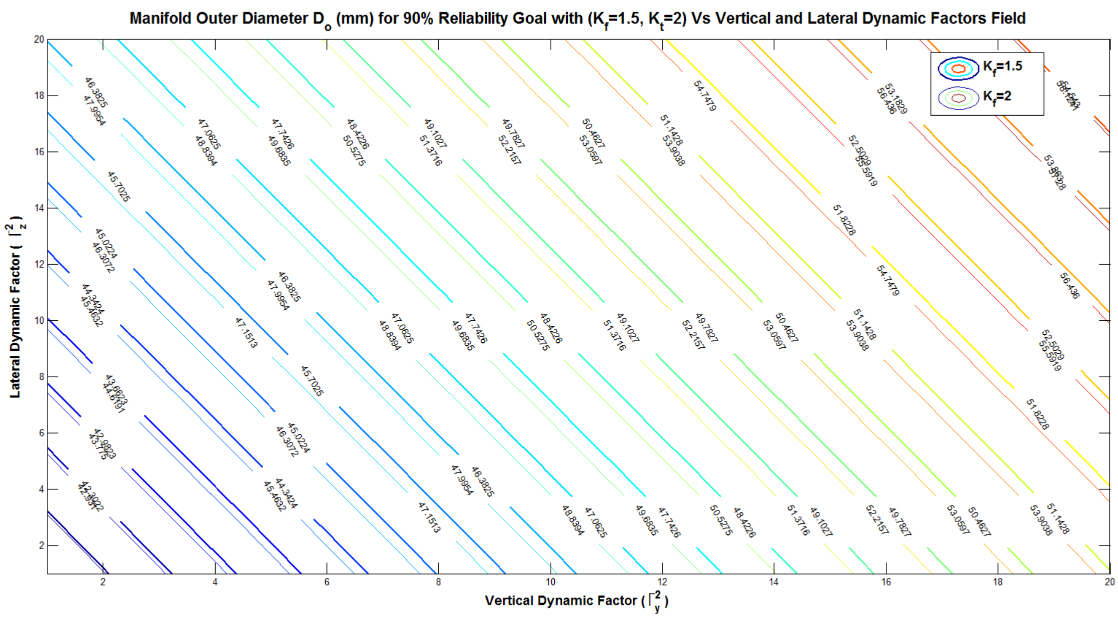

Figure 5-33: Manifold Outer Diameter to satisfy 90% Reliability Goal for $\left(k_f = 1.5, k_t = 2\right)$ versus Vertical and Lateral Dynamic Factors Loading

The design form developed at the end of conceptual design phase, using averaged stress generated from the cycles sum process (79MPa), underestimated the outer diameter needed to pass the reliability goal. Adding design “cushions” during the conceptual design phase could have reduced the time needed to design a sufficient form to pass reliability goals during the embodiment design phase.

Numerical modeling for the design form (FEA in this case) was very valuable to assess the mechanical stress responses due to engine mechanical vibration; in this specific project, accelerometer data was available to use as inputs to the FEM, which is not the typical situation; for newly developed designs, where data for simulation is not available during early phases of the design process, reliance on history knowledge and/or expert judgment might bridge this gap.

The equivalent damage process provided an economic solution to the reliability process; the number of samples generated for 25 operations dropped from 7.89E169 6.25E6.

If the system analyst is interested in one specific subsystem or component, he needs to sufficiently capture all of its functionalities and interactions besides the functionality and interactions of its surrounding components and environments. The operations/components interaction matrix ($\boldsymbol{OCI}$) can also be used as a tool to assist in testing-for-reliability where components can economically be tested by identifying the minimum number of system components to be included in the test activity.

Chapter 6 Discussion and Conclusions

One of Reliability Engineering definitions is: “the science of designing products and processes to be reliable” [43]; Design Research provides rich taxonomy to describe the design as an entity and a process; it provides models of representation that can be leveraged in reliability engineering science. This research work touched on many engineering fields like: system theory, solid mechanics, dynamic system theory, fracture mechanics, design research and stochastic simulation to be able to realize the main building blocks of MDRV.

6.1 Conclusions

The framework of mechanistic reliability requires the following attributes:

1. Design synthesis that describes the mechanical system in context of reliability as an engineering goal
2. Expert knowledge that uses the system synthesis to describe “how ” the system functions and “how” the system it gets affected by delivering its design goals, i.e. to develop (*W-,H- and D- relationships*)
3. Damage mathematical algorithm that uses: (*W-,H- and D- relationships*), system environmental stresses and material damage parameters to calculate the TTF distribution of the system.

The MDRV version presented here, allows efficient data management with the merging of many operations through the damage equivalent method (Appendix A.1); this is only possible for linear damage accumulation processes. The MDRV process was tested with a detailed ideal example and a specific design and validation case study; the results achieved by the case study shows MDRV to be somewhere between conservative or within the reliability uncertainty captured by field data. The case study showed a conservative estimation to reliability at short lives as shown by Figure 5-32; these results are judged conservative due to its impact on design; which (the design form) would have performed in the field better than the estimated reliability using MDRV; on the other side, at the long life regime we observe MDRV to be within the 95% uncertainty margins of the field data. This suggests that MDRV performance is reasonable to be adopted for design-for-reliability; yet it needs to be coupled with a reliability testing procedure for the final system at the end of PDP to better understand the uncertainty due to MDRV following necessary assumptions:

- Operations are independent of each other and are the main damage drivers
- System: operations/functions descriptive models, functions/components coupling relationships and component interactions are assumed linear.
- Linear damage accumulation model: Palmgren-Miner damage hypothesis applies to life consumed by different stress levels
- Components damages are independent of each other: damage accumulated on one component doesn't affect the degradation of another component.
- Independence of the following main parameters affecting system reliability from each other:
    - Customer Usage (determines the distribution of operations and periodical customer demand)
    - Stress (determines forces deriving the damage)
    - Stress cycle duration (determines frequency)
    - Material Properties (material resistance to damage, quality of material used)

MDRV approach is reliability-centered; design as a whole has more perspectives that can be synthesized differently than the reliability one (see Figure 6-1); being able to extract and model those perspectives is a time-consuming endeavor; it is recommended to improve the automation of MDRV and/or provide sufficient resources and time to successfully implementing it.

6.2 Discussion

More research focus is needed in the field of integrating design representation to reliability engineering to make reliability an emergent property of the system being investigated. This work contribute some of the building blocks to the foundations of design synthesis integration to reliability engineering; for this process to be effective, it's important to understand the contextual aspect of design synthesis (see Figure 6-1).

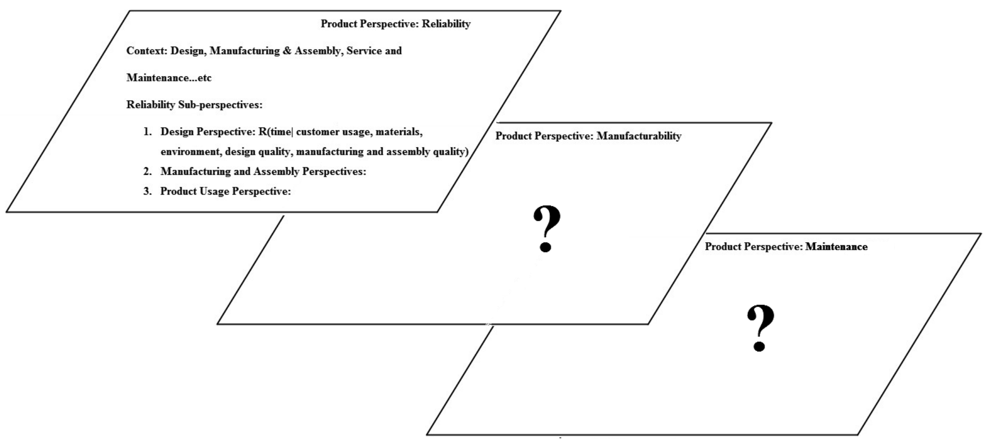

Figure 6-1: Perspectives of the Product in PDP; shown just three perspectives, the complete list is more

As presented in the previous sections, the current available design integrated reliability processes do not integrate all of the functional, behavioral, structural and physical aspects of the design in a cohesive framework while MDRV does; it leverages the functional-basis and axiomatic design methodologies to synthesize the designed system of components. In summary, MDRV reliability has three main attributed:

- Structure: realization of the system components and relationships critical to its operational reliability; besides, identifying the logic governing the system reliability. The latter needs to be captured from designer knowledge and integrate it into the system reliability evaluation process.
- Physics: the science governing the failure behavior of system entities formulated into mathematical models describing it.
- Procedures: knowledge about how to assess reliability of mechanical system, what tools and governing relationships (i.e. for instance failure paths, damage simulation process …etc.) to use.

The system representation, in MDRV framework, separates the functional flow (energy, mass and signal) aspects of the system representation from the structural aspect and superimposed the two representation to get an amalgamation of the two system representations to capture the operations/component interaction relationship. As the design progresses from conceptual phase to embodiment phase, the interaction relationships between components increase and become more complicated and less obvious and that has negative impact on system reliability; hence every time a new realization or design additions are implemented all design matrices ($\boldsymbol{OF}$), ($\boldsymbol{FC}$), ($\boldsymbol{I}$) and ($\boldsymbol{OCI}$) need to be updated and system reliability to be reevaluated.

The system design and reliability experts are the main links between the design synthesis and the mechanistic reliability models; they leverage and interpret the W-relationship statements to produce D-relationships and H-relationships; which are crucial to the assessment of components and system reliability. Numerical modeling for the design form (FEA in this case) was very valuable to assess the mechanical stress responses generated by IC engine mechanical vibrations and external base excitations. In this specific project, accelerometer data was available which is not typical. Relying on other numerical models like DSM (dynamic system modeling) would have been another alternative to accelerometer data, that could have led to spending more time developing these models besides increasing the model uncertainty and lowering the confidence in the final results.

MDRV relies heavily on statistical simulation in which controlled randomness for: component stresses, system usage, material properties...etc. allows assessment of TTF for components and complete systems. Considering the engine manifold case study, statistical simulation consumed significant time especially during conceptual design; developing a physics-based methodology that recognizes parameters' stochastic significance is important to reduce the TTF vector size without reducing stochastic confidence; more focus on data management would improve the efficiency of this process.

As shown by the case study example, the process is flexible in managing the amount of details required for representing the system and/or the depth of analysis (capturing system internal interactions and/or external stimuli); the system representation can be focused on a specific subsystem, that need to be analyzed, and simplify the rest of the system that's is not the central focus of analysis.

MDRV system representation lacks function sequence modeling; for the case study functional model example, actuate power generation happens before channeling air or regulating fuel intake, but the function model developed doesn't structurally recognize that. MDRV focuses on system operations, and the functions delivering them, as the main system goals; intended and unintended operations and/or functions are not separated.

6.3 Recommendations

6.3.1 Improving Effectiveness

The mechanistic process provides strong integration between design and reliability engineering but relies heavily on stochastic simulation and consumes significant amount of time; efficient numerical modeling and program coding; better data management, faster computer processors and large memory storage is needed for the process to be more effective and less time consuming. Besides, investing in Equivalent Damage models, similar to the one developed for mechanical stresses (Appendix A.1), will have positive impact on MDRV run-time; the amount of data required to solve for operational damages drops by many orders of magnitudes when equivalent damage models are used.

The accuracy of MDRV depends on the accuracy of product data and availability of experts to provide reasonable estimates to: product usage, operational stresses, material damage parameters…etc.; the process can integrate Bayesian inference as more information and data becomes available during design progression from a concept to a physical entity. The process has the capacity to maximize the benefit of using most of available information to address the design reliability problem; besides, the process has the ability to identify the parameters and variable that has significant impact on reliability; which allows the development of reliability optimization algorithms in the future.

6.3.2 Improving Inclusiveness

Expanding the framework from “material damage models” focus to “system damage models” will allow the process to address other engineered systems beside mechanical systems; although damage models would still be central to understanding systems reliability during the design phase, the definition of system failure might shift to “failure of the system physical form and/or any other forms”.

Identifying damaging stresses from functional structure can miss some of the stresses that are byproducts of the function output goals, for example: mechanical energy is the output functional goal of internal combustion engines, yet thermal stresses has significant impact on the degradation behavior of its components but they might not be recognized as damaging stresses. A model that captures, the function’s “*goal*” and “*how*” that goal is being achieved should be investigated in the future. Assessing the viability of other system representations would improve the H-relationship description; to reduce reliance on subjective judgment. Methods like Biomatrix system representation has more degrees of representation than functional structures’ and might better capture internal effects within system entities.

Investigating different damage accumulation models, comparing them to Palmegren-Miner’s and explore their advantages and effects on process accuracy is recommended. Studying multi-failure mechanisms damage models through a case study to test the applicability of the aggravating damage model would improve MDRV capabilities.

Distinguishing between operations that are design-intent and operations that are unintended is needed. Besides, expanding the model to recognize operations and functions that has compliance impacts (e.g. emission control); safety impact (e.g. lifting machines); and/or ergonomic impact (e.g. steering and machine control) type functions to go beyond the current customer focus perspective.

6.3.3 Improving Process Capability

Studying the linearity vs. nonlinearity limitations of mechanical systems' descriptive, coupling and interrelationship models is important to expand the process to also cover nonlinear models.

Importance and priority of system operations, functions and components needs to be studied and modeled to improve MDRV capabilities during the design phase; besides understanding the physical meaning of $(\boldsymbol{OF})$, $(\boldsymbol{FC})$ matrix elements and the applicability of those coupling factors is recommended to improve the system reliability assessment process.

6.3.4 Improving Accuracy

The current process doesn't distinguish between intended and unintended functions (or operations); it assumes all operations are intended and the damage affecting the system is produced by those operations. Exploring the value of separating the system functions (or operations) into intended or unintended functions (or operations) needs to be explored in the future. Operations/component interaction matrix, $(\boldsymbol{OCI})$, can be used as a tool to assist in testing-for-reliability setups and planning; where components' sufficient surroundings, subsystems , joints and environments can easily be identified and included in the test-for-reliability procedure using the revealed $(\boldsymbol{OCI})$ system relationships.

Equivalent-damage stress process (Appendix A.1 & Appendix B.3) was used in (Chapter 5-Case Study) to reduce the number of TTF samples; Comparing the results outcome of this process with complete-operations solution results is needed. This process coupled with improving the mechanistic reliability code efficiency (Appendix B.1) would allow higher number of TTF samples to be generated and higher confidence on reliability output results to be achieved.

Appendix A Mathematical and Numerical Models

Appendix A.1 The Equivalent Damage Stress

Sometimes, due to the high number of system operations and TTF samples, computer memory limitations became an obstacle to solve for random TTF data generated by the mechanistic reliability stochastic simulation. To better manage this problem, a method to generate an equivalent damaging stress with equivalent cycle goals is developed. The goal of this process is to reduce the number of TTF samples generated from $(L \times M \times N \times P^2)^n$ to $(L \times M \times N \times P^2)$; where: $\{L, M, N, P\}$ are the number of random: stress cycle duration, stress amplitude, usage time, material fatigue properties samples and (n) is the number of system operations

Considering two sinusoidal stress signals, shown by Equation A-1

$$S_1(t) = S_{amp_1} \sin(\omega_1 t)\,;$$
$$S_2(t) = S_{amp_2} \sin(\omega_2 t) \qquad \textbf{Equation A-1}$$

where: $S_1(t)$ and $S_2(t) \equiv$ two stress signals affecting same location on a structure at different time intervals

S_{amp_1} and S_{amp_2} $\equiv$ the maximum signals amplitudes

ω_1 and ω_2 $\equiv$ signals frequencies

$S(t)$ and $n(t)$ shown by Equation A-2and Equation A-3, represent the stress amplitude and number of cycles that produces an equivalent damage summation produced by $S_1(t)$ and $S_2(t)$ collectively

$$S(t) = S_{amp} \sin(\omega t) \qquad \textbf{Equation A-2}$$

$$n(t) = ft = \left(\frac{\omega}{2\pi}\right)t \qquad \textbf{Equation A-3}$$

where: $n(t)$ ≡ number of cycles accumulated during time (t)

f ≡ frequency in (Hz)

ω ≡ frequency in (rad/sec)

The fatigue damage produced by Equation A-1 stress cycles, can be calculated using Equation 3-51 :

$$\Lambda_1(t) = \frac{n_1}{N_{f_1}} = \frac{n_1(t)}{C_\sigma\, exp\left[A_\sigma\, ln\left(S_{amp_1}\right)\right]}$$

Equation A-4

$$\Lambda_2(t) = \frac{n_2}{N_{f_2}} = \frac{n_2(t)}{C_\sigma\, exp\left[A_\sigma\, ln\left(S_{amp_2}\right)\right]}$$

Summing the damage generate by the two stress signals and generalizing the summation formula:

$$\Lambda(t) = \frac{n_1}{N_{f_1}} + \frac{n_2}{N_{f_2}} + \cdots + \frac{n_m}{N_{f_m}} = \sum_{j=1}^{m}\left(\frac{n_j}{N_{f_j}}\right) \qquad \textbf{Equation A-5}$$

The damage generated from $\left(S_{amp}, n(t)\right)$, the equivalent stress signal, is presented in Equation A-6:

$$\Lambda(t) = \frac{n}{N_f} = \frac{n(t)}{C_\sigma\, exp\left[A_\sigma\, ln\left(S_{amp}\right)\right]} \qquad \textbf{Equation A-6}$$

Equating the damage generated from the set $\{S_1(t), S_2(t)\}$ to the equivalent stress damage presented in Equation A-6 produces Equation A-7 :

$$\frac{n}{C_\sigma\, exp\left[A_\sigma\, ln\left(S_{amp}\right)\right]} = \sum_{j=1}^{m}\left(\frac{n_j}{N_{f_j}}\right) \qquad \textbf{Equation A-7}$$

Rearranging Equation A-7 creates Equation A-8 to Equation A-12:

$$exp\left[A_\sigma\ ln\left(S_{amp}\right)\right] = \frac{n}{C_\sigma \sum_{j=1}^{m}\left(\frac{n_j}{N_{f_j}}\right)}$$ **Equation A-8**

$$A_\sigma\ ln\left(S_{amp}\right) = ln\left(\frac{n}{C_\sigma \sum_{j=1}^{m}\left(\frac{n_j}{N_{f_j}}\right)}\right)$$ **Equation A-9**

$$ln\left(S_{amp}\right) = \frac{ln\left(\frac{n}{C_\sigma \sum_{j=1}^{m}\left(\frac{n_j}{N_{f_j}}\right)}\right)}{A_\sigma}$$ **Equation A-10**

$$S_{amp} = exp\left(\left(\frac{1}{A_\sigma}\right) ln\left(\frac{n}{C_\sigma \sum_{j=1}^{m}\left(\frac{n_j}{N_{f_j}}\right)}\right)\right)$$ **Equation A-11**

$$S_{amp} = \left(exp\left(ln\left(\frac{n}{C_\sigma \sum_{j=1}^{m}\left(\frac{n_j}{N_{f_j}}\right)}\right)\right)\right)^{\frac{1}{A_\sigma}}$$ **Equation A-12**

The equivalent stress amplitude for a specific number of cycles (n) is presented in Equation A-13

$$S_{amp} = \left(\frac{n}{C_\sigma \sum_{j=1}^{m} \left(\frac{n_j}{N_{f_j}} \right)} \right)^{\frac{1}{A_\sigma}} \qquad \textbf{Equation A-13}$$

The equivalent number of cycles for a specific stress amplitude (S_{amp}) is presented in Equation A-14:

$$n = C_\sigma (S_{amp})^{A_\sigma} \sum_{j=1}^{m} \left(\frac{n_j}{N_{f_j}} \right) \qquad \textbf{Equation A-14}$$

Equation A-13 and Equation A-14 represents the equivalent stress amplitude and cycle counts that produces the same amount of damage generated by $S_1(t)$ and $S_2(t)$. The stress (S_{amp}) can be assesses for arbitrary $(n) \geq 0$ from Equation A-13 and the cycles counts (n) can also be assessed for arbitrary $(S_{amp}) \geq 0$ from Equation A-14.

Appendix A.2 Manifold External Tube Diameter: Detailed Calculations

The body forces passing through the manifold structure is produced by the dynamics response of the turbocharger inertia due to the engine base excitation. Figure 6-2 and Figure 6-3 and show two schematic projections to the manifold problem; Since the dominant vibration amplitudes are occurring along the lateral and vertical engine directions, i.e. (Y,Z) plane, we can simplify the loading passing through the manifold as a bending behavior influences by a dynamic set $(\Gamma_y g, \Gamma_z g)$ acceleration field $(\overrightarrow{A_{T,(y,z)}})$ centered around the turbocharger center of gravity, i.e.: $\overrightarrow{A_{T,(y,z)}} = \Gamma_y g\hat{\jmath} + \Gamma_z g\hat{k}$. The dynamic responses of internal combustion engines are typically measured by accelerometers that are mounted on the engine block. The (x) moment reaction at the joint connecting the manifold to the engine block is presented in Equation 5-7.

$$M_{xx} = m_T g\left(\Gamma_y L_z + \Gamma_z L_y\right) \qquad \textbf{Equation A-15}$$

where: $M_{xx} \equiv$ resultant x-moment at the joint connecting the manifold to the engine block

$m_T \equiv$ distributed tube sharing of turbocharger mass, see Table 5-9

$g \equiv$ gravity

$\Gamma_y \equiv$ dynamic y-direction factor (gravity scaling)

$\Gamma_z \equiv$ dynamic z-direction factor (gravity scaling)

$L_y \equiv$ turbocharger center of gravity distance to manifold center line joint with engine block, see Figure 6-2

$L_z \equiv$ turbocharger center of gravity distance to manifold joint face with engine block, see Figure 6-2

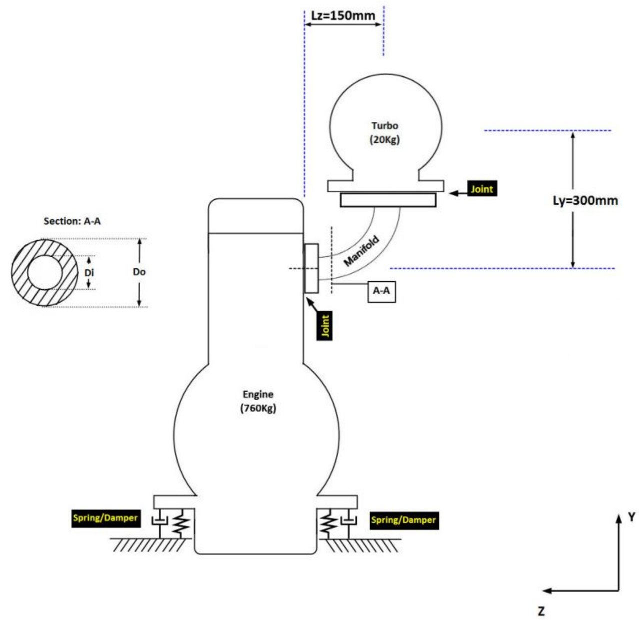

Figure 6-2: Schematic Representation to Manifold and Components Affecting its Design (Y-Z) Plane

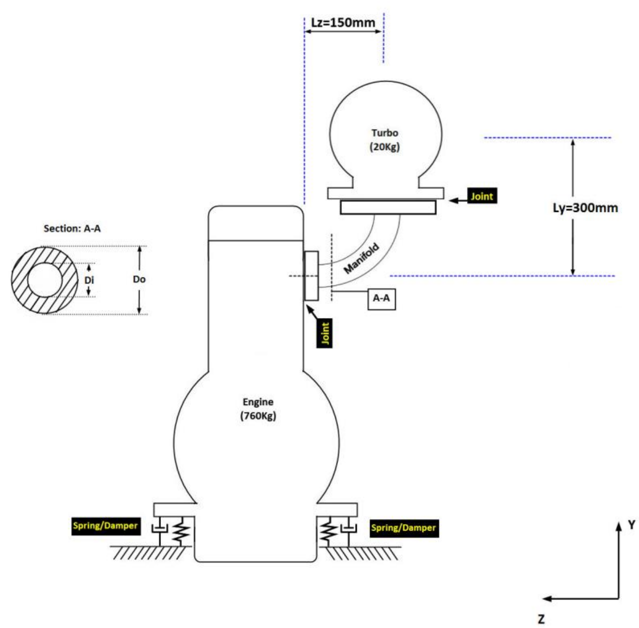

Figure 6-3: Schematic Representation to Manifold and Components Affecting its Design (Y-Z) Plane

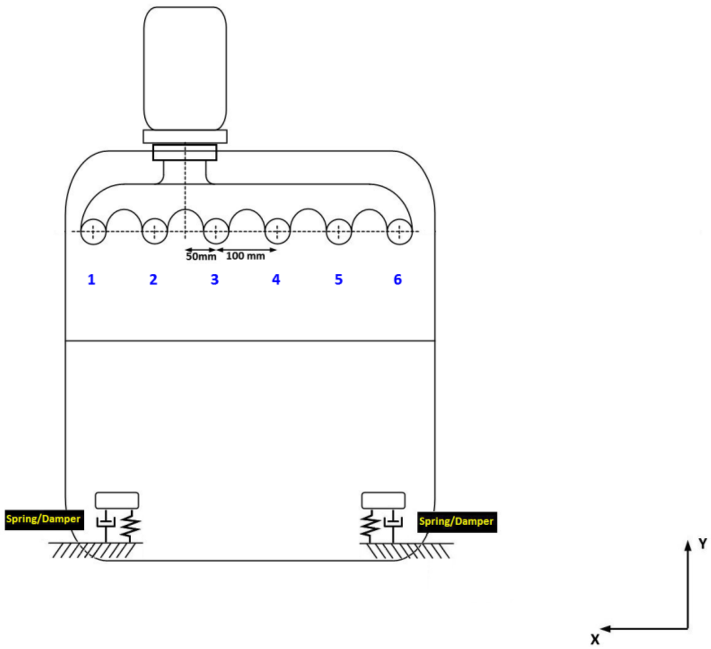

Figure 6-4: Schematic Representation to Manifold and Components Affecting its Design (X-Y) Plane

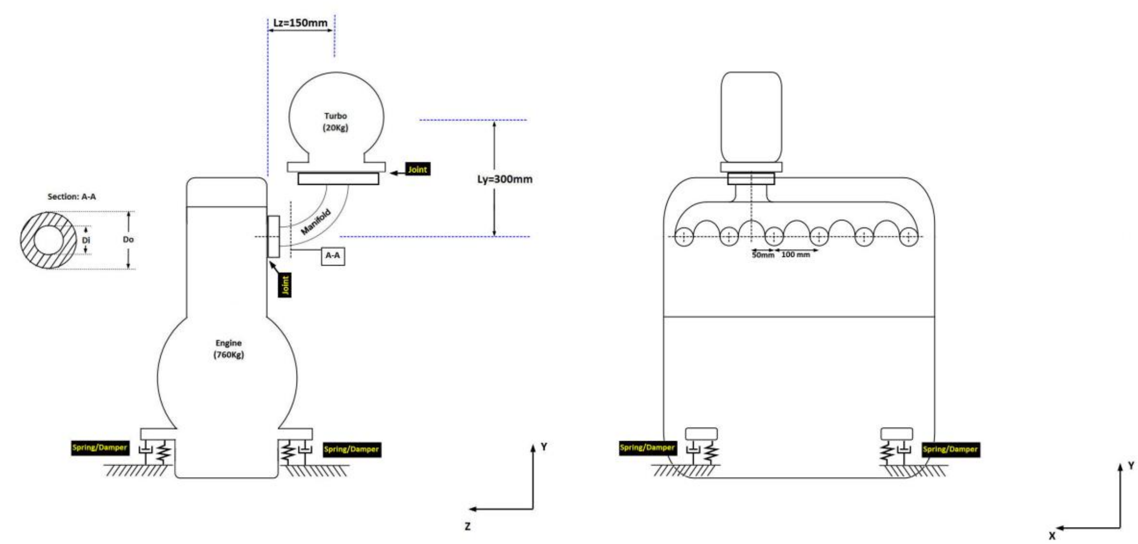

Figure 6-5: Schematic Representation to Manifold and Components Affecting its Design

Table 6-1: Distribution of Turbocharger Mass (used for load sharing calculations)

Tube number (see Figure 6-4)	X-Distance from Turbo (mm)	Mass Distribution Ratio Inversely Proportional with Distance (X)
1	150	11.08%
2	50	33.23%
3	50	33.23%
4	150	11.08%
5	250	6.65%
6	350	4.75%

The mass distribution presented in Table 6-1 shows tube-2 and 3 to be carrying more loading than others; their mass share (6.65Kg), or 33.23% of 20 Kg, will be used for designing each tube cross section.

Designing for a circular tube section for the manifold under bending stresses (Equation A-16 and Equation A-17); taking into account the stress concentration generated by the manifold/engine interface; a fatigue notch factor of 1.5 and 2 will be used to assess the stress concentration effects on fatigue; $(k_f = 1.5), (k_t = 2)$ will be used as design goal for the manifold shape.

$$\sigma_{xx} = \frac{M_{xx}\left(D_o/2\right)}{\frac{\pi}{64}\left(D_o{}^4 - D_i{}^4\right)} \qquad \textbf{Equation A-16}$$

$$\sigma_{xx} = \frac{32\, M_{xx} D_o}{\pi\left(D_o{}^4 - D_i{}^4\right)} \qquad \textbf{Equation A-17}$$

where: $\sigma_{xx} \equiv$ bending stress at the outer upper fiber on the tube section

$D_o \equiv$ tube outer diameter, see section presented in Figure 6-3

$D_i \equiv$ tube inner diameter, see section presented in Figure 6-3

Considering there is a requirement for 40 mm internal diameter for optimum air flow to the engine, the problem becomes a one geometric parameter unknown, (D_o) and two dynamic factors (Γ_y, Γ_z).

Rewriting Equation A-17 and considering $\frac{32\, M_{xx}}{\pi \sigma_{xx}} = c$, Equation A-18 is generated,

$$D_o{}^4 - cD_o - D_i{}^4 = 0 \qquad \textbf{Equation A-18}$$

Numerically solving Equation 5-9 for (D_o), given: $(D_i = 40mm)$, $\left(\sigma_{xx} = \frac{74MPa}{k_f=1.5} = 49MPa \text{ and } \sigma_{xx} = \frac{74MPa}{k_f=2} = 37MPa\right)$ for a 90% reliability goal and a variable (Γ_y, Γ_z) field matrix from 1 to 20 dynamic factors, can be executed. This equation has one real and three imaginary roots.

```
function [ExtDia] = manifold_outerDiameter(Di,Mt,Ly,Lz,sigma,GammaY,GammaZ)
%Matlab sunction to solve for D0^4-C*D0-Di^4=0; for manifold diameter
%solution
%  Di: inner tube diameter
%  Mt: turbo mass
%  Ly: vertical moment arm
%  Lz: horizontal moment arm
%  sigma: stress goal (for reliable design)
%  GammaY: vertical dynamic factor (applied to gravity, 9.81 m/sec^2)
%  GammaZ: horizontal dynamic factor (applied to gravity, 9.81 m/sec^2)
m=length(GammaY);
n=length(GammaZ);
ExtDia=zeros(m,n);
for i=1:m
    for j=1:n
        C=32*Mt*9.81*(GammaY(i)*Lz+GammaZ(j)*Ly)/(sigma*pi);
        syms D0
        eqn=D0^4-C*D0-Di^4==0;
        solx=solve(eqn,D0);
        ExtDia(i,j)=double(solx(1,1));
    end
end

end
```

Figure 6-6: Numerical Solution for $\left(D_o{}^4 - cD_o - D_i{}^4 = 0\right)$

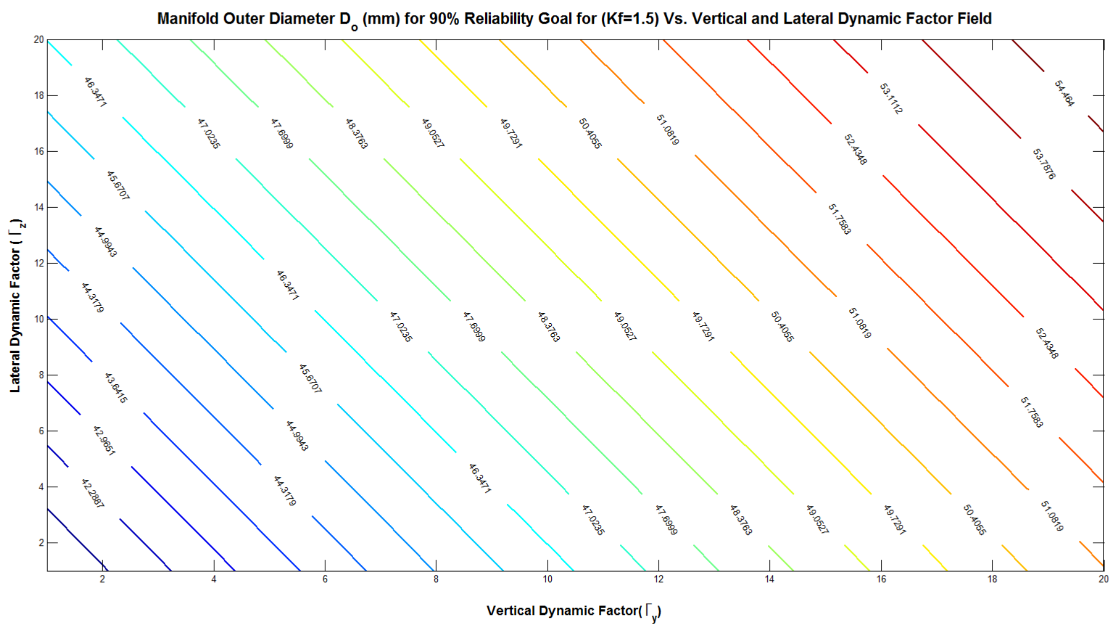

Figure 6-7: Manifold Outer Diameter to satisfy 90% Reliability Goal for (k_f=1.5) versus Vertical and Lateral Dynamic Factors Loading

Table 6-2: Stiffness Calculations for Manifold Variable sections for a Constant 40 mm Internal Diameter

Inner Diameter (mm)	Outer Diameter (mm)	Translational Axial Stiffness due to Sectional Tension/ Compression Force $\left(K_z = \frac{AE}{L}\right)$ (N/mm)	Translational Vertical and Fore/Aft Stiffness due to Bending Forces $\left(K_x = K_y = \frac{3EI}{L^3}\right)$ (N/mm)	Rotational Stiffness due to Bending Force $\left(K_{\theta_x} = K_{\theta_y} = \frac{2EI}{L^2}\right)$ (N-rad)	Torsional Stiffness due to Localized Torsion $\left(K_{\theta_z} = \frac{GJ}{L}\right)$ (N-mm/rad)
40	45	5.32E+05	1739	1.85E+06	1.49E+09
40	46	6.45E+05	2165	2.31E+06	1.86E+09
40	47	7.62E+05	2619	2.79E+06	2.25E+09
40	48	8.80E+05	3103	3.30E+06	2.66E+09
40	49	1.00E+06	3618	3.85E+06	3.11E+09
40	50	1.13E+06	4166	4.44E+06	3.58E+09
40	51	1.25E+06	4748	5.06E+06	4.08E+09
40	52	1.38E+06	5365	5.71E+06	4.61E+09

40	53	1.51E+06	6018	6.41E+06	5.17E+09
40	54	1.65E+06	6710	7.15E+06	5.76E+09
40	55	1.78E+06	7441	7.93E+06	6.39E+09
40	56	1.92E+06	8213	8.75E+06	7.05E+09
40	57	2.06E+06	9028	9.62E+06	7.75E+09
40	58	2.21E+06	9886	1.05E+07	8.49E+09
40	59	2.35E+06	10790	1.15E+07	9.27E+09
40	60	2.50E+06	11742	1.25E+07	1.01E+10
40	61	2.65E+06	12742	1.36E+07	1.09E+10
40	62	2.81E+06	13792	1.47E+07	1.18E+10
40	63	2.96E+06	14895	1.59E+07	1.28E+10
40	64	3.12E+06	16051	1.71E+07	1.38E+10
40	65	3.28E+06	17263	1.84E+07	1.48E+10

Considering the turbocharger mass (20 Kg) compared to the engine's (760 Kg) it's reasonable to assume the turbocharger mass to have minimal effects on the engines base-excitation.

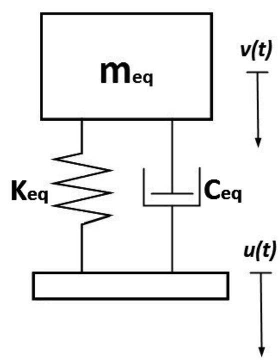

Figure 6-8: Simplified One Degree of Freedom Spring/Damper Dynamic System

Considering the dynamic spring/damper system presented in Figure 6-8 which represents a harmonic support excitation $u(t)$ influencing a mass (m_{eq}) connected to the support base with stiffness (K_{eq}) and damper (C_{eq}); the support motion is presented by Equation A-19 below.

$$u(t) = U\sin(\omega t) \qquad \textbf{Equation A-19}$$

where: $U \equiv$ base max displacement, also amplitude of harmonic base excitation

$\omega \equiv$ excitation frequency

$t \equiv$ time

The absolute displacement of (m_{eq}) is governed by [76] Equation A-20

$$\ddot{v} + 2\xi\omega_n\dot{v} + \omega_n^2 v = \omega_n^2 U\sin(\omega t) + 2\xi\omega_n\cos(\omega t) \qquad \textbf{Equation A-20}$$

where: $v \equiv m_{eq}$ displacement; time dependent

$\dot{v} \equiv$ time differentiation of (v)= (m_{eq}) velocity

$\dot{v} \equiv$ time differentiation of $(\dot{v})$= (m_{eq}) acceleration

$\xi \equiv \frac{C_{eq}}{2\sqrt{m_{eq}K_{eq}}}$, damping ratio, C_{eq} is equivalent system damping coefficient and K_{eq} is equivalent system stiffness

$\omega_n \equiv$ natural frequency

$\omega \equiv$ excitation frequency

$t \equiv$ time

The steady-state amplitude of absolute displacement is given by Equation A-21

$$T(r,\xi) = \frac{V}{U} = \sqrt{\frac{1 + (2\xi r)^2}{(1 - r^2)^2 + (2\xi r)^2}} \qquad \textbf{Equation A-21}$$

where: $T(r,\xi) \equiv$ Steady state transmissibility

$U \equiv$ base max displacement, also amplitude of harmonic base excitation

$V \equiv (m_{eq})$ max displacement dynamic response

$r \equiv (\omega/\omega_n)$, ratio between excitation frequency (ω) and natural frequency (ω_n)

where: $\left(\omega_n = \frac{K_{eq}}{m_{eq}}\right)$

$\xi \equiv \frac{C_{eq}}{2\sqrt{m_{eq}K_{eq}}}$, damping ratio, (C_{eq}) is equivalent system damping coefficient and (K_{eq}) is equivalent system stiffness

Considering the manifold tubes stiffness shown in Table 6-2, the natural frequency (for the joint of 6 tubes-stiffness of one tube was multiplied by 6), and the Transmissibility for $(\xi = 0.01)$ for lateral bending (z-displacement, see Figure 6-5) are presented in Table 6-3.

Table 6-3: Natural Frequency and Transmissibility

Inner Diameter (mm)	Outer Diameter (mm)	Natural frequency (for joint of 6-tubes) (ω_n) (rad/sec)	Transmissibility: $T(r, \xi)$
40	45	9326	1.043
40	46	25484	1.006
40	47	28030	1.005
40	48	30511	1.004
40	49	32947	1.003
40	50	35353	1.003
40	51	37740	1.003
40	52	40117	1.002
40	53	42491	1.002
40	54	44866	1.002
40	55	47247	1.002
40	56	49638	1.001
40	57	52041	1.001
40	58	54460	1.001
40	59	56896	1.001
40	60	59351	1.001
40	61	61827	1.001
40	62	64325	1.001
40	63	66847	1.001
40	64	69393	1.001
40	65	71965	1.001

The averaged acceleration on the engine top, around the engine/manifold joint, (see Figure 6-3), is $\overrightarrow{A_{E,(x,y,z)}} = 5g\hat{\imath} + 3.2g\hat{\jmath} + 8.5g\hat{k}$. Considering the natural frequency and transmissibility factors presented in Table 6-3 a conservative response of the turbocharger would be: $\overrightarrow{A_{T,(x,y,z)}} = 5.2g\hat{\imath} + 3.3g\hat{\jmath} + 8.9g\hat{k}$. Using $(\Gamma_y = 3.3, \Gamma_z = 8.9)$ an external diameter of 44.6 mm would be sufficient for 90%, 10 years reliability given the assumptions the analysis started with; see Figure 6-9.

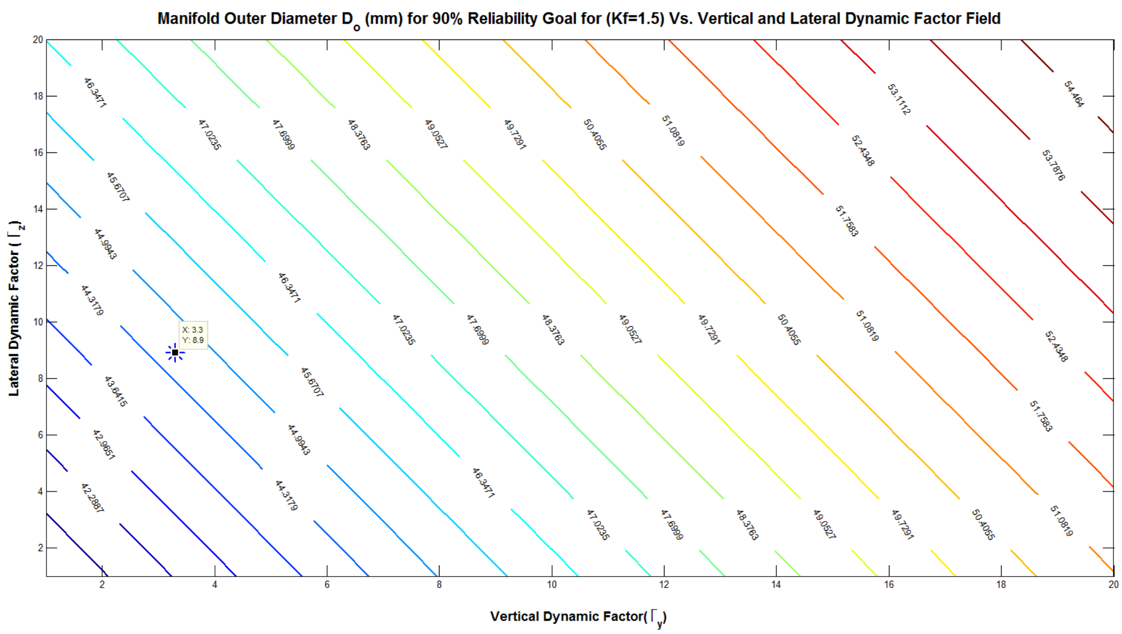

Figure 6-9: Manifold Outer Diameter Target Field for 90% Reliability Vs Averaged Manifold Loading (Shown as a point asterisk)

Appendix A.3 Finite Element Modeling of Intake Manifold

Due to the high number of manifold finite element solid meshing degrees of freedom and the long time duration needed to solve the dynamic FEM, a simplified mass/spring dynamic FEM that represents the engine and turbo masses connected through 6 DOFS spring representing the manifold stiffness was created to generate the body dynamic forces passing through the manifold structure. Spring stiffness: $\left(K_x, K_y, K_z, K_{\theta_x}, K_{\theta_y}, K_{\theta_z}\right)$ for the manifold were assessed from a second model: a linear solid mesh FEA. A third static 3D FEM for the manifold, to assess the static stress responses to unit loads was developed. The dynamic body force responses created by the dynamic FEM were used as scale factors to the static unit loads stress responses generated by the static FEM forces; to produce the dynamic stress/ time data response on points of interest on the structure. The dynamic stresses produced on highly stressed areas were then used to assess TTF and reliability of the manifold.

The finite element software Abaqus CAE was used to model the engine manifold problem. Abaqus Modal Dynamics solver and Abaqus Standard Static solver were used to solve the engine base-excitation problem. As mentioned above three FEA models were created:

1. Static model to assess an accurate manifold stiffness, $\left(K_x, K_y, K_z, K_{\theta_x}, K_{\theta_y}, K_{\theta_z}\right)$; in which, the manifold CAD volume was meshed with 3D second-order tetrahedron elements. Unit displacement loading was applied to the model at the turbocharger center of gravity. The manifold joint with the engine was constraint from displacement. The

resultant reaction forces on the manifold center of gravity for the 6 displacements were used to calculate $\left(K_x, K_y, K_z, K_{\theta_x}, K_{\theta_y}, K_{\theta_z}\right)$

2. Dynamic model to assess the body dynamic forces passing through the manifold structure due to engine vibration and external vehicle loading, in which the engine and the air turbocharger were modeled as lumped point masses. The manifold was modeled as 6 DOFS spring elements, $\left(K_x, K_y, K_z, K_{\theta_x}, K_{\theta_y}, K_{\theta_z}\right)$, resembling the manifold stiffness assessed from the first FE model. Samples of 25 operations were modeled as dynamic base-excitation using accelerometer data collected on engine mounts with the rigid frame. Table 6-4 and Table 6-5 show the operations accelerometers time duration samples used for the dynamic model. Figure 6-10 shows the dynamic FEA model.
3. Static 3D FEA model exposed to 3 unit forces to identify the highly stressed areas on the manifold and to assess the stress field response to these unit loads that are going to be linearly scaled and superimposed to create the resultant stress/time data. Virtual gage locations were identified from this model based on stress responses to the unit loads applied and high stress concentration areas.

Table 6-4: Sample Durations of Accelerometer Data used for Continuous Operations

Continuous Operations	
Operation	Sample duration (sec)
O1	19.2
O2	4.8
O3	42
O4	9.6
O5	2.4
O6	12
O7	12
O8	18
SUM	120

Table 6-5: Sample Durations of Accelerometer Data used for Discrete Operations

Discrete Operations		
Operation	Sample duration (sec)	Counts
O9	9	1 event
O10	9	1 event
O11	4	1 event
O12	4	1 event
O13	10	1 event
O14	1.5	1 event
O15	1.5	1 event
O16	1.5	1 event
O17	1.5	1 event
O18	4.5	1 event
O19	2	1 event
O20	5	1 event
O21	20	1 event
O22	1.5	1 event
O23	1.5	1 event
O24	2	1 event
O25	7.5	1 event

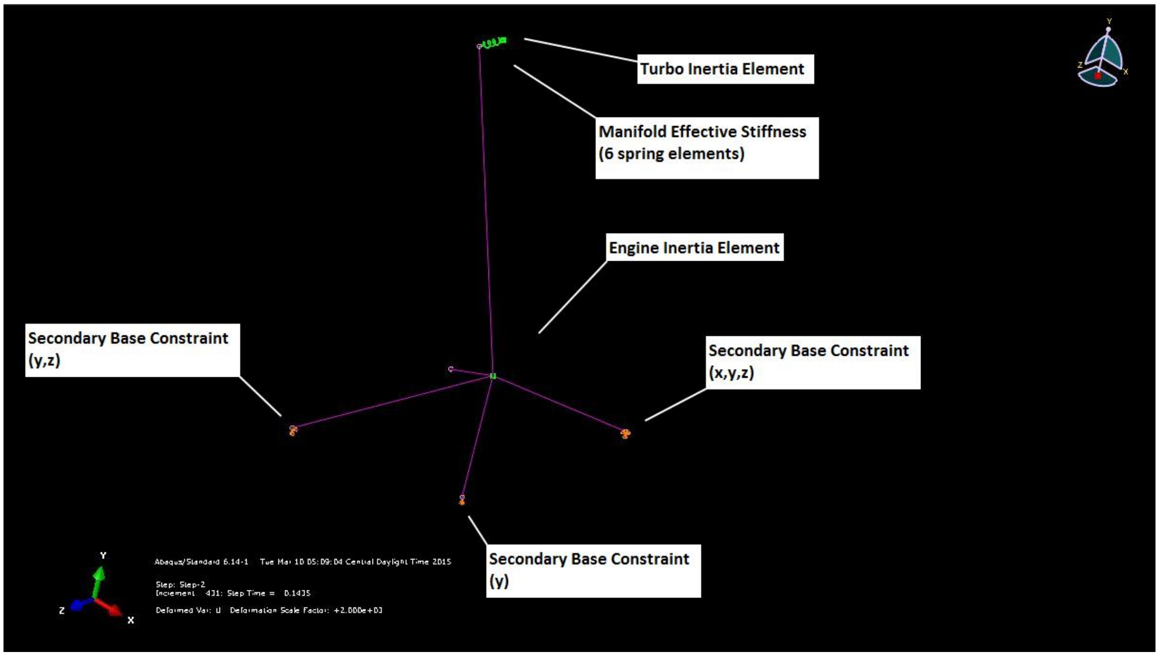

Figure 6-10: Dynamic FEA Model Setup in Abaqus CAE

Seven virtual gages were identified but one location, consistently, had the highest stress response amplitude and was identified as the lowest life area, further damage and reliability analyses were performed on this area.

Appendix B Matlab Computer Codes

Appendix B.1 Component Mechanistic Reliability Parametric Assessment

```
function[OPERsN,FMsN,COMPsN,SIM_STRESS,SIM_t,...
    SIM_System_Usage_Time,stress_agents_MU,...
    stress_agents_STD_DEV_percentage,t_MU,t_STD_DEV_percentage,...
    damage_time_domain_cells,TTF_Samples,TTF_from_Medians,...
    TTF_mu,TTF_sigma,TTF_muln,TTF_sigmaln,Reliability_at_Tg]=...

Mechanistic_Reliability_Parametric_Assessment(stress_agents_Excel,...
    system_usage_sheet,customer_usage_MU_field,...
    customer_usage_STD_DEV_percentage_field,...
    stress_agents_sheet,component_usage_MU_fields,...

component_usage_STD_DEV_percentage_fields,stress_agents_MU_fields,...
    stress_agents_STD_DEV_percentage_fields,material,Tg,L,M,N,P)
%%%%%%%%%%%%%%%%%%%%%%%%%%%%%%%%%%%%%%%%%%%%%%%%%%%%%%%%%%%%%%%%%%%%%%%%%
%%%%
% Mechanistic Reliability Assessemnt of a Mechanical System
%%%%%%%%%%%%%%%%%%
% Program Inputs
%%%%%%%%%%%%%%%%%%%%%%%%%%%%%%%%%%%
% stress_agents_Excel
% stress_agents_sheet
% component_usage_MU_fields
% component_usage_STD_DEV_percentage_fields
% stress_agents_MU_fields
% stress_agents_STD_DEV_percentage_fields
% material
% M
%%%%%%%%%%%%%%%%%%
% Program Outputs
%%%%%%%%%%%%%%%%%%%%%%%%%%%%%%%%%%
% OPERsN: Number of System Operations
% FMsN: Number of Mechanical Failure Mechanisms affecting Mechanical
System
% COMPsN: Number of System Components
% SIM_STRESS: Stochastically Simulated Stresses for Operations,Failure
%Mechanisms,Components; stored in (OPERsN,FMsN,COMPsN,M) matrix
% SIM_t: Stochastically Simulated Duration of Single Stress Cycle for
%Operations,Failure Mechanisms,Components; stored in
(OPERsN,FMsN,COMPsN,M)
%matrix
% stress_agents_MU
% stress_agents_STD_DEV_percentage
% t_MU
% t_STD_DEV_percentage
% stress_time_samples_cells
% universal_damage_cells
```

```
%% Import Stress Agents Median and Standard Deviation
[OPERsN,~,~]=xlsread(stress_agents_Excel,system_usage_sheet,'B1:B1','ba
sic'); % loading number of operations
[COMPsN,~,~]=xlsread(stress_agents_Excel,system_usage_sheet,'B2:B2','ba
sic'); % loading number of components
[FMsN,~,~]=xlsread(stress_agents_Excel,system_usage_sheet,'B3:B3','basi
c'); % loading number of failure mechanisms
stress_agents_MU=zeros(OPERsN,FMsN,COMPsN);% storage room for median
value of stress agents
stress_agents_STD_DEV_percentage=zeros(OPERsN,FMsN,COMPsN);% storage
room for std. dev. percentage value of stress agents (off median)
for i=1:COMPsN

stress_agents_MU(:,:,i)=xlsread(stress_agents_Excel,stress_agents_sheet
,char(stress_agents_MU_fields(i,:)),'basic');

stress_agents_STD_DEV_percentage(:,:,i)=xlsread(stress_agents_Excel,str
ess_agents_sheet,char(stress_agents_STD_DEV_percentage_fields(i,:)),'ba
sic');
end

%% Generate Random Stress Agents Matrix Data
if M==1
    SIM_STRESS=stress_agents_MU;
else

[SIM_STRESS]=STRESS_RANDOMIZER(stress_agents_MU,stress_agents_STD_DEV_p
ercentage,M);% M stress samples distributed along
(Operations,FMs,Components) domain, matrix size (OPERsN,FMsN,COMPsN,M)
end

%% Import Stress Agents Cycle Duration (this should be called
characteristic time, it would have a different name for corrosion for
instance)
t_MU=zeros(OPERsN,FMsN,COMPsN); % data space for median value of stress
agent cycle duration
t_STD_DEV_percentage=zeros(OPERsN,FMsN,COMPsN); % data space for std
dev value of stress agent cycle duration
for k=1:COMPsN
    for j=1:FMsN

t_MU(:,j,k)=xlsread(stress_agents_Excel,stress_agents_sheet,char(compon
ent_usage_MU_fields(k,j)),'basic'); % Import component operation time;
One cycle duration; this time is being used for all failure mechanisms
(no looping along FMs index), this might change as any stress agent
could have a different cycle duration

t_STD_DEV_percentage(:,j,k)=xlsread(stress_agents_Excel,stress_agents_s
heet,char(component_usage_STD_DEV_percentage_fields(k,j)),'basic');
    end
end
```

```
%% Generate Random Stress Cycle Duration Time Vector Data
if L==1
    SIM_t=t_MU;
else
    [SIM_t]=RANDOMIZER(t_MU,t_STD_DEV_percentage,'Stress Cycle Duration
(sec)',L);
end

%% Import System Usage Time
[Customer_Usage_MU,~,~]=xlsread(stress_agents_Excel,system_usage_sheet,
customer_usage_MU_field,'basic'); % loading sytem usage time (mean) in
unit time/yr
[Customer_Usage_STD_DEV,~,~]=xlsread(stress_agents_Excel,system_usage_s
heet,customer_usage_STD_DEV_percentage_field,'basic'); % loading sytem
usage time (std deviation) in unit time/yr

%% Generate Random System Usage Time
if N==1
    SIM_System_Usage_Time=Customer_Usage_MU;
else

[SIM_System_Usage_Time]=RANDOMIZER(Customer_Usage_MU,Customer_Usage_STD
_DEV,'System Usage',N);
    for i=1:OPERsN
        hold on
        subplot(OPERsN,1,i);
        str1=strcat('System:',' ',' Operation-',num2str(i),':','Trial
Simulation Results');
        title(num2str(str1))
        hold on
    end
end

%% Solving for TTF value using median values
MedianStress=stress_agents_MU;
MedianStressCycleDuration=t_MU;
CustomerUsage=Customer_Usage_MU;

Comp_Damage_from_Medians=zeros(OPERsN,FMsN,COMPsN);
Comp_Degradation_from_Medians=zeros(OPERsN,FMsN,COMPsN);
CompDamagefromMedian=zeros(OPERsN,FMsN);
TTF_from_Medians=zeros(1,FMsN,COMPsN); %storing TTF into 3D matrix, the
first matrix, (:,:,1) is reserved for component-1, the first column in
that matrix is for FM1 time to failure and so on.

for k=1:COMPsN

[CompDegradMedian]=Single_Component_Degradation(MedianStress(:,:,k),Med
ianStressCycleDuration(:,:,k),material);% Single_Component_Degradation
calculates the median degradation, material stochastic variation is not
present; remember the material needs to be a variable dependant on the
component, needs an update here later
    Comp_Degradation_from_Medians(:,:,k)=CompDegradMedian;
    for j=1:FMsN
```

```
        CompDamagefromMedian(:,j)=CompDegradMedian(:,j).*CustomerUsage;
    end
    for i=1:OPERsN
        Comp_Damage_from_Medians(:,:,k)=CompDamagefromMedian;
    end
end

for k=1:COMPsN
    for j=1:FMsN

[~,~,TTF_from_Medians(1,j,k),~]=Damage_Path(Comp_Degradation_from_Media
ns(:,j,k),CustomerUsage);
    end
end




%% Solving for Random Sample Degradation and Damage Generated from One
Cycle Operation: this would lead to generating (L*M*N) time-damage-
degradation samples
damage_time_domain_cells=cell(OPERsN,FMsN,COMPsN);
if P==1
    for k=1:COMPsN
        for j=1:FMsN
            for i=1:OPERsN
                %Resolve Degradation Domain
                SIMSTRESS(1,:)=SIM_STRESS(i,j,k,:);
                SIM_Char_t(1,:)=SIM_t(i,j,k,:);

[SIM_STRESS_SIM_t_U_ProbSpace]=ProbSpace([M,L],[SIMSTRESS,SIM_Char_t],2
);% Stress Characteristic-Time Universal Probability Domain

[Comp_Degradation_Sample]=Single_Component_Degradation(SIM_STRESS_SIM_t
_U_ProbSpace(:,1),SIM_STRESS_SIM_t_U_ProbSpace(:,2),material);%
remember the material needs to be a variable dependant on the
component, needs an update here later
                CompDegradationSample=Comp_Degradation_Sample;% convert
"comp_degradation_sample" back to matrix
                C_D_S=CompDegradationSample';% rearrange matrix to
become a vector
                comp_degradation_sample=C_D_S(:);

                %Resolve Damage Domain
                SIMUsageTime(1,:)=SIM_System_Usage_Time(i,:,:,:);

[comp_degradation_SIMUsage_U_ProbSpace]=ProbSpace([L*M*P^2,N],[comp_deg
radation_sample',SIMUsageTime],2);% this section is reflecting
mechanical fatigue, as it has 2 parameters (hence P^2)

comp_damage_sample=comp_degradation_SIMUsage_U_ProbSpace(:,1).*comp_deg
radation_SIMUsage_U_ProbSpace(:,2);

damage_time_domain_cells(i,j,k)={[comp_degradation_SIMUsage_U_ProbSpace
(:,2),comp_damage_sample,comp_degradation_SIMUsage_U_ProbSpace(:,1)]};
```

```
                clear Comp_Degradation_Sample CompDegradationSample
C_D_S; % release memory
            end
        end
    end
else
    for k=1:COMPsN
        for j=1:FMsN
            for i=1:OPERsN
                %Resolve Degradation Domain
                SIMSTRESS(1,:)=SIM_STRESS(i,j,k,:);
                SIM_Char_t(1,:)=SIM_t(i,j,k,:);

[SIM_STRESS_SIM_t_U_ProbSpace]=ProbSpace([M,L],[SIMSTRESS,SIM_Char_t],2
);% Stress Characteristic-Time Universal Probability Domain

[Comp_Degradation_Sample]=Single_Component_Stochastic_Degradation(SIM_S
TRESS_SIM_t_U_ProbSpace(:,1),SIM_STRESS_SIM_t_U_ProbSpace(:,2),material
,P);% remember the material needs to be a variable dependant on the
component, needs an update here later

CompDegradationSample=cell2mat(Comp_Degradation_Sample);% convert
"comp_degradation_sample" back to matrix
                C_D_S=CompDegradationSample';% rearrange matrix to
become a vector
                comp_degradation_sample=C_D_S(:);

                %Resolve Damage Domain
                SIMUsageTime(1,:)=SIM_System_Usage_Time(i,:,:,:);

[comp_degradation_SIMUsage_U_ProbSpace]=ProbSpace([L*M*P^2,N],[comp_deg
radation_sample',SIMUsageTime],2);% this section is reflecting
mechanical fatigue, as it has 2 parameters (hence P^2)

comp_damage_sample=comp_degradation_SIMUsage_U_ProbSpace(:,1).*comp_deg
radation_SIMUsage_U_ProbSpace(:,2);

damage_time_domain_cells(i,j,k)={[comp_degradation_SIMUsage_U_ProbSpace
(:,2),comp_damage_sample,comp_degradation_SIMUsage_U_ProbSpace(:,1)]};
                clear Comp_Degradation_Sample CompDegradationSample
C_D_S; % release memory
            end
        end
    end
end

%% Create TTF Samples and Plot UPL and LPL: Damage vs Time (TTF is at
damage =1)
TTF_Samples=cell(1,FMsN,COMPsN);
TTF_mu=zeros(COMPsN,FMsN);% store TTF mean value
TTF_sigma=zeros(COMPsN,FMsN);% store TTF sigma value
TTF_muln=zeros(COMPsN,FMsN);% store TTF mu-parameter for lognormal
distribution value
TTF_sigmaln=zeros(COMPsN,FMsN);% store TTF sigma-parameter for
lognormal distribution value
```

```
Reliability_at_Tg=zeros(COMPsN,FMsN);% store Reliability at design goal
time
for k=1:COMPsN
    for j=1:FMsN
        figure

[COMP_FM_TTF_Samples,~,~]=Regular_Damage_Path(OPERsN,damage_time_domain
_cells(:,j,k));% create TTF_Samples for component (k), failure
mechanism (j)
        TTF_sample_median=median(COMP_FM_TTF_Samples);% median of the
sample generated
        nTTF_Dist=length(COMP_FM_TTF_Samples);
        line([TTF_from_Medians(1,j,k)
TTF_from_Medians(1,j,k)],[0,1],'LineStyle','--','Color','k');% plot the
median TTF line
        hold on
        line([Tg Tg],[0,1],'LineStyle','--','Color','c');% ploting Tg
        str2=strcat('Component-',num2str(k),' Failure Mechanism-
',num2str(j));
        title(num2str(str2))
        legend({'TTF Samples','UFP','LFP','TTF from
Medians','Tg'},'Location','SouthEast');% overwrite the legend to add
Median TTF.
        xlabel('time')
        ylabel('damage')
        TTF_Plot_Limits=xlim;
        TTF_Samples(:,j,k)={COMP_FM_TTF_Samples}; %store
COMP_FM_TTF_Samples in TTF_Samples cell array
    end
end

end
```

Appendix B.2 Random equivalent stress output of deterministic cycles and random material input:

```
function[StressGoal]=Mechanical_Fatigue_Stress_Goal(n_goal,material,P)
%This program takes material mechanical fatigue inputs from an Excel
file called 'mechanical_fatigue_db.xlsx'; uses the sheet named
'material' and returns:
% 1- equivalent stress distribution due to n cycles damage

%%%%%%%%%%%%%%%
%Program Inputs
%%%%%%%%%%%%%%%%
% n_goal: cycle goals
% material: name of material used, 'string'; either use material='MAT
NAME' or input the material in the form of 'MAT_NAME'
% P: number of material properties samples used for simulation
%%%%%%%%%%%%%%%%
%Program Outputs
%%%%%%%%%%%%%%%%
% StressGoal: stress goal distribution; further statistical analysis
need to follow. Statistical analysis should identify the stress
amplitude to use to produce any expected reliability levels for the
component being designed
%%
[~,PROPERTY_NAME1,~]=xlsread('mechanical_fatigue_db.xlsx',material,'A3:
A12','basic'); % loading monotonic property names
[~,PROPERTY_NAME2,~]=xlsread('mechanical_fatigue_db.xlsx',material,'A15
:A20','basic'); % loading fatigue property names
PROPERTY_NAME=[PROPERTY_NAME1;PROPERTY_NAME2];
[MEDIAN1,~,~]=xlsread('mechanical_fatigue_db.xlsx',material,'C3:C12','b
asic'); % loading median monotonic numerical values
[MEDIAN2,~,~]=xlsread('mechanical_fatigue_db.xlsx',material,'C15:C20','
basic'); % loading median fatigue numerical values
MEDIAN=[MEDIAN1;MEDIAN2];
[STD_DEV1,~,~]=xlsread('mechanical_fatigue_db.xlsx',material,'D3:D12','
basic'); % loading standard deviation monotonic numerical values
[STD_DEV2,~,~]=xlsread('mechanical_fatigue_db.xlsx',material,'D15:D20',
'basic'); % loading standard deviation fatigue numerical values
STD_DEV=[STD_DEV1;STD_DEV2];
%%

% Fatigue Strength Coefficient Median (MPa); Stochastic Simulated Data
[SIM_DATA]=MAT_PROP_RANDOMIZER(MEDIAN(11),STD_DEV(11),PROPERTY_NAME(11)
,P); %LogNormally Distributed
sigmaprimef_SimData(:,1)=SIM_DATA;

% Fatigue Strength Exponent Median; Stochastic Simulated Data
[SIM_DATA]=MAT_PROP_RANDOMIZER(MEDIAN(12),STD_DEV(12),PROPERTY_NAME(12)
,P); %LogNormally Distributed with negative sign
b_SimData(:,1)=-SIM_DATA;

clear SIM_DATA
```

```
%[epsilonprimef_c_U_ProbSpace]=ProbSpace([P,P],[epsilonprimef_SimData',
c_SimData'],2);
[sigmaprimef_b_U_ProbSpace]=ProbSpace([P,P],[sigmaprimef_SimData',b_Sim
Data'],2);
%[Kprime_nprime_U_ProbSpace]=ProbSpace([P,P],[Kprime_SimData',nprime_Si
mData'],2);

n_goalVectorLength=length(n_goal);
StressGoal=zeros(n_goalVectorLength,P^2);

for i=1:n_goalVectorLength
    for j=1:P^2
        for k=1:P
            for m=1:P^2
                Csigma=exp(-(log(sigmaprimef_b_U_ProbSpace(m,1)) ...
                /sigmaprimef_b_U_ProbSpace(m,2)));
                Asigma=1/sigmaprimef_b_U_ProbSpace(m,2);
                Sigma=exp((1/Asigma)*log(n_goal(i)/Csigma));
                StressGoal(i,m)=Sigma;
            end
        end
    end
end

end
```

Appendix B.3 Equivalent damage stochastic stress output

```
function[Eq_Sigma_Median,Eq_Sigma_Mean,Eq_Sigma_Std_Dev_Percentage,...
    Stress_Samples]=EquivalentDamageStress_Stochastic(C,A,Stress_MU,...
    Stress_STD_DEV_percentage,UsageCycle,CycleGoal,M)
%EquivalentDamageStress_Stochastic calculates the equivalent stress
that
%produces the same amount of damage generated by a set of stress fields
%   C: material parameter, see my PhD thesis
%   A: material parameter, see my PhD thesis
%   Stress_MU: stress amplitudes means (column vector)
%   Stress_STD_DEV_percentage: stress standard deviation percentage
(column vector)
%   UsageCycle: number of usage cycles for the stress field (column
vector); this is a determinstic value in this program
%   CycleGoal: number of cycles as a goal for the equilalent stress to
produce the same amount of damage produced by the stress field of
(Stress_MU,Stress_STD_DEV_percentage)
%   M: number of stress samples
m=length(Stress_MU);
Stress_Samples=zeros(M,m);

%% Create Stress Samples
for i=1:m
```

```
[SIM_STRESS]=STRESS_RANDOMIZER(Stress_MU(i),Stress_STD_DEV_percentage(i
),M);
    Stress_Samples(:,i)=SIM_STRESS;
    % close;
end

%% Create Probability Space
Sets_Index=M*ones(1,m);
Set=reshape(Stress_Samples,1,M*m);
Num_of_Sets=m;
[U_ProbSpace] = ProbSpace(Sets_Index,Set,Num_of_Sets);

%% Calculate the equivalent-damage stress for every sample from
probability space and store in Eq_Sigma
[Nr,~]=size(U_ProbSpace);
Eq_Sigma=zeros(Nr,1); % Equivalent-damage stress storage space
for i=1:Nr

[EquivalentDamageStress]=EquivalentStress(C,A,U_ProbSpace(i,:),UsageCyc
le,CycleGoal); % calculate equivalent-damage stress
    Eq_Sigma(i)=EquivalentDamageStress;
end
% figure

%% plot stress samples and Eq_Sigma

for i=1:m
    subplot(2,1,1);plot(Stress_Samples(:,i))
    hold on
end
subplot(2,1,1);title('Stress
Samples');xlabel('trials');ylabel('Stress');

subplot(2,1,2);plot(Eq_Sigma)
subplot(2,1,2);title('Equivalent Damage Stress
Samples');xlabel('trials');ylabel('Stress');

%% Calculate equivalent-damage stress statistics
Eq_Sigma_Median=median(Eq_Sigma);
Eq_Sigma_Mean=mean(Eq_Sigma);
Eq_Sigma_Std_Dev_Percentage=std(Eq_Sigma)/Eq_Sigma_Mean;

End
```

Appendix B.4 Mechanical fatigue stochastic damage

```
function[one_cycle_sigma_damage,one_cycle_sigma_degradation,Nf]=...
    Mechanical_Fatigue_Stochastic_Damage(sigma,t,material,P)
%This program takes material mechanical fatigue inputs from an Excel
file
% called 'mechanical_fatigue_db.xlsx'; uses the sheet named 'material'
and
% returns:
% 1-damage due to a single stress cycle (one_cycle_sigma_damage)
% 2-degradation (damage rate) due to a single stress cycle
%   (one_cycle_sigma_degradation)
% 3-number of cycles to failure (Nf)
%%%%%%%%%%%%%%%
%Program Inputs
%%%%%%%%%%%%%%%%
% sigma: true stress amplitude
% t: time duration of a single stress cycle
% material: name of material used, 'string'; either use material='MAT
NAME'
% or input the material in the form of 'MAT_NAME'
%%%%%%%%%%%%%%%%
%Program Outputs
%%%%%%%%%%%%%%%%
%damage_sigma: damage due to a single stress cycle
%degradation: damage rate (damage per stress cycle/stress cycle
duration)
%Nf: number of cycles unlil failure happens
%%
[~,PROPERTY_NAME1,~]=xlsread('mechanical_fatigue_db.xlsx',material,'A3:
A12','basic'); % loading monotonic property names
[~,PROPERTY_NAME2,~]=xlsread('mechanical_fatigue_db.xlsx',material,'A15
:A20','basic'); % loading fatigue property names
PROPERTY_NAME=[PROPERTY_NAME1;PROPERTY_NAME2];
[MEDIAN1,~,~]=xlsread('mechanical_fatigue_db.xlsx',material,'C3:C12','b
asic'); % loading median monotonic numerical values
[MEDIAN2,~,~]=xlsread('mechanical_fatigue_db.xlsx',material,'C15:C20','
basic'); % loading median fatigue numerical values
MEDIAN=[MEDIAN1;MEDIAN2];
[STD_DEV1,~,~]=xlsread('mechanical_fatigue_db.xlsx',material,'D3:D12','
basic'); % loading standard deviation monotonic numerical values
[STD_DEV2,~,~]=xlsread('mechanical_fatigue_db.xlsx',material,'D15:D20',
'basic'); % loading standard deviation fatigue numerical values
STD_DEV=[STD_DEV1;STD_DEV2];
%%

% Yield Strength Median (MPa); Stochastic Simulated Data
[SIM_DATA]=MAT_PROP_RANDOMIZER(MEDIAN(2),STD_DEV(2),PROPERTY_NAME(2),P)
; %LogNormally Distributed
sigmayield_SimData(:,1)=SIM_DATA;
```

```
E=MEDIAN(7); % Modulus of Elasticity Median (MPa)

% Fatigue Strength Coefficient Median (MPa); Stochastic Simulated Data
[SIM_DATA]=MAT_PROP_RANDOMIZER(MEDIAN(11),STD_DEV(11),PROPERTY_NAME(11)
,P); %LogNormally Distributed
sigmaprimef_SimData(:,1)=SIM_DATA;

% Fatigue Strength Exponent Median; Stochastic Simulated Data
[SIM_DATA]=MAT_PROP_RANDOMIZER(MEDIAN(12),STD_DEV(12),PROPERTY_NAME(12)
,P); %LogNormally Distributed with negative sign
b_SimData(:,1)=-SIM_DATA;


% Fatigue Ductility Coefficient Median; Stochastic Simulated Data
[SIM_DATA]=MAT_PROP_RANDOMIZER(MEDIAN(13),STD_DEV(13),PROPERTY_NAME(13)
,P); %LogNormally Distributed
epsilonprimef_SimData(:,1)=SIM_DATA;


% Fatigue Ductility Exponent Median; Stochastic Simulated Data
[SIM_DATA]=MAT_PROP_RANDOMIZER(MEDIAN(14),STD_DEV(14),PROPERTY_NAME(14)
,P);  %LogNormally Distributed with negative sign
c_SimData(:,1)=-SIM_DATA;

% Cyclical Strength Coefficient (MPa) Stochastic Simulated Data
[SIM_DATA]=MAT_PROP_RANDOMIZER(MEDIAN(15),STD_DEV(15),PROPERTY_NAME(15)
,P); %LogNormally Distributed
Kprime_SimData(:,1)=SIM_DATA;

% Cyclical Strain Hardening Exponent Stochastic Simulated Data
[SIM_DATA]=MAT_PROP_RANDOMIZER(MEDIAN(16),STD_DEV(16),PROPERTY_NAME(16)
,P); %LogNormally Distributed
nprime_SimData(:,1)=SIM_DATA;

clear SIM_DATA

[epsilonprimef_c_U_ProbSpace]=ProbSpace([P,P],[epsilonprimef_SimData',c
_SimData'],2);
[sigmaprimef_b_U_ProbSpace]=ProbSpace([P,P],[sigmaprimef_SimData',b_Sim
Data'],2);
[Kprime_nprime_U_ProbSpace]=ProbSpace([P,P],[Kprime_SimData',nprime_Sim
Data'],2);

%%

StressVectorLength=length(sigma);
Nf=zeros(StressVectorLength,P^2);
one_cycle_sigma_damage=zeros(StressVectorLength,P^2);
one_cycle_sigma_degradation=zeros(StressVectorLength,P^2);

for i=1:StressVectorLength
    for j=1:P^2
```

```
plastic_epsilon=(sigma(i)/Kprime_nprime_U_ProbSpace(j,1))^(1/Kprime_npr
ime_U_ProbSpace(j,2)); %plastic true strain amplitude
        %true_epsilon=elastic_epsilon+plastic_epsilon; %true strain
amplitude
        for k=1:P
            if sigma(i)<=sigmayield_SimData(k)
                for m=1:P^2
                    Csigma=exp(-
(log(sigmaprimef_b_U_ProbSpace(m,1))/sigmaprimef_b_U_ProbSpace(m,2)));
                    Asigma=1/sigmaprimef_b_U_ProbSpace(m,2);
                    NfSigma=Csigma*exp(Asigma*log(sigma(i)));
                    Nf(i,m)=NfSigma;
                    one_cycle_sigma_damage(i,m)=1/Nf(i,m);

one_cycle_sigma_degradation(i,m)=one_cycle_sigma_damage(i,m)./t(i);
                end
            else
                for n=1:P^2
                    Cepsilon=exp(-
(log(epsilonprimef_c_U_ProbSpace(n,1))/epsilonprimef_c_U_ProbSpace(n,2)
));
                    Aepsilon=1/epsilonprimef_c_U_ProbSpace(n,2);

NfEpsilon=Cepsilon*exp(Aepsilon*log(plastic_epsilon));
                    Nf(i,n)=NfEpsilon;
                    one_cycle_sigma_damage(i,n)=1/Nf(i,n);

one_cycle_sigma_degradation(i,n)=one_cycle_sigma_damage(i,n)./t(i);
                end
            end
        end
    end
end

end
```

Appendix B.5 Stress Randomizer

```
function[SIM_STRESS]=STRESS_RANDOMIZER(stress_agents_MU,stress_agents_S
TD_DEV_percentage,M)
% This computer program takes 1D, 2D and 3D stress matrix fileds mean
values and
% provides simulated stress fields that reflects a similar stattistical
distribution
% stress_agents_MU: mean or median of normally distributed stress data
in the form of 1D vector,
% 2D or 3D matrix
% stress_agents_STD_DEV_percentage: standard deviation percentage of
mean in the form of
% 1D vector, 2D or 3D matrix
% M: number of random numbers required to represent the
size_operations_sigma=size(stress_agents_MU);
OPERsN=size_operations_sigma(1);
FMsN=size_operations_sigma(2);
if size(size_operations_sigma)==[1 3] % resolving 3D stress field for
more than one component
    COMPsN=size_operations_sigma(3);
else % resolving stress field for one component
    COMPsN=1;
end
SIGMA=stress_agents_MU.*stress_agents_STD_DEV_percentage;
SIM_STRESS=zeros(OPERsN,FMsN,COMPsN,M); % space to store: simulated
stress agents magnitudes
for k=1:COMPsN
    for j=1:FMsN
        figure
        for i=1:OPERsN
            mu =
log((stress_agents_MU(i,j,k)^2)/sqrt(SIGMA(i,j,k)^2+stress_agents_MU(i,
j,k)^2));% lognormal mu parameter
            sigma =
sqrt(log(SIGMA(i,j,k)^2/(stress_agents_MU(i,j,k)^2)+1));% lognormal
sigma parameter
            Sim_Stress=lognrnd(mu,sigma,M,1); % lognormally distributed
data
            SIM_STRESS(i,j,k,:)=Sim_Stress;
            subplot(OPERsN,1,i);
            plot(Sim_Stress);title('Trial Simulation
Results');xlabel('trials');ylabel('Stress');
            str1=strcat('Component-',num2str(k),',',' Operation-
',num2str(i),',',' Failure Mechanism-',num2str(j),':','Trial Simulation
Results');
            title(num2str(str1))
            hold on
        end
    end
end
end
```

Appendix B.6 Randomizer

```
function[SIM_DATA]=RANDOMIZER(MU,STD_DEV_percentage,input_name,M)
% RANDOMIZER(MU,SIGMA,M) is a program that takes 1D, 2D and 3D matrix
% fileds mean values and provides simulated data that reflects similar
% stattistical distribution
% MU: mean or median of normally distributed data in the form of 1D
vector, 2D or 3D matrix
% STD_DEV_percentage: standard deviation percentage of mean in the form
of 1D vector, 2D or 3D matrix
% 'input_name': parameter name as a string
% M: number of random numbers required to represent the
size_MU=size(MU);
OPERsN=size_MU(1);
FMsN=size_MU(2);
if size(size_MU)==[1 3] % resolving 3D stress field for more than one
component
    COMPsN=size_MU(3);
else % resolving stress field for one component
    COMPsN=1 ;
end
SIGMA=MU.*STD_DEV_percentage;% Calculating Absolute std dev
SIM_DATA=zeros(OPERsN,FMsN,COMPsN,M);
for k=1:COMPsN
    for j=1:FMsN
        figure
        for i=1:OPERsN
%             SimData=MU(i,j,k)+SIGMA(i,j,k)*randn(M,1); % normally
distributed data
            mu=log((MU(i,j,k)^2)/sqrt(SIGMA(i,j,k)^2+MU(i,j,k)^2)); %
lognormal mu parameter
            sigma=sqrt(log(SIGMA(i,j,k)^2/(MU(i,j,k)^2)+1)); %
lognormal sigma parameter
            SimData=lognrnd(mu,sigma,M,1); % lognormally distributed
data
            SIM_DATA(i,j,k,:)=SimData;
            subplot(OPERsN,1,i);
            plot(SimData);xlabel('trials');ylabel(input_name);
            str1=strcat('Component-',num2str(k),',',' Operation-
',num2str(i),',',' Failure Mechanism-',num2str(j),':','Trial Simulation
Results');
            title(num2str(str1))
            hold on
        end
    end
end
```

Appendix B.7 Single Component Degradation

```
function[comp_degradation]=Single_Component_Degradation(operations_sigm
a...
    ,t,material)
%% This program takes material failure mechanisms parameters as inputs
and
%returns: component degradation matrix
%as of now one failure mechanism is considered mechanical fatigue
%%%%%%%%%%%%%%%%%%%%%%%%%%%%%%%%%%%%%%%%%%%%%%%%%%%%%%%%%%%%%%%%%%%%%%%
%%%%
% Monotonic Properties (SAE-J1099)
%%%%%%%%%%%%%%%%%%%%%%%%%%%%%%%%%%%
%BHN: Brinnnel Hardness #
% Yield Strength (MPa), measured at 0.2% strain offset
% Ultimate Tensile Strength (MPa)
% Reduction in area after fracture (%)
% Monotonic Strength Coefficient (MPa)
% Monotonic Strain Hardening Exponent
% Modulus of Elasticity (MPa)
% Engineering strain at Yield
% True strain at Yield
%?f: True Fracture Ductility (true plastic strain after fracture)
%%%%%%%%%%%%%%%%%%%%%%%%%%%%%%%%%%%%%%%%%%%%%%%%%%%%%%%%%%%%%%%%%%%%%%%
%%%%
% Cyclic Properties (SAE-J1099)
%%%%%%%%%%%%%%%%%%%%%%%%%%%%%%%%
%?'f: Fatigue Strength Coefficient (MPa)
%b: Fatigue Strength Exponent
%?'f: Fatigue Ductility Coefficient
%c: Fatigue Ductility Exponent
%K': Cyclical Strength Coefficient (MPa)
%n': Cyclical Strain Hardening Exponent
%sigmayield= ?ys: Yield Strength (MPa)
%E: Modulus of Elasticity (MPa)
%sigmaprimef= ?'f: Fatigue Strength Coefficient (MPa)
%b: Fatigue Strength Exponent
%epsilonprimef= ?'f: Fatigue Ductility Coefficient
%c: Fatigue Ductility Exponent
%Kprime= K': Cyclical Strength Coefficient (MPa)
%nprime= n': Cyclical Strain Hardening Exponent
%%%%%%%%%%%%%%%%%%%%%%%%%%%%%%%%%%%%%%%%%%%%%%%%%%%%%%%%%%%%%%%%%%%%%%%
%%%%
% Program Inputs
%%%%%%%%%%%%%%%%%%
% operations_sigma: stress agents matrix; for different operations
% (organized in rows) and for different failure mechanisms(organized in
% columns):
%   1st column of this matrix: true mechanical stress amplitudes matrix
%   due to operations,
%   2nd column of this matrix: true corrosion stress amplitudes due to
%   operations environment
% t: characteristic time for damage progression:
```

```
%   for mechanical fatigue this is one cycle duration time duration
vector
%   of single stress cycles
%
% material: name of the material as specified in the material database
file
% mechanical_fatigue_db.xlsx (this file needs to be input as a variable
in
% case the user needed to use a different database)


%%%%%%%%%%%%%%%%%%%%%%%%%%%%%%%%%%%%%%%%%%%%%%%%%%%%%%%%%%%%%%%%%%%%%%%
%%%%
% Program Outputs
%%%%%%%%%%%%%%%%%%
%damage_sigma: damage due to a single stress cycle
%degradation: damage rate (damage per stress cycle/stress cycle
duration)
%Nf: number of cycles unlil failure happens
%%
SIZE_operations_sigma=size(operations_sigma); % extract number of
operations;
% equal to the number of operations_sigma rows
OPERsN=SIZE_operations_sigma(1);
FMsN=SIZE_operations_sigma(2); %extract number of failure
mechanisms;equal
% to the number of operations_sigma columns
comp_degradation=zeros(OPERsN,FMsN);% create storage for component
degradation
for i=1:OPERsN
    for j=1:FMsN
        if j==1 % Mechanical Fatigue Degradation
            if operations_sigma(i,j)==0
                comp_degradation(i,j)=0;% zero mechanical stress
creates zero damage
            else
                sigma=operations_sigma(i,j);
                operation_cycle_duration=t(i);
                [~,degradation,~]=Mechanical_Fatigue_Damage(sigma,...
                    operation_cycle_duration,material);
                comp_degradation(i,j)=degradation;
            end
        elseif j==2 % Corrosion Degradation
            if operations_sigma(i,j)==0
                comp_degradation(i,j)=0;
            else
                sigma=operations_sigma(i,j);
                operation_cycle_duration=t(i);

[~,degradation,~]=Mechanical_Fatigue_Damage(sigma,operation_cycle_durat
ion,material);
                comp_degradation(i,j)=degradation;% this should be
updated with damage modeling for corrossion
            end
        elseif j==3 % Wear Degradation
```

```
            if operations_sigma(i,j)==0
                comp_degradation(i,j)=0;
            else
                sigma=operations_sigma(i,j);
                operation_cycle_duration=t(i);

[~,degradation,~]=Mechanical_Fatigue_Damage(sigma,operation_cycle_durat
ion,material);
                comp_degradation(i,j)=degradation;% this should be
updated with damage modeling for wear
            end
        end
    end
end
```

Appendix B.8 Single Component Stochastic Degradation

```
function[comp_degradation]=Single_Component_Stochastic_Degradation(oper
ations_sigma...
    ,t,material,P)
%% This program takes material failure mechanisms parameters as inputs
and
%returns: component degradation matrix
%as of now one failure mechanism is considered mechanical fatigue
%%%%%%%%%%%%%%%%%%%%%%%%%%%%%%%%%%%%%%%%%%%%%%%%%%%%%%%%%%%%%%%%%%%%%%%%
%%%%
% Monotonic Properties (SAE-J1099)
%%%%%%%%%%%%%%%%%%%%%%%%%%%%%%%%%%%
%BHN: Brinnnel Hardness #
% Yield Strength (MPa), measured at 0.2% strain offset
% Ultimate Tensile Strength (MPa)
% Reduction in area after fracture (%)
% Monotonic Strength Coefficient (MPa)
% Monotonic Strain Hardening Exponent
% Modulus of Elasticity (MPa)
% Engineering strain at Yield
% True strain at Yield
%?f: True Fracture Ductility (true plastic strain after fracture)
%%%%%%%%%%%%%%%%%%%%%%%%%%%%%%%%%%%%%%%%%%%%%%%%%%%%%%%%%%%%%%%%%%%%%%%%
%%%%
% Cyclic Properties (SAE-J1099)
%%%%%%%%%%%%%%%%%%%%%%%%%%%%%%%%
%?'f: Fatigue Strength Coefficient (MPa)
%b: Fatigue Strength Exponent
%?'f: Fatigue Ductility Coefficient
%c: Fatigue Ductility Exponent
%K': Cyclical Strength Coefficient (MPa)
%n': Cyclical Strain Hardening Exponent
%sigmayield= ?ys: Yield Strength (MPa)
%E: Modulus of Elasticity (MPa)
%sigmaprimef= ?'f: Fatigue Strength Coefficient (MPa)
%b: Fatigue Strength Exponent
%epsilonprimef= ?'f: Fatigue Ductility Coefficient
%c: Fatigue Ductility Exponent
%Kprime= K': Cyclical Strength Coefficient (MPa)
%nprime= n': Cyclical Strain Hardening Exponent
%%%%%%%%%%%%%%%%%%%%%%%%%%%%%%%%%%%%%%%%%%%%%%%%%%%%%%%%%%%%%%%%%%%%%%%%
%%%%
% Program Inputs
%%%%%%%%%%%%%%%%%%
% operations_sigma: stress agents matrix; for different operations
% (organized in rows) and for different failure mechanisms(organized in
% columns):
%   1st column of this matrix: true mechanical stress amplitudes matrix
%   due to operations,
%   2nd column of this matrix: true corrosion stress amplitudes due to
%   operations environment
% t: characteristic time for damage progression:
```

```
%   for mechanical fatigue this is one cycle duration time duration
vector
%   of single stress cycles
%
% material: name of the material as specified in the material database
file
% mechanical_fatigue_db.xlsx (this file needs to be input as a variable
in
% case the user needed to use a different database)


%%%%%%%%%%%%%%%%%%%%%%%%%%%%%%%%%%%%%%%%%%%%%%%%%%%%%%%%%%%%%%%%%%%%%%%
%%%%
% Program Outputs
%%%%%%%%%%%%%%%%%%
%damage_sigma: damage due to a single stress cycle
%degradation: damage rate (damage per stress cycle/stress cycle
duration)
%Nf: number of cycles unlil failure happens
%%
SIZE_operations_sigma=size(operations_sigma); % extract number of
operations;
% equal to the number of operations_sigma rows
OPERsN=SIZE_operations_sigma(1);
FMsN=SIZE_operations_sigma(2); %extract number of failure
mechanisms;equal
% to the number of operations_sigma columns
comp_degradation=cell(OPERsN,FMsN);% create storage for component
degradation
for i=1:OPERsN
    for j=1:FMsN
        if j==1 % Mechanical Fatigue Degradation
            if operations_sigma(i,j)==0
                comp_degradation(i,j)=0;% zero echanical stress creates
zero damage
            else
                sigma=operations_sigma(i,j);
                operation_cycle_duration=t(i);

[~,degradation,~]=Mechanical_Fatigue_Stochastic_Damage(sigma,...
                    operation_cycle_duration,material,P);
                comp_degradation(i,j,:)={degradation};
            end
        elseif j==2 % Corrosion Degradation
            if operations_sigma(i,j)==0
                comp_degradation(i,j)=0;
            else
                sigma=operations_sigma(i,j);
                operation_cycle_duration=t(i);

[~,degradation,~]=Mechanical_Fatigue_Stochastic_Damage(sigma,operation_
cycle_duration,material,P);
                comp_degradation(i,j,:)={degradation};% this should be
updated with damage modeling for corrossion
            end
```

```
        elseif j==3 % Wear Degradation
            if operations_sigma(i,j)==0
                comp_degradation(i,j)=0;
            else
                sigma=operations_sigma(i,j);
                operation_cycle_duration=t(i);

[~,degradation,~]=Mechanical_Fatigue_Stochastic_Damage(sigma,operation_
cycle_duration,material,P);
                comp_degradation(i,j,:)={degradation};% this should be
updated with damage modeling for wear
            end
        end
    end
end
```

Appendix B.9 Damage Path

```
function[FP_t,FP_Damage,TTF,Delta_Matrix]=Damage_Path(Rho,t)
% This function takes the degration rate vector (degradation of many
% operations), usage time vector (usage time for the operations) and
% produces a damage path (TTF_t,TTF_Damage) and calculated time to
failure
% (TTF)
%%%%%%%%%%%%%%%%%%%%%%%%%%%%%%%%%%%%%%%%%%%%%%%%%%%%%%%%%%%%%%%%%%%%%%%%%
%%%%
% Inputs:
%#########
% OPERsN: number of operations
% Rho: degradation vector (damage rate vector; for every operation)
% t: periodical operations usage-time vector; this vector takes into
account the percentage of
% usage over a specified period (ex. annually)
%%%%%%%%%%%%%%%%%%%%%%%%%%%%%%%%%%%%%%%%%%%%%%%%%%%%%%%%%%%%%%%%%%%%%%%%%
%%%%
% Outputs:
%##########
% FP_t: path to failure (time component)
% FP_Damage: path to failure (damage component)
% TTF: time to failure
% No data sorting; failure path will be developed from the data 'as-
received'
%%

OPERsN=length(Rho); % number of operations
cum_t=zeros(OPERsN,1); % space for cumulative time
cum_t(1)=t(1);
for i=2:OPERsN
    cum_t(i)=t(i)+cum_t(i-1);
end

Delta_Matrix=zeros(OPERsN); % matrix coupling damage to usage time
Delta_Matrix(1,1)=Rho(1);
for i=2:OPERsN
    Delta_Matrix(i,i)=Rho(i);
    Delta_Matrix(i,i-1)=Rho(i-1)-Rho(i);
    if i>2
        for j=(i-2):-1:1
        Delta_Matrix(i,j)=Delta_Matrix(i-1,j);
        end
    end
end

% Damage per period (hourly, daily, annually...etc for example)
periodical_Damage=Delta_Matrix*cum_t;
T=[0;cum_t]; % adding zero initial conditions to time vector
```

```
Delta=[0;periodical_Damage]; % adding zero initial conditions to damage
vector

% figure
% plot(T,Delta); %Uncomment if you want to plot Delta vs T

% TTF (time to failure: hours, days, years...etc for example) Based on
the
% period used for evaluating Delta)
Damage_Sum=periodical_Damage(OPERsN);
% FP_Damage=periodical_Damage./Damage_Sum % another method that might
be
% more efficient
FP_Damage=(Delta_Matrix./Damage_Sum)*cum_t;
% FP_t=cum_t./Damage_Sum; % another method that might be
% more efficient
FP_t=(inv(Delta_Matrix))*FP_Damage;
TTF=FP_t(OPERsN);
FP_Damage=[0;FP_Damage]; % adding zero initial conditions to damage
vector
FP_t=[0;FP_t]; % adding zero initial conditions to time vector
```

Appendix B.10 Regular Damage Path

```
function[TTF_Samples,t_ProbSpace,Rho_ProbSpace]=Regular_Damage_Path(OPE
RsN,damage_time_domain_cells)
%
%%
[TTF_Samples,Rho,t]=Regular_Damage_Path(OPERsN,damage_time_domain_cells
)
%%
% this program will identify the damage path from the
% damage_time_domain_cells; damage_time_domain_cells is one of the
output
% cell arrays of Mechanistic_Reliability.m script
%%%%%%%%%%%%%%%%%%
%% Program Inputs
%%%%%%%%%%%%%%%%%%%%%%%%%%%%%%%%%%%
%  OPERsN: number of operations
%
% damage_time_domain_cells: one cell array of all operations affecting
one
% component under one failure mechanism
%
%
%%%%%%%%%%%%%%%%%
%% Program Ouputs
%%%%%%%%%%%%%%%%%%%%%%%%%%%%%%%%%%%
% Rho: degradation probability space
%
% t: usage time probability space
%
% TTF_Samples: time to failure of all samples
%
% this program will plot the maximum damage path (t,Rho)
%%

Index=zeros(1,OPERsN); % column space for OPERs degradation samples
r=0;
for i=1:OPERsN
    DegradSamplesIJK=cell2mat(damage_time_domain_cells(i,:,:)); %
extract degradation samples for every operation
    [n,~]=size(DegradSamplesIJK);% number of degradation samples
    Index(i)=n; % number of similar degradation samples stored in Index
    Rho1(r+1:sum(Index))=(DegradSamplesIJK(:,3)); % store all
degradation in Rho1 vector (Index will track operations degradation
within vector)
    t1(r+1:sum(Index))=DegradSamplesIJK(:,1);% store all sample
operations time in t1 vector (Index will track operations time within
vector)
    r=sum(Index);
end

[t_ProbSpace] = ProbSpace(Index,t1,OPERsN);
[Rho_ProbSpace] = ProbSpace(Index,Rho1,OPERsN);
```

```
[P,~]=size(Rho_ProbSpace); % just need the number of raws
TTF_Samples=zeros(P,1);

for i=1:P
    [~,~,TTF,~]=Damage_Path((Rho_ProbSpace(i,:))',(t_ProbSpace(i,:))');
    TTF_Samples(i)=TTF;
end
Damage_at_Failure=ones(P,1);
plot(TTF_Samples,Damage_at_Failure,'go','MarkerSize',8)
hold on

minTTF=min(TTF_Samples);
maxTTF=max(TTF_Samples);
for i=1:P
    TTF_Sample=TTF_Samples(i);
    if TTF_Sample==minTTF
        identifier1=i;

[FP_t1,FP_Damage1,~,~]=Damage_Path_Descend_Degradation((Rho_ProbSpace(i
dentifier1,:))',(t_ProbSpace(identifier1,:))');
        plot(FP_t1,FP_Damage1,'b-o','LineWidth',2)
        break
    else
    end
end
for i=1:P
    TTF_Sample=TTF_Samples(i);
    if TTF_Sample==maxTTF
        identifier2=i;

[FP_t2,FP_Damage2,~,~]=Damage_Path_Ascend_Degradation((Rho_ProbSpace(id
entifier2,:))',(t_ProbSpace(identifier2,:))');
        plot(FP_t2,FP_Damage2,'r-o','LineWidth',2)
        break
    else
    end
end
legend({'TTF Samples','UFP','LFP'},'Location','SouthEast')

end
```

Appendix B.11 Synchronous Damage-1

```
function[subsys_mean,subsys_stddev,subsys_lognormal_mu,subsys_lognormal
_sigma]...
    =SYNCHRONOUS_MAX_DAMAGE_LN_Dist(mu,sigma,M)
% SYNCHRONOUS_MAX_DAMAGE(mu,sigma,M) is a function that selects the min
TTF
% of two "Synchronous Damage" lognormal signals defined by LN(mu,sigma)
% parameters and returns the system TTF: mean, standard deviation,and
% lognormal parameters for the Synchronous Damage System
%%%%%%%%%%%%%%%%%%%%%%%%%%%%%%%%%%%%%%%%%%%%%%%%%%%%%%%%%%%%%%%%%%%%%%%%
%%%
%%Program inputs:
% M is number of each vector simulated data points; scalar
% mu is the lognormal distribution mu parameter
% sigma is lognormal distribution sigma parameter
%%
n=length(mu);
y=zeros(n,M);
for i=1:n
%      y(i,:)=MU(i)+SIGMA(i)*randn(M,1);
    y(i,:)=lognrnd(mu(i),sigma(i),M,1); % generating randomly
distributed data from lognormal params (mu,sigma)
    subplot(3,1,1);
    plot(y(i,:));
    hold on
end
subplot(3,1,1);title('Trial Simulation
Results');xlabel('trials');ylabel('TTF');
Sets_Index=M*ones(1,n);
Set=reshape(y',1,n*M);% convert (y) to a line vector from nXM matrix
[U_ProbSpace] = ProbSpace(Sets_Index,Set,n);

s=zeros(1,M^n);
for i=1:(M^n)
    s(i)=min(U_ProbSpace(i,:));
end
subplot(3,1,2);
for i=1:n
    plot(U_ProbSpace(:,i))
    hold on
end
plot(s,':r');
hold on
for i=1:n
    step=(max(y(i,:))-min(y(i,:)))/1000;
%      MU=mean(y(i));
%      SIGMA=std(y(i));
%      mu=log((MU^2)/sqrt(SIGMA^2+MU^2)) % lognormal mu parameter
%      sigma=sqrt(log(SIGMA^2/(MU^2)+1)) % lognormal sigma parameter
    PDF_DATA= lognpdf(min(y(i,:)):step:max(y(i,:)),mu(i),sigma(i));
    subplot(3,1,3);
    plot(min(y(i,:)):step:max(y(i,:)),PDF_DATA);
```

```
    hold on
end
step=(max(s)-min(s))/1000;
MU=mean(s);
SIGMA=std(s);
mu=log((MU^2)/sqrt(SIGMA^2+MU^2)); % lognormal mu parameter
sigma=sqrt(log(SIGMA^2/(MU^2)+1)); % lognormal sigma parameter
PDFs = lognpdf(min(s):step:max(s),mu,sigma);
% subplot(3,1,3);
plot(min(s):step:max(s),PDFs,':r');
subplot(3,1,3);title('pdf(TTF)');xlabel('TTF');ylabel('pdf(TTF)');
subsys_mean=mean(s);
subsys_stddev=std(s);
subsys_lognormal_mu=mu;
subsys_lognormal_sigma=sigma;
```

Appendix B.12 Synchronous Damag-2

```
function[subsys_mean,subsys_stddev,subsys_lognormal_mu,subsys_lognormal
_sigma]...
    =SYNCHRONOUS_MAX_DAMAGE_LN_Dist(mu,sigma,M)
% SYNCHRONOUS_MAX_DAMAGE(mu,sigma,M) is a function that selects the min
TTF
% of two "Synchronous Damage" lognormal signals defined by LN(mu,sigma)
% parameters and returns the system TTF: mean, standard deviation,and
% lognormal parameters for the Synchronous Damage System
%%%%%%%%%%%%%%%%%%%%%%%%%%%%%%%%%%%%%%%%%%%%%%%%%%%%%%%%%%%%%%%%%%%%%%%%%
%%%
%%Program inputs:
% M is number of each vector simulated data points; scalar
% mu is the lognormal distribution mu parameter
% sigma is lognormal distribution sigma parameter
%%
n=length(mu);
y=zeros(n,M);
for i=1:n
%     y(i,:)=MU(i)+SIGMA(i)*randn(M,1);
    y(i,:)=lognrnd(mu(i),sigma(i),M,1); % generating randomly
distributed data from lognormal params (mu,sigma)
    subplot(3,1,1);
    plot(y(i,:));
    hold on
end
subplot(3,1,1);title('Trial Simulation
Results');xlabel('trials');ylabel('TTF');
Sets_Index=M*ones(1,n);
Set=reshape(y',1,n*M);% convert (y) to a line vector from nXM matrix
[U_ProbSpace] = ProbSpace(Sets_Index,Set,n);

s=zeros(1,M^n);
for i=1:(M^n)
    s(i)=min(U_ProbSpace(i,:));
end
subplot(3,1,2);
for i=1:n
    plot(U_ProbSpace(:,i))
    hold on
end
plot(s,':r');
hold on
for i=1:n
    step=(max(y(i,:))-min(y(i,:)))/1000;
%     MU=mean(y(i));
%     SIGMA=std(y(i));
%     mu=log((MU^2)/sqrt(SIGMA^2+MU^2)) % lognormal mu parameter
%     sigma=sqrt(log(SIGMA^2/(MU^2)+1)) % lognormal sigma parameter
    PDF_DATA= lognpdf(min(y(i,:)):step:max(y(i,:)),mu(i),sigma(i));
    subplot(3,1,3);
    plot(min(y(i,:)):step:max(y(i,:)),PDF_DATA);
```

```
    hold on
end
step=(max(s)-min(s))/1000;
MU=mean(s);
SIGMA=std(s);
mu=log((MU^2)/sqrt(SIGMA^2+MU^2)); % lognormal mu parameter
sigma=sqrt(log(SIGMA^2/(MU^2)+1)); % lognormal sigma parameter
PDFs = lognpdf(min(s):step:max(s),mu,sigma);
% subplot(3,1,3);
plot(min(s):step:max(s),PDFs,':r');
subplot(3,1,3);title('pdf(TTF)');xlabel('TTF');ylabel('pdf(TTF)');
subsys_mean=mean(s);
subsys_stddev=std(s);
subsys_lognormal_mu=mu;
subsys_lognormal_sigma=sigma;
```

Appendix B.13 Asynchrouous Damage

```
function[subsys_mean,subsys_stddev,subsys_lognormal_mu,subsys_lognormal
_sigma]...
    =ASYNCHRONOUS_DAMAGE_LN_Dist(mu,sigma,M)
% ASYNCHRONOUS_DAMAGE(mu,sigma,M) is a function that calculates the sum
of TTF
% of two "Asynchronous Damage" lognormal signals defined by
LN(mu,sigma)
% parameters and returns the system TTF: mean, standard deviation,and
% lognormal parameters for the Asynchronous Damage System
%%%%%%%%%%%%%%%%%%%%%%%%%%%%%%%%%%%%%%%%%%%%%%%%%%%%%%%%%%%%%%%%%%%%%%%%
%%%
%%Program inputs:
% M is number of each vector simulated data points; scalar
% mu is the lognormal distribution mu parameter
% sigma is lognormal distribution sigma parameter
%%
n=length(mu);
y=zeros(n,M);
for i=1:n
%     y(i,:)=MU(i)+SIGMA(i)*randn(M,1);
    y(i,:)=lognrnd(mu(i),sigma(i),M,1); % generating randomly
distributed data from lognormal params (mu,sigma)
    subplot(3,1,1);
    plot(y(i,:));
    hold on
end
subplot(3,1,1);title('Trial Simulation
Results');xlabel('trials');ylabel('TTF');
Sets_Index=M*ones(1,n);
Set=reshape(y',1,n*M);% convert (y) to a line vector from nXM matrix
[U_ProbSpace] = ProbSpace(Sets_Index,Set,n);

s=zeros(1,M^n);
for i=1:(M^n)
    s(i)=sum(U_ProbSpace(i,:));
end
subplot(3,1,2);
for i=1:n
    plot(U_ProbSpace(:,i))
    hold on
end
plot(s,':r');
hold on
for i=1:n
    step=(max(y(i,:))-min(y(i,:)))/1000;
%     MU=mean(y(i));
%     SIGMA=std(y(i));
%     mu=log((MU^2)/sqrt(SIGMA^2+MU^2)) % lognormal mu parameter
%     sigma=sqrt(log(SIGMA^2/(MU^2)+1)) % lognormal sigma parameter
    PDF_DATA= lognpdf(min(y(i,:)):step:max(y(i,:)),mu(i),sigma(i));
    subplot(3,1,3);
```

```
    plot(min(y(i,:)):step:max(y(i,:)),PDF_DATA);
    hold on
end
step=(max(s)-min(s))/1000;
MU=mean(s);
SIGMA=std(s);
mu=log((MU^2)/sqrt(SIGMA^2+MU^2)); % lognormal mu parameter
sigma=sqrt(log(SIGMA^2/(MU^2)+1)); % lognormal sigma parameter
PDFs = lognpdf(min(s):step:max(s),mu,sigma);
% subplot(3,1,3);
plot(min(s):step:max(s),PDFs,':r');
subplot(3,1,3);title('pdf(TTF)');xlabel('TTF');ylabel('pdf(TTF)');
subsys_mean=mean(s);
subsys_stddev=std(s);
subsys_lognormal_mu=mu;
subsys_lognormal_sigma=sigma;
```

Bibliography

[1] D. W. Benbow and H. W. Broome, The Certified Reliability Engineer Handbook, Milwaukee: American Society of Quality, 2008.

[2] A. Z. Palmgren, "Die Lebensdauer von Kugellagern," *Z. Ver. Deutsch.,* no. 68, p. 339, 1924.

[3] M. A. Miner, "Cumulative Damage in Fatigue," *Journal of Applied Mechanics,* no. 12, 1945.

[4] J. ,. M. K. Saleh, "Highlights from the early (and pre-) history of reliability engineering," vol. 91, no. (2006) 249–256, 2005.

[5] W. Denson, "The History of Reliability Prediction," Vols. 47, NO. 3-SP, 1998.

[6] N. Bayazit, "Investigating Design: A Review of Forty Years of Design Research," *Design Issues,* vol. 20, no. 1, pp. 16-29, 2004.

[7] J. S. Gero, "Design Prototypes: A Knowledge Representation Schema for Design," *AI Magazine,* vol. 4, no. 11, pp. 26-36, 1990.

[8] A. Chakrabarti, K. Shea, R. Stone, J. Cagan, M. Campbell, N. V. Hernandez and K. L. Wood, "Computer-Based Design Synthesis Research: An Overview," *Journal of Computing and Information Science in Engineering,* vol. 11, pp. 116-126, 2011.

[9] G. E. Dieter and L. C. Schmidt, Engineering Design, 4th Edition, New York, NY: McGraw Hill Higher Education, 2009.

[10] L. Y. a. S. N. Zhang W.J., "On the Function-Behavior-Structure Model for Design," in *Proceedings of the Canadian Design Engineering Network (CDEN) Conference*, Kaninaskis, Alberta, 2005.

[11] G. Pahl, W. Beitz, J. Feldhusen and K. H. Heinrich, Engineering Design: A Systematic Approach, 3rd Edition, 2007.

[12] W. Hsu and B. Liu, "Conceptual design: issues and challenges," *Computer-Aided Design,* vol. 32, no. 14, pp. 849-850, 2000.

[13] B. Lotter, Manufacturing Assembly Handbook, Boston: Butterworths, 1986.

[14] D. A. McAdams, J. Johnson, C. Bryant, V. Rajagopalan, R. Stone, T. Kurtoglu and M. I. Campbell, "CREATION OF ASSEMBLY MODELS TO SUPPORT AUTOMATED CONCEPT GENERATION," in *Proceedings of IDETC/CIE 2005*, Long Beach, California USA, 2005.

[15] G. C. Avontuur and K. v. d. Werff, "An Implementation of Reliability Analysis in the Conceptual Design Phase of Drive Trains," *Reliability Engineering & Syatem Safety,* vol. 73, pp. 155-165, 2001.

[16] V. Hubka and W. E. Eder, Theory of Technical Systems, Berlin: Springer, 1988.

[17] D. S. Cochran, W. Eversheim, G. Kubin and M. L. Sesterhenn, "The Application of

Axiomatic Design and Lean Management Principles in the Scope of Production System Segmentation," vol. 38, no. 6, pp. 1377-1396, 2000.

[18] N. P. Suh, The Principles of Design, New York: Oxford University Press, 1990.

[19] N. P. Suh, Complexity: Theory and Applications, Oxford New York: Oxford University Press, 2003.

[20] Y. M. Deng, S. B. Tor and G. A. Britton, "A COMPREHENSIVE REPRESENTATION MODEL FOR FUNCTIONALDESIGN OF MECHANICAL PRODUCTS," in *INTERNATIONAL CONFERENCE ON ENGINEERING DESIGN*, Munich, 1999.

[21] A. Gofuku, "A Consideration to Apply Functional Modeling Techniques to Mechanical Designs," in *Proceedings of the Third International Workshop on Functional Modeling of Complex Technical Systems*, College Park, MD, 1995.

[22] C. L. Schmidt, E. Chang and X. Li, "The Need for a Form, Function, and Behavior-based Representation System," Design Assistance Tool Lab, College Park, 2000.

[23] M. A. Rosenman and J. S. Gero, "Purpose and function in a collaborative CAD environment," *Reliability Engineering & System Safety*, no. 64, pp. 167-179, 1999.

[24] Y. Umeda, H. Takeda, T. Tomiyama and H. Yoshikawa, "Function, Behaviour, and Structure," *Applications of artificial intelligence in engineering*, vol. 1, no. 5, pp. 177-194, 1990.

[25] M. A. Rosenman and J. S. Gero, "Purpose and Function in Design: From the Socio-Cultural to the Techno-Physical," *Design Studies*, vol. 19, pp. 161-186, 1998.

[26] J. S. Gero and U. Kannengiesser, "The Situated Function – Behaviour – Structure Framework," *Artificial Intelligence in Design'02,,* vol. 2, pp. 89-104., 2002.

[27] L. Bogoni, "More than just shape: a representation for functionality," *Artificial Intelligence in Engineering*, no. 12, pp. 337-354, 1998.

[28] Y. Umeda and T. Tomiyama, "Functional Reasoning in Design," *Artificial Intelligence in Design*, pp. 42-48, 1997.

[29] M. S. HUNDAL, "A Systematic Method for Developing Function Structures, Solutions and Concept Variants," *Mechanism and Machine Theory*, vol. 25, no. 3, pp. 243-256, 1990.

[30] J. A. Collins, B. T. Hagan and H. M. Bratt, "The Failure-Experience Matrix - A Useful Design Tool," in *Design Engineering Technical Conference*, Washington, DC, 1975.

[31] G. M. Fadel, C. F. Kirschman and C. C. Jara–Almonte, "CLASSIFYING FUNCTIONS FOR MECHANICAL DESIGN," in *Proceedings of The 1996 ASME Design Engineering Technical Conference and Computers in Engineering Conference*, Irvine, California, 1996.

[32] R. B. Stone, J. Hirtz, D. A. McAdams, S. Szykman and K. L. Wood, "A Functional Basis for Engineering Design: Reconciling and Evolving Previous Efforts," National Institute of Standards and Technology, Washington, DC, 2002.

[33] D. Karnopp and R. Rosenberg, System Dynamics: A Unified Approach, John Wiley

& Sons, Inc, 1975.

[34] M. Lind, "Multilevel Flow Modeling," in *Proceedings of the First International Workshop on Functionality Modeling of Complex Technical Systems*, Ispra, Italy, 1993.

[35] M. Modarres, "Functional Modeling of Complex Systems Using GTST MPLD Framework," in *Proceedings of the First International Workshop on Functional Modeling of Complex Technical Systems*, Ispra, Italy, 1993.

[36] M. Modarres and S. W. Cheon, "Function-centered modeling of engineering systems using the goal tree–success tree technique and functional primitives," *Reliability Engineering & System Safety,* vol. 64, no. 2, p. 181–200, May 1999.

[37] J. Smith and P. J. Clarkson, "Design Concept Modelling to Improve Reliability," *Journal of Engineering Design,* vol. 16, no. 5, pp. 473-492, October 2005.

[38] Y. M. Deng, G. A. Britton and S. B. Tor, "Constraint-based functional design verifcation for conceptual design," *Computer-Aided Design,* vol. 32, pp. 889-899, 2000.

[39] B. Chandrasekaran, "Functional Representation: A Brief Historical Perspective," *Applied Artificial Intelligence,* vol. 8, no. 2, pp. 173-197, 1994.

[40] Y. Umeda, M. Ishii, Y. Shimomura and Y. Tomiyama, "Supporting Conceptual Design Based on the Function-Behavior-State Modeler," *Artificial Intelligence for Engineering Design, Analysis and Manufacturing,* vol. 10, pp. 275-288, 1995.

[41] C. M. Mitchell, "The Importance of Modeling Operator Functions in Complex Dynamic Systems; A Conceptual Overview and Proposed Methodology," College Park, MD, 1995.

[42] C. M. Mitchell, "The Importance of Modeling Operator Functions in Complex Dynamic Systems; A Conceptual Overview and Proposed Methodology," in *Proceedings of the Third International Workshop on Functional Modeling of Complex Systems*, College Park, MD, 1995.

[43] RAC and R. A. Center, Practical Statistical Tools for the Reliability Engineer.

[44] M. R. Azarkhail and M. Modarres, "The Evolution and History of Reliability Engineering - Rise of Mechanistc Reliability Modeling," *International Journal of Performability Engineering,* vol. 7, no. 6, pp. 595-606, November 2011.

[45] I. Y. T. M. V. W. Robert B. Stone, "The Function-Failure Design Method".

[46] C. K. S. a. I. K. Eubanks, "Advanced Failure Modes and Effects Analysis using Behavior Modeling," in *ASME Design Engineering Technical Conferences*, Sacramento,CA, 1997.

[47] I. Y. Tumer and R. B. Stone, "ANALYTICAL METHODS TO EVALUATE FAILURE POTENTIAL DURING HIGH-RISK COMPONENT DEVELOPMENT," in *Proceedings of DETC'01; 2001 ASME Design Engineering Technical Conferences*, Pennsylvania, USA, September 9-12, 2001.

[48] C. A.D.S., Mechanical Reliability and Design, New York Toronto: John Wiley and Sons Inc, 1997.

[49] K. H. Henley E. J., System Reliability Theory: Models, Statistical Methods, and Applications, IEEE, 1991.

[50] U. D. o. Defence, "Military Handbook: Electronic Reliability Design Handbook (MIL-HDBK-338B)," DoD, 1998.

[51] . I. Horváth , "CONCEPTUAL DESIGN: INSIDE AND OUTSIDE," in *Proceedings of the EDIProD*, 2000.

[52] I. Y. Tumer and R. B. Stone, "MAPPING FUNCTION TO FAILURE DURING HIGH-RISK COMPONENT DEVELOPMENT," *Research in Engineering Design 14(1):25-33,* vol. 14, no. 1, pp. 25-33, 2003.

[53] S. W. Ormon, C. R. Cassady and A. G. Green, "A Simulation-Based Reliability Prediction Model for Conceptual Design," in *PROCEEDINGS Annual RELIABILITY and MAINTAINABILITY Symposium*, Philadelphia, Pennsylvania USA, 2001.

[54] S. W. Ormon, C. R. Cassady and A. G. Greenwood, "Reliability Prediction Models to Support Conceptual Design," *IEEE TRANSACTIONS ON RELIABILITY,* vol. 51, no. 2, pp. 151-157, JUNE 2002.

[55] A. M. Law and W. D. Kelton, Simulation Modeling and Analysis, 2nd ed., McGraw-Hill, 1991.

[56] I. Y. Tumer, B. O'Halloran, Y. Zhang and T. . Kurtoglu, "System-Level Reliability Analysis for Conceptual Design of Electrical Power System," in *CSER*, Long Beach, CA, 2011.

[57] M. Modarres, M. Kaminsky and V. Krivtsov, Reliability Engineering and Risk Analysis, Boca Raton, Florida: CRC Press; Taylor & Francis Group, 1999.

[58] J. Trewn and K. Yang, "A Treatise on System Reliability and Design Complexity," in *First International Conference on Axiomatic Design*, Cambridge, MA, 2000.

[59] P. Citti, G. Arcidiacono, M. Delogu and L. Michelini, "The Theoretical Aspects of Reliability Design Analysed Using Axiomatic Design," in *First International Conference on Axiomatic Design*, Cambridge, MA, 2000.

[60] A. Dasgupta and M. Pecht, "Material Failure Mechanisms and Damage Models," *IEEE Transactions on Reliability,* vol. 40, no. 5, December 1991.

[61] N. D. Singpurwalla, Reliability and Risk: A Bayesian Perspective, West Sussex, England: John Wiley & Sons Ltd, , 2006.

[62] J. L. Bogdanoff and F. Kozin, Probabilistic Models of Cummulative Damage, New York: John Wiley & Sons, 1985.

[63] A. Fatemi and L. Yang, "Cumulative Fatigue Damage and Life Prediction Theories: A Survey of the State of the Art for Homogeneous Materials," *International Journal of Fatigue,* vol. 20, no. 1, pp. 9-34, 1998.

[64] F. E. Richart and N. M. Newmark, "An Hypothesis for the Determination of Cumulative Damage in Fatigue," in *Proceedings, American Society for Testing and Materials*, 1948.

[65] S. M. Marco and W. L. Starkey, "A Concept of Fatigue Damage," *Transactions of ASME*, vol. 76, pp. 627-732, 1954.

[66] J. B. Kommers, "The Effect of Overstress in Fatigue on the Endurance Life of Steel," in *Proceedings, American Society for Testing and Materials,* 1945.

[67] J. A. Bennett, "A Study of the Damaging Effect of Fatigue Stressing on X4130 Steel," in *Proceedings, American Society for Testing and Materials,* 1946.

[68] D. L. Henry, "A Theory of Fatigue Damage Accumulation on Steel," *Transactions of the ASME,* vol. 77, pp. 913-918, 1955.

[69] R. R. Gatts, "Application of a Cumulative Damage Concept to Fatigue," *ASME Journal of Basic Engineering,* vol. 83, pp. 529-540, 1961.

[70] R. R. Gatts, "Cumulative Fatigue Damage with Random Loading," *ASME Journal of Basic Engineering,* vol. 84, pp. 403-409, 1962.

[71] J. I. Bluhm, "A Note on Fatigue Damage," *Material Research and Standards,* 1962.

[72] J. Pearl, Causality : Models, Reasoning, and Inference, Cambridge, NY: Canbridge University Press, 2013, p. 44.

[73] J. A. Collins, Failure of Materials in Mechanical Design: Analysis, Prediction, Prevention., Wiley Interscience Publication, 1993.

[74] S. International, "J1099- Technical Report on Low Cycle Fatigue Properties: Ferrous and Non-Ferrous Materials," SAE International, Warrendale, PA, 2002.

[75] S. International, "Technical Report on Low Cycle Fatigue Properties Ferrous and Non-Ferrous Materials," SAE International, Warrendale, PA, 2002.

[76] S. G. Kelly, Schaum's Outline of Theory and Problems of Mechanical Vibrations, McGraw-Hill, 1996.

[77] G. Yang, Life Cycle Reliability Engineering, John Wiley & Sons, Inc, 2007.

[78] T. Levitt, "Exploit the Product Life Cycle," Nov.-Dec. 1965.

[79] B. J. Zirger and M. A. Maidique, "A Model of New Product Development: An Empirical Test," *Management Science,* vol. 36, no. No. 7, pp. 867-883, July 1990.

[80] M. A. M. David E. Lee, "ISSUES IN PRODUCT LIFE CYCLE ENGINEERING ANALYSIS," in *Advances in Design Automation, ASME 1993; ASME Design Automation Conference,* Albuquerque, NM, September 1993, 1993.

[81] S. Szykman, J. W. Racz and R. D. Sriram, "The Representation of Function in Computer-based Design," in *ASME Design Engineering Technical Conferences (11th International Conference on Design Theory and Methodology)*, Las Vegas, NV, 1999.

[82] S. Szykman, S. J. Fenves, W. Keirouz and S. Shooter, "A Foundation for Interoperability in Next-generation Product Development Systems," *Computer-Aided Design,* no. 33, pp. 545-559, 2001.

[83] A. Little, K. Wood and D. McAdams, "Functional Analysis: A Fundamental Empirical Study for Reverse Engineering, Benchmarking and Redesign," in *ASME Design Theory and Methodology Conference,* Sacramento, CA, 1997.

[84] R. Stone, K. Wood and R. Crawford, "Product Architecture Development with Quantitative Functional Models," in *ASME Design Engineering Technical Conferences; Proceedings of DETC99,* Las Vegas, NV, 1999.

[85] R. Stone, K. Wood and R. Crawford, "A Heuristic Method to Identify Modules from a Functional Description of a Product," in *ASME Design Engineering Technical Conferences; Proceedings of DETC98*, Atlanta, GA, 1998.

[86] R. Stone and K. Wood, "Development of a Functional Basis for Design," in *ASME Design Engineering Technical Conferences; Proceedings of DETC99*, Las Vegas, NV, 1999.

[87] D. McAdams, R. Stone and K. Wood, "Functional Interdependence and Product Similarity Based on Customer Needs," *The Journal of Research in Engineering Design*, no. 11, pp. 1-19, 1999.

[88] D. McAdams and K. Wood, "Quantitative Measures for Design by Analogy," in *ASME Design Engineering Technical Conferences; DETC'00*, Baltimore, Maryland, USA, 2000.

[89] D. McAdams and K. Wood, "Methods and Principles for Concurrent Functional Tolerance Design," in *ASME Design For Manufacturing Conference; 99-DETC/DFM49*, Las Vegas, Nevada, 1999.

[90] K. Dorst and P. E. Vermaas, "John Gero’s Function-Behaviour-Structure model of designing: a critical analysis," *Research in Engineering Design (2005) 16: 17–26,* vol. 16, pp. 17-26, 2005.

[91] D. Socie, "www.efatigue.com," [Online]. Available: https://www.efatigue.com/constantamplitude/stresslife/#a. [Accessed 14 April 2013].

[92] T. Ming, "Overview of Mechanistic Modelling Techniques," Newcastle University, Department of Chemical Engineering and Advanced Materials, 2000. [Online]. Available: http://lorien.ncl.ac.uk/ming/dynamics/modelling.pdf. [Accessed 6 April 2015].

[93] ANSI/PMI, *A Guide to the Project Management Body of Knowledge,* Newtown Square, PA: Project Management Institution, Inc, 2004.

[94] N. Papakonstantinou, S. Sierla, D. Jensen and I. Yumer, "Simulation of Interactions and Emergent Failure Behavior During Complex System Design," *Journal of Computing and Information Science in Engineering*, vol. 12, no. September 2012, 2012.